TECHNISCHE UNIVERSITÄT MÜNCHEN

Lehrstuhl für Technische Mikrobiologie

Analysis of the interaction of gushing inducing hydrophobins with beer foam proteins

Claudia Specker

Vollständiger Abdruck der von der Fakultät Wissenschaftszentrum Weihenstephan für Ernährung, Landnutzung und Umwelt der Technischen Universität München zur Erlangung des akademischen Grades eines

Doktors der Naturwissenschaften

genehmigten Dissertation.

Vorsitzender:	Univ.-Prof. Dr. H.-C. Langowski
Prüfer der Dissertation:	1. Univ.-Prof. Dr. R. F. Vogel
	2. Univ.-Prof. Dr. D. Langosch

Die Dissertation wurde am 18.08.2014 bei der Technischen Universität München eingereicht und durch die Fakultät Wissenschaftszentrum Weihenstephan für Ernährung, Landnutzung und Umwelt am 26.10.2014 angenommen.

Danksagung

An dieser Stelle möchte ich mich herzlich bei meinem Doktorvater Prof. Dr. Rudi Vogel für die Möglichkeit bedanken, an diesem interessanten Thema an seinem Lehrstuhl zu arbeiten. Ich danke für die fachliche Unterstützung, Anregungen und Ideen, fördernde Diskussionen, sowie für das Ermöglichen eines Forschungsaufenthalt an der technischen Universität Eindhoven.

Ein weiterer großer Dank geht an Prof. Dr. Ludwig Niessen, meinen Betreuer und Ansprechpartner in Sachen Gushing. Dabei ist die stete Diskussionsbereitschaft, sowie Hilfe bei der Präsentation der Arbeit hervorzuheben.

Mein Dank gilt ebenso Prof. Dr. Dieter Langosch für die Übernahme des Koreferats und Prof. Dr. Horst-Christian Langowski für die Übernahme des Prüfungsvorsitzes.

Ich danke meinen Projektkollegen Ekaterina Minkenko und Carla Denschlag für das Einbringen neuer Ideen und die stete Bereitschaft zur Diskussion, sowie das Bereitstellen von Versuchsproben.
Bei meinen Bürokollegen Juliane Schnabel, Christian Lenz, Frank Jakob und Mandy Stetina, sowie allen Doktoranden- und Arbeitskollegen bedanke ich mich für das angenehme und freundschaftliche Klima.

Ich bedanke mich weiterhin bei Dr. Ilja Voets für die Möglichkeit AFM und DLS Messungen am Department of Chemical Engineering and Chemistry, an der technischen Universität Eindhoven durchzuführen, sowie das große Interesse und die Bereitschaft für Diskussion in Bezug auf meine Arbeit.

Bei meinen Projektpartnern Michael Ammer und Dr.-Ing. Martina Gastl möchte ich mich für die Durchführungen der Brauversuche und Bereitstellung von Brauproben bedanken.

Dem Lehrstuhl für Lebensmittelverfahrenstechnik und Molkereitechnologie danke ich für die Möglichkeit und Hilfe bei der Messung von Partikelgröße, sowie Benutzung des Tropfentensiometers.

Ebenso gilt mein Dank der Arbeitsgemeinschaft industrieller Forschungsvereinigungen "Otto von Guericke" e.V. (Projekt AiF 16508) und der Wissenschaftsförderung der Deutschen Brauwirtschaft e.V. (WiFö) für die Finanzierung der Arbeit.

Sue Law danke ich für die sprachliche Korrektur der Arbeit. Ein großer Dank geht an meine Eltern und Familie, die mich während des Studiums und der Promotion unterstützten. Besonders bedanke ich mich bei Matthias Jakob für seine Geduld, seelische Unterstützung und Motivation, sowie für das Korrekturlesen der Arbeit.

Abbreviations

abs	Absorbance
AFM	atomic force microscopy
aa	amino acid
ANS	8-anilino-1-naphatlene sulfonic acid
AOX	alcohol oxygenase
AP	alkaline phosphatase
APS	ammonium persulfate
BCIP	5-bromo-4-chloro-3'-indoly phosphate p-toluidine salt
BLAST	basic local alignment search tool
bp	base pair
BSA	bovine serum albumin
'btl'	fraction of beverage that stayed in the bottle after gushing
CAPS	3-(cyclohexylamino)-1-propanesulfonic acid
CHAPS	3-[(3-cholamid-opropyl)-dimethylammonio]-1-propane sulfonate
DDL	3,5-diacetyl-1,4-dihydrolutidine
DDLS	depolymerized dynamic light scattering
dist.	Distilled
DLS	dynamic light scattering
DNA	desoxyribo nucleic acid
DMSO	dimethyl sulfoxide
DTT	Dithiothreitol
EDC	1-ethyl-3-(3-dimethylaminopropyl)-carbodiimide
EDTA	ethylenediaminetetraacetic acid
ELISA	enzyme-linked immunosorbent assay
FcHyd5p	class 2 hydrophobin from *Fusarium culmorum*
FcHyd3p	class 1 hydrophobin from *Fusarium culmorum*
FHB	*Fusarium* head blight
g	acceleration constant
HCCA	α-cyano-4-hydroxycinnamic acid
HEPES	4-(2-hydroxyethyl)-1-piperazine-ethanesulfonic acid
Hfb2	class 2 hydrophobin from *Trichoderma reesei*

IgG	immunoglobin G
kbp	kilo base pair
kDa	kilo Dalton
MALDI TOF	matrix-assisted laser desorption/ionization
MCT	modified Carlsberg test
NBT	nitro-blue tetrazolium chloride
NHS	N-hydroxysuccinimide
nsLtp1	non specific lipid transfer protein 1 from *Hordeum vulgare*
nsLtp1 b	heat treated nsLtp1
OD	optical density
‘of’	fraction of beverage that overfoamed by gushing
PAGE	polyacrylamide gel electrophoresis
PBS	phosphate-buffered saline
PCR	polymerase chain reaction
PNPP	p-nitrophenyl phosphate
RCL	reactive center loop
RU	resonance unit
SDS	sodium dodecyl sulfate
SPR	surface plasmon resonance
serpin	serine protease inhibitor
TAE	Tris-acetate-EDTA
TBS	Tris-buffered saline
TCEP	Tris-(2-carboxyethyl)-phosphine
TEMED	tetramethylethylenediamine
TFA	trifluoractetic acid
TMW	Technische Mikrobiologie Weihenstephan
Tricine	N-(2-hydroxy-1,1-bis(hydroxymethyl)ethyl)glycine
Tris	Tris-(hydroxymethyl)-aminomethane
Tween20	polyoxyethylene (20) sorbitan monolaurate
YNB	yeast nitrogen base
Z4 b	heat treated protein Z4 from *Hordeum vulgare*

Table of Contents

1 Introduction

1.1 Beer gushing

Gushing denotes a physical phenomenon occurring in a wide variety of carbonated beverages. It describes the spontaneous overfoaming of a bottled drink upon opening, without previous agitation. Gushing was described in carbonated fruit juices, sparkling wines and ciders, but is most remarkable in beer (Beattie, 1951; Fischer, 2001; Pellaud, 2002; Schumacher, 2002) with high annual economic losses for the brewing industry. Gushing beer batches are unsaleable and have to be withdrawn from the market. Moreover, if gushing occurs in the consumer's hand, the brewery's image and market share might suffer considerably (Bellmer, 1995).

Even though the phenomenon is known since bottling of beer became popular in England around 1650 (Beattie, 1951), the first scientific treatment of beer gushing was published only in 1909 (Pellaud, 2002). Since this first publication a lot of research has been carried out to describe, evaluate, and analyze the overfoaming of beer and other beverages. Further, even more important to industries is the fact that research has been focused on finding ways to prevent gushing incidence and on elucidating the mechanisms involved. However, since gushing proved to be a multicausal phenomenon, no clear mechanism has been devised by research to date (Gastl et al., 2008; Pellaud, 2002).

Basically, the occurrence of beer gushing is first of all driven by carbon dioxide, which is produced by yeast cells during beer fermentation under anaerobic conditions (Deckers et al., 2010; Pellaud, 2002). It can be demonstrated that 99 % of the beer's carbon dioxide is freely dissolved in the liquid part of a beer when it is in a bottle (Guggenberger, 1962). Bottle opening results in a pressure decrease from 4 to 1 bar, leading to an abrupt change in the solution equilibrium of CO_2 and forces a portion of the carbon dioxide from the water soluble state into the gas phase. This leads to depletion of CO_2 super saturation by bubble formation and ascendance of gas into the atmosphere as bubbles (Liger-Belair, 2005; Pellaud, 2002). Bubble formation has been described as one of the key factors in gushing-research. A homogenous nucleation process with de novo bubble formation, which describes the bubble development in absolutely pure water, can be excluded for the regarded system beer. The necessary super saturation of CO_2 (25 g/L at 10 °C) is never reached in beer or any other carbonated beverage. As a consequence, evaporation of CO_2 in beer happens through aggregation at condensation nuclei (Draeger, 1996; Fischer, 2001; Gardner, 1973; Pellaud, 2002). This type of bubble formation is called heterologous nucleation, and is limited by the

concentration of nucleation sites present in the beverage (Draeger, 1996). It is therefore widely assumed that in gushing beverages the concentration of such nuclei, present and accessible for gas to evaporate, is much higher as compared to non-gushing beverages, leading to faster bubble formation and liberation (Draeger, 1996; Pellaud, 2002). Depending on the type of nuclei present for bubble formation, gushing is classified into secondary and primary gushing (Gjertsen et al., 1963).

1.1.1 Secondary gushing

Secondary gushing results from organic or inorganic particulate matter present in the beer and from other failures clearly assignable to the brewing technology currently used to produce a particular batch of beer. Small particles can act as nucleation sites for evaporation of CO_2, which results in fast release of gas and leads to overfoaming of the beverage. Particles that cause secondary gushing can be crystals of calcium oxalate, *Kieselgur*, metal ions, such as iron or heavy metals, or bottle surface roughness as summarized by Pellaud (2002). Residues of cleansing agents, abrasion of crown caps and residual filter materials were also reported to cause gushing (Draeger, 1996; Wershofen, 2004). Other detrimental physical factors can be over-carbonation, high temperature during filling as well as high volume of air in the headspace of a bottle (Pellaud, 2002; Wershofen, 2004). Secondary gushing is characterized by sporadic occurrence in a particular brewery (Garbe et al., 2004). This type of gushing can generally be handled using good manufacturing practice and appropriate management and process design.

1.1.2 Primary gushing

In contrast to secondary gushing, primary gushing occurs periodically and epidemically after extremely humid summers. It affects the entire production volume of beer produced from one malt lot (Bellmer, 1995; Casey, 1996). Curtis et al. (1961) speculated that the factors inducing primary gushing might originate from the malt used for beer production. In those early days of gushing research it was already suspected that mould infestation of grain with fungi of the genus *Fusarium* may be the cause of beer gushing (Draeger, 1996). Today it is generally accepted that *Fusarium* infected grain is the major cause of primary gushing in beer. Some *Fusarium* spp. are causal agents for the Fusarium head blight (FHB) disease of cereals, including brewing crops such as barley and wheat. Next to yield loss and mycotoxin contamination, gushing was found to be a great damage due to FHB outbreaks. *Fusarium* infection is greater in years with high humidity and rainfall during vegetation periods. This

explains the periodic and regional nature of the occurrence of the gushing phenomenon (Goswami & Kistler, 2004; Sarlin et al., 2005a; Schwarz et al., 1996; Wagacha & Muthomi, 2007). It was shown that species such as *F. graminearum, F. culmorum, F. avenaceum* and *F. sporotrichioides* had more impact on gushing than others (Niessen et al., 1992; Sarlin et al., 2012). However, it has also been postulated that non *Fusarium* fungi such as *Aspergillus* spp*., Alternaria alternata, Microdochium nivale* or *Rhizopus stolonifer* may be connected to the occurrence of gushing (Casey, 1996; Narziß, 1995).

In recent research it was demonstrated that hydrophobin proteins act as gushing factors (Haikara et al., 1999; Kleemola et al., 2001). These proteins are produced and secreted by filamentous fungi during plant infection (Ebbole, 1997; Wösten & Wessels, 1997). By usage of contaminated grain and malt for brewing, hydrophobin proteins are transferred into the finished beer where they can promote gushing.

1.2 Approaches for the prevention of gushing in beer

1.2.1 Technical methods to prevent gushing

The occurrence of gushing is a problematic issue in breweries due to losses of beer and unsaleability of affected batches. To avoid primary gushing as induced by hydrophobins, several approaches have been proposed. One approach to overcome gushing has been shown to be the addition of gushing reducing substances during the brewing process. Hop oils have been proven to exhibit gushing reducing properties and can be added into the brewing process, although the taste and flavor of the beer may suffer (Gardner et al., 1973; Shokribousjein et al., 2011). Also the addition of proteases, which would degrade hydrophobin proteins, was suggested as a strategy for gushing reduction. However, the success of such a measure remains doubtful because also other beer proteins important for foam formation or haze stability may also be degraded along with hydrophobins (Shokribousjein et al., 2011). In addition, at least class 1 hydrophobins show high stability against proteolytic cleavage (Aimanianda et al., 2009; Wösten & Wessels, 1997). Moreover, for German breweries, which produce beer according to the German law of purity (*Reinheitsgebot*), no other ingredients except water, malt, hop and yeast are permitted as raw materials. The company Erbslöh (Erbslöh Geisenheim AG, Geisenheim, Germany) markets a substance called AnGus^{1516}®, which is comprised of a mixture of silicates enriched with calcium. The addition of AnGus^{1516}® into the mashing phase during brewing results in

aggregation and binding of oxalate. According to the company, this addition would comply with the law of purity. Various proteins, including hydrophobins present in the mash, will be bound and removed from the mash with the spent grain fraction (Müller et al., 2013). However, as with the application of proteases, not only hydrophobin proteins are likely to be affected, but also proteins with positive impact on beer flavor and foam.

In another approach filtration of gushing beer through nylon powder was suggested as a means of removing gushing inducing materials from the beverage. The hydrophobic nylon material will bind and remove hydrophobic particles, including hydrophobin proteins. Because of the high amount of nylon powder needed, application in the industry is, however, not realistic (Deckers et al., 2010; Gardner, 1973; Hudson, 1962). In effect, all measures proposed to influence and reduce gushing directly, either during beer production or in the finished product, are not always easily applied and include disadvantages, such as the removal of beer foam proteins and flavor components, or are in contradiction to the German law of purity.

1.2.2 Tests for gushing prediction

The addition of gushing-reducing substances during brewing is not suitable for the purpose of brewing. Therefore, avoidance of gushing is attempted to be achieved by use of raw material without gushing potential. Currently, it is common practice in the brewing industry to determine the gushing potential of malt prior to its actual processing. A malt lot, which has been tested to have a potential to induce gushing, will be either rejected by a brewery or is blended with gushing negative malt in order to reduce the gushing potential. By blending, the concentration of gushing inducing material, i.e. hydrophobin proteins, is thought to reach a level below a critical limit (Garbe et al., 2004, Christian et al., 2009). Sarlin and co-workers experimentally determined a minimum level of 250 ppm hydrophobin in malt, above which malt shows a positive gushing potential. However, because of the different gushing inducing capabilities of different hydrophobin proteins, the critical level cannot be clearly defined (Sarlin et al., 2005b).

Counting of *Fusarium*-infected kernels or the determination of mycotoxin levels as a marker for *Fusarium* infection have been used as an indirect measure to determine the gushing inducing potential of malt lots. However, estimating a gushing potential by means of calculating fungal contamination of barley or malt proved to be insufficient (Bellmer, 1995; Narziß et al., 1990). Also the determination of mycotoxins produced by fungi, which was linked to the fungal biomass only to a limited extent, was used as predictive test for gushing

occurrence (Garbe et al., 2004; Niessen, 1993; Schwarz et al., 1996). However, different levels of mycotoxins are produced by different fungal species, and the production of the compounds varies with factors such as environmental conditions, agricultural practice or cereal cultivar (Bellmer, 1995; Sarlin et al., 2005a). Therefore, also mycotoxins proved not to be a reliable predictor for gushing. Furthermore, both values, fungal biomass and mycotoxin level, can only be correlated to a limited extent to the severity of gushing and to the level of the gushing factor hydrophobin (Sarlin et al., 2005b; Schwarz et al, 1996).

In previous research, two predictive gushing tests were developed and are currently widely used to determine the gushing potential of raw materials. The Donhauser test uses unmalted wheat or barley but can also be performed with malted grain. The sample is ground in a lab mill and extracted with water under boiling (in case of malt) or without boiling (in case of unmalted cereals). In the latter case, extracts are filtered and boiled. After cooling, trub is separated from both types of extracts by centrifugation. Clear extracts are carbonated to a standardized CO_2 content and filled in new standard glass bottles common in trade, which are shaken under standardized conditions. After opening, the amount of overflowing extract is used as an indirect measure for the gushing potential (Donhauser et al., 1990; *MEBAK III*, 1996). In the more commonly used modified Carlsberg test (MCT), ground malted or unmalted cereals are extracted with water. After filtration and reduction of the volume by boiling, extracts are added to standardize carbonated water (Bonaqa®) followed by defined shaking of the bottles. The weight of the overflow upon opening is used as a measure of the gushing potential of the examined sample (*MEBAK III*, 1996; Rath, 2008).

Furthermore, a PCR based method named loop-mediated isothermal amplification assay (LAMP) has recently been developed. Results of the assay correlated to gushing potentials of malt samples determined with the MCT. In the assay procedure, a partial sequence of the hydrophobin coding *hyd5* gene is amplified from typical gushing inducing *Fusarium* spp. under isothermal conditions. Analysis of malt and grain samples was done to evaluate the assay and authors claimed it to be more convincing than results of the MCT in corresponding samples (Denschlag et al., 2013).

A new method was recently proposed, which can be additionally performed on samples previously tested by the MCT. Micro bubbles, which were found to be associated with beer gushing, are detected by dynamic light scattering (DLS). Presence of 100 nm particles indicating the presence of micro bubbles stabilized by hydrophobin proteins, are used as evidence for the presence of a gushing potential (Deckers et al., 2012b; Deckers et al. 2011).

Direct detection of hydrophobin proteins would allow the most reliable gushing prediction. An ELISA assay was developed by Sarlin and co-workers, which can be used to quantify hydrophobin proteins in order to predict the gushing potential of raw materials (Sarlin et al., 2005b; Sarlin et al., 2007). In this procedure, the used antibodies detect a hydrophobin of *Fusarium poae*. To the author's knowledge, this method is not yet applied widely for gushing prediction in the brewing industry.

1.3 Stability of micro bubbles

As already mentioned in section 1.1, the amount of active condensation nuclei present in a bottled beverage is important for bubble development and gushing occurrence. Micro bubbles are believed to act as condensation sites for evaporation of CO_2 (Draeger, 1996; Gardner, 1973). According to the Laplace equation (1), stable micro bubbles can be formed when the pressure inside the bubble (P_B) is equal to the pressure on the outside of the bubble (P_S) (Yount, 1982). In a system which is in equilibrium, however, the surface tension at the gas/water interface surrounding the bubble (σ) exerts high pressure on the bubble, according to Laplace equation. Because surface tension σ increases with decreasing bubble diameter (D), this pressure component is more pronounced in small bubbles than in bigger ones. Smaller bubbles are therefore forced to shrink in order to fit the Laplace equation. This results in the evanescence and eventually disappearance of small bubbles.

Laplace equation $$\Delta P = P_B - P_S = \frac{4 \cdot \sigma}{D}$$

In contrast, bubbles with a size exceeding the critical diameter will be lifted to the surface of the liquid due to buoyancy. As a consequence no stable bubble will remain in a pure system since they either shrink or ascend depending on the original bubble size.

Stable micro bubbles, which can act as condensation nuclei for carbon dioxide, are only possible if the surface tension σ at the gas/water interfaces tends against zero. A decrease of the surface tension will result if surface active substances are present in the interface layer surrounding the bubble. However, a surface tension near zero cannot be reached by mere adsorption of surface active molecules (Fischer, 2001). The varying permeability model designed by Yount and co-workers proposes a stable micro bubble formation by formation of rigid surfactant films at the bubble surface under compression (Yount, 1979, 1982). They

postulated that if during compression the time for diffusion equilibrium is too short, the surfactant film will become impermeable. The increasing skin compression will act against surface tension, thus preventing further shrinkage of bubbles and promotion of the formation of stable micro bubbles (Yount, 1979, 1982). If proteins serve as surface active particles, the protein film formed at the bubble surface further provides mechanical strength upon compression by bubble shrinkage, preventing further bubble reduction (Fischer, 2001; Pellaud, 2002). This permeability model can explain the occurrence of micro bubbles in carbonated beverages, which are the actual gushing driving force.

1.4 Surface active beer proteins

As previously explained in chapter 1.3, micro bubble stabilization can be achieved by adsorption of surface active substances at the bubble surface. In beer particular hop compounds as well as fatty acids and proteins are highly surface active and may be relevant in micro bubble stabilization and gushing. Some hop compounds were observed to be gushing promoters: dehydrated humulinic acid as well as oxidated forms of iso-α-acids induce gushing and positively influence over foaming (Shokribousjein et al., 2011). However, most of the surface active hop substances present in beer cannot form a solid surface layer at hydrophobic/hydrophilic interfaces and therefore play no role in primary micro bubble formation according to the permeability model (Gardner, 1972; Yount, 1979, 1982). In fact some hop compounds, such like iso-α-acids, dry hop oil and linalool were shown to have a reducing impact on beer gushing (Gardner, 1972; Gardner et al, 1973; Lutterschmid et al., 2010, 2011). Next to hop acids, high molecular protein molecules mainly play a role in formation and stability of beer foam since they are surface active compounds (Evans & Bamforth, 2008; Narziß, 1995). Interactions between surface active compounds on a molecular level is believed to be important for accomplishing high quality beer foam (Jégou et al., 2000; Simpson & Hughes, 1994; Sørensen et al., 1993). Proteins nsLtp1, protein Z, and species derived from hordein and glutelin were found to be associated with beer foam formation and stability (Evans & Bamforth, 2008; Sørensen et al., 1993). The major beer protein is protein Z with 50-200 mg/L, followed by nsLtp1 with 50-90 mg/L (Leisegang & Stahl, 2005).

1.4.1 nsLtp1

Beer protein nsLtp1 derives from the barley grain. This alkaline protein of *Hordeum vulgare* is present in the aleuron layer in high concentrations. Its primary structure consists of 91 aa and has a molecular weight of 9.7 kDa. nsLtp1 belongs to a multigenic class of proteins, which are ubiquitous in the plant kingdom. Their name stands for non-specific lipid transfer protein since they were shown to have *in vitro* lipid transfer activity (Breu et al., 1989; Douliez et al., 2000). However, their *in vivo* function within the plant is still unknown. Because of the presence of a signal peptide domain in the mRNA translated protein sequence, secretion and extracellular functions can be assumed (Douliez et al., 2000; Kader, 1996).

Induced expression of *nsltp* genes in barley plants upon infection with fungi, as well as the antimicrobial activity of barley nsLtp proteins *in vitro,* have led to the assumption of a role in pathogen defense (Garcia-Olmedo et al., 1995; Molina et al., 1993). For the nsLtp protein of rough lemon also an increased expression upon fungal infection and antifungal activity was shown (Nishimura et al., 2008). Also gene induction by stress factors such as cold, drought, and high salt concentrations was reported (Dunn et al., 1991; Hughes et. al, 1992; Soufleri et al., 1996; Torres-Schumann et al., 1992). In addition, a protease inhibiting property was shown for barley nsLtp1. The activity of some serine proteases, cysteine proteases, and green malt proteases was reduced upon contact with the protein. A role of nsLtp1 in silencing such proteases during germination until their activity is required was suggested for malting (Jones & Marinac, 2000).

All plant nsLtp proteins contain a conserved pattern of 8 cysteine residues, which are involved in 4 intramolecular disulphide bonds (Kader, 1996). The secondary structure is characterized by a four helix topology. Involving conserved hydrophobic residues, a hydrophobic cavity is formed in the secondary structure of the protein. This is a potential site for interaction with lipids or amphiphilic ligands (Douliez et al., 2000; Heinemann et al., 1996). nsLtp1 is capable of binding a wide variety of lipids (Pacios et al., 2012). By capturing and removing foam negative lipids, this lipid binding property probably contributes to beer foam stability (Evans & Bamforth, 2008; van Nierop et al., 2004).

Barley nsLtp1 is highly stable against protease activity and heat denaturation with a melting point above 100 °C. This results in stability and survival of the protein during the brewing process (Lindorff-Larsen & Winther, 2001). It is surface active and able to bind to air/water interfaces (Subirade et al., 1995). However, native barley nsLtp1 exhibits only poor foaming potential, in contrast to the modified form, which is found in beer (Sørensen et al., 1993). Glycation of the protein by Maillard reaction as well as acylation were demonstrated during

malting and mashing. Furthermore, structural unfolding during the boiling process occurs under the chemically reducing conditions prevailing in the wort (Jégou et al., 2000, 2001; Mills et al., 2009; Perrocheau et al., 2006). All these modifications increase the amphiphilic character of the protein (Douliez et al., 2000). Substances which have a reducing effect on gushing are believed to be surface active, which is the case for barley or wheat nsLtp1 present in beer. Indeed, a correlation between the severity of gushing and the level of nsLtp1 in beer has been described. Zapf et al. (2005) found that only half of the level of wheat nsLtp was present in a gushing wheat beer as compared to non-gushing wheat beer of comparable make. Hippeli and Hecht reported similar results in gushing wheat beer. They supposed that degradation of nsLtp1 may occur in infected malt due to activity of *Fusarium* proteases as an explanation for the decrease in nsLtp1 levels. Authors suggested that proteolytic degradation products of nsLtp1 might work as gushing inducers (Hippeli & Hecht, 2007). Still in current literature this assumption leads to the ambiguous conclusion that nsLtp1 serves as gushing promoter. However, Lutterschimd and co-workers (2011) were able to demonstrate that transgenic barley nsLtp1 reduced hydrophobin induced gushing, especially after previous heat treatment in synthetic wort. As an alternative to the nsLtp1 fragmentation theory, Niessen et al. (2006) speculated that nsLtp1 together with amphiphilic fungal proteins, e.g. hydrophobins, might accumulate at the water/gas interface of CO_2 bubbles in the beer to result in a mixed protein layer surrounding a bubble. As a result, the bubble layer becomes more unstable against expansion and will burst upon pressure release and bubble growth. Deriving fragments of the bubble skin will act as further condensation nuclei for additional liberation of CO_2. Thus, although nsLtp1 may not be the agent stabilizing micro bubbles responsible for gushing, the level of nsLtp1 can be presumed to be an important gushing determinator.

1.4.2 Protein Z4

Protein Z is another main beer protein, which is present in even higher concentrations than nsLtp1. It makes up 10-25 % of total dialyzable beer protein (Hejgaard & Kaersgaard, 1983; Kaersgaard & Hejgaard, 1979). As with nsLtp1, albumin protein Z derives from *H. vulgare*, where three isoforms occur. Of these, mainly proteins Z4 and Z7 are found in beer, whereas isoform Zx is generally less abundant and only present in traces in beer (Fasoli et al., 2010; Østergaard et al., 2004; Roberts et al., 2003). Proteins Z7 and Z4, which are encoded on chromosomes 7 and 4 (hence the name), respectively, share 75 % protein identity (Hejgaard

& Kaersgaard, 1983; Østergaard et al., 2000). 80 % of the total beer protein Z content, however, accounts to Z4 (Evans & Hejgaard, 1999).

Z4 is encoded by the *Paz1* gene, which consists of 3133 bp with a 334 bp long intronic sequence. The mature protein has a size of 43.1 kDa with 399 aa in length. No signal peptide is known to exist. However, an internal 21 aa long hydrophobic region may serve as signal, targeting Z4 into the endoplasmatic reticulum (Brandt et al., 1990). Both isoforms, Z4 and Z7, are mainly expressed in the maturing grain. Proteins are deposited into the starchy endosperm and into the subaleuron layer. In addition, some expression of genes was also found in vegetative plant tissues such like roots and leaves. Zx, on the other hand, was not found in germinating barley (Roberts et al., 2003). Because of a high content of lysine, a role for protein Z as storage protein in the grain was suggested (Finnie et al., 2002). Protein Z contains 20 lysine residues per molecule and makes up 5 % of total grain lysine (Hejgaard, 1982). Moreover, protein Z is present in the grain as thiol-bound and free form, and during germination, a significant number of bound forms are released (Hejgaard & Boisen, 1980; Østergaard et al., 2004; Rosenkrands et al., 1994). Yet the function as storage protein is controversial. Because of sequence similarities, protein Z belongs to the serpin protein family, which is an acronym for serine protease inhibitor (Hejgaard et al., 1985). Serpin proteins are metastable. Their native form is relatively instable, but it gains high stability after structural change during protease inhibition. Protein Z in the grain can function as a protease inhibitor of proteolytic enzymes produced during germination. Thus, protein Z becomes resistant to degradation and consequently is inappropriate as a storage protein (Roberts et al., 2003).

Protein Z was the first serpin that was identified in plants (Brandt et al., 1990; Hejgaard et al., 1985). Protein Z4 shows 25-30 % homology to mammalian serpin proteins with highly conserved internal amino acid clusters also conserved in Z4 (Brandt et al., 1990). Serpins are a family of serine protease inhibitors that inactivate serine proteases in an irreversible suicide like inhibition process. The native serpin structure contains, next to a reactive centre loop (RCL), three β-sheets (A-C) and eight to nine α-helices (A-I) (Devlin & Bottomley, 2005).

During the process of inhibition, a serpin-protease complex is formed. The reactive site, i.e. the active serine, of the protease interacts with the RCL of the serpin protein which mimics a protease's bait. By this the catalytic site of the protease is disrupted, inactivating the enzyme. The structurally disordered protease is now accessible to degradation. On the other hand, the serpin protein is cleaved at the RCL and is structurally rearranged. The cleaved RCL is inserted into one β-sheet of the molecule, leading to a relaxation state comprising lower free

energy (Devlin & Bottomley, 2005; Huntington et al., 2000). A more stable form of the serpin results, which possesses enhanced thermal stability and conformational stability (Bruch et al., 1988; Horvath et al., 2005; Huntington et al., 2000). The structural changes of serpin upon protease inactivation are shown in Figure 1.

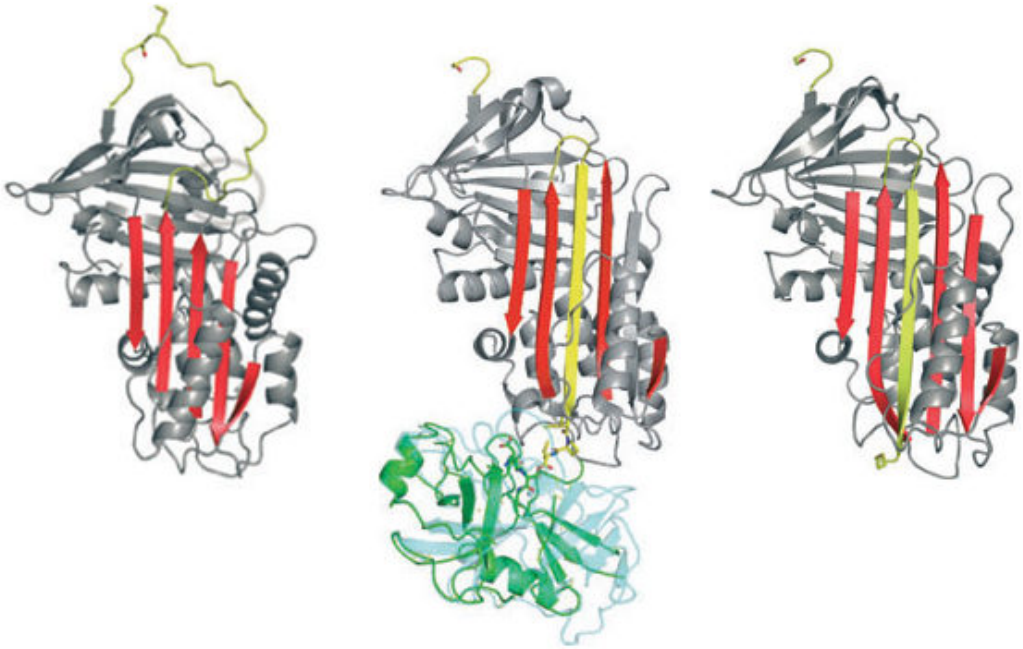

Figure 1: Structural rearrangement of a serpin molecule during protease inhibition according to Huntington et al., 2011. Left: the serpin in native form is displayed with the hinge region indicated by a circle. By binding a protease a serpin-protease complex (middle) is formed by which the RCL is cleaved resulting after release in a cleaved serpin form (right) with the RCL inserted into a β-sheet. The RCL is shown in light yellow. β-sheets in the molecule are marked red.

Instead of having a role as storage protein, it was suggested that protein Z functions as a protector for storage proteins. Protein Z protects by either shielding grain proteins from endogenous plant proteases by regulating endogenous proteolytic events, or by inactivating gut enzymes such as trypsin or chymotrypsin and thus enabling seed dispersal by animals (Roberts et al., 2003). A function in pathogen defense has also been assumed since expression of protease inhibitors was increased in plants upon fungal infection or contact with insects (Casaretto & Corcuera, 1998; Cordero et al., 1994). Further, a plant serpin protein was correlated to a reduction of survival and reproduction rates in aphids (Yoo et al., 2000). For the barley serpin protein Z, no endogenous target proteases are known to date. *In vitro* studies showed that Z4 was no inactivator for the mammalian proteases trypsin, chymotrypsin or elastase. However, it was able to inhibit cathepsin G (Dahl et al., 1996; Hejgaard et al., 1985).

The stability, which is acquired by structural unfolding during protease inactivation, is believed to enable protein Z to survive the brewing process. During germination most of the

proteins Z4 and Z7 were converted to the cleaved serpin form. However, during the kilning process of malting 10-30 % of protein Z is lost (Evans & Hejgaard, 1999). In fact the proposed temperature and pH stability of protein Z only was shown by application of an immunoelectrophoretic detection method (Hejgaard, 1982). Similar to nsLtp1, also protein Z is modified during the malting process. Glycation occurs predominantly at the lysine residues with both pentoses and hexoses (Bobálová et al., 2010; Hejgaard & Kaersgaard, 1983; Leiper et al., 2003). Apart from glycation, virtually no further detectable changes of protein Z occurred throughout malting and brewing processes (Mills et al., 1998). The presence of different modified forms in beer can be visualized by SDS-PAGE analysis with a diffuse protein cloud detectable in gels in a size range corresponding to protein Z (Curioni et al., 1995; Hejgaard & Kaersgaard, 1983; Tanner et al., 2013).

The ability to withstand the conditions present during brewing with simultaneous glycation makes protein Z a candidate protein for foam formation. In addition, protein Z is generally rich in hydrophobic amino acids (Hejgaard, 1982), resembling structural features of an amphiphilic protein. Based on its high surface activity, protein Z was claimed to be the beer protein with the highest surface viscosity and elasticity properties (Maeda et al., 1991; Yokoi et al., 1989) and was thus presumed to be a major foam protein in beer (Evans et al., 1999; Kaersgaard & Hejgaard, 1979). Experimental evidence linking protein Z to beer foam stability, however, resulted in contradictory conclusions. According to part of the literature, protein Z was not detected in the foam fraction of beer at all (Leiper et al., 2003). Moreover, the stability and quantity of beer foam was not influenced by partial removal of protein Z from beer through immune affinity chromatography (Hollemans & Tonies, 1989; Vaag et al., 1999). Also beers brewed with barley deficient in protein Z species showed no decrease in foam stability (Iimure et al., 2012). In other studies, foam positive properties of protein Z were confirmed. Protein Z was linked to foam stability by demonstrating its presence in beer foam (Hejgaard & Kaersgaard, 1983; Yokoi et al., 1989). In 2-D gel analysis of different beers the intensity of the spot corresponding to protein Z was increased in beers with better foaming properties. Thus, a link between protein Z and foam stability was shown to exist (Iimure et al., 2008). Also Evans and co-workers positively correlated protein Z4, but not Z7, to foam stability. It was thus suggested, that only a specific form of protein Z, namely protein Z4, may contribute to foam stability (Evans et al., 1999).

In conclusion, from the results described, an interaction of protein Z4 and other beer proteins, such as nsLtp1, has been proposed to be necessary for the formation of proper beer foam (Douma et al., 1997). Also the assumption was made, that nsLtp1 proteins and hops are

responsible for foam formation, whereas protein Z plays a role in further stabilizing the foam once it has formed (Leiper et al., 2003; Sørensen et al., 1993). To date no data have been presented which would indicate a link between protein Z and the gushing phenomenon.

1.5 Hydrophobins

A gushing factor responsible for primary gushing was identified as hydrophobin proteins (Haikara et al., 1999; Kleemola et al., 2001). These fungal proteins are structurally amphiphilic and display great surface activity (Linder et al., 2005; Wösten et al., 1999). They are secreted by filamentous fungi during plant infection and thereby can be present in grain or malt used for brewing (Ebbole, 1997; Wösten & Wessels, 1997). Growth and hydrophobin production may further continue during malting (Oliveira et al., 2012; Sarlin et al., 2007; Schwarz et al, 1995). Since hydrophobins are quite stable and can at least partly withstand the conditions of brewing, they may even get into the finished product. Sarlin et al. (2007) speculated that about 10 % of the initial hydrophobin concentration found in malt might end up in the finished beer. Since only low amounts of hydrophobin are necessary to induce gushing, this is in the end sufficient to result in gushing beers (Deckers et al., 2013; Sarlin et al., 2005b, 2012).

Hydrophobins are small amphiphilic fungal proteins. They are about 100 amino acids in size and have a molecular weight between 7 and 20 kDa. Hydrophobins have been found to be present in filamentous fungi within the *Ascomycetes* and *Basidiomycetes* (de Vries et al., 1993; Wösten & Wessels, 1997; Wösten, 2001). Many of the fungal species analyzed contain several distinctive genes coding for hydrophobin type proteins, which may be produced and secreted under different growth conditions (Askolin et al., 2005; Ebbole, 1997; Kershaw & Talbot, 1998; Kubicek et al., 2008; Mosbach et al., 2011; Wösten, 2001). Hydrophobin proteins can display various different functions. They cover cell walls of aerial hyphae and conidial spores where they are responsible for the water repellent properties of those structures. In fruiting bodies of mushrooms, hydrophobins cover the walls of pores and thus prevent them from being water soaked during rainfall. But they were also found to cover submerged conidia (Bidochka et al., 1995; Stringer & Timberlake, 1995; Wessels et al., 1991a). By lowering the surface tension of coated hyphae, hydrophobins enable the fungal mycelia to escape the aqueous environment of the substrate and form aerial structures (Wösten et al., 1999). Hydrophobins are also involved in plant infection (Carpenter et al., 1992; Stringer & Timberlake, 1993; Talbot et al., 1993). By changing the hydrophobicity

through assembly of the proteins at hydrophobic surfaces of plant tissues, close contact of fungal cells and plant surface facilitates infection in many plant pathogenic fungi (Talbot et al., 1993; Viterbo & Chet, 2006). Moreover a role of hydrophobins in the symbiosis of ectomycorrhizal fungi has been discussed such that the hydrophobin layer allows close contact between the fungus and the roots of a plant (Tagu et al., 1996). Because of the coating of spores, a function in dissemination and protection against antimicrobial compounds was also suggested (Ebbole, 1997).

The primary structure of hydrophobin proteins is very diverse. They all contain 8 cysteine residues at conserved positions as the common feature of the primary structure. Those residues form 4 strong disulphide bonds resulting in a secondary structure of a four–loop protein (de Vries et al., 1993; Hakanpää et al., 2004; Mackay et al., 2001; Wessels, 1994). The disulfide bonds provide the protein with high structural stability against defolding, self aggregation and solvent treatment, resulting in heat stability even at 90 °C (Askolin et al., 2006; de Vocht et al., 2000; Torkkeli et al., 2002; Sunde et al., 2008; Wösten & Wessels, 1997). The core of the globular protein, consisting of a small β-barrel, is stabilized by the network of disulfide bonds (Kallio et al., 2007; Linder, 2009). Originally, depending on their hydrophobicity pattern, hydrophobins were classified into two types, class 1 and class 2 (Wessels, 1994). Further, classification is based on the length of the intervening sequences between the conserved cysteine residues, with class 2 hydrophobins being more conserved in the space length as is illustrated in Figure 2 (Kershaw & Talbot, 1998; Linder et al., 2005). Moreover, class 2 hydrophobins are generally shorter and show different solubility properties (Linder et al., 2005).

Class I X_{26-85} - C - X_{5-8} - C - C - X_{17-39} - C - X_{8-23} - C - X_{5-6} - C - C - X_{6-18} - C - X_{2-13}

Class II X_{17-67} - C - X_{9-10}- C - C - X_{11} - C - X_{16} - C - X_{6-9} - C - C - X_{10} - C - X_{3-7}

Figure 2: Length of the sequences in between the eight conserved cysteine residues of class 1 and class 2 hydrophobins according to Wösten & Wessels, 1997.

Hydrophobin proteins form films at hydrophobic/hydrophilic interfaces by spontaneous assemblage. Assembled films of class 1 hydrophobins are quite stable and assemblies can only be dissolved with 100 % formic acid or trifluoroacetic acid (de Vries et al., 1993; Wösten et al., 1993; Wessels et al., 1991b). Polymers appear as distinct amyloid like rodlets (de Vocht et al., 2000; Kwan et al., 2006; Mackay et al., 2001; Wösten et al., 1993). In contrast, hydrophobins classified as class 2 exhibit a higher solubility and aggregates dissolve

already after addition of organic solvents or hot SDS (Carpenter et al., 1992; Szilvay et al., 2006). Interface assemblies formed by class 2 hydrophobins resemble needle like structures (Askolin et al., 2006; Torkkeli et al., 2002). Another difference between the two classes of hydrophobins is their dissemination throughout the fungal phyla. Class 2 hydrophobins appear to be restricted to the *Ascomycetes*, whereas class 1 hydrophobins are present in both phyla of the dikarya, *Acsomycetes* and *Basidiomycetes* (Linder et al., 2005). Most knowledge of hydrophobin proteins derives from investigations of the class 1 hydrophobin SC3 produced by the basidiomycete *Schizophyllum commune* and the class 2 hydrophobins Hfb1 and Hfb2 produced by the ascomyceteous fungus *Trichoderma reesei*. For class 2 hydrophobins the particular amino acids which are important for structure formation are highly conserved, suggesting a more conserved pattern of folding (Hakanpää et al., 2004, 2006). Proteins of both hydrophobin classes contain hydrophobic and hydrophilic surface domains. In class 2 hydrophobins this is in form of a hydrophobic patch, created by hydrophobic aliphatic amino acid side chains present on the otherwise hydrophilic protein surface (see Figure 3) (Hakanpää et al., 2004; Linder et al., 2005). Despite the similarities between the hydrophobin groups, only class 2 hydrophobins were shown to induce gushing in carbonated beverages to a degree which was dependent on the type of class 2 hydrophobin analyzed (Lutterschmid et al., 2011; Sarlin et al., 2012, 2005b; Stübner et al., 2010; Zapf et al., 2006).

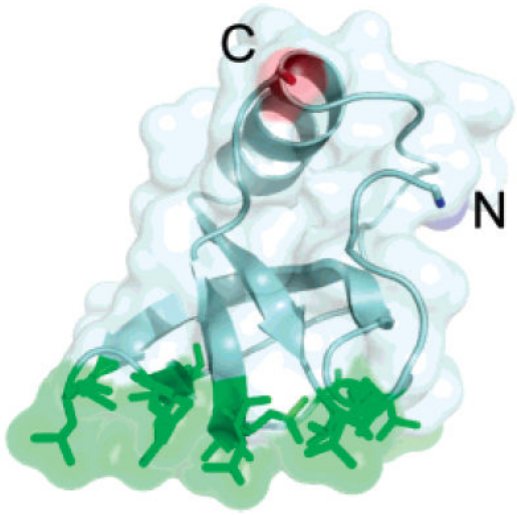

Figure 3: Space filling model of class 2 hydrophobin Hfb2 molecule of *T. reesei* with hydrophobic and hydrophilic domains according to Szilvay et al., 2007. The hydrophobic patch is shown in green, in contrast to the hydrophilic protein surface (light blue). In blue and red C and N-termini are marked, respectively.

The amphiphility of hydrophobin molecules is the reason for their ability to assemble at hydrophobic/hydrophilic interfaces. Self assembly at solid surfaces leads to a change of the displayed hydrophobicity and hence wettability of surfaces. Use of this property was proposed for several medical or industrial applications (for a review see Scholtmeijer et al., 2001). Because of their amphiphility, hydrophobin molecules form dimers and tetramers in solution by lateral hydrophobic interaction in a concentration dependent manner, explaining also their solubility in aqueous solutions (Kisko et al., 2008; Szilvay et al., 2006; Torkkeli et al., 2002; Wang et al., 2004). The arrangement of the hydrophobic surface areas at one side of the dimer thereby allows further assembly of dimers to tetramers (Kallio et al., 2007). Assembly driven by amphiphile molecules at air/water interfaces was suggested for the monomeric, dimeric and tetrameric molecules (Hakanpää et al., 2004, 2006; Kallio et al., 2007; Paananen et al., 2003). The hydrophobin assembly mechanism is shown in Figure 4 according to the latest research results derived by x-ray diffraction of hydrophobin crystals done by the group of Kallio (2007). Polymeric hydrophobin fibers, which were suggested to occur by this group, can be thought of representing nucleation sites for heterologous bubble formation (Shokribousjein et al., 2010), which may be determinative for gushing occurrence and may explain the inducing properties of hydrophobin proteins.

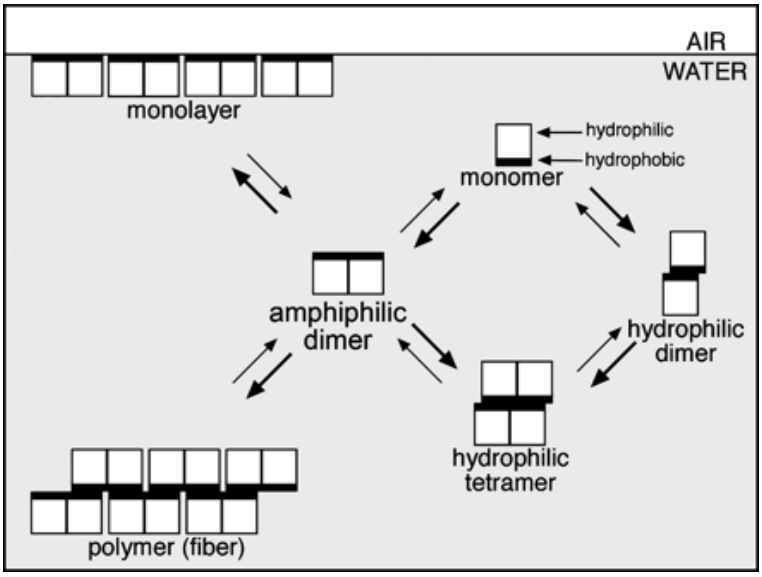

Figure 4: Multimerization and surface assembly of class 2 hydrophobin Hfb2 driven by the hydrophobic patch at the protein surface (black) according to Kallio et al., 2007.

For class 2 hydrophobins no change in protein structure was observed upon interface adsorption (Askolin et al., 2006; Cheung, 2012; Szilvay et al., 2007). A stable amphipathic membrane, consisting of a protein monolayer is formed at interfaces. This provides a

remarkably high elasticity and has a great impact on surface tension (Alexandrov et al., 2012; Blijdenstein et al., 2010; Cox et al., 2009, 2007; Milani et al., 2013; Murray, 2007). Hydrophobins are the proteins with the highest surface activity, lowering the surface tension of water from 72 mJ m^{-2} to down to 24 mJ m^{-2} (Askolin, 2006; Wösten et al., 1999). These film properties give rise to exceptional stability of foams and emulsions that are formed in the presence of hydrophobin proteins (Cox et al., 2009; Linder, 2009; Lumsdon et al., 2005; Niu et al., 2012). The densely packed and highly ordered layer of hydrophobin molecules consists of a monolayer, which upon compression shows wrinkle structures (Basheva et al., 2011a; Blijdenstein et al., 2010, 2013; Kisko et al., 2005, 2007; Paananen et al., 2003; Szilvay et al., 2007). Wrinkles on drop surfaces are depicted in Figure 5. They are believed to arise from superimposing of molecules into trilayers as result of a combination of pressure derived surface space reduction and the inability of hydrophobins to desorb off the interface (Cheung, 2012; Cox et al., 2007; Paananen et al., 2003; Stanimirova et al., 2013).

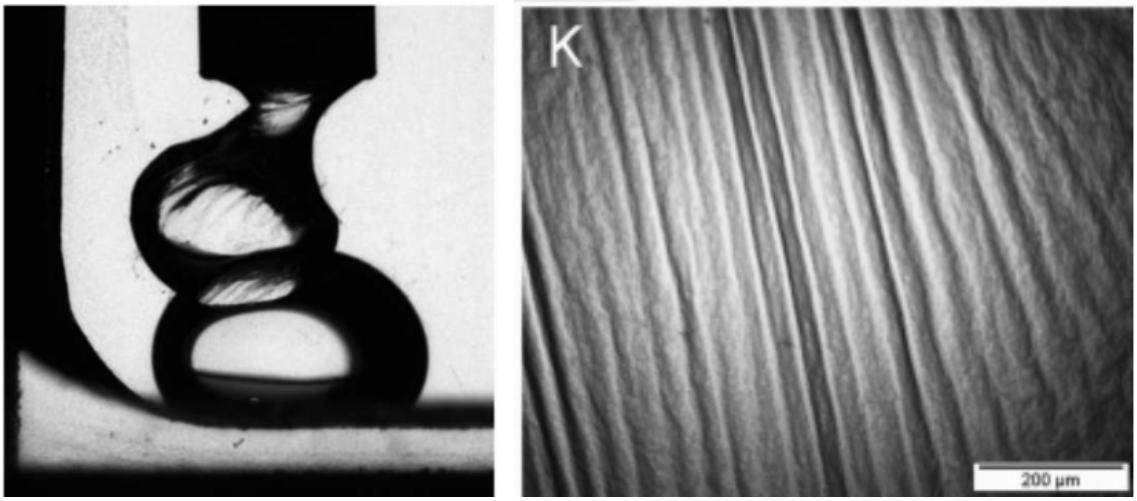

Figure 5: Wrinkle formation of hydrophobin films at air/liquid interfaces occurring after film compression. Images of Hfb1 formed films at air/oil interface according to Milani et al., 2013 (right) and at air/water interface according to Szilvay et al., 2007 (left).

1.5.1 FcHyd5p

In this study, experiments on hydrophobin-gushing evaluation were performed with the class 2 hydrophobin FcHyd5p of *F. culmorum*. Stübner and co-workers constructed a transformant *Pichia pastoris* strain that heterologously expresses and excretes this hydrophobin protein. The incorporated nucleotide sequence of the *hyd5* gene did not contain sequences of the intron nor of the fungal signal peptide. The nucleotide sequence was further optimized for the codon usage of the yeast *Saccharomyces cerevisiae* (Stübner et al., 2010; Zapf et al., 2006).

Although the size of FcHyd5p was predicted to be 8.4 kDa, the transgenic protein ran at 12 kDa in SDS-PAGE. This resulted in the assumption of incomplete cleavage of the signal site during production, or protein modification such as acylation or glycoslyation. Nevertheless, FcHyd5p was highly surface active and inverted the hydrophobicity of hydrophobic surfaces. It formed stable foams and aggregates that were dissolvable only in strong denaturating acids (Stübner et al., 2010). FcHyd5p caused gushing in beer, carbonated water, and other carbonated beverages (Lutterschmid et al., 2010; Stübner et al., 2010). The gushing inducing ability was maintained after heating. Boiling in synthetic wort, however, reduced the overfoaming volume. Authors suspected that glycation, occurring during this process, decreased the hydrophobin's surface activity and hence lowered the gushing effect (Lutterschmid et al., 2010).

Mature and secreted FcHyd5p from *F. culmorum,* was found to share 100 % homology with the aa sequence of FgHyd5p from *F. graminearum* (Zapf et al., 2006). Both fungi are mainly responsible for grain infection and FHB outbreaks with *F. graminearum* being the causal agent in warmer and more humid regions and *F. culmorum* being more widespread in cooler and dry areas (Wagacha & Muthomi, 2007). Representing a class 2 hydrophobin produced by major gushing inducing fungi, FcHyd5p provides a highly attractive model for investigations on the mechanisms leading to gushing of carbonated drinks.

1.6 Presumed gushing mechanism

1.6.1 Gushing by hydrophobins

Stable micro bubbles that can act as condensation nuclei for CO_2 diffusion are required to induce gushing. Surface active layer formation around the bubbles by surface active substances was already proposed in 1973 by Gardner, and later connected with hydrophobins by Pellaud (Gardner, 1973; Pellaud, 2002). Hydrophobin proteins have the properties needed as prerequisite for the formation of stable micro bubbles as described previously (see chapter 1.3). They are highly surface active and form a monomolecular film, compression of which leads to increased surface density rather than protein desorption. Optical evidence of this behavior is shown in Figure 5, where the wrinkled appearance of a hydrophobin layer upon pressure application is demonstrated. Thus, hydrophobin layers fulfill the basic assumptions made in the varying permeability model (for review see Pellaud, 2002). Simulation of molecular dynamics of carbon dioxide condensation resulted in evidence for a clustering of

CO_2 molecules at the hydrophobin's hydrophobic patch, thus, supporting the interaction of CO_2 and hydrophobins (Deckers et al., 2012a).

Deckers' group postulated and created a model for bubble stabilization by hydrophobins. They coined the "nano-bombs" for such bubbles which lead to an immediate and fast release of gas. The events which happen according to that theory prior to and during the process of gushing are schematically displayed in Figure 6. Small particles of 5-10 nm in diameter represent hydrophobin coated CO_2 micro bubbles. These develop during yeast fermentation, filling, shaking and the carbonation process. At a critical diameter the hydrophobic/hydrophilic monolayer hydrophobin film becomes impermeable and thus prevents further shrinkage according to the varying permeability model. The resulting micro bubbles were calculated to possess an internal pressure of about 4 bar (Deckers et al., 2010, 2012b). By opening of the bottle, the gas-liquid equilibrium between beer and the atmosphere is abruptly disbalanced. Because of the pressure release, micro bubbles present in the beverage will expand. CO_2 from the surrounding liquid phase diffuses into the bubble leading to uncontrolled bubble growth (Pellaud, 2002). The rapid expansion of micro bubbles will cause the surrounding surface film to disrupt in an explosion like manner. During explosive disruption energy is released locally, which can then break bonds between surrounding CO_2 molecules and water. This immediately forces CO_2 molecules to transit from the water soluble state into the gas phase by free diffusion and formation of bubbles, which rise to the surface in masses resulting in gushing (Deckers et al., 2010).

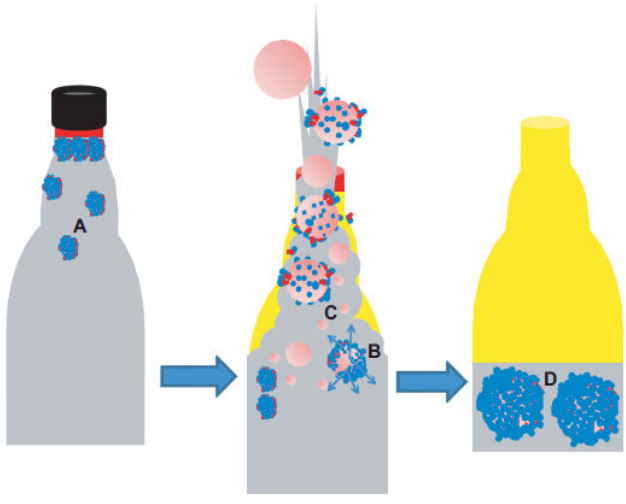

Figure 6: Schematic view on the theoretical evolution of gushing by hydrophobin stabilized nano bubbles according to Deckers et al., 2010. A: closed bottle with hydrophobin coated micro bubbles, diameter determined by internal pressure; B and C: after bottle opening, micro bubbles grow and explode, which results in rapid CO_2 release inducing gushing; D: micro bubbles are formed by the hydrophobin containing micro bubble fragments, diameter determined by the atmospheric pressure.

After degassing of the beer, a fraction of the hydrophobin molecules can still be found in the beer remained in the bottle. They assemble at residual gaseous CO_2, resulting in the formation of new micro bubbles with a critical diameter of 100 nm at atmospheric pressure. These can be detected in gushing beer using the dynamic light scattering (DLS) technology. Recently, Deckers et al. (2011, 2012a, 2012b) proposed the use of this technology as a new method for gushing prediction in beer.

The model also stresses the importance of carbonization in relation to gushing. Not only the amount of hydrophobin, but also the level of carbonization of the beverage determines gushing. This is supported by the observation that increased entry of CO_2 into the liquid by increased shaking of a bottle will result in a more pronounced occurrence of gushing (Christian et al., 2009; Deckers et al., 2013). As a result, most of the tests for prediction of gushing potential used in the brewing industry include more or less intensive shaking during incubation periods.

1.6.2 Reduction of hydrophobin induced gushing by surface active compounds

Already in 1972, Gardener stated that substances with anti-gushing properties, e.g. particular hop compounds such as humolones and fatty acids, should be highly surface active compounds which cannot form a solid surface layer at hydrophobic/hydrophilic interfaces (Gardner, 1972). Surface active substances of beer that have the ability to at least partly suppress gushing are mainly hop compounds but also unsaturated fatty acids (Gardner, 1972, 1973; Gardner et al., 1973; Shokribousjein et al., 2011). The fact that hydrophobin induced gushing can indeed be negatively influenced has recently been demonstrated for hop constituents such as modified iso-α-acids, dry hop oil, and linalool (Lutterschmid et al., 2011, 2010). Another surface active compound of beer, which has been demonstrated to impair hydrophobin induced gushing, is the beer foam protein nsLtp1 (Lutterschmid et al., 2011). It was speculated that due to the surface activity and the inability of formation of a solid surface layer these compounds, fatty acids, hop oil and beer foam proteins, may be able to compete with gushing inducing hydrophobin proteins for adsorption to the hydrophobic/hydrophilic interface (Gardner, 1972; Niessen et al., 2006). Speculation about the mechanism involved went along a line according to which the solidity and strength of the hydrophobin layer is disturbed, leading to destabilization and disappearance of gushing inducing micro bubbles and consequently to reduction of gushing.

1.7 Aim of the study

This dissertation is based on the following thesis: Prevalence of surface active beer proteins in the brewing process and their interaction with hydrophobin proteins are determinant factors in the gushing occurrence of beer.

The aim of the current study was therefore to analyze the prevalence of the gushing inducing protein hydrophobin FcHyd5p and the beer foam protein nsLtp1 in raw materials and beer using immunochemical (ELISA) assays and to investigate their fate during the brewing process. A further aim was to study the mutual influences of reducing and promoting proteins on gushing and on the formation of amphiphilic protein films in emulsions and surface films.

2 Materials and Methods

2.1 Materials

2.1.1 Equipment

The different devices used for experiments in this work are recorded in Table 1.

Table 1: List of equipment used in this work.

Equipment	Type	Manufacturer
agarose gel chamber 13.8 x 12 cm	Easy Cast electrophoresis system	Owl Separation Systems, Portsmouth, NH, USA
atomic force microscope	MFP-3D	Atomic force F+E GmbH, Mannheim, Germany
drop tensiometer	TVT2 Lauda	Lauda, Königshofen, Germany
dynamic light scattering instrument	Zetasizer μV, Model ZMV2000	Malvern instruments, Malvern, UK
dynamic light scattering instrument	ALV instrument CGS-3, compact GonimeterSystem	ALV GmbH, Langen, Germany
electroporation system	GenePulser II	Bio-Rad Laboratories, Hercules, CA, USA
freeze dryer	FreeZone 2.5plus	Labconco, Kansas City, MO, USA
Grinder	DFLU disc mill	Bühler GmbH, Braunschweig, Germany
homogenizer	FastPrep®-24 instrument	MP Biomedicals, Solon OH, USA
MALDI-TOF mass spectrometer	microflex LT	Bruker Daltonics, Bremen, Germany
microtiter plate-reader	FluoStar Omega	BMG Labtech GmbH, Ortenberg, Germany
microtiter plate-reader	Tecan SUNRISE	TECAN Austria GmbH, Grödig, Austria
microtiter plate-reader	Tecan Spectrafluor fluorimeter	TECAN Deutschland GmbH, Crailsheim, Germany
Nanodrop	Nanodrop 1000 spectrophotometer	Peqlab Biotechnologie GmbH, Erlangen, Germany
particle size analyzer	Mastersizer Malvern Hydro 2000 S	Malvern Instruments, Herrenberg, Germany
PCR cycler	Primus 96 plus	MWG Biotech AG, Ebersberg, Germany
PCR cycler	Mastercycler gradient	Eppendorf AG, Hamburg, Germany

Equipment	Type	Manufacturer
pH meter	Knick pH 761 Calimatic	Knick elektronische Geräte, Berlin, Germany
pH-electrode	InLab 412, pH 0-14	Mettler-Toledo, Gießen, Germany
polyacrylamide gel electrophoresis unit	Mini Protean III Cell	Bio-Rad Laboratories, Hercules, CA, USA
protein interaction analyzer, BR-1100-28	BIAcoreX	Biacore AB, Uppsala, Sweden
scanner	Bio-5000, Microtek	Microtek, Hsinchu, Taiwan
semi-dry blotter	HEP-1	peqLab, Erlangen, Germany
spectrophotometer	Novaspellq	Pharmacia Biotech, Cambridge, England
ultrasonic bath	Sonorex Super RK 1034	Bandelin, Berlin, Germany

2.1.2 Chemicals

The sources of the chemicals used during the current work, are listed in Table 2.

Table 2: List of chemicals used in this study.

Chemical	Manufacturer
2-butanol	Carl Roth GmbH & Co. KG, Karlsruhe, Germany
2-propanol	Carl Roth GmbH & Co. KG, Karlsruhe, Germany
BCIP	GERBU Biotechnik GmbH, Gailberg, Germany
ANS	Sigma-Aldrich Chemie GmbH, Schnelldorf, Germany
acetic acid (99 - 100 %, glacial)	Merck, Darmstadt, Germany
acetonitrile (HPLC-grade)	Mallinkrodt Baker B. V., Deventer, The Netherlands
acetylacetone	Merck, KGaA, Darmstadt, Germany
acrylamide (30 %, 37.3)	Bio-Rad Laboratories, Munich, Germany
agar	Difco, BD Sciences, Heidelberg, Germany
agarose	Biozym Scientific GmbH, Oldendorf, Germany
ammonium acetate	Merck, KGaA, Darmstadt, Germany
APS (p.a.)	SERVA, Heidelberg, Germany
ampicillin sodium salt	GERBU Biotechnik GmbH, Gaiberg, Germany
Berol 840	Akzo Nobel Surface Chemistry AB, Stenungsund, Sweden
biotin	GERBU Biotechnik GmbH, Gailberg, Germany
bromphenole blue	SIGMA–Aldrich, Steinheim, Germany
$CaCl_2$ x 2 H_2O (p.a.)	Merck, KGaA, Darmstadt, Germany
CAPS	SIGMA-Aldrich, Steinheim, Germany
CHAPS	SIGMA-Aldrich, Steinheim, Germany
citric acid	SIGMA–Aldrich, Steinheim, Germany

Chemical	Manufacturer
Coomassie-Blue, R350 PhastGel™ Blue R	Amersham Pharmacia Biotech AB, Uppsala, Sweden
diethanolamine (p.a.)	Merck, KGaA, Darmstadt, Germany
DL-lactic acid (Ph. Eur.)	Merck, KGaA, Darmstadt, Germany
DL-malic acid	FLUKA, Steinheim, Germany
DMSO	Carl Roth GmbH & Co. KG, Karlsruhe, Germany
D-sorbit	Carl Roth GmbH & Co. KG, Karlsruhe, Germany
DTT	GERBU Biotechnik GmbH, Gaiberg, Germany
EDC	Sigma-Aldrich Chemie GmbH, Schnelldorf, Germany
EDTA	GERBU Biotechnik GmbH, Gaiberg, Germany
ethanol, absolute	VWR, Prolabo, Foutenay-sous-Bois, France
ethanolamide hydrochloride	Sigma-Aldrich Chemie GmbH, Steinheim, Germany
Fast-AP	Thermo Fisher Scientific Biosciences GmbH, St. Leon-Rot, Germany
FD restriction buffer	Thermo Fisher Scientific Biosciences GmbH, St. Leon-Rot, Germany
FD restriction enzymes	Thermo Fisher Scientific Biosciences GmbH, St. Leon-Rot, Germany
formic acid (p.a.)	Merck, KGaA, Darmstadt, Germany
fructose (for microbiology)	Merck, KGaA, Darmstadt, Germany
glucose monohydrate	Merck, KGaA, Darmstadt, Germany
glycerol (87 %, p.a.)	GERBU Biotechnik GmbH, Gaiberg, Germany
glycine (p.a.)	Merck, KGaA, Darmstadt, Germany
HCl (Ph. Eur.)	Merck, KGaA, Darmstadt, Germany
HEPES	GERBU Biotechnik GmbH, Gaiberg, Germany
KCl	Carl Roth GmbH & Co. KG, Karlsruhe, Germany
KH_2PO_4	Carl Roth GmbH & Co. KG, Karlsruhe, Germany
maltodextrin	SIGMA-Aldrich, Steinheim, Germany
maltose monohydrate	GERBU Biotechnik GmbH, Gaiberg, Germany
methanol (HPLC-grade)	Mallinkrodt Baker B. V., Deventer, The Netherlands
$MgCl_2$ x 6 H_2O	FLUKA, Steinheim, Germany
$MnCl_2$ (p.a.)	Merck, Darmstadt, Germany
MOPS (ultra pure)	GERBU Biotechnik GmbH, Gaiberg, Germany
Na_2CO_3	Carl Roth GmbH & Co. KG, Karlsruhe, Germany
Na_2HPO_4 x 2 H_2O	Merck, KGaA, Darmstadt, Germany
NaCl	Carl Roth GmbH & Co. KG, Karlsruhe, Germany
NaH_2PO_4	Carl Roth GmbH & Co. KG, Karlsruhe, Germany
$NaHCO_3$	GERBU Biotechnik GmbH, Gaiberg, Germany
$NaIO_4$	Merck, KGaA, Darmstadt, Germany
NaOH	Merck, KGaA, Darmstadt, Germany
NHS	Sigma-Aldrich Chemie GmbH, Schnelldorf, Germany
NBT (analytical grade)	GERBU Biotechnik GmbH, Gaiberg, Germany

Chemical	Manufacturer
o-phosphoric acid (85 %, p.a.)	Carl Roth GmbH & Co. KG, Karlsruhe, Germany
peptone of casein	Merck, KGaA, Darmstadt, Germany
PNPP	GERBU Biotechnik GmbH, Gaiberg, Germany
Proteinase K	Omega Bio-Tek, Norcross, GA, USA
pyruvic acid (p.a.)	FLUKA, Steinheim, Germany
RbCl	Merck, KGaA, Darmstadt, Germany
Roti®-Blue, 5 x concentrated, colloidal CBB G-250	Carl Roth GmbH & Co. KG, Karlsruhe, Germany
saccharose (p.a)	SIGMA-Aldrich, Steinheim, Germany
sodium acetate	Merck, KGaA, Darmstadt, Germany
sodium citrate x 2 H_2O	Carl Roth GmbH & Co. KG, Karlsruhe, Germany
SDS (research grade)	Serva, Heidelberg, Germany
T4 DNA ligase	Thermo Fisher Scientific Biosciences GmbH, St. Leon-Rot, Germany
TEMED (p.a.)	Merck, KGaA, Darmstadt, Germany
Tricine (ultra pure)	GERBU Biotechnik GmbH, Heidelberg, Germany
Tris HCl (p.a.)	GERBU Biotechnik GmbH, Gaiberg, Germany
Tris-Base (ultra pure)	MP Biomedicals, Solon, OH, USA
trypsin	SIGMA-Aldrich, Steinheim, Germany
Tween20	GERBU Biotechnik GmbH, Gaiberg, Germany
urea	GERBU Biotechnik GmbH, Gaiberg, Germany
yeast extract	Carl Roth GmbH & Co. KG, Karlsruhe, Germany
YNB, Difco™	Becton, Dickinson and Company, Sparks, MB, USA
Zeocin™	InvivoGen, San Diego, CA, USA

2.1.3 Consumables

Other materials used in this work are shown in Table 3.

Table 3: Overview of consumables used in this study.

Material	Type	Manufacturer
AFM discs	specimen disc, 15 mm dia	TED Pella Inc, Redding, CA, USA
AFM glass cover slide	glass cover slip, round 15 mm dia	TED Pella Inc, Redding, CA, USA
AFM tip	silicon-SPM-sensor, point probe-plus, PPP-NCHR-50	Nanosensor, Neuchtal, Switzerland
cuvettes	UV transparent disposable cuvettes	Sarstedt, Nümbrecht, Germany
dialysis tube	molecular weight cut off 3500 Da	Serva Electrophoresis GmbH, Heidelberg, Germany
DNA purification kit	MasterPure Yeast DNA Purification Kit™	Epicentre, Biotechnologies, Madison, WI, USA

Material	Type	Manufacturer
EasySelect™ Pichia Expression Kit		Invitrogen, Paisley, UK
electroporation cuvettes		Biozym scientific GmbH, Oldendorf, Germany
gel extraction kit	PeqGold gel extraction kit	PEQLAB Biotechnologie GMBH, Erlangen, Germany
microscopy glass slides		Marienfeld, Lauda-Königshofen, Germany
microtiter plates	96-well plate, transparent, flat bottom, with lid	Sarstedt, Nümbrecht, Germany
microtiter plates	96-well FIA-plate, black, flat bottom	Greiner Bio-One GmbH, Frickenhausen, Germany
microtiter plates	Immnuo Module F8 x 12, PS, 96 wells, MaxiSorp, transparent	Thermo Fisher Scientific Nunc A/S, Roskilde, Denmark
nitrocellulose membrane	Hybond™ ECL™ nitrocellulose	Amersham pharmacia biotech, AB, Uppsala, Sweden
NMR sample tubes	thin walled	VWR, international
Parafilm®		Pechiney Plastic Packing, Menasha, WI, USA
plasmid extraction kit	peqGOLD plasmid miniprep kit	PEQLAB Biotechnologie GMBH, Erlangen, Germany
protein ladder	PageRuler™ prestained protein ladder	Thermo Fisher Scientific Biosciences GmbH, St. Leon-Rot, Germany
protein ladder	PageRuler™ plus prestained protein ladder	Thermo Fisher Scientific Biosciences GmbH, St. Leon-Rot, Germany
rapid-flow bottle top filter	0.2 µm PES membrane	Thermo Fisher Scientific Biosciences GmbH, St. Leon-Rot, Germany
reaction tubes	2 mL, 1.5 mL, 200 µL	Eppendorf, Hamburg, Germany
sensor Chip CM5		GE Healthcare Bio-Science AB, Uppsala, Sweden
sterile ml tubes	5 ml, 15 ml, 50 ml	Sarstedt, Nümbrecht, Germany
Taq Core Kit		MP Biomedicals Solon, OH, USA

2.1.4 Organisms

Escherichia coli strains were used for the preparation and construction of plasmids in order to perform cloning of the *Paz1* gene into yeast cells. Genetically modified *Pichia pastoris* strains were used for the heterologous protein production of hydrophobins FcHyd5p, Hfb2, FcHyd3p and barley proteins nsLtp1 and protein Z4. Strains are listed in Table 4.

Table 4: List of microorganisms used in this work.

Organism	TMW number	Reference/Supplier
Escherichia coli TOP 10	2.580	Invitrogen, Carslbad, USA
Escherichia coli TOP 10 / pPICZαA_Z4	2.1180	this work
Escherichia coli TOP 10 / pMA-T_Z4	2.1181	this work
Pichia pastoris X33	3.177	EasySelect™ Pichia Kit, Invitrogen, Paisley, UK
Pichia pastoris X33 [pPICZαA _Z4]	3.383	this work
Pichia pastoris X33 [pPICZαA _FcHyd5p]	3.213	Stübner et al., 2010
Pichia pastoris X33 [pPICZαA _Hfb2]	3.219	Lutterschmid et al., 2011
Pichia pastoris X33 [pPICZαA _FcHyd3p]	3.218	Lutterschmid et al., 2011
Pichia pastoris X33 [pPICZαA _nsLtp1]	3.214	Lutterschmid et al., 2011

2.1.5 Oligonucleotides and plasmids

Oligonucleotides used for amplification of DNA sequences by PCR are given in Table 5. Primer pair AOX1-r/AOX1-f resulted in an amplificate covering parts of the promoter sequence and the complete AOX gene of methylotrophic yeast cells. These oligonucleotides served for the validation of genes inserted into the cloning vector pPICZαA, or to check for the cross over event of these plasmids into *P. pastoris* transformants. Amplification of the modified *Paz1* gene from plasmid pMA-T_Z4 was achieved by oligonucleotides for_Z4_EcoR1 and rev_Z4_Age1.

Table 5: Sequences of oligonucleotides used in this work. Restriction sites are marked in bold.

Primer	Sequence	Supplier
AOX1-r	5′-GCA AAT GGC ATT CTG ACA TCC-3′	Eurofins, Ebersberg, Germany
AOX1-f	5′-GAC TGG TTC CAA TTG ACA AGC-3′	Eurofins, Ebersberg, Germany
for_Z4_EcoR1	5′-C**GA ATT C**AT GGC TAC TAC TTT GGC-3′	Eurofins, Ebersberg, Germany
rev_Z4_Age1	5′-G**AC CGG T**TT AAG CGG AGA TCA ATG-3′	Eurofins, Ebersberg, Germany

Vector pMA-T_Z4, which contained the modified form of the protein Z4 encoding *Paz1* gene, was acquired for reproducing and storage of the corresponding gene sequence. Vector pPICZαA was used for cloning of the *Paz1* gene, resulting in the plasmid pPICZαA_Z4. All plasmids are given in Table 6.

Table 6: Plasmids and their corresponding selection markers used in this work.

Plasmid	Selection marker	Reference/Supplier
pPICZαA	Zeocin™ resistance	EasySelect™ Pichia Kit, Invitrogen, Paisley, UK
pMA-T_Z4	ampicillin resistance	Geneart, Regensburg, Germany
pPICZαA_Z4	Zeocin™ resistance	this work

2.1.6 Antibodies

The antibodies that were used in Western blot analysis and for ELISA experiments in this study are listed in Table 7.

Table 7: Antibodies used in this study. Given protein positions (pos.) refer to protein sequence without signal peptide.

Plasmid	Description	Supplier
goat-anti-rabbit-IgG-AP	anti-rabbit IgG (whole molecule) F(ab')2 fragment - alkaline phosphatase antibody produced in goat	Sigma Aldrich, Saint Louis, MO, USA
anti-FcHyd5p-P2-IgG	polyclonal rabbit antibody directed against a peptide of FcHyd5p (pos. 1-22)	ImmnuoK, Amsbio, AMS Biotechnology, Oxfordshire, UK
anti-FcHyd5p-P3-IgG	polyclonal rabbit antibody directed against a peptide of FcHyd5p (pos. 62-81)	
anti-nsLtp1-P2-IgG	polyclonal rabbit antibody directed against a peptide of nsLtp1 (pos. 71-86)	

2.2 Bioinformatical methods

Software programs used during this work are listed in Table 8.

Table 8: Software programs used in this work and their corresponding application.

Program	Application	Reference	Web link
AfterALV	analysis of MultiAngle dynamic light scattering results		www.dullware.nl/products/afteralv/afteralv.htm
Bioedit	alignment of DNA or proteins	Hall, 1999	
clustalW	alignment of DNA or proteins	Goujon et al., 2010	www.ebi.ac.uk/Tools/msa/clustalw2/
Gwyddion 2.31	SPM data visualization and analysis of height field and image analysis (AFM)	Nečas & Klapetek, 2012	http://gwyddion.net
Image J 1.46	image processing and analysis	Rasband, W.S. (U. S. National Institutes of Health & Maryland)	http://imagej.nih.gov/ij/
ProtScale	computing profiles produced by amino acid scales, used for protein's hydrophobicity plot (Kyte & Doolittle, 1982)	Gasteiger et al., 2005	http://web.expasy.org/protscale/
SignalP 4.0	prediction of signal cleavage sites in amino acid sequences	Petersen et al., 2011	www.cbs.dtu.dk/services/SignalP-4.0/
SigmaPlot 8.0	significance testing, creation of diagrams	SPSS Inc., Chicago, IL, USA	
Yaspin	prediction of protein secondary structure	Lin et al., 2005	www.ibi.vu.nl/programs/yaspinwww/

2.3 Microbiological methods

2.3.1 Media and growth conditions

2.3.1.1 LB medium

Composition of LB medium is shown in Table 9. LB medium was used for the cultivation of *E. coli* cells. Low salt medium had to be used when cells were selected by the antibiotic Zeocin™. Cultivation was performed at 37 °C, for liquid cultures under shaking at 180 rpm.

Table 9: Composition of media LB and low salt LB used for cultivation of *E. coli* cells.

Ingredients	Amount [g/L]
LB	
peptone of casein	10
yeast extract	5
NaCl	10
low salt LB, pH 6.5	
peptone of casein	10
yeast extract	5
NaCl	5

In low salt LB medium the pH had to be adjusted to pH 6.5 by addition of NaOH. For preparation of agar plates, 15 g/L agar was added.

Media were sterilized by autoclaving at 121 °C for 20 min. If the medium was used for selection of *E. coli* clones or for cultivation of *E. coli* strains containing plasmids encoding a Zeocin™ resistance gene, antibiotic Zeocin™ was added in low salt LB medium to result in a concentration of 25 µg/mL. Ampicillin was used in a concentration of 100 µg/mL.

2.3.1.2 YPD and YPDS medium

For cultivation of *P. pastoris* strains prior to cryo-conservation or DNA isolation, YPD medium (yeast extract peptone dextrose medium) was used. YDPS agar plates containing 100 µg/mL Zeocin™ served for growth and selection of clones after electro-transformation. Cells were cultivated at 30 °C, with shaking at 180 rpm when cultured in liquid medium. Composition of media is given in Table 10.

Table 10: Composition of media YPD and YPDS used for cultivation of yeast cells.

Ingredients	Amount [g/L]
peptone of casein	20
yeast extract	10
Glucose	20
sorbitol (only in YPDS)	182.2

For medium preparation peptone, yeast extract, and sorbitol (only for YPDS) were dissolved in 800 mL deionized water. Glucose was weighed separately and dissolved in 200 mL deionized water. The solutions were separately autoclaved for 20 min at 121 °C. For preparation of agar plates, 20 g agar/L medium were added.

2.3.1.3 BMGY and BMMH medium

BMGY medium (buffered glycerol-complex medium) and BMMH medium (buffered minimal methanol medium) were used for cultivation of transgenic *P. pastoris* strains for heterologous protein production. Pre-culturing of yeast clones was done in BMGY (Table 11). Cells were then transferred into BMMH medium, which contained methanol as an inducer for heterologous gene expression (Table 12). Cultivation took place under vigorous shaking at 30 °C.

Table 11: Composition of BMGY medium used for yeast pre-culturing.

Ingredients	Amount per L
peptone of casein	20 g
yeast extract	10 g
YNB	13.4 g
1 M potassium phosphate buffer, pH 6.0	100 mL
biotin (500 x 4 x 10^{-5} %)	2 mL
glycerol	12.8 g

For preparation of BMGY, peptone and yeast extract were dissolved in 700 mL deionized water followed by autoclaving for 20 min at 121 °C. YNB, dissolved in 100 mL deionized water, was mixed with 100 mL potassium phosphate buffer, biotin and glycerol in 100 mL deionized water and mixed into the residual medium after sterile filtration.

Table 12: Composition of BMMH medium used for cultivation of *P. pastoris* cells in order to produce transgenic protein.

Ingredients	Amount per L
YNB	13.4 g
1 M potassium phosphate buffer, pH 6.0	100 mL
biotin (500 x 4 x 10^{-5} %)	2 mL
methanol	5 mL

In order to prepare BMMH medium, YNB was dissolved in 195 mL deionized water and mixed with 100 mL potassium phosphate buffer, biotin and methanol. The solution was added to sterile deionized water (121 °C, 20 min) under sterile filtration. The medium was freshly prepared for each cultivation.

2.3.1.4 Synthetic wort

Synthetic wort was prepared as described by Zapf (2006). According to Zapf it contains the wort characteristic concentrations of sugars and organic acids, which were orientated on

values given by Narziß and MEBAK III, respectively (Narziß, 1995; *MEBAK*, 1996, S. 87-88). Only maltotriose was omitted from the preparation. In Table 13 the ingredients of the two components are listed. Sugar component was set up as a 5 fold concentrated stock solution. The organic acidic components were prepared as a 10 fold concentrated stock solution in order to enable proper weighing of the ingredients.

Table 13: Composition of sugar and acid component of synthetic wort

Ingredients	Amount [g/100 mL]
sugar component, 5 x	
glucose monohydrate	11.5
Fructose	3.0
Saccharose	3.0
maltose monohydrate	50.0
Maltodextrin	10.0
acid component, 10 x	
DL-malic acid	0.075
pyruvic acid	0.075
citric acid	0.2
acetic acid	0.1
DL-lactic acid	0.26
formic acid	0.02

Ingredients for both components were dissolved separately in 100 mL deionized water and sterilized by autoclaving (121 °C, 20 min). Immediately before use the components 5 fold sugar, 10 fold acid and deionized water were mixed 2:1:7 (sugar component : acid component : water; v/v) to result in a solution containing 1 fold sugar and 1 fold acid component. Synthetic wort prepared in this way had a pH value of 3.0. For pH adjustment, 3 M NaOH was added to a part of the synthetic wort, which was then mixed to the original wort until the desired pH was reached.

2.3.2 Production of chemically competent *E. coli* and transformation conditions

Chemically competent *E. coli* TOP10 cells were prepared using the rubidium chloride method. The solutions used are given in Table 14. pH values of the media were adjusted with acetic acid for RF1 and with NaOH for RF2 medium. Both media were sterile filtered over 0.2 µm filters before use. The TOP10 *E. coli* strain was cultivated at 37 °C in 100 mL LB

medium until a OD_{600} of 0.3-0.5 was reached. Cells were pelleted by centrifugation at 4 °C for 15 min at 5,000 x g. Cells were resuspended in 30 mL of ice-cooled RF1 medium and incubated on ice for 15 min. Following a second centrifugation step the pellet was resuspended in 4 mL RF2 medium. Competent cells were aliquoted in 200 µL portions in 1.5 mL tubes and frozen at -80 °C until used.

Table 14: Composition of media RF1 and RF2 used for production of chemically competent *E. coli* cells.

Ingredients	Amount per L
RF1-medium, pH 5.8	
RbCl	12 g
$MnCl_2$	9.9 g
$CaCl_2$ x 2 H_2O	1.5 g
potassium acetate	2.9 g
glycerol (87 %)	121 mL
RF2-medium, pH 6.8	
MOPS	2.1 g
RbCl	1.2 g
$CaCl_2$ x 2 H_2O	11 g
glycerol (87 %)	121 mL

Prior to performance of transformations the competent cells were thawed at room temperature. After 5 min of incubation on ice, 0.1 µg of to transformed DNA was added and the mixture was incubated on ice for 20 min. Heat shock was performed at 42 °C for 90 s. Following the heat shock, tubes were directly put on ice for 2 min. 1 mL of LB medium was added to the cells, which were then allowed to grow under shaking conditions at 37 °C for 1 h. 100 µL of the cell suspension was then plated on LB plates containing antibiotics for selection.

2.3.3 Production of electrocompetent *P. pastoris* and transformation conditions

The preparation of electrocompetent *P. pastoris* cells followed the protocol provided with the EasySelect™ Pichia Expression Kit (Invitrogen, Paisley, UK). An overnight culture of wild type *P. pastoris* strain X33 was harvested after a DO_{600} of 1.3-1.5 was reached. The cells were washed twice in pre-chilled sterile deionized water and once in 2 mL of 1 M cooled sterile sorbitol. Competent cells were then resuspended in 100 µL chilled 1 M sterile sorbitol.

For transformation, plasmid-DNA was linearized by restriction with restriction endonuclease *Sac1*. After restriction at 37 °C for 25 min the DNA was precipitated with 10 % sodium acetate (3 M) and 250 % ethanol at -20 °C overnight. Precipitated DNA was washed in 70 % ethanol and suspended in 15 µL water. 80 µL of competent cells and the whole DNA sample were mixed in a pre-chilled electroporation cuvette. A 5 min incubation on ice was followed by electro-transformation using a GenePulser II Electroporation System with conditions set to 1.5 kV, 200 Ω and 25 µF. 1 mL of cold 1 M sterile sorbitol was instantly added to the mixture and cells were incubated for 1-2 h at 30 °C. Cells were plated in different concentrations on YPDS agar plates containing the required antibiotic for selection.

2.4 Molecular biological methods

2.4.1 Sequence analysis and bioinformatics

Plasmids constructed for expression or multiplication in *E. coli* and genomic DNA of all *P. pastoris* clones produced during the study were checked for correct insertion and sequence identity of the inserted DNA by nucleotide sequence analysis. Plasmids were isolated from overnight cultures of *E. coli* strains using the peqGOLD plasmid miniprep kit. For constructs transformed into *P. pastoris* cells, genomic DNA of the clones was isolated using the MasterPure™ Yeast DNA Purification Kit. The transformed DNA region was checked by amplifying the insert with the primer pair AOX1-f and AOX1-r. After electrophoresis, the DNA fragments were purified from agarose gels. The purity and concentration of DNA samples was checked photometrically by measurements in a Nanodrop spectrophotometer against deionized water. The recommended DNA concentration of 10-30 ng/µL for plasmids and 10-50 ng/µl for PCR products was adjusted. 30 µL DNA and 30 µL of the corresponding primer (10 pmol/µL) were sent to GATC biotech (Konstanz, Germany) to perform single read DNA sequencing. The software packages BioEdit sequences alignment editor and clustalW were used for evaluation of the sequences.

2.4.2 Nanodrop analysis

Concentration and purity of isolated plasmids from *E. coli* strains or of purified genomic DNA of *P. pastoris* clones, as well as DNA concentration of PCR products, was determined by Nanodrop analysis. 1 µL of test solution was applied to a Nanodrop spectrophotometer

and absorbance was measured at 260 nm in comparison to a blank value obtained with deionized water, resulting in value output of DNA concentration in ng/µL. In parallel the ratio of absorbance at 260/280 nm was calculated. Values of 1.8 or above represent highly pure DNA without protein or other contaminants.

2.4.3 Agarose gel electrophoresis

DNA fragments amplified by PCR were separated in 1 % agarose gels by electrophoresis. Gels were prepared by adding 1 % (v/w) agarose to 1 x TAE buffer (stored as 50 x TAE buffer: 2.0 M Tris, 1.0 M acetic acid, 0.1 M EDTA, pH 8.2). Melting agarose was achieved by boiling in a micro wave oven. After cooling to about 60 °C, the agarose solution was used for gel casting. Solidified gels were placed into the electrophoresis chamber, which was filled with 1 x TAE buffer covering the gel. DNA was applied to the gel after mixing in a 5:1 (v/v) ratio with gel loading dye (5 x 0.25 % bromphenole blue, 40 % saccharose) to achieve sinking of the sample into the pockets of the gel. In each run a DNA size marker standard was run in parallel for evaluation of DNA fragment size. Separation of DNA was performed at about 9 V/cm for 1-1.5 h. The run was stopped when the bromphenole blue front passed 2/3 of the gel length. For visualization, gels were incubated in a dimidium bromide bath for 20 min. Gels were documented in an UV chamber at 320 nm using a video camera in combination with Intas® GDS equipment and software. If DNA of the band was needed for further experiments, bands were cut off and DNA extraction was performed using the peqGOLD gel extraction kit according to the manufacturer's protocol.

2.4.4 Cloning of the protein Z4 encoding *Paz1* gene

Sequence of the protein Z4 encoding gene *Paz1* of *H. vulgare* provided by Brandt et al. (1990) was available under GenBank accession number X51726.1. An artificial gene based on nucleotides 10 to 1212 of the mRNA sequence of protein Z4 (GenBank: X97636) was synthesized by Geneart. Thereby an optimization of the nucleotide sequence according to the codon usage of *P. pastoris* was carried out without resulting in changes in the primary structure of the corresponding protein. A plasmid (pMA-T_Z4) was provided containing the optimized gene as insert. After replication in *E. coli* cells, the artificial gene was amplified by PCR from the resulting vector by using primers for_Z4_EcoR1 and rev_Z4_Age1. Amplification with *Taq* DNA polymerase was carried out for 35 cycles with an annealing temperature of 56 °C according to the following scheme:

[95 °C, 4 min – (95 °C, 1 min – 56 °C, 1 min – 72 °C, 7 min) x 35 – 72 °C, 7 min]

The resulting fragment with a length of 1214 bp had *EcoR1* and *Age1* restriction sites added with the primers at the 5' and 3' ends, respectively. The fragment was purified from the agarose gel by using a gel extraction kit. Extraction was followed by digestion of the PCR product with endonucleases *EcoR1* and *Age1*. After digestion, the construct was ligated into plasmid pPICZαA with the help of T4 DNA Ligase according to manufacturer's protocol. By this cloning procedure the insert containing *Paz1* gene fragment was positioned between the methanol inducible AOX1 promoter of *P. pastoris* (5′-end) and the *S. cerevisiae* α factor for protein secretion (3'-end). Both these sequences were present in the unmodified pPICZαA vector. In addition, pPICZαA contains the *sh-ble* gene, conferring resistance against Zeocin™ as selective marker and a replication site for *E. coli.* The resulting vector pPICZαA_Z4 was transformed in *E. coli* TOP10 and transformants were selected against Zeocin™.

After plasmid isolation with a plasmid miniprep kit, the purified vector pPICZαA_Z4 was transformed into *P. pastoris* X33 cells as described in 2.3.3. By a single crossover event, the vector and the contained *Paz1* gene integrated at the 5'AOX1 locus into the genome of *P. pastoris*. Several transformants were selected on Zeocin™ containing media and further cultured. Transformants were checked for containing the insert using genomic DNA extracted from clones (see 2.4.5) as template and amplification of the integrated construct using primers AOX1-f and AOX1-r. The resulting amplification products were checked for size and DNA was sequenced (see 2.4.1) for verification of integrity and correct integration of the cloned gene into the genome of the *P. pastoris* clones. One of the confirmed clones of *P. pastoris* X33 [pPICZαA_Z4] was prepared for cryo-preservation in glycerol and stored at -80 °C under collection no. TMW 3.383 in the culture collection of Lehrstuhl für Technische Mikrobiologie.

2.4.5 Extraction of genomic DNA from *P. pastoris* clones

Genomic DNA of *P. pastoris* clones was extracted with the Master Pure™ yeast DNA extraction kit, following the manufacturer's protocol. 1 mL of a culture of the respective *Pichia* strain grown overnight in YPD liquid medium was pelleted by centrifugation (2-5 min, ambient temperature, 12,300 x g). Cells were suspended in 300 µL yeast cell lysis solution. After 15 min of incubation at 65 °C, samples were set on ice for 5 min. 150 µL of MPC precipitation agent were added and the formed precipitate removed by centrifugation

(10 min, ambient temperature, 12,300 x g). The DNA was precipitated from the supernatant by addition of 500 µL 2-propanol and pelleted by centrifugation (10 min, ambient temperature, 12,300 x g). The DNA-containing pellet was washed with 500 µL 70 % ethanol (v/v) and suspended in 35 µL sterile deionized water after air drying. DNA was stored at 4 °C until further analysis.

2.5 Protein chemical methods

2.5.1 Expression and preparation of recombinant protein Z4

Paz1 gene encoding protein Z4 was inserted behind the AOX1 promoter, which is methanol dependent. For verification of transgenic protein expression by the transformant strain *P. pastoris* X33 [pPICZαA_Z4], clones were cultivated in BMMH medium under inducing conditions by addition of methanol (see 2.5.10). Expressed heterologous protein was expected to be in the medium because of the presence of an α factor secretion signal sequence as part of the primary transcript. After removal of cells the BMMH medium was dialyzed and freeze dried. Lyophilisate of purified recombinant proteins was then analyzed by SDS-PAGE. Amino acid sequence identity of the protein Z4, produced by clone *P. pastoris* X33 [pPICZαA_Z4] with the original sequence of the barley protein Z4 (accession no. CAA36015) was verified by peptide mass fingerprint analysis of the excised protein band at a size of about 45 kDa (Protein analysis unit, Ludwigs-Maximilians-Universität München, Munich, Germany).

2.5.2 SDS-PAGE

To detect heterologously produced proteins, SDS-PAGE was carried out according to the protocol described by Schägger & von Jagow (1987). 16 % Tris-Tricine gels were used to ensure proper separation of proteins in the low molecular weight range. Compositions of solutions for preparation and running of the gels are listed in Table 15. SDS-PAGE was carried out in a Mini Protean III cell with gels of 0.75 mm thickness. Glass plates were cleaned with ethanol prior to casting the gel. APS and TEMED were added to the separating and stacking gel solution immediately before gel pouring. The surface of the separating gel was covered with 2-propanol to prevent surface irregularities. After solidification of the separating gel alcohol was removed and a 4 % stacking gel was poured on top of the

separating gel. Gels were either used directly or wrapped in wet tissue and aluminum foil for storage at 4 °C.

For running gels, protein samples were mixed in a 1:1 (v/v) ratio with incubation buffer in a maximum volume of 20 µL and loaded onto 16 % Tris-Tricine gels. Prior to loading samples were heated in incubation buffer to 75 °C for 10 min. When lyophilisate contained hydrophobin it was first dissolved in CHAPS/SDS buffer (Table 16) and mixed for 15 min to enable dissolving and to prevent protein aggregation. Gels were run using cathode and anode buffers as running buffers (Table 15). Proteins were separated at a constant voltage of 120 V until the running front nearly reached the end of the gel.

Table 15: Composition of 16 %-Tris-Tricine gels and running buffer for SDS-PAGE.

Ingredients	Amount
gel buffer	250 mL
Tris	90.86 g
HCl	until pH 8.45
separating gel (16 %)	
acrylamide, 30 %, 37.3:1	5.30 mL
gel buffer	3.33 mL
deionized water	1.26 mL
SDS-solution, 25 %	40 µL
TEMED	7 µL
APS, 10 %	5 µL
running buffer for cathode, 5x	1 L
Tris	60.57 g
Tricine	89.58 g
SDS-solution, 25 %	20 mL
running buffer for anode, 5x	1 L
Tris	121.14 g
HCl	until pH 8.9
incubation buffer	10 mL
Tris-HCl, 1 M, pH 6.8	1.0 mL
SDS	0.8 g
glycerol	3.0 g
DTT	0.31 g
TCEP	20 mg
bromphenole blue	1.0 mg

For preparation of CHAPS buffer, urea and thiocarbamide were dissolved in deionized water and filled to 50 mL. After filtration of CHAPS, DTT and pharmalyte were added to 48 mL of the filtrate. The ingredients for SDS buffer were dissolved in water and adjusted to pH 8.6 with HCl. After aliquotation, SDS and CHAPS buffers were stored separately at -20 °C. Aliquots of both buffers were thawed immediately before usage and mixed in a 5:2 = CHAPS:SDS (v/v) ratio

Table 16: Composition of SDS buffer and CHAPS buffer for sample preparation prior to SDS-PAGE.

Ingredients	Amount (g/50 mL)
CHAPS buffer	
urea	21.0
thiocarbamide	7.1
CHAPS	2.0
DTT	0.5
Pharmalyte 3-10, 0.5 %	0.75
SDS buffer, pH 8.6	
DTT	0.5
Tris-base	0.72

2.5.3 Colloidal Coomassie Blue staining of polyacrylamide gels

Following gel runs, gels were rinsed in deionized water and then treated according to the different staining methods applied.

For colloid Coomassie Blue staining, fixation and staining was achieved by incubating the gels in staining solution (25 % 2-propanol (v/v), 10 % acetic acid (v/v), 0.05 % PhatGel™BlueR (w/v)) overnight at room temperature. After destaining with 10 % acetic acid (v/v) for about 1 h, gels were rinsed in deionized water and documented by scanning data into an electronic file.

As an alternative Coomassie staining procedure Roti®-Blue concentrate was used, following the manufacturer's protocol. In this protocol fixation and staining is combined in one step by the presence of phosphoric acid in the staining solution. Gels were incubated in staining solution (5 % Roti®-blue concentrate (5 x) (v/v), 5 % methanol (v/v), 1 % o-phosphoric acid (85 %) (v/v)) at room temperature for about 16 h. To obtain higher resolution of stained protein bands, the gel was destained with methanol solution (5 % methanol (v/v), 1 % o-phosphoric acid (85 %) (v/v)) by shaking it 1-3 times for about 1 min, followed by stopping of the destaining with deionized water.

2.5.4 Western blot analysis

To detect proteins by specific antibodies and to test the sensitivity of the antibodies applied against FcHyd5p and nsLtp1, respectively, a semi-dry Western blot was carried out. Buffer solutions used during blotting procedures are listed in Table 17. Following separation by SDS-PAGE, proteins were blotted onto nitrocellulose membrane in blotting buffer. Blotting was performed for 1.5 h in a semi dry-blotter at 35 V and 50 mA, corresponding to 0.8-1 mA/cm^2. For the specific analysis of Western blots, membrane was blocked with 3 % BSA in blocking buffer overnight at 4 °C followed by incubation with the specific antibody (1:2,000 (v/v)) in TBS buffer for 1.5 h at 37 °C. After washing with buffers TBS and TBS-T, the membrane was rinsed in TBS containing the secondary "antibody goat-anti-rabbit-IgG-AP", which is coupled to alkaline phosphatase (1:5,000 in TBS (v/v)). The 1.5 h of incubation at 37 °C was followed by repeated washing of the membrane after which the enzyme reaction for detection of bound antibody was started. For detection the membrane was incubated in developer solution containing NBT (50 mg/mL in 70 % DMSO) and BCIP (50 mg/mL in 100 % DMSO). The color reaction was stopped by addition of EDTA. Blots were documented with a hand held digital camera.

Table 17: Composition of buffers used in Western blot analysis.

Ingredients	Amount per L
blotting buffer, pH 11.0	
CAPS	2.21 g
Methanol	100 mL
TBS buffer, TBS-T buffer, pH 7.5	
Tris-base	2.42 g
NaCl	2.29 g
Tween20 (only in TBS-T buffer)	0.5 mL
blocking buffer, pH 7.5	
Tris-base	2.42 g
NaCl	8.76 g

For buffer preparation the ingredients were weighed and dissolved in 900 mL distilled water. After adjusting the pH with NaOH for blotting buffer and HCl for TBS and TBS-T buffer, respectively, each buffer was filled to 1,000 mL with deionized water.

2.5.5 Ponceau S red staining of Western blots

Successful transfer of proteins from SDS-gels onto nitrocellulose membranes by semi-dry blotting was checked by staining membranes with Ponceau S. This azo dye binds unselectively to positively charged amino groups of proteins. Directly after blotting, the membrane was incubated in Ponceau S solution (Table 18) for 2-3 min. The staining was stopped with deionized water followed by documentation of the membrane with a hand held digital camera. Destaining was achieved by washing in deionized water. Membranes could further be used for specific detection of proteins as described in 2.5.4.

Table 18: Composition of 10 x solution for Ponceau S protein staining of Western blot membranes.

Ingredients	Amount per L
Ponceau S red	2.5 g
Methanol	400 mL
glacial acetic acid	150 mL

2.5.6 Protein quantification by using Bradford assay

For protein quantification the method according to Bradford (1976) was performed by using the Bio-Rad Protein assay. 20 µL of the protein sample were added to a 1.5 mL tube. The corresponding buffer without protein was used as a blank sample. The 5 x Bio-Rad color reagent was diluted 1:5 (v/v) with deionized water and 1 mL was added to each sample. After mixing and incubation for 5 to 60 min at room temperature the absorption at 595 nm was measured in a photometer. For quantification a standard curve with BSA in a range of 0 mg/mL to 1.5 mg/mL in the corresponding buffer was analyzed along with the samples.

2.5.7 Heat stability testing of proteins

To test the heat stability of transgenic protein Z4, freeze dried preparations of the protein were dissolved in deionized water to result in a concentration of 16 mg/mL. 100 µL of the solution were incubated at different temperatures of 70 °C, 90 °C and 100 °C for 1 h. A control without heat treatment was left at ambient temperature. 25 µL from each of the treated samples were subjected to SDS-PAGE analysis, representing 0.3 µg protein, respectively. Freeze dried cell culture supernatant of the *P. pastoris* wild type strain X33 served as negative control. Gels were stained with Coomassie Blue and band intensities were analyzed in the resulting gels. The presence or absence of bands and their intensities were compared in order to determine the effect of heat treatment upon the protein. Intensity was

determined with the image analysis software package Image J 1.46 relative to the intensities of bands occurring after treatment at ambient temperature.

2.5.8 MALDI-TOF MS analysis

Purified freeze dried FcHyd5p produced by clone *P. pastoris* X33 [pPICZαA_FcHyd5p] was applied to MALDI-TOF MS analysis. 0.6-0.8 mg lyophilisate was dissolved in 5 µL deionized water. In order to compare native and heat treated transgenic FcHyd5p, lyophilisate was dissolved in synthetic wort (pH 3.0) to a concentration of 2 mg/mL, and part of it was incubated at 100 °C for 1 h. After dialysis for 1 day against deionized water at 4 °C this solution was directly used for analysis. Aqueous samples were mixed with acetonitrile and 0.1 % TFA in a 1:1:1 (v/v) ratio. 1 µL of this mixture was applied to a stainless steel target plate. After air dying of the samples 1 µL of matrix solution (10 mg/ml HCCA in acetonitrile, water and TFA (50:47.5:2.5, v/v) was overlaid and applied to measurement after further air drying. Measurements were performed with a MALDI-TOF mass spectrometer equipped with a nitrogen laser (λ = 337 nm) operating in linear positive ion detection mode under Biotyper Automation Control 2.0. The mass spectrum with a range of 7,000 to 10,000 Da was acquired and occurring peak values were further analyzed with Microsoft-Excel.

2.5.9 Glycation assay

A glycation assay adapted to the protocol of Ahmed & Furth (1991) was performed to relatively quantify the glycation state of protein FcHyd5p. The colorimetric assay in microtiter scale was based on the periodate method. By addition of periodate, formaldehyde is released from the C1 hydroxyl in amadori forms of glycated proteins via oxidation of periodate. By reaction of acetylactone in ammonia, the released formaldehyde is then converted to the chromophor diacetyl-dihydrolutidine (DDL). Determination of the absorbance of DDL serves as relative quantification of glycation of a protein.

Freeze dried preparations of FcHyd5p were dissolved in synthetic wort with pH 3.0, 5.0, 7.0, 9.0 and 11.0 to a final concentration of 2 mg/mL. One portion of each sample solution was heat treated at 100 °C for 1 h. A portion of each unboiled and boiled sample fraction was used for comparative gushing experiments (see 2.9.2). The rest of each sample fraction was dialyzed overnight against deionized water at 4 °C in order to remove unbound sugar molecules from the sample. Glycated and non glycated BSA served as control. To glycoslyate this protein, it was incubated in 0.5 M glucose solution at 37 °C for 12 d. After

dialysis for 3 d against deionized water at 4 °C, it was applied to the glycation assay together with the hydrophobin samples.

The glycation assay was carried out by mixing 20 µL sample with 20 µL deionized water followed by addition of 20 µL 0.1 M HCl and 20 µL 0.05 M $NaIO_4$. After 30 min of incubation at ambient temperature samples were cooled on ice for 10 min in order to terminate the oxidation. The formed zinc iodate was precipitated by addition of 20 µL pre-chilled 15 % $ZnSO_4$ (w/v) and 20 µL pre-chilled 0.7 M NaOH. After mixing by vortexing, the precipitate was removed by centrifugation (10 min, 9,000 x g). 100 µL of the supernatant was transferred to a microtiter plate and formaldehyde was detected by addition of 200 µL formaldehyde detection reagent (0.46 % acetylacetone in 3.3 M ammonium acetate (v/v), freshly prepared). After incubation for 1 h at 37 °C the formed DDL was measured via absorbance at 405 nm.

2.5.10 Preparation of recombinant proteins

For expression of recombinant proteins, heterologous transformant strains of *P. pastoris* were cultured in protein free medium BMMH under inducing conditions. First, pre-cultures were incubated in BMGY medium (chapter 2.3.1.3) for 24 h at 30 °C at 180 rpm. After centrifugation (10 min, 6,000 x g) cells were applied to 300 mL BMMH medium (chapter 2.3.1.3) in Fernbach flasks. By addition of 0.5 % methanol every 24 h, the expression of the recombinant genes and the production of heterologous protein was induced. Methanol metabolism of *P. pastoris* requires copious oxygen, which could be supplied by shaking at 180 rpm and the usage of sterile bandages as lid to cover cultivation flasks. Because the proteins are linked to the secretion signal α factor of *S. cerevisiae*, they were secreted into the medium. BMMH medium is nearly protein free so that the supernatant of the cultivation mainly contained the transgenic protein (Barr et al., 1992). After 3 d of cultivation at 30 °C the supernatant was harvested by centrifugation for 30 min at 10 °C and 6,000 x g. In order to remove salts and small molecules, the cell free supernatants were dialyzed for at least 3 d against deionized water at 4 °C in dialysis tubes with a molecular weight cut off of 3,500 Da. For concentration and storage the protein solutions were freeze dried. The resulting lyophilisates were used in this form for experiments unless otherwise stated.

2.5.11 Protease inhibition experiments

Protease inhibition experiments were done by determining the zone of inhibition of test solutions containing proteases in combination with protein Z4 or nsLtp1, respectively, on caseinate agar (2 % casein, 1.5 % agar, pH 8.0). Solutions of 10 mg/mL lyophilisate of transgenic proteins in PBS buffer (0.8 % NaCl (w/v), 0.02 % KH_2PO_4 (w/v), 0.02 % KCl (w/v), 0.15 % Na_2HPO_4 (w/v), pH 7.4) were prepared. One portion of the solution served as untreated control. The other part of the solution was heat treated for 1 h in a boiling water bath. Tested proteases were proteinase K and trypsin, which were adjusted to a concentration of 120 µg/mL in PBS buffer. Further influence of protein Z4 and nsLtp1 on proteases present in barley malt were analyzed by utilization of a 1:2 (v/v) dilution of malt extract in deionized water. Therefore, proteins present in barley malt obtained from Lehrstuhl für Brauerei- und Getränketechnik (TU-München, Freising, Germany) were extracted by mixing the malt with PBS buffer in a 1:1 (w/v) ratio. After vortexing for 30 s the extract was incubated for 3 h at ambient temperature. The supernatant of this extract was used in further gushing and protease inhibition experiments.

For protease inhibition testing, equal volumes of the protein solution and protease solutions were mixed resulting in concentrations of 5 mg/mL protein Z4 or nsLtp1, respectively, and 60 µg/mL protease. Final malt extract dilution was 1:4 (v/v). Addition of PBS buffer instead of nsLtp1 or protein Z4 solutions served as negative control. For testing the inhibition, 50 µL of each mix was transferred to a well (5.5 mm diameter) punched into caseinate agar plates. After incubation at 37 °C for 22 h, diameters of inhibition zones in all experiments were determined.

2.6 ELISA assays for the detection of FcHyd5p and nsLtp1

2.6.1 Antibody production

Antibodies against FcHyd5p and nsLtp1 were acquired by companies via ‘custom polyclonal antibody service’. Protein sequences of FcHyd5p (GenBank: ABE27986.1) and nsLtp1 (GenBank: CAA41946.1) missing the predicted signal peptide sequence were analyzed by the online available secondary structure software Yaspin in order to choose for appropriate peptides for antibody production. For protein nsLtp1, the available 3D structure as determined by Heinemann et al. (1996) was also taken into account. Antibodies were

delivered in concentration of 0.25-2.5 mg/mL and were stored in PBS buffer with NaN_3 at 4 °C. Peptides were delivered as lyophilisates in a purity of at least 85 %. For utilization they were dissolved in sterile deionized water to concentrations of 1.5 to 5 mg/mL. NaN_3 was added and dissolved peptides were stored at -20 °C.

2.6.2 Buffers for ELISA assay

Buffers used in ELISA assays for the detection of FcHyd5p and nsLtp1 and their composition are listed in Table 19.

Table 19: Composition of buffers used in ELISA experiments.

Ingredients	Amount per L
bicarbonate buffer, pH 9.6	
Na_2CO_3	5.3 g
$NaHCO_3$	4.2 g
NaN_3	0.2 g
PBS buffer, PBS-T buffer, pH 7.5	
NaCl	8.0 g
KH_2PO_4	0.2 g
Na_2HPO_4	1.15 g
KCl	0.2 g
Tween20 (only in PBS-T buffer)	0.5 mL
diethanolamine buffer, pH 9.8	
diethanolamine	96 mL
$MgCl_2$ x 6 H_2O	0.2 g

PBS buffer was prepared by dissolving all components in deionized water and adjusting the pH with either HCl (2 M) or NaOH (2 M). PBS-T buffer was prepared by addition of 0.5 mL Tween20 to PBS buffer as described before. For preparation of bicarbonate buffer, Na_2CO_3 was dissolved in 950 mL deionized water, followed by addition of $NaHCO_3$ until a pH of 9.6 resulted. Deionized water was added to 1 L.

PNPP substrate solution was prepared in diethanolamine buffer in a concentration of 2 mg/mL. This stock was stored at 4 °C for up to one week. Immediately before utilization as enzyme substrate in ELISA, a dilution of the stock was prepared in diethanolamine buffer to result in a working concentration of 0.5 mg/mL pNPP.

2.6.3 ELISA protocol for relative quantification of FcHyd5p

A competitive ELISA assay was established for the relative quantification of FcHyd5p in sample materials. Different samples of beer, grain or malt extract as well as emulsion solutions were applied to ELISA assays. Samples were either used directly or diluted in PBS buffer prior to analysis. The relative amount of FcHyd5p present in the samples was determined by relating the corresponding absorbance values to the absorbance without addition of protein. Therefore, the percentage of decrease in absorbance in the sample as compared to absorbance of the control without protein addition (0 %) was calculated. In addition, the hydrophobin level of grain and malt samples was related to the whole protein content of unheated extracts. The following protocol was established and used for relative quantification of FcHyd5p. The assay was carried out in transparent 96 well Maxisorp microtiter plates. Following each washing step plates were dried by tapping the plates on a dry paper towel.

- **coating**: 1.5 ng peptide FcHyd5p-P3 in bicarbonate buffer (100 µL/well)
  incubation 1.5 h, ambient temperature
- washing three times with PBS-T (200 µL/well)
- **sample-antibody incubation:** 100 µL sample directly or diluted in PBS + 2 µL anti-FcHyd5p-P3-IgG diluted 1:10 in PBS (end dilution 1:500)
  incubation 1.5 h, ambient temperature
- washing three times with PBS-T (200 µL/well)
- **secondary antibody incubation:** 100 µL/well goat-anti-rabbit-IgG-AP 1:500 in PBS
  incubation 0.5 h, ambient temperature
- washing three times with PBS-T (200 µL/well)
- washing two times with PBS (200 µL/well)
- **substrate incubation:** 0.5 mg/mL PNPP in diethanolamine buffer (100 µL/well)
  incubation 0.5 h, ambient temperature
- **absorbance measurement:** abs 405 nm in plate reader TecanSunrise or Omega

2.6.4 ELISA protocol for relative quantification of nsLtp1

ELISA assay for the detection of nsLtp1 was applied on different samples of beer, grain or malt extract, as well as emulsion solutions. Samples were measured either directly or after

dilution in PBS buffer. For grain and malt samples the relative nsLtp1 level was calculated per whole protein content of the unheated extracts. The reciprocal determined absorbance values were used as measure for the relative quantification, which represented the average amount of nsLtp1 of barley and wheat. ELSIA assays were performed in transparent 96 well Maxisorp microtiter plates, following the subsequent protocol. After washing steps, prior to addition of next substance, plates were dried by tapping the plates on a dry paper towel.

- **coating**: 1.5 ng peptide nsLtp1-P2 in bicarbonate buffer (100 µL/well)
  incubation 1.5 h, ambient temperature
- washing three times with PBS-T (200 µL/well)
- **sample-antibody incubation:** 100 µL sample directly or diluted in PBS + 2 µL anti-nsLtp1-P2-IgG diluted 1:10 in PBS (end dilution 1:500)
  incubation 1.5 h, ambient temperature
- washing three times with PBS-T (200 µL/well)
- **secondary antibody incubation:** 100 µL/well goat-anti-rabbit-IgG-AP 1:500 in PBS
  incubation 0.5 h, ambient temperature
- washing three times with PBS-T (200 µL/well)
- washing two times with PBS (200 µL/well)
- **substrate incubation:** 0.5 mg/mL PNPP in diethanolamine buffer (100 µL/well)
  incubation 0.5 h, ambient temperature
- **absorbance measurement:** abs 405 nm in plate reader TecanSunrise or Omega

2.6.5 Sample preparation

2.6.5.1 Protein extraction from of grain for Western blot analysis

Grains from barley and wheat cereals were finely ground. Proteins were extracted by mixing 4 g flour with PBS buffer, pH 7.4 in a 1:2 (w/v) ratio and rotating the mixture for 2 h over head at ambient temperature. After centrifugation (10 min, 8,000 x g) the supernatant was heat treated by incubation at 100 °C for 1 h. Precipitated proteins were removed by centrifugation at 9,000 x g for 10 min. The resulting extracts containing heat stable proteins of wheat or barley grain, respectively, were analyzed using SDS-PAGE and Western blot

analysis (see chapters 2.5.2 and 0) in order to check for their recognition by hydrophobin- and nsLtp1-specific antibodies.

2.6.5.2 Protein extraction from malt and grain for ELISA analysis

For analysis of grains or malt with the ELISA tests developed for detection of FcHyd5p and nsLtp1, respectively, extraction of protein was done as follows. The grain or malt was finely ground and 4 g flour were mixed with PBS buffer, pH 7.4 (1:2, w/v). Extraction of total protein present in malt or grain was achieved by rotating the mixture for 4 h over head at ambient temperature. After centrifugation (7,000 x g, 10 min) a Bradford protein assay (see 2.5.6) of the soluble extract was performed and the protein concentration was calculated. To eliminate heat labile proteins, extracts were then incubated in a boiling water bath for 1 h. After centrifugation (12,000 x g, 10 min) extracts were stored at -20 °C until further utilization in ELISA assays.

2.6.5.3 Berol purification

Amphiphilic proteins can be purified from samples by the use of non-ionic surfactants. These compounds are composed of two parts. An alkyl chain represents the hydrophobic part, whereas the hydrophilic head group consists of a polyoxyethylene chain. At a certain temperature, amphiphilic molecules concentrate within the micellar non-ionic surfactant phase, and can thus be separated and concentrated in one step. By adding a solvent, the micellar phase is disrupted and the amphiphilic proteins are released. Based on this principle, Linder and co-workers (2004; 2001) developed a method for purification of hydrophobins from a *T. reesei* culture supernatant by utilization of the non-ionic surfactant Berol. An adapted protocol for Berol purification of hydrophobin FcHyd5p and nsLtp1 was used in this current work. These proteins were purified from samples of beer and grain in order to be able to apply samples with higher concentrations of the tested proteins to the ELISA assays. 2 % of Berol 840 (v/v) were mixed in a separation funnel with the sample or in case of grain, sample extract (chapter 2.6.5.2). Phase separation was allowed to take place for at least 4 h at 4 °C. The aqueous phase was removed and one Berol 840 volume of deionized water was added. For protein release from the non-ionic surfactant phase into the water phase, five Berol 840 volumes of 2-butanol were added. After mixing, the water phase was separated from the 2-butanol phase and used in further experiments.

2.6.6 Beer titration with FcHyd5p

Comparative gushing potentials of beers from different lots produced in one brewery was determined by titrating the beer with hydrophobin FcHyd5p in order to compare the effect of nsLtp1 content in beers with different gushing potentials. For titration experiments, 5 bottles from three different batches of bottom fermented lager beer (0.5 L, purchased from retail) were pre-chilled to 4 °C. After bottle opening, 1 mL of beer was withdrawn from each bottle for application in ELISA assays and the volume was replaced by 1 mL of hydrophobin solution. To each of the 5 bottles of one batch a different FcHyd5p concentration, ranging from 0.0625 mg/mL to 1 mg/mL in deionized water, was added. Bottles were re-sealed with sterile crown corks and agitated overnight at 130 rpm at ambient temperature. After 1 h rest, bottles were opened and loss of volume was determined by weighing the bottles before and after opening. Loss of volume per bottle relative to hydrophobin concentrations was compared between the three batches and correlated to average levels of nsLtp1 in the batches. The nsLtp1 content was measured using the nsLtp1 specific ELISA. The experiment was repeated once with another three batches of beer produced in a different brewery.

2.6.7 Brewing experiments

Brewing experiments using barley malt were performed with addition of transgenic proteins FcHyd5p and nsLtp1 at different segments of the brewing process. Brewing was performed in a 10 L pilot brewing system at Lehrstuhl für Brau- und Getränketechnologie, TU München (Freising, Germany). A bottom fermented beer was produced from barley malt according to the protocol given in Table 20. Boiling temperatures as well as amounts and varieties of hops added varied between different batches as part of the experimental set up.

Table 20: Protocol used for brewing of bottom fermented beer under addition of transgenic protein FcHyd5p or nsLtp1.

Brew parameter	Setting	
malt grist	1,500 g	
malt grinding	Miag 2-laboratory roller mill, roller gap 0.8 mm	
infusion mashing process	restings, heating rate 1.0 °C/min	30 min, 52 °C
		30 min, 62 °C
		30 min, 72 °C
		10 min, 76 °C
lautering	90-100 min	
main wash	6 L H_2O dist.	
secondary washes	1. 3 L H_2O dist. with 78 °C	
	2. 2 L H_2O dist. with 78 °C	
	3. 1 L H_2O dist. with 78 °C	
wort boiling:	90/70 min hop addition 65 mg alpha acid at boiling start (hop: Opal 10 % alpha/Taurus 15.3%)	
hot break removal	sedimentation, 20 min	
inoculation	15 x 10^6 cells/ml, brewing yeast strain 34/70	
main fermentation	until fermentation degree of 70 % isothermally at 12 °C	
ripening/maturation	warm-ripening: 3 days at 16 °C until total diacetyl < 0.12 mg/L	
storage	28 days at 0 °C	
filtration	sheet filtration	
filling	0.5 L Longneck bottles (new glass)	
bottle storage:	upright at 20 °C	

2.7 Protein-protein interaction studies

2.7.1 BIAcore SPR experiments

Interaction studies were performed with the BIAcore X protein interaction analyzer instrument. A change in detection angle of surface plasmon resonance (SRP) measured by the instrument is a measure of interaction of immobilized ligand with a dissolved analyte. Two different approaches to test interactions between hydrophobin FcHyd5p and nsLtp1 or FcHyd5p and protein Z4 by BIAcore were carried out. One was to immobilize the antibody anti-FcHyd5p-P3-IgG and to check for differences in binding behavior between pure FcHyd5p and mixtures of hydrophobin with beer foam proteins. The other approach was to use FcHyd5p directly as ligand and to test binding of analytes Z4 or nsLtp1.

For both methods ligand immobilization onto a sensor chip CM5 was achieved at 24 °C by amino coupling during which the ligand is attached covalently to the sensor surface via primary amine groups. During the ligand immobilization procedure, HBS-EP (pH 7.4, see Table 21) was used as running buffer at a constant flow rate of 5 µL/min. For immobilization of FcHyd5p, no Tween 20 was added to buffers to minimize the effect on hydrophobic interactions. The surface of the sensor chip CM5 was activated by addition of 35 µL NHS (0.1 M) and EDC (0.4 M) in a 1:1 (v/v) ratio resulting in a contact time of 7 min. Following activation, the ligand solution was injected with a volume of 55 µL, representing 10 min contact time with the surface. For antibody coupling, antibody anti-FcHyd5p-P3-IgG dissolved in sodium acetate buffer (10 mM) in a concentration of 50 µg/mL was used. FcHyd5p was coupled to the chip by using a concentration of 2.3 mg/mL in HBS-EP buffer. Deactivation of excess reactive groups was achieved by injection of 35 µL 1 M ethanolamine-HCl.

For experiments using the sensor chip with immobilized antibody, running buffer HBS-EP (pH 7.4) was used at a flow rate of 10 µL/min at constant temperature of 24 °C. After each injection of analyte the surface of the sensor chip was regenerated with glycine-HCl buffer (10 mM glycine, 10 mM NaCl, pH 1.5) with an injection volume of 10 µL in order to remove the bound analyte prior to testing the next analyte sample. Analyte samples were injected in a volume of 15 µL in HBS-EP buffer. For interaction studies, FcHyd5p was used either directly as first analyte followed by injection of nsLtp1 or Z4 without intermittent regeneration or a mixture of both proteins was injected directly.

Interaction studies on the sensor chip with immobilized FcHyd5p were carried out at 24 °C with a flow rate of 10 µL/min of HBS-EP buffer (pH 7.5) without Tween20 added in order to enable hydrophobic interactions. Regeneration was achieved by injection of 20 µL NaOH (124 mM). Analytes were injected in a volume of 20 µL with concentrations ranging from 2.5 mg/mL to 3.8 mg/mL.

Composition of HBS-EP buffer is given in Table 21. Buffer was sterile filtered through a 0.2 µm membrane filter and degassed under vacuum.

Table 21: Composition of HBS-EP buffer used in BIAcore interaction studies.

Ingredients	Amount per 0.5 L
HEPES	1.19 g
NaCl	4.20 g
EDTA	0.632 g
Tween20	250 µL

2.7.2 Dynamic light scattering (DLS)

To investigate the size of particles in solutions containing freeze dried proteins FcHyd5p, nsLtp1 or Z4, dynamic light scattering was applied. A comparison of particle size distributions was performed in solutions with pure proteins and samples with mixtures of hydrophobin protein with nsLtp1, or hydrophobin with Z4, respectively. Two different instruments were used for determination of particles with dynamic light scattering.

2.7.2.1 Single angle

First experiments were performed in a single angle 90° light scattering instrument (Zetasizer μV) with laser beam wave length of 830 nm. Samples contained 2.5 mg/mL total protein in 50 mM sodium acetate buffer (pH 5.0). A protein ratio of 1:1 (v/v) was used in combination experiments. Samples of nsLtp1 and Z4 were also analyzed after heat treatment by incubation at 99 °C for 1 h. After filtering through 0.2 μm inorganic membrane filters, 100 μL of samples were analyzed in single angle measurement. Values for viscosity and refractive index were set to 0.8872 and 1.330, respectively, representing water as the solvent. 13 runs were performed at 25 °C with 120 s equilibration time prior to each measurement. Experiments were run in replicates. Runs were automatically summarized in two independent measurement output data files by the standard operating procedures of Zetasizer software, which also converted the measured intensities into a particle size distribution profile.

2.7.2.2 Multiple angles

To get a more accurate insight into particle size, DLS was also carried out at multiple angles with the instrument ALV instrument CGS-3. Scattering was measured in a toluene bath at a wavelength of 532 nm at a temperature of 25 °C. 300 μL of sample with a total protein concentration of 30 mg/mL in sodium acetate buffer (pH 5.0) were applied. In protein mixtures, a ratio of 1:1 (v/v) of hydrophobin:beer protein was adjusted. Detection of light scattering was conducted 5 times for 300 s in the single angle detection mode in the range of 30° to 150° in 10° steps. ALV-MultiAngle software was used for data acquisition and correction for toluene and water, as well as for correlation functions. Since measurements were done in an aqueous system, settings for refractive index (1.332) and viscosity (0.97505, 25 °C) corresponded to the ones typical for water. Sample refractive index increment dn/dc was set to 0.185 mL/g, representing protein. The software package AfterALV was used for calculation of the particle size distribution. Direct comparison of particle size distribution in the different samples was performed for each angle. Mean values for the peak sizes at angles

of 50° and upwards were compared. Data of measurements under 30° and 40° angles were omitted since they showed too high noise of scattering.

2.7.2.3 Depolymerized DLS

Depolymerized DLS (DDLS) was conducted with the ALV instrument CGS-3 by placing a depolymerisation filter in front of the detector. A 45° angle was used for the analysis. Pure toluene without sample added served as control. Samples used were FcHyd5p and FcHyd5:nsLtp1 (1:1, v/v) at 30 mg/mL in sodium acetate buffer (pH 5.0).

2.7.3 Surface hydrophobicity

ANS (8-anilino-1-naphatlene sulfonic acid) interacts with hydrophobic domains of proteins and was therefore used during the current study to measure surface hydrophobicity of protein solutions. Interaction of ANS with hydrophobic protein domains induces ANS fluorescence and can thus be used for relative quantification of surface hydrophobicity. The method used here was described by Nakai &Li-Chan (1980), Kato & Nakai (1988) and also by Uruakpa & Arntfield (2006). Protein samples were adjusted to 10 mg/mL in NaCl-solution (0.5% (w/v)). If heat treatment was done, solutions were incubated at 100 °C for 1 h in a water bath prior to ANS measurement. Protein samples were diluted 1:1 (v/v) in 0.5 % NaCl. Mixtures of proteins in the ratio 1:1 contained 5 mg/mL of each protein. For quantification, different protein concentrations ranging from 0.0025 % to 0.1 % were prepared in 50 mM citrate buffer (pH 5.0). 100 µL of each dilution was pipetted into wells of a 96 well microtiter plate (FIA-plate, black) and 5 µL of ANS (8.46 mM in 0.1 M potassium phosphate buffer, pH 7.0) were added. The fluorescence of at least three parallel analyses per sample was measured in a Tecan Spectrafluor fluorimeter with excitation at 380 nm, emission at 465 nm and gain set to 110.

2.8 Investigation of influences of nsLtp1 and Z4 on surface properties of FcHyd5p

2.8.1 Emulsion properties

Stability of oil-in-water emulsions prepared with water phases containing FcHyd5p was compared to emulsions containing nsLtp1 and protein Z4 or mixtures of those proteins. The time needed for the respective emulsions to clear was compared and correlated to the proteins

and protein mixtures used. In addition, oil droplets in the respective emulsions were compared in respect of their size distribution. For this purpose, 20 % (v/v) oil-in-water emulsions were prepared. Protein solutions of FcHyd5p, protein Z4, Z4 b, nsLtp1 and nsLtp1 b in distilled water served as aqueous phase. Heat treatment (b) was done by incubating the protein solutions for 1 h at 100 °C in a water bath. Sun flower oil (purchased from retail) was added for preparation of emulsions, and the samples were homogenized in a FastPrep®-24 instrument for 30 s at 4 m/s followed by sonification at ambient temperature for 10 min in an ultrasound bath.

2.8.1.1 Emulsion stability

Stability of emulsions containing protein in concentrations of 0.01 mM and 0.75 mg/mL (0.75 mg/mL protein correspond to 0.09 mM for FcHyd5p, 0.08 mM for nsLtp1 and 0.02 mM for protein Z4), respectively, was determined by observing the clearing as a function of time. Samples were kept in polystyrol/polystyrene cuvettes sealed with Parafilm® to prevent evaporation and stored at ambient temperature. The absorbance at 590 nm was recorded with a spectrophotometer every 24 h for at least 4 days. In instable emulsions the phase separation was supposed to be more rapid, leading to a faster clearing of the solution.

2.8.1.2 Droplet size determination

Particle size distribution in emulsions containing 0.01 mM protein was measured in a particle size analyzer equipped with a Hydro 2000S sample handling unit. About 0.6 mL of sample was added to the sample handling unit containing water. The dispersed sample is re-circulated continuously through the measurement zone to keep it suspended and homogenized. Particle size was measured by laser diffraction in the dispersed sample. The particle's refractive index was set to the value usually used in the analysis of milk fat (1.46), the dispersant refractive index was defined as 1.330, representing water, and absorption was set to 0.001. Scattering volumes were calculated towards numerical size distribution by the instrument's built in software. Oil droplet diameters were calculated volumetrically with polydispersed model for size distribution.

2.8.1.3 Protein binding to oil

Oil-in-water emulsions were prepared by homogenizing 33 % (v/v) sun flower oil in aqueous protein solutions of the proteins to be tested. Binding of protein FcHyd5p or nsLtp1 to the oil was examined by measuring the loss of protein in the water phase using ELISA assays.

Protein solutions of 10 mg/mL freeze dried protein mixed with either water or the second protein (10 mg/mL) in a 1:1 (v/v) ratio were examined. If heat treatment was applied, this was performed by incubation in a boiling water bath for 1 h prior to dilution and mixing. To each sample (100 µL) 50 µL sun flower oil was added. Emulsions were produced by homogenizing mixtures for 30 s at 4 m/s in a FastPrep®-24 homogenizer followed by incubation in an ultrasonic bath for 10 min. Phases were then separated by centrifugation at 12,300 x g for 10 min. The aqueous phase was transferred to ELISA measurements. The relative amount of FcHyd5p or nsLtp1 was determined and compared to the control, which was a sample solution containing 5 mg/mL nsLtp1 or FcHyd5p, respectively, without addition of oil.

2.8.2 Foaming properties

To investigate the foaming rates and foam stability of aqueous solutions of pure proteins and the influence of beer proteins nsLtp1 and Z4 on foaming properties of FcHyd5p, lyophilisates of proteins were dissolved in distilled water to a concentration of 2 mg/mL. If heat treatment was applied, samples were used after boiling for 1 h in a water bath. Protein solutions were either used directly or diluted 1:2 in water. For testing combinations of proteins, protein solutions were mixed in a 1:1 (v/v) ratio. 5 mL of each sample was added to 15 mL-tubes followed by mixing and foaming in a FastPrep®-24 homogenizer at 4 m/s for 1 min. Foam collapse and stability were determined after 0 and 1 h by measuring the height of the foam and the serum fractions, respectively. Based on these parameters the percentage of foam present directly after preparation and after 1 h was calculated as the foaming rate which was defined as the ratio of foam height to the height of the total volume (foam height + serum height). Foam decay was determined via the quotient of foaming rate at 1 h and the foaming rate at time point zero, and was used as a measure for foam stability.

Examination of the influence of temperature on foaming capacity of FcHyd5p followed the same scheme. Proteins in concentrations of 2 mg/mL were dissolved in deionized water or synthetic wort and incubated for 1 h at different temperatures. After foaming of 5 mL protein solution of FcHyd5p, foam height was documented after 0 h and 1 h.

2.8.3 Surface tension

Surface tension was determined using a volume drop tensiometer TVT2 Lauda. Ten cycles with three drops per cycle were measured for each sample. A temperature of 20 °C was

chosen for measurements in dynamic mode to measure the interface tension as a function of the drop age against air. Sampling was performed of protein solutions containing 0.1 mM proteins FcHyd5p, nsLtp1 or Z4, or a combination of proteins in a 1:1 (v/v) ratio, respectively, in deionized water. Drops were formed with a 2.5 mL syringe. The pH of the samples was 5.9. Instrument settings were set to drop formation time between 0.08 and 5 µL/s with drop slow down switched off. The capillary used had a radius of 1.385 nm. Density difference between the used phases, as calculated from density measurements with values of 0.0011 g/cm^3 for air and 0.9985 g/cm^3 for protein samples were set for calculation of the surface tension by the instruments built in software.

2.8.4 Coating properties

In order to prepare glass coatings, 5 mg/mL freeze dried proteins were dissolved in distilled water and mixed by inversion. Heat treatment of nsLtp1 and protein Z4 was performed of part of the sample in a boiling water bath for 1 h. Combination of hydrophobin FcHyd5p with nsLtp1 or protein Z4, respectively, were prepared in the ratios of 10:1 (v/v) and 1:1 (v/v). 90 µL of each protein solution was pipetted onto microscopy glass slides and allowed to dry by evaporation at ambient temperature resulting in a surface protein film. Coatings of FcHyd5p mixed with water served as controls for testing the influence of the beer foam proteins on coating properties.

In order to investigate the hydrophobicity displayed by prepared protein films, the radial distribution of oil droplets on the surface of the coatings was measured. On each protein film 1 µL of sun flower oil (purchased in free trade) was applied. For measuring the oil droplet size, close up photographs of the oil droplets were taken after 10 min, after 1 h and after 3 d. Image analysis software package Image J 1.46 was used to analyze the average droplets diameters from digital images.

Contact angles of oil droplets on pure protein coatings and on coatings of 10:1 (v/v) protein mixtures were calculated from close up images taken laterally with a digital camera set to manual focusing. For each droplet the angle was calculated from both sides using Image J 1.46 software package.

2.8.5 Structure of protein films at air/water interface

Atomic force microscopy (AFM) was applied to protein films to investigate formation and topography of films of pure and mixed proteins.

The drop surface transfer method was used for preparation of protein films on a hydrophobic substrate. A drop of a protein containing aqueous solution was applied onto a Parafilm® surface and incubated for 30 min at ambient temperature to enable the proteins to assemble at the air/water interface at the drop surface. This protein film then was transferred onto a hydrophobic substrate by tapping the substrate on top of the droplet as illustrated in Figure 7. The hydrophobic part of the protein which is directed outwards from the aqueous phase of the droplet can be attached to the hydrophobic substrate in this way. The protein film of the drop surface is transferred onto the substrate displaying its hydrophilic surface.

The method was adapted according to protocols used by Kirkland & Keyhani (2011) and Szilvay et al. (2007). Hydrophobic glass cover slides served as substrate for tapping. They were cleaned and defatted by washing in 100 % ethanol and drying under a stream of N_2 directly prior to use. A working concentration of 100 µg/mL protein at pH 5.0 was found to work best. The preparation procedure of AFM substrates with desired protein film is described in Figure 7.

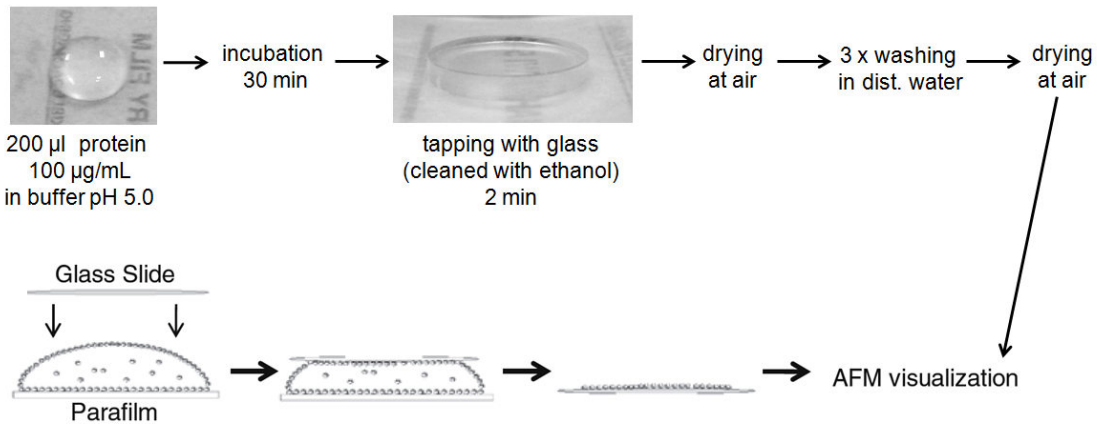

Figure 7: Schematic diagram of the drop surface transfer method used for preparation of protein films on glass surface, modified after Kirkland & Keyhani (2011).

Solutions of FcHyd5p, nsLtp1 and Z4 were prepared in sodium acetate buffer (50 mM, pH 5.0) in a final concentration of 100 µg/mL. Droplets (200 µL) of 1:1 (v/v) mixtures of FcHyd5p and Z4 or nsLtp1, respectively, as well as of pure protein solutions, were applied onto Parafilm® and incubated at ambient temperature for 30 min. Tapping was done by touching the droplet with a clean glass cover slide for 2 min, followed by air drying. After three rinses with distilled water the glass surface was air dried again. After three days of storage, samples were used for AFM analysis. Glass cover slides without coating served as negative control.

Substrates were applied to measurements in an AFM instrument in the dynamic non contact tapping mode with H*silicon tips of 4 ± 1 µm thickness. Scanning was operated at ambient temperature with a scanning rate of at least 0.5 Hz. Size scan was set between 10 and 0.5 µm with a resolution at least 256. AFM images were analyzed with the data visualization and analysis program Gwyddion. The lowest point of the topography in each image was set to zero prior to analysis. Data were de-noised by line by line height median matching. Height profiles of height retrace-images of the different surfaces were compared to each other.

2.9 Gushing experiments

Bottom fermented beer with 0.5 L per bottle (purchased from local retail markets) was used for gushing experiments. Experiments with addition of hydrophobins and/or beer foam proteins were performed with beer bottles from the same production lot and from the same brewery for comparison of results. Control beers did not show any gushing as was checked for each lot by parallel testing a bottle without protein addition. Bonaqa® was used in gushing experiments involving carbonated water. Bottles contained 0.33 L. For testing of gushing activity of added proteins, bottles of beer or carbonated water were subjected to horizontal shaking in an incubator shaker. Shaking was set to 100 rpm during incubation time of 16 h at room temperature. Following shaking, bottles were stored for 1 h standing upright at ambient temperature prior to opening. Overflow volumes were determined by measuring the weight loss. For examination of gushing inducing properties of hydrophobins, lyophilisates of the proteins were dissolved in synthetic wort or deionized water and added to the beverages. Bottles were pre-chilled to 4 °C prior to protein addition in order to minimize CO_2 loss. After addition of proteins, bottles were tightly re-sealed with sterile crown caps. In beer, 1 mL of a hydrophobin solution with a concentration of 2 mg/mL was added routinely whereas 1 mg/mL was sufficient in carbonated water. The influence of beer foam proteins on gushing was analyzed by adding transgenic proteins Z4 and nsLtp1 dissolved in water or synthetic wort in addition to hydrophobins. To examine the influence of heat treatment on the gushing activity, solutions of the transgenic proteins Z4 and nsLtp1 either in water or in synthetic wort were incubated for 1 h in a boiling water bath. To test the influence on gushing of possible cleavage of serpin protein Z4 upon protease inhibition, protein Z4 was pre-incubated with the barley malt extract described in chapter 2.5.11. 10 mg/mL Z4 in malt extract in a 1:2 (v/v) dilution in deionized water was incubated at 37 °C for 1.5 h. 1 mL of the

mixture of malt extract with protein Z4 was transferred to pre-chilled Bonaqa® water previously treated with hydrophobin FcHyd5p.

2.9.1 Influence of pH on FcHyd5p induced gushing

Freeze-dried FcHyd5p was suspended in synthetic wort or deionized water, respectively, at pH values of 3.0, 5.0, 7.0, 9.0 and 11.0. A part of the 2 mg/mL hydrophobin containing samples was heated at 100 °C for 1 h in a water bath. After cooling to room temperature, 1 mL of each the heat treated hydrophobin and untreated hydrophobin samples were added to lager beer in 0.5 L bottles. Bottles were re-sealed with sterile crown caps and rotated (28 rpm) for 16 h at ambient temperature. After resting the bottles for 1 h in upright position they were opened and the overflow volume was determined as previously described.

2.9.2 Influence of FcHyd5p-glycation on gushing

Samples of FcHyd5p previously analyzed in glycation assay (see 2.5.9) were analyzed for their gushing potential. Lyophilized FcHyd5p was suspended in synthetic wort at different pH values (3.0, 5.0, 7.0, 9.0, 11.0) resulting in a concentration of 2 mg/mL. A portion of each sample was heat treated at 100 °C for 1 h in a water bath. After cooling to room temperature, 1 mL of each boiled and unboiled sample was added to lager beer in 0.5 L bottles. Bottles were re-sealed with sterile crown caps and rotated (28 rpm) for 16 h at ambient temperature. After resting the bottles for 1 h in upright position they were opened and the overflow volume was determined as previously described.

3 Results

3.1 Parameters influencing hydrophobin induced gushing

3.1.1 Influence of pH combined with heat treatment

The influence of pH value on the hydrophobin FcHyd5p in terms of gushing was tested by comparing the hydrophobin induced overflow volumes of beer. Addition of 1 mL water containing 2 mg of FcHyd5p to 0.5 L beer resulted in an overflow volume of 200 to 270 mL. The overflow volume did not significantly differ when the hydrophobin was dissolved in water at pH 3.0, 5.0, 7.0, 9.0 or 11.0. Also heat treatment of the solutions containing FcHyd5p prior to addition to beer resulted in no difference in gushing volumes at pH values between 3.0 and 9.0. However, heat treatment of the FcHyd5p solution at pH 11.0 resulted in a reduction of gushing volumes. The loss of beer volume decreased to 90 mL.

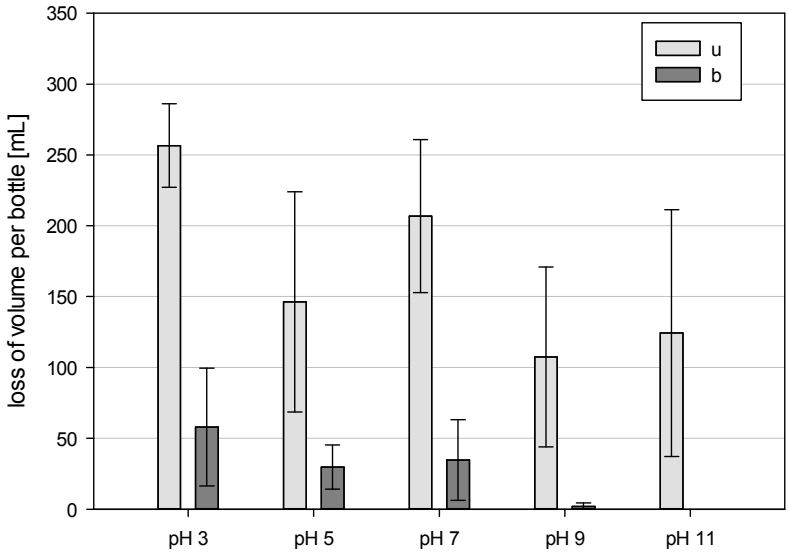

Figure 8: Influence of pH on gushing inducing properties of FcHyd5p. Loss of volume of beer per bottle upon addition of 2 mg FcHyd5p dissolved in synthetic wort of different pH values; u: unboiled samples; b: boiled samples.

When FcHyd5p was dissolved in synthetic wort before addition to beer, an effect of the pH value on the gushing volume per bottle of beer was observed. Hydrophobin in synthetic wort at pH 3.0 induced gushing with a loss of volume of 256.6 ± 29.4 mL. Increasing the pH resulted in a reduction of the gushing volume with a significant decrease at pH values of 9.0 ($P = 0.024$) or 11.0 ($P = 0.048$) as compared to pH 3.0. At these pH values the gushing volumes decreased to 107.4 ± 63.5 mL and 124.3 ± 87.0 mL, respectively (Figure 8). In

contrast to FcHyd5p dissolved in water, a considerable effect of the heat treatment was observed in synthetic wort. A decrease of the gushing volume of about 20 % compared to unboiled samples was observed at lower pH values (pH 3.0 - pH 7.0). Almost no gushing was induced by heat treated FcHyd5p in synthetic wort at pH 9.0. At pH 11.0 no gushing occurred under these conditions (Figure 8).

3.1.2 Influence of temperature on foaming properties of FcHyd5p

Incubating FcHyd5p at different temperatures prior to the foaming experiments had no effect on the initial foam formation, neither in aqueous solution nor in synthetic wort. A foaming rate of about 29 % in water and 45 % in synthetic wort was observed at all tested temperatures. Foam decay, however, was affected by the heat treatment of FcHyd5p. Foam decay rates after 1 h of incubation at ambient temperature are shown in Figure 9.

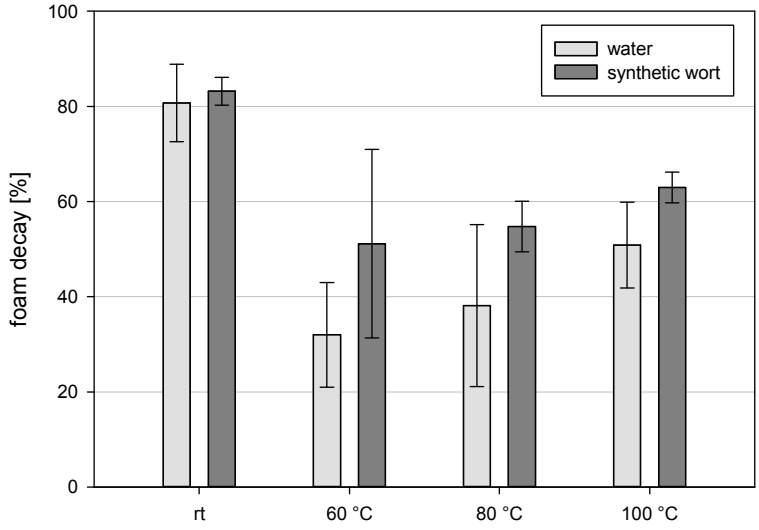

Figure 9: Foam decay of foams prepared with FcHyd5p heat treated prior to foaming. Foam decay of foamed solutions of water and synthetic wort containing 2 mg/mL FcHyd5p after 1h at ambient temperature.

For samples in aqueous solution at ambient temperature 80 ± 8 % of the foam collapsed, for samples incubated at 60 °C the decay rate sank to 32 ± 11 %. Further increase of incubation temperatures again led to a higher foam decay rate. 38 ± 17 % and 51 ± 9 % of the foam collapsed at 80 °C and 100 °C, respectively. The effect of thermal treatment of FcHyd5p on foam decay was less pronounced in synthetic wort. In synthetic wort foam collapse was highest after incubation at room temperature, with a rate of 83 ± 3 %. Thermal treatment stabilized the foam. After incubation at 60 °C, a foam decay of 51 ± 20 % was observed. Further increase in incubation temperatures resulted in decreasing foam stabilization effect.

In samples treated at 80 °C and 100 °C, 55 ± 5 % and 63 ± 3 % of foam collapsed after 1 h (Figure 9).

3.1.3 Glycation

The decrease of gushing, caused by FcHyd5p dissolved and boiled in synthetic wort, was thought to be due to changes of the protein during the boiling process. Since this effect was not observed when FcHyd5p was boiled in deionized water, defolding was excluded. Instead, protein glycation was assumed. Therefore, the glycation state of FcHyd5p was examined by MALDI-TOF analysis and glycation assays.

The spectrum obtained by MALDI-TOF analysis of the native hydrophobin is shown in the lower part of Figure 10. Double peaks occurred in a mass range from 7,500 to 8,100 Da. The detected double peaks had a mass difference of 162 Da representing the mass of a hexose molecule. Since this spectrum of peaks was observed in untreated FcHyd5p it was assumed that enzymatic glycation alias glycosylation had already occurred during the heterologous protein production in the *P. pastoris* host. Within all the double peaks the interval mass differences of local maxima was 17 Da (Figure 10).

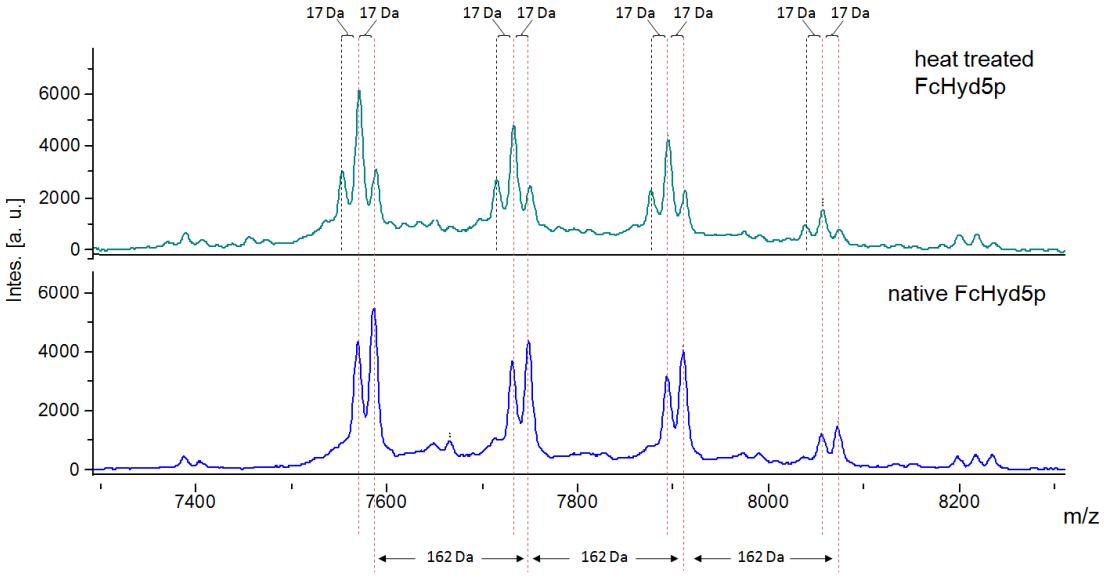

Figure 10: MALDI-TOF MS spectra of lyophilized FcHyd5p produced by transgenic *P. pastoris* [pPICZ*α*A_FcHyd5p] in native form (bottom) and after heat treatment in synthetic wort (pH 3) (top). The main peaks are displayed with the intervals of mass differences marked.

When FcHyd5p was incubated in synthetic wort and submitted to heat treatment, the same mass range was covered and peaks at the same sizes as in untreated samples occurred with an interval of 162 Da (Figure 10). However, each of these peaks consisted of three local maxima

instead of two, with a distance of 17 Da. The two rightmost local maxima in each triple peak, corresponding to higher mass, matched with the maxima of a double peak in the untreated sample. However, boiling resulted in a shift in the intensity of local maxima. The intensity of the maxima at highest mass decreased, whereas the intensity of the maxima corresponding to the one with lower mass in the double peak was increased. As illustrated in Figure 10, this scheme was visible at all of the occurring triple peaks of the mass spectrum.

Samples of FcHyd5p in synthetic wort of different pH values and incubated in a boiling water bath were analyzed for the extent of glycation in a glycation assay. Results were compared to samples incubated at ambient temperature. The results are displayed in Figure 11. At all tested pH values the absorbance in the glycation assay increased after heat treatment. The highest increase of 606 % was observed at pH 11.

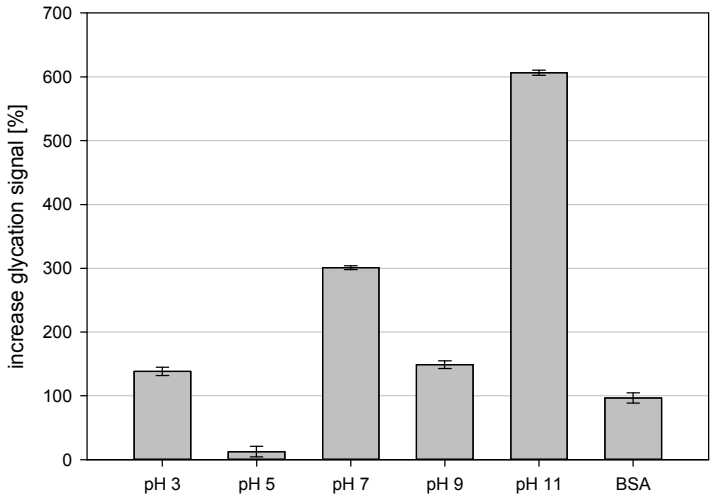

Figure 11: Increase of glycation signal of FcHyd5p after heat treatment in synthetic wort at different pH values. Glycation was determined by glycation assay. Glycated BSA served as positive control.

3.2 Establishing an ELISA assay for the detection of FcHyd5p

3.2.1 Antibody production and sensitivity

To develop an ELISA assay for the detection of the hydrophobin FcHyd5p, a specific antibody against this protein was obtained by immunization of rabbits. The amino acid sequence of FcHyd5p without the predicted signal sequence was deduced from translation of the nucleotide sequence of the *fchyd5* gene (Stübner et al., 2010; GenBank: ABE27986.1) as given below.

```
1  LPANEKRQAY IPCSGLYGTS QCCATDVLGV ADLDCGNPPS SPTDADNFSA
51 VCAEIGQRAR CCVLPILDQG ILCNTPTGVQ D
```

Custom polyclonal antibody service was used for the production of peptides used to immunize animals for antibody production. Two different peptides (FcHyd5p-P2 and FcHyd5p-P3) were deduced from FcHyd5p protein sequence, both covering different parts of the protein. Peptides were produced with a chemical modification to protect the internal cysteines during immunization by addition of acetamidomethyl (acm). The sequences of immunization peptides FcHyd5p-P2 and FcHyd5p-P3 with their respective positions within the FcHyd5p protein sequence are given in Table 22.

Table 22: aa sequences of peptides FcHyd5p-P2 and FcHyd5p-P3 used for polyclonal antibody production.

Peptide	Peptide sequence	Position in FcHyd5p	Length (#aa)
FcHyd5p-P2	LPANEKRQAYIPC(acm)SGLYGTSQC	N-terminal, 1-22	22
FcHyd5p-P3	CVLPILDQGILC(acm)NTPTGVQD	C-terminal, 62-81	20

FcHyd5p-P2 covered a region mainly predicted to be random coiled. FcHyd5p-P3 covered a region partly predicted to form ß-sheets. The peptides were positioned at the N (P2) and C (P3) termini of the protein, as they were assumed to be at the outer surface of native FcHyd5p.

BLAST analysis (Altschul et al. 1990) for each of the peptides resulted in matches with the Hyd5 proteins of *F. graminearum* and *F. culmorum* with an alignment score of 74.4 and 68.1 for FcHyd5p-P2 and FcHyd5p-P3, respectively. Both peptides did not match with any proteins of *H. vulgare*, *P. pastoris* or *Saccharomycetes* with an alignment score above 30.

For databases of *Ascomycetes*, BLAST analysis revealed that 52.8 % of class 2 hydrophobins with > 80 % identity to FcHyd5p contained a peptide with high alignment score to FcHyd5p-P2. Accordingly, 86.4 % of those peptides matching the FcHyd5p-P2 peptide with high alignment score lay within hydrophobins with > 80 % amino acid sequence identity to FcHyd5p. The second peptide, FcHyd5-P3, matched 66.7 % of those hydrophobins which displayed > 80 % sequence identity to FcHyd5p. Of those peptides matching the FcHyd5p-P3 peptide with high alignment score 92.3 % belonged to hydrophobins with > 80 % amino acid sequence identity to FcHyd5p. Peptide FcHyd5p-P3 matched to hydrophobin proteins of 27 fungi within the *Ascomycetes* with an alignment score > 35. The species are listed in **Fehler! Verweisquelle konnte nicht gefunden werden.**.

Table 23: Proteins of *Ascomycetes* matching to peptide FcHyd5p-P3 with a max alignment score above 35. Matching was calculated by the BLAST program.

Organism	Protein	max alignment score	Accession	% query coverage
Fusarium fujikuroi	related to trihydrophobin precursor *	68.1	CCT72002.1	100
Fusarium oxysporum	trihydrophobin *	68.1	ENH66835.1	100
Fusarium pseudograminearum	hypothetical protein FPSE 11324 *	68.1	EKJ68316.1	100
Fusarium oxysporum	hypothetical protein FOXB 00066 *	68.1	EGU89442.1	100
Fusarium poae	putative hydrophobin precursor *	68.1	CBJ94531.1	100
Fusarium verticillioides	hydrophobin, class 2 hydrophobin*	68.1	AAN78355.1	100
Fusarium culmorum Fusarium graminearum	hydrophobin 5 precursor, Hyd5 *	68.1	XP_382007.1	100
Colletotrichum orbiculare	fungal hydrophobin *	65.1	ENH84086.1	100
Colletotrichum gloeosoroides	hydrophobin precursor *	62.6	ELA33409.1	100
Glomerella graminicola	fungal hydrophobin, class 2 hydrophobin*	62.6	EFQ36046.1	100
Colletotrichum higginsianum	fungal hydrophobin *	61.3	CCF32111.1	100
Togninia minima	putative hydrophobin precursor protein *	57.9	EON97461.1	100
Magnaporthe oryzae	hydrophobin *	57.9	XP_003714057.1	90
Nectria haematococca	hypothetical protein NECHADRAFT 51212, no class relatable	57.1	XP_003041182.1	100
Podospora anserina	hypothetical protein, unnamed protein product *	52.4	XP_001907576.1	95
Verticillium dahliae	cerato-ulmin *	51.5	EGY16674.1	90
Eutypa lata	putative hydrophobin precursor protein *	45.6	EMR62638.1	90
Gaeumannomyces graminis	hypothetical protein GGTG 03085 *	44.3	EJT77982.1	95
Neurospora tetrasperma	hypothetical proteins NEUTE1DRAFT 101200 and NEUTE2DRAFT 128739 *	41.8	EGO58333.1	85

Organism	Protein	max alignment score	Accession	% query coverage
Neurospora crassa	hypothetical protein NCU08192*	41.8	XP_989282.2	85
Sclerotinia scleotiorum	predicted protein *	41.4	XP_001597020.1	75
Eutypa lata	putative hydrophobin precursor protein *	41.1	EMR67611.1	90
Colletotrichum gloeosporioides	cerato-ulmin *	39.2	ELA32569.1	90
Gaeumannomyces graminis	hypothetical protein GGTG 02383 *	37.1	EJT82410.1	90
Trichoderma atroviride	hydrophobin **	35.4	ABS59370.1	85
Trichoderma atroviride	hydrophobin *	35.4	EHK49783.1	85

** probable class 2 hydrophobin, * classified as class 2 hydrophobin, as determined by analysis of the primary sequence and comparison to general hydrophobin structure based on conserved cysteines residues (Wösten & Wessels, 1997).

Antibodies acquired by immunization with peptides FcHyd5p-P2 and FcHyd5p-P3 were termed anti-FcHyd5p-P2-IgG and anti-FcHyd5p-P2-IgG, respectively.

Western blot analysis was applied to a freeze dried preparation of FcHyd5p after separation by SDS-PAGE. A 12 kDa protein band was stained after application of both antibodies in separate reactions. However, application of the anti-FcHyd5p-P3-IgG antibody resulted in highly intensive staining whereas application of the anti-FcHyd5p-P2-IgG antibody resulted in a considerably weaker signal. This indicated that the antibody against P3 had a higher sensitivity towards FcHyd5p. Thus, further experiments were performed with the anti-FcHyd5p-P3-IgG antibody. Specificity of this antibody was evaluated by Western blot analysis of beer proteins nsLtp1 and protein Z4, as well as hydrophobin Hfb2 from *T. reesei*. Proteins isolated from the culture supernatant of the *P. pastoris* wild type strain X33 were used as negative control. As illustrated in Figure 12, Western blots of lyophilized proteins separated by SDS-PAGE showed a distinctive band with FcHyd5p whereas all other tested proteins were not recognized by anti-FcHyd5p-P3-IgG. However, in the negative control as well as in samples of protein Z4 and nsLtp1, bands between 55 and 70 kDa in size were stained. This band, in addition to genuine FcHyd5p, was also observed in the FcHyd5p sample. It can therefore be speculated that the protein might be produced by the host yeast

P. pastoris used for transgenic protein production and may be present in all the lyophilisates, although BLAST analysis had not resulted in a hit for any *P. pastoris* protein.

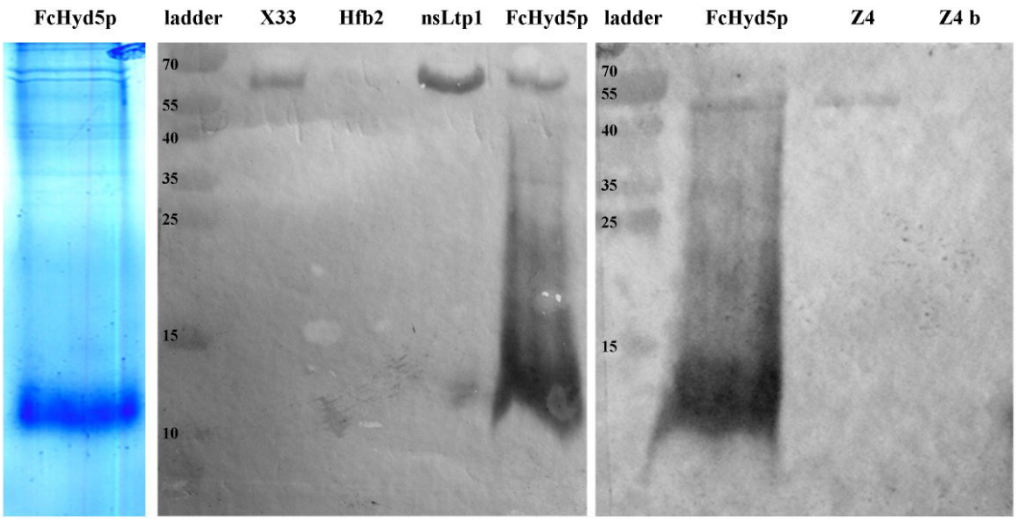

Figure 12: Reactivity of anti-FcHyd5p-P3-IgG with lyophilisates of *P. pastoris* wild type X33 (negative control), Hfb2, nsLtp1, protein Z4, heat treated protein Z4 (Z4 b) and FcHyd5p, separated by SDS-PAGE and transferred to Western blot analysis. Protein sizes are indicated in kDa; FcHyd5p on Coomassie stained SDS-gel is shown in lane 1.

To check whether the antibody was able to detect FcHyd5p in samples from the brewing process and in beer, Western blot analysis from pure and Berol purified samples was performed. German lager beer and a brewing process sample taken at the end of mashing from an experimental brew, with FcHyd5p lyophilisate added at the start of mashing, was examined after protein separation by SDS-PAGE. By Western blot analyses with antibody anti-FcHyd5p-P3-IgG, no bands were detected in the beer sample without using sample pre-treatment. After using Berol extraction to concentrate amphiphilic proteins, a weak band was visible in the range of the size of FcHyd5p (12 kDa). No other beer proteins showed cross reactions with the anti-FcHyd5p-P3-IgG antibody. In the mashing sample, in which a concentration of about 100 mg/mL of FcHyd5p was expected, a band in the size range of FcHyd5p was already visible when the sample was applied without further sample processing. Berol treatment of the mashing sample did not result in a further increase of signal intensity.

3.2.2 Development of FcHyd5p-ELISA

To test the hypothesis that hydrophobins are the causal agents for primary gushing in beer as well as to analyze the proposed negative impact of nsLtp1 on hydrophobin induced gushing,

an assay for the detection and monitoring of the class 2 hydrophobin FcHyd5p was developed.

To set up a competitive ELISA type assay, the surface of a microwell plate is coated with the antigen recognized by the specific antibody. The coating step is followed by incubation of the sample together with the specific antibody (primary antibody) in the microplate wells. Competitive binding of the antibody occurs by either interacting with the coated peptide or with the target antigen present in the sample. The more target protein is present in the sample, the lesser antibody will bind to the coating antigen on the solid phase. After washing steps and incubation with a labeled secondary antibody, the amount of primary antibody in the wells can be detected. Because of the competitive type of ELISA set up here, signal read out will be inversely proportionate to the antigen concentration present in a sample.

For test evaluation and application, the anti-FcHyd5p-P3-IgG antibody was used. Purified peptide FcHyd5p-P3 served as the coating antigen. For evaluation of the optimal working concentrations, a checkerboard titration of coating peptide FcHyd5p-P3 against optimal secondary antibody dilution was performed. The primary antibody concentration was kept constant in a dilution of 1:500 (v/v) in PBS buffer. In the same experiment the incubation time with PNPP substrate was also varied and evaluated.

Absorbance measurement was done using a serial dilution of the coating peptide in combination with four different dilutions of the secondary antibody (1:250, 1:500, 1:1,000 and 1:2,000 (v/v) in PBS). Optimum concentrations were compared at 4 different substrate incubation periods (0, 15, 30, 45 and 60 min) of substrate solution.

Color formation occurred immediately after PNPP addition. Increasing incubation times resulted in an increase in absorbance values in relation to the antibody dilution. The curves of lower dilutions showed a lower increase in absorbance values during the incubation period. At time point 30 min still all dilution curves had different absorbance values. These values of 3.7 (1:250), 3.6 (1:500), 3.2 (1:1,000) and 2.6 (1:2,000) were 2.6 to 3.8 times higher as compared to absorbances at time point zero (Figure 13). With further incubation time the absorbance values approached a saturation value of 4 for all secondary antibody dilutions.

The concentration of coating peptide FcHyd5p-P3 for which absorbance saturation was reached was also related to incubation time. With increased incubation times, saturation was already reached at lower FcHyd5p-P3 levels. After 15 min saturation was reached at 4-5 ng/100 µL, after 30 min at 3-4 ng/100 µL for all antibody dilutions tested. For incubation periods of 45 min and 60 min, the minimum saturation concentration further decreased to

2-3 ng/100 µL and 1-2 ng/100 µL, respectively. Exemplarily, results of the checkerboard assay are displayed for an incubation period of 30 min in Figure 13.

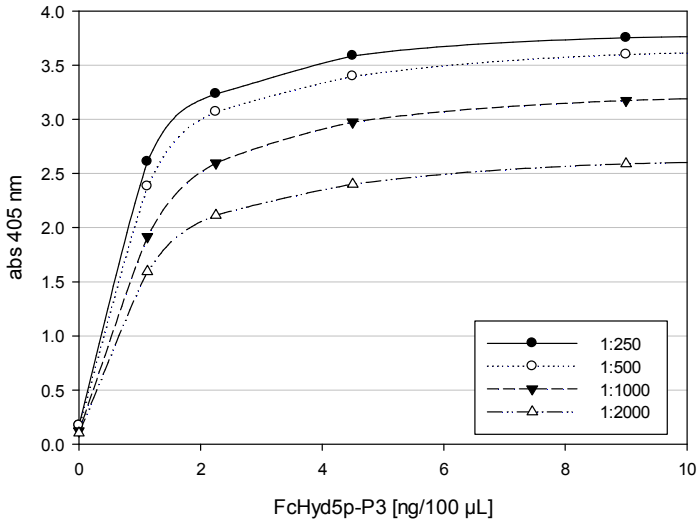

Figure 13: Absorbance values for FcHyd5p-ELISA checkerboard experiments with serial dilutions of coating peptide FcHyd5p-P3 and secondary antibody. Measurements were performed after 30 min incubation time with PNPP as the enzyme substrate.

Since no great differences between the curves obtained with secondary antibody dilutions of 1:250 and 1:500 were detectable, a goat-anti-rabbit-IgG-AP dilution of 1:500 for was used in further experiments. The optimum coating peptide concentration was below 4 ng/100 µL. The highest and most linear increase in absorbance occurred at concentrations between 1.125 and 2.25 ng/100 µL. As a consequence, an FcHyd5p-P3 concentration of 1.5 ng/100 µL was used in further experiments. 30 min substrate incubation time was used for ELISA experiments. For selected coating concentrations this time lay in the linear range of plots of time vs. coating-concentration, thus, quantitative measurement of absorbance decrease upon antigen detection was possible.

3.2.3 Evaluation of ELISA for the detection of FcHyd5p

A calibration curve for the ELISA assay was set up in order to quantify the amount of FcHyd5p in samples. Freeze dried transgenic FcHyd5p was dissolved to a concentration of 10 mg/mL in PBS and a serial 10 fold dilution (v/v) was directly applied to the ELISA and treated as described in 3.2.2. By this, a calibration curve in the concentration range from 0.016 mg/mL to 1 mg/mL was obtained, which showed a maximum absorbance of 1.8 at a concentration of 0.016 mg/mL. In the tested concentration range, a linear curve was obtained when FcHyd5p concentrations were plotted in half logarithmic scale against absorbance at

405 nm. The correlation coefficient calculated from the linear regression of the curve was $R^2 = 0.97$, indicating a strong correlation between parameters.

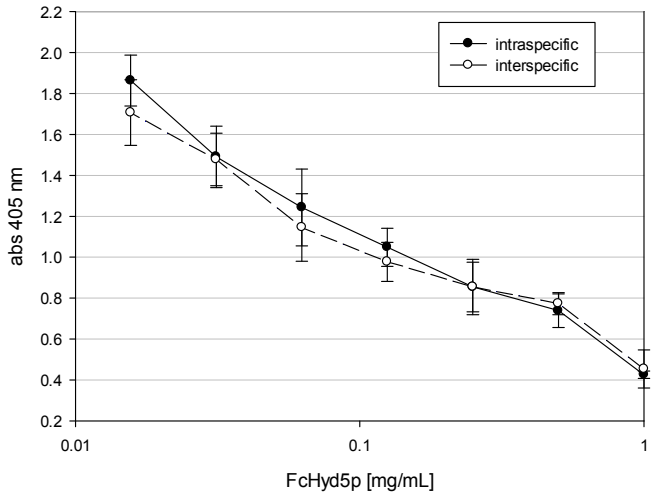

Figure 14: Intra- and interspecific variation of absorbance values for the calibration curve of the FcHyd5p-ELISA within one plate or three replicate plates, respectively.

The intraspecific and interspecific reproducibility of the standard curve was determined by incubation and measuring the standard samples three times within the same plate, or in parallel in three plates, respectively. As shown in Figure 14, a high reproducibility of the calibration curve was observed. The coefficient of variation, which is the ratio of the standard deviation to the mean value, was below 15 % for intraspecific variation for all FcHyd5p concentrations. For interspecific tests, the coefficient of variation was 20 % for the higher FcHyd5p concentrations, and also below 15 % at lower concentrations of the protein.

The recovery rate of the evaluated test was determined by applying a known concentration of FcHyd5p and calculating the concentration as measured with the ELISA assay. As shown in Figure **15**, the standard deviations of determined hydrophobin concentrations increased considerably at concentrations ≥ 50 µg/100 µl, indicating the assay was more reliable for FcHyd5p concentrations ≤ 30 µg/100 µl. However, deviations from applied concentrations were still high in lower concentrations. The overall recovery rate ranged from 85.9 % to 162.8 % over the range of tested concentrations.

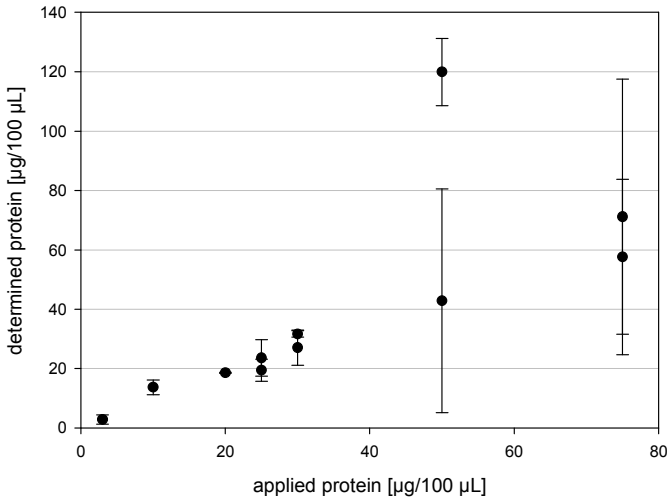

Figure 15: Recovery of applied protein lyophilisate FcHyd5p by the standard curve of the ELISA assay. Concentrations of 25-75 µg/100 µL FcHyd5p were measured two times in parallel ELISAs.

Experiments, in which the FcHyd5p ELISA assay was applied to analyze samples of beer and malt, resulted in high variation of the FcHyd5p concentrations upon repetitive measurement of individual samples. As a consequence, absolute determination of FcHyd5p concentrations in samples was not possible with the ELISA assay developed during the current study. Therefore, the assay was used only for the determination of FcHyd5p relative to concentrations found in a negative control by directly comparing absorbance values rather than concentrations.

Because the ELISA assay had been established mainly for the determination of FcHyd5p within the brewing process, where temperatures of up to 100 °C occur, the influence of temperature on the detectability of FcHyd5p was evaluated. Incubation for 1 h at 60 °C or 70 °C in deionized water increased the ELISA signal by 10 % compared to a sample incubated at 25 °C. For 90 °C the signal increased by 23 % and for 100 °C by 28 %.

Thermal treatment by incubation in synthetic wort resulted in a smaller increase in the ELISA signal. The signal increase after treatment at 70 °C was statistically insignificant compared to the signal at 25 °C. Only after incubation at 80 °C or 90 °C did a significant increase of 7.1 % ($P = 0.025$) occur. Upon boiling, the signal decreased by 7.9 % (see Figure 16).

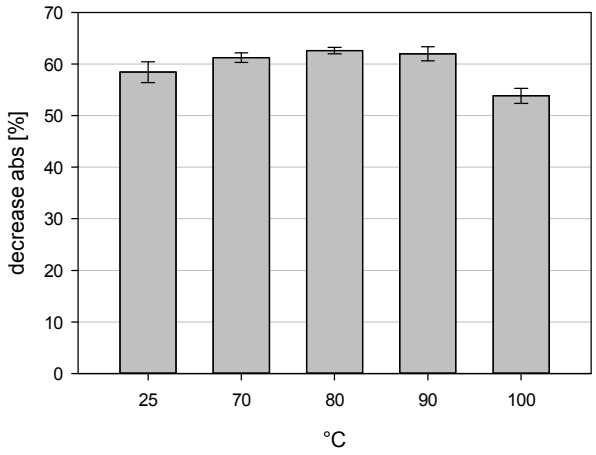

Figure 16: Influence of thermal treatment on the detectability of FcHyd5p in synthetic wort by the FcHyd5p ELISA assay.

3.3 Establishing an ELISA assay for the detection of nsLtp1

3.3.1 Antibody production and sensitivity

Polyclonal antibodies against a part of the protein sequence of nsLtp1 were acquired via the 'custom polyclonal antibody service'. The chosen peptide nsLtp1-P2, with a length of 16 aa, is equal to the sequence SKCNVNVPYTISPDID at position 71-86 of nsLtp1. It covers a region of relatively high hydrophobicity, where, according to secondary structure prediction and 3D model, no α helix is formed. nsLtp1-P2 lies at the N-terminal end of the protein and is, according to 3D structure, on the protein surface (Figure 17).

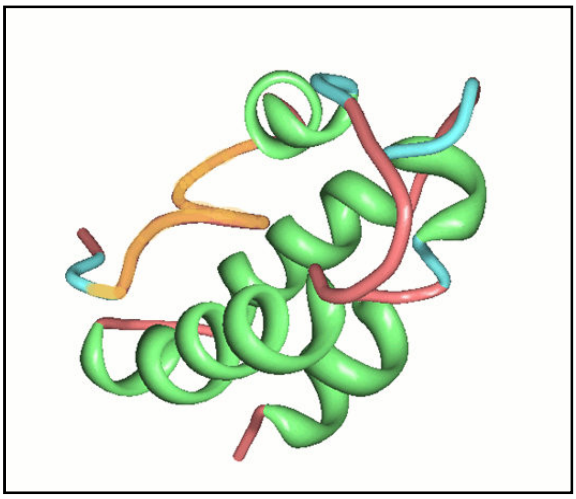

Figure 17: 3D structure of nsLtp1 without signal peptide sequence based on the NMR 3D structure provided by Heinemann et al. (1996) (PDB ID 1LIP). Peptide nsLtp1-P2 used for second antibody production is marked in yellow; green display: helix; turquoise display: turn; red display: coil.

According to BLAST analysis (Altschul et al., 1990), peptide nsLtp1-P2 matched the nsLTP1 protein of *H. vulgare*. BLASTing against non redundant protein databases of *Ascomycetes*, *P. pastoris* or *Saccharomycetes* resulted in no matches with max scores > 30. A search for matches with the nsLtp1-P2 peptide in the general non-redundant protein database resulted in several hits, partly matching lipid transfer proteins of cereals and grasses such as *Triticum aestivum* (wheat), *Oryza sativa* (rice), *Sorghum bicolor* (millet), *Setaria italica* (millet) and *Dactylis glomerata* (orchard grass). Also, Ltp proteins of non grassy plants such as *Stevia rebaudiana* (syn. *Eupatorium rebaudianum*, stevia), *Brachypodium distachyon*, *Dianthus caryophyllus*, *Solanum lycopersicum*, *Aegilops tauschii*, *Theobroma cacao, Nicotiana tabacum, N. attenuate* and *Glycine max* had alignment scores > 30.

The polyclonal antibody raised against peptide nsLtp1-P2 was designated as anti-nsLtp1-P2-IgG. Freeze dried preparations of transgenic nsLtp1 dissolved in water or synthetic wort were applied to SDS-PAGE followed by Western blot using antibody anti-nsLtp1-P2-IgG to check for specificity. As displayed in Figure 18, nsLtp1 in its native form was not recognized by the antibody. Only after heat treatment a band at the size of about 15 kDa became visible. This size matched with the protein band of nsLtp1 in Coomassie Blue stained SDS-PAGE gels. A band at about 70 kDa was also stained.

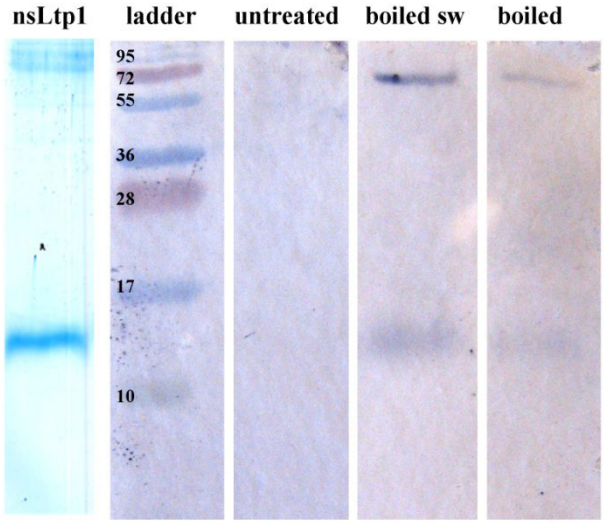

Figure 18: Reactivity of anti-nsLtp1-P2-IgG with nsLtp1 in native (untreated) and boiled form, separated by SDS-PAGE and analyzed by Western blot analysis. Heat treatment was performed in synthetic wort (boiled sw) and deionized water (boiled). Protein standards in kDa are present in lane 2; nsLtp1 on Coomassie stained SDS-gel is shown in lane 1.

Cross reactivity of the anti-nsLtp1-P2-IgG antibody was evaluated for lyophilisates of transgenic proteins FcHyd5p, FcHyd3p, protein Z4 as well as for lyophilisate obtained from the culture supernatant of the *P. pastoris* wild type strain X33, and a cytosolic extract of

P. pastoris X33 cells. After SDS-PAGE and Western blotting, no reaction of anti-nsLtp1-P2-IgG with Z4 or with any of the *F. culmorum* hydrophobins FcHyd5p and FcHyd3p was observed. Also after heat treatment of these proteins, no detection by the antibody occurred. However, a band at about 70 kDa was detected in Western blots prepared from the cytosolic extract as well as from the culture supernatant of the *P. pastoris* X33 strain. It was concluded that the lyophilisate contained a protein naturally produced as by-product during cultivation which was recognized by the nsLtp1 specific antibody.

anti-nsLtp1-P2-IgG was proposed to be used for nsLtp1 quantification in brewing and beer samples. Since beer made of barley malt and also beers containing a considerable portion of wheat malt were used, sensitivity of the antibody to the detection of wheat nsLtp1 was examined. Wheat nsLtp1 has a sequence homology of 72 % towards the barley nsLtp1 protein. BLAST analysis showed that 11 out of the 16 amino acids contained in the peptide nsLtp1-P2 used for immunization were homolog to the sequence of wheat nsLtp1 (GenBank: AAB22334) as shown in Figure 19. Also, peptide BLASTing of nsLtp1-P2 against databases of non redundant proteins gave a hit with wheat nsLtp1 with a maximum alignment score of 35.8 and query coverage of 93 %.

```
wheat.nsLtp1    IDCGHVDSLVRPCLSYVQGGPGPSGQCCDGVKNLHNQARSQSDRQSACNCLKGIARGIHN 60
nsLtp1-P2       ------------------------------------------------------------

wheat.nsLtp1    LNEDNARSIPPKCGVNLPYTISLNIDCSRV 90
nsLtp1-P2       ----------SKCNVNVPYTISPDID---- 16
                          .**.**:***** :**
```

Figure 19: Homology between peptide nsLtp1-P2, used for antibody production, and nsLtp1 of wheat (accession number AAB22334).

Western blot analysis of SDS-PAGE separated protein extracts of barley and wheat showed that proteins of wheat and barley were detected by the antibody. In case of barley extract, bands had the size of a monomer (about 10 kDa), and multimers (dimer, trimer, tetramer, and pentamer) of nsLtp1. In wheat samples no band corresponding to the nsLtp1 monomer with a predicted size of 9.6 kDa occurred. However, bands at 20 and 30 kDa were detected, corresponding to the size of the dimer and the trimer of nsLtp1, respectively.

Since the nsLtp1 specific ELISA should be used for the quantification of protein sample materials such as beer, grain and brewing process samples, the reactivity of the anti-nsLtp1-P2-IgG antibody was checked in Western blot analysis. For this purpose, proteins from samples taken at different steps within the brewing process (‘end of mashing’, ‘kettle wort’, ‘cooling wort’, ‘malt’) and from three different beers (lager, wheat, pilsner) were separated

by SDS-PAGE. After blotting, the transferred proteins were reversibly stained with Ponceau S to visualize all proteins before specific detection with anti-nsLtp1-P2-IgG.

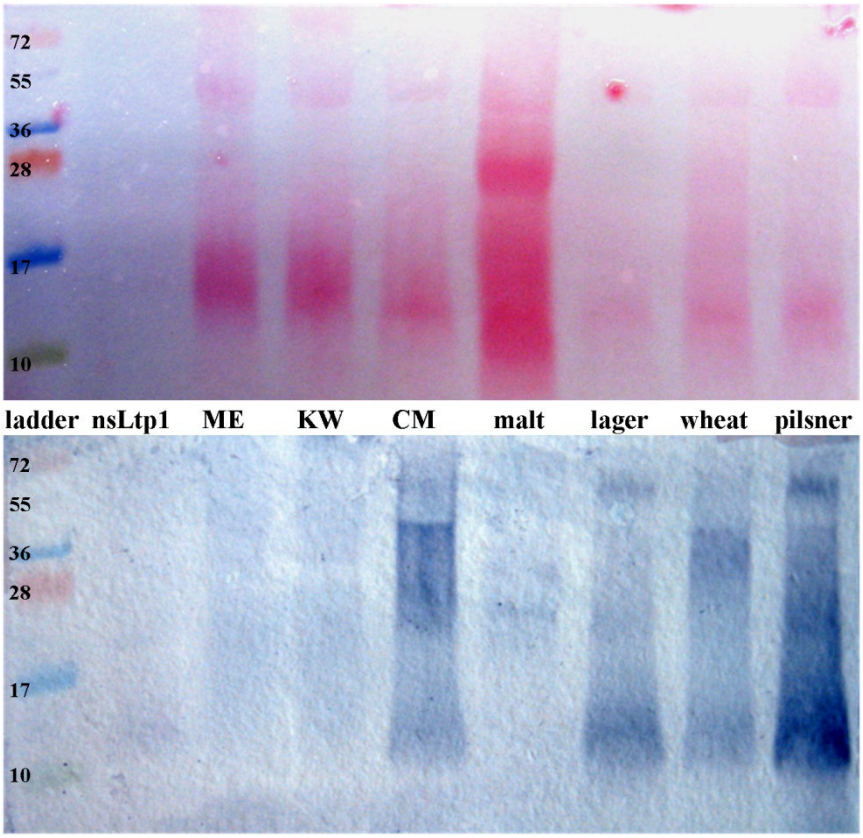

Figure 20: Western blot of brewing and beer samples separated by SDS-PAGE stained by Ponceau S (top) and after specific detection by anti-nsLtp1-P2-IgG (bottom). Samples applied were heat treated transgenic nsLtp1 (nsLtp1); brewing samples mashing end (ME), kettle wort (KW), cooling wort (CM), barley malt (malt) and beer samples (lager, wheat and pilsner). Protein standards in kDa are present in lane 1.

As shown in Figure 20, heat treated nsLtp1 could not be detected during Ponceau S staining. However, with the specific antibody the nsLtp1 was detected at a size of 12 kDa. Regarding the Ponceau S stain a clear decrease in total protein content from malt to samples of the subsequent brewing steps was detected. This indicates the presence of proteolytic processes during the brewing process. However, a band of 12 kDa was visible in all samples in the predicted size of nsLtp1 (Figure 20). In addition, in all samples a protein was present at about 40 kDa, corresponding to the size of barley protein Z. Specific detection of proteins with anti-nsLtp1-P2-IgG did not result in a clear resolution of the blot. However, in all samples apart from malt, a band corresponding to nsLtp1 was visible. These results indicate that the antibody recognized nsLtp1 in brewing samples and in beer. In cooling wort, lager, and pilsner beer an additional band between 55 and 72 kDa was observed. Furthermore, in

cooling wort, malt and beer samples a protein band of 20 kDa in size was stained which may represent a dimer of nsLtp1. Also bands between 36 and 55 kDa were detected by anti-nsLtp1-P2-IgG in these samples but not in the malt sample (Figure 20). An improper separation of nsLtp1 was assumed. As already shown, a cross reaction with protein Z, having a size of 40 kDa, can be excluded.

3.3.2 Development of nsLtp1-ELISA

For quantification and monitoring of nsLtp1 in beer and brewing samples, an indirect competitive ELISA assay with the specific antibody anti-nsLtp1-P2 was established. A checkerboard analysis with coating antigen nsLtp1-P2 against optimal secondary antibody dilution was performed in order to determine the optimum combination of concentrations for both components. Also the incubation time of the PNPP substrate was evaluated. The primary antibody concentration was kept constant at 1:500 (v/v) in PBS buffer.

Absorbance measurement directly after addition of PNPP substrate already resulted in saturation curves with higher absorbance at higher antigen concentration, reaching a plateau at a coating peptide concentration between 2 and 3 ng/100 µL. At antibody dilutions of 1:100, 1:200, 1:250 and 1:500, absorbance values 0.4, 0.3, 0.7 and 0.6 were reached. After 15 min of substrate incubation, curves were similar but smoother, and absorbance values had increased about 5 fold. Again, a plateau was reached for all antibody dilutions for a coating concentration between 2 and 3 ng/100 µl nsLtp1-P2. With further increasing incubation time of PNPP the difference in absorbance values between the different antibody dilutions decreased. Figure 21 gives an example of the data for a substrate incubation time of 30 min. After 30 min of incubation with the secondary antibody in dilutions of 1:250 and 1:500 a maximum absorbance of 3.8 and 3.6 was reached. Dilutions of 1:100 and 1:200 with absorbance values of 3.2 and 2.5, respectively, showed an eight fold increase of the absorbance signal as compared to time point 0 (Figure 21). After 60 min all curves had reached saturation at an absorbance of 4.0.

The curves' inflection points, at which saturation was reached, decreased with incubation times. After 15 min it lay between 2 and 3 ng/100 µL nsLtp1-P2, after 30 min it was 2 ng/100 µL. After 45 min of incubation, 1.5 ng/100 µL were sufficient, and after 1 h incubation reflection points lay between 1 and 1.5 ng/100 µL nsLtp1-P2.

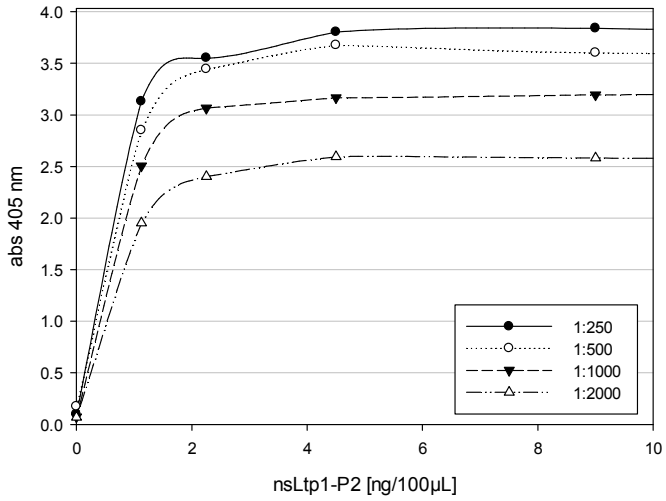

Figure 21: Absorbance values for nsLtp1-ELISA checkerboard experiments with serial dilutions of coating peptide nsLtp1-P2 and secondary antibody. Measurements were performed after 30 min incubation time with substrate PNPP.

Because of the saturation levels gained by these experiments for peptide concentration above 2 ng/100 µL, a concentration of 1.5 ng/100 µL was used in further experiments with the nsLtp1-ELISA assay. Substrate incubation time of 30 min was chosen since this lay in a linear range of a curve resulting from plotting the substrate incubation times against the absorbance values for coating of 2.25 ng/100 µL and 1.125 ng/100 µL of nsLtp1-P2 peptide. Dilutions of secondary antibody of 1:250 and 1:500 gave similar curves in plots of absorbance against coating peptide concentration. A dilution of 1:500 was chosen because less secondary antibody was necessary in the test.

3.3.3 Evaluation of ELISA for the detection of nsLtp1

To be able to quantify the tested samples used in the nsLtp1-ELISA and as positive control, a calibration curve was set up with an aqueous solution of transgenic nsLtp1. Since the antibody only recognized denatured nsLtp1, lyophilisate was dissolved in PBS and incubated in a boiling water bath for 1 h prior to dilution and testing.

Using a 1:1.5 (v/v) serial dilution of transgenic nsLtp1 resulted in a reproducible calibration curve with a linear range in a half logarithmic scale. Intraspecific variation coefficient for parallel applied standard curves in one plate lay between 0.2 % and 11.5 % with a correlation coefficient of $R^2 = 0.9394$. Interspecific variation within three plates was between 5.0 % and 19.8 %. The resulting linear curve had a correlation coefficient of $R^2 = 0.9774$ (Figure 22). Heat treatment of nsLtp1 dissolved in synthetic wort resulted in a comparable signal measured by ELISA.

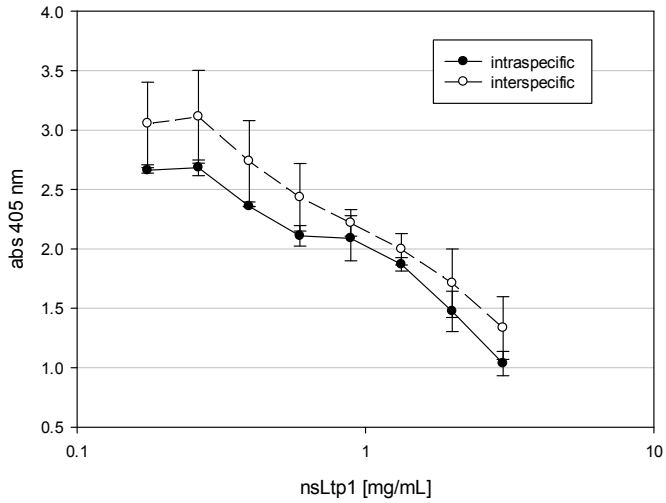

Figure 22: Intra- and interspecific variation of absorbance values for the calibration curve of the nsLtp1-ELISA within one plate or three plates, respectively.

To confirm that the established ELISA was suitable to detect and quantify nsLtp1 in beer samples, beer was applied to the assay, which had previously been examined for the occurrence of nsLtp1 by Western blot analysis. As shown in Figure 23, the signal obtained by ELISA correlated with the amount of nsLtp1 as assessed in Western blot analysis. In contrast to beers A, F and Ö, samples of beer S showed no band in Western blots. In accordance with the Western blot results, by ELISA a higher amount of nsLtp1 was detected in beers A, F and Ö compared to beer S. However, big differences between results were observed when the ELISA was replicated with the same samples. Again, beer A contained more nsLtp1 than beer S, however, values were much higher and increased from 122 mg/mL in the first ELISA assay run to 400 mg/mL nsLtp1 in the second ELISA assay in beer A. A similar increase was detected in beer samples F and Ö (Figure 23).

As a consequence of these results, the ELISA was used to determine relative amounts of nsLtp1 in tested samples. The reciprocal absorbance values were evaluated and used for comparison of samples without calculating concentrations of the antigen.

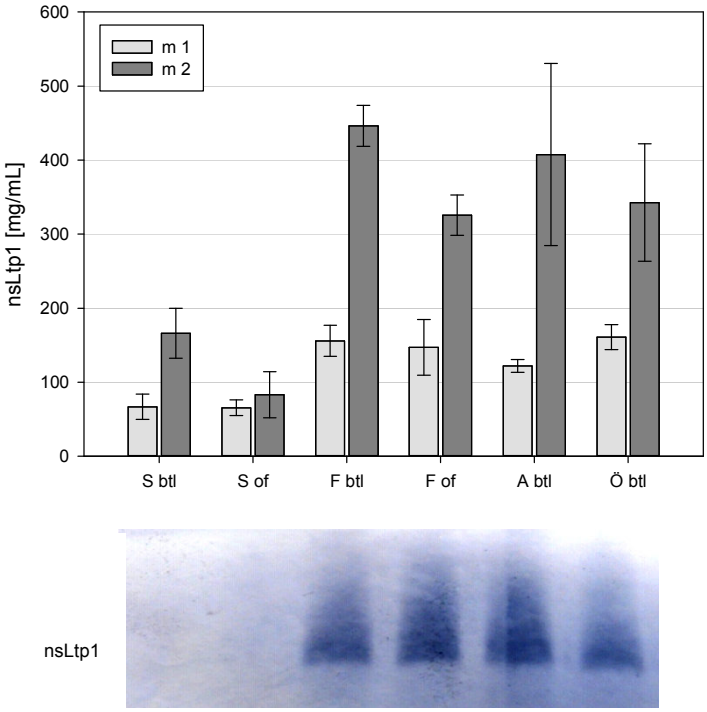

Figure 23: nsLtp1 content in beer detected by ELISA in two different test runs, m 1 and m 2 (top), and Western blot of samples of the same beers (bottom). Samples of beers S, F, A, and Ö; for gushing beers both fractions 'of' (overfoamed beer) and 'btl' (beer remaining in the bottle after gushing) were analyzed.

3.4 Monitoring FcHyd5p during the brewing process

To monitor FcHyd5p during the brewing process, samples from experimental brews were examined to which hydrophobin FcHyd5p had been added at different steps of the brewing process. Preliminary experiments in which 10 g and 20 g of freeze dried cell free culture supernatant from an FcHyd5p producing transformant of *P. pastoris* were added at the start of mashing, did not result in the production of a gushing beer. Nonetheless, samples taken at different steps of the brewing process in the experiments were analyzed for FcHyd5p using the ELISA developed during the current study. The by ELISA assay determined relative amounts of FcHyd5p per volume of examined samples multiplied per volume of the corresponding brewing step were used for experimental evaluation. No initial difference was found in the amount of FcHyd5p in samples 'mashing end' when experiments with addition of 10 g and 20 g of the lyophilisate were compared. In the finished beer, the content of FcHyd5p was even higher for the sample produced with addition of 10 g. Both experiments showed elevated levels of FcHyd5p upon lautering with high signals in 'kettle wort' and in 'last running'. In 'spent grain' the amount of FcHyd5p was comparable to the one of

'mashing end'. After wort boiling, in 'cast wort' an increased amount of FcHyd5p as compared to 'mashing end' was detected. However, the level detected was lower than in lautering samples. The processes of fermentation and filtration had a positive influence on the detection of FcHyd5p. In beer the amount of the hydrophobin increased as compared to the beginning of the brewing process (Figure 24).

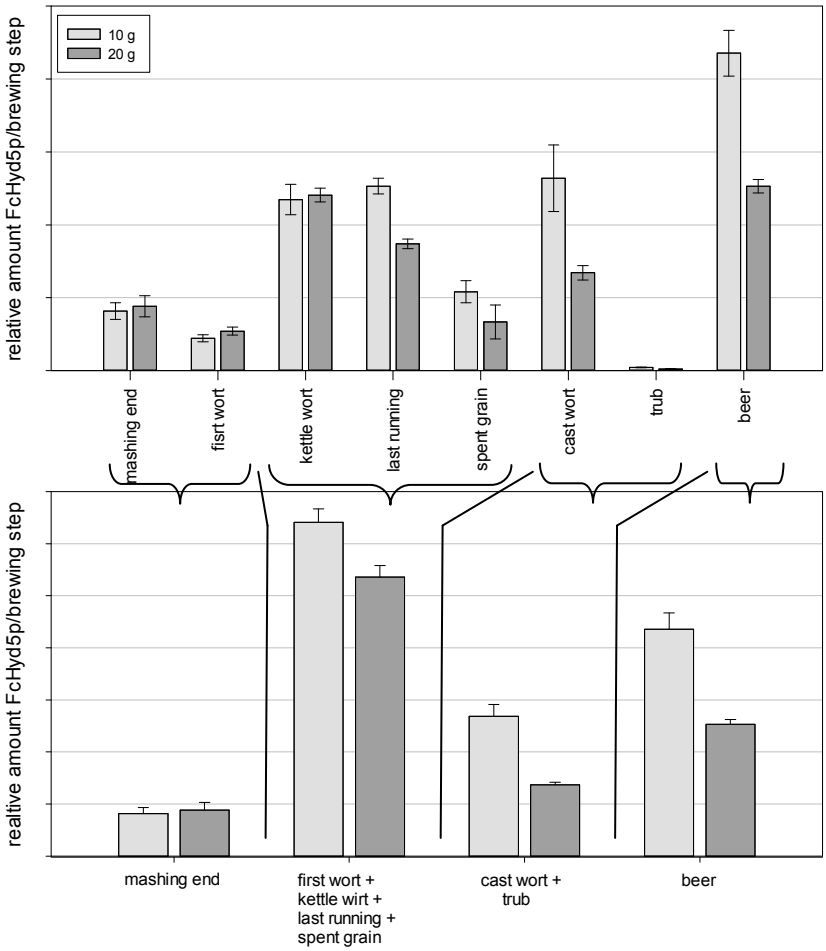

Figure 24: Content of FcHyd5p as relative amount as determined by ELISA per volume of brewing sample of brews with addition of 10 g or 20 g lyophilisate of FcHyd5p at begin of mashing, determined by ELISA. The relative content in each brewing sample (top) and the summarized amounts of FcHyd5p within corresponding brewing steps (bottom) are shown.

Samples of four brewing experiments with addition of freeze dried cell free culture supernatant of an FcHyd5p producing *P. pastoris* transformant strain (120 mg/L) at different steps of the brewing process were analyzed.

The addition of 120 mg/L lyophilisate should result in 6 mg/0.5 L in finished beer under the assumption that no loss occurred during brewing. Addition of 6 mg hydrophobin lyophilisate to non-gushing beer had resulted in 180 mL gushing volume from a 0.5 L bottle. This means

that addition of 120 mg/L into the brewing process should result in similar gushing of the produced beer provided that no loss of hydrophobin occurred.

Figure 25 shows the brewing process with sampling points and time points of protein addition in brews b1-b4. Points of addition were designated as ‘mashing begin’ (b1), ‘kettle wort’ (b2), ‘begin boiling’ (b3) and ‘whirlpool’ (b4). In effect, none of the beers produced showed gushing. Relative amounts of FcHyd5p determined in the brewing samples with the ELISA assay are given in Figure 26.

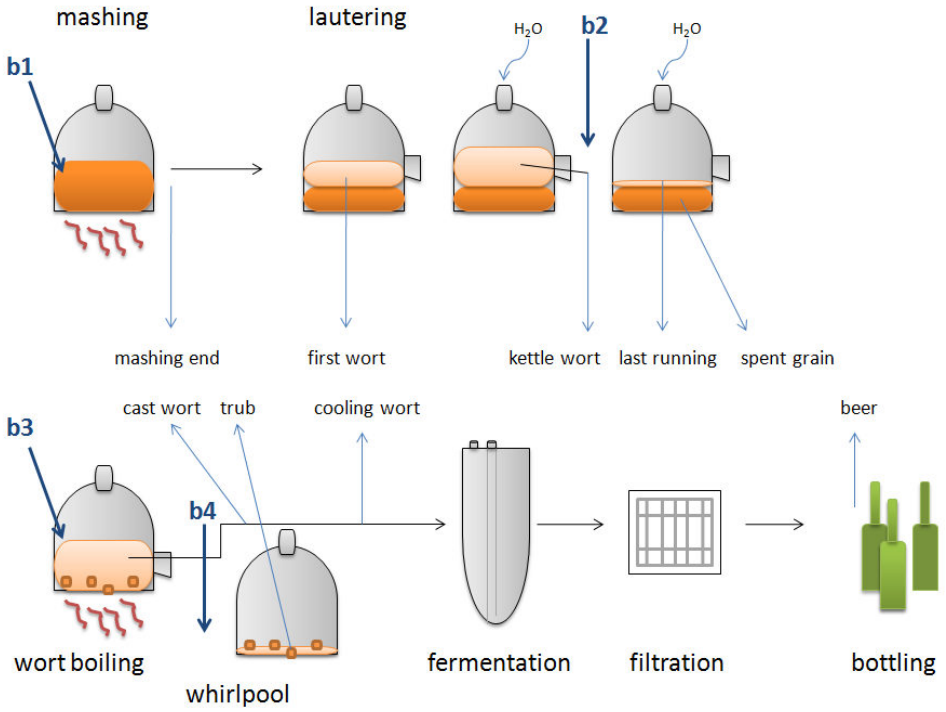

Figure 25: Schematic representation of the brewing process with addition of FcHyd5p or nsLtp1 (120 mg/L). The addition points in brews b1-b4 and the sampling points are indicated (arrows).

In brews b2 and b3, where FcHyd5p was added to ‘kettle wort’ or to ‘begin of wort boiling’, respectively, an increased content of FcHyd5p was detected upon addition. In both brews, for samples of ‘kettle wort’ taken after hydrophobin addition, the inverse ELISA signal was increased as compared to samples taken before hydrophobin addition. In b4 the ‘cooling wort’, where FcHyd5p was added, a similar absorbance as in ‘cooling wort’ samples of the other brews was detected. No explicit increase was observed at this stage despite the addition of hydrophobin (see Figure 26A).

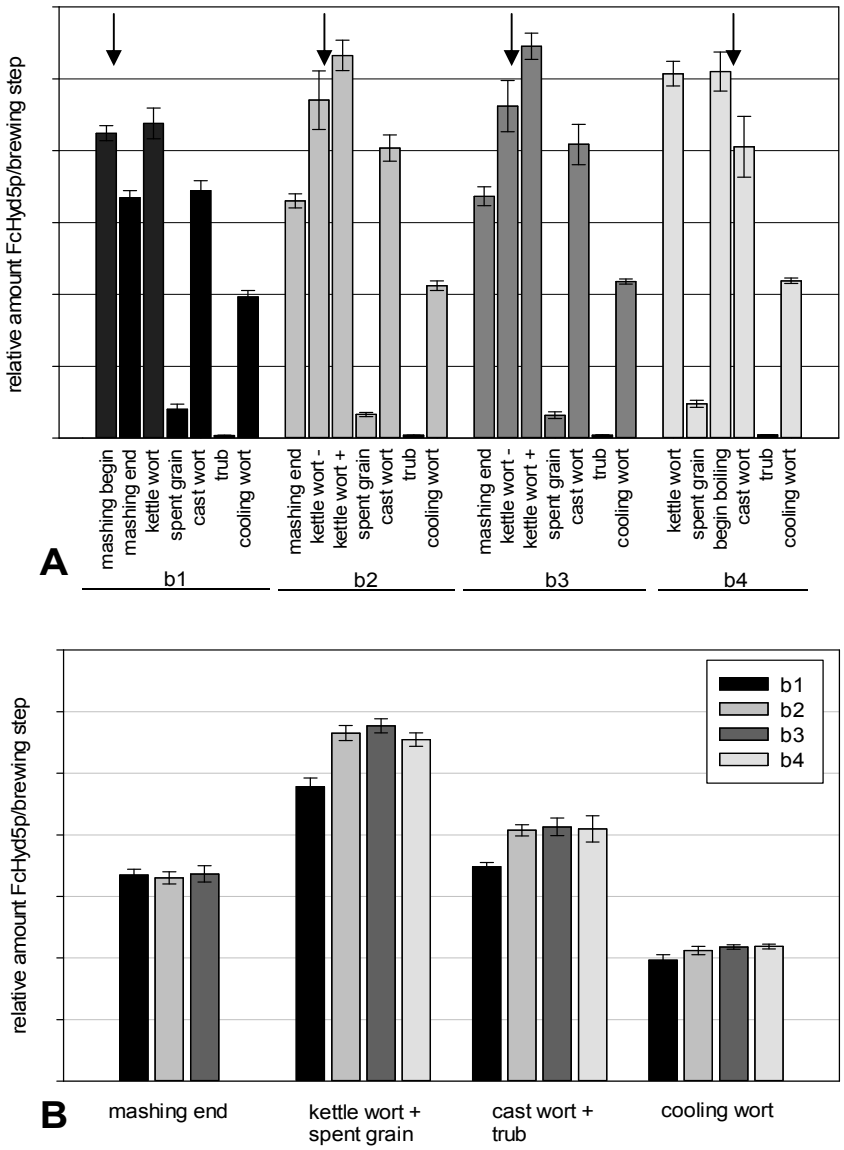

Figure 26: Content of FcHyd5p as relative amount as determined by ELISA per volume of brewing sample of brews after addition of transgenic FcHyd5p protein (120 mg/L) at different brewing steps (marked with arrows for brews b1-b4). A: amount of FcHyd5p per brewing sample; B: summarized amounts of FcHyd5p within corresponding brewing steps.

In all four brewing experiments, no signal was detected in 'trub' samples, indicating that no loss of hydrophobin occurred via the trub. A minor loss occurred via 'spent grain', containing only small amounts of FcHyd5p. However, the detection of FcHyd5p decreased in the wort boiling process. In 'cast wort' samples of all brewing experiments, less FcHyd5p was present as compared to 'kettle wort' before boiling. Also in b4, the sample 'cast wort' taken after boiling process showed a decreased signal as compared to 'begin boiling' (Figure 26A). The sum of relative amounts of FcHyd5p per brewing steps belonging together are shown in Figure 26B. For all brews, detected FcHyd5p increased during lautering as compared to

‘mashing end’ samples, whereas after wort boiling the signal decreased again. In the following ‘cooling wort’ even less FcHyd5p was detected than in ‘mashing end’ samples.
Addition of FcHyd5p in the ‘begin of mashing’ (b1) seemed to lead to reduced accessibility of FcHyd5p during brewing, with the signal being smaller in all samples compared to the other brews after FcHyd5p addition. Mashing led to a loss of FcHyd5p. This also was visible by comparison of amounts of FcHyd5p in ‘mashing end’ samples of different brews. Here, in b1 with FcHyd5p addition a similar signal was detected as in b2 and b3, although hydrophobin was not yet added to these brews (see Figure 26A, B).

3.5 Monitoring nsLtp1 during the brewing process

In separate experiments nsLtp1 lyophilisate (120 mg/L) was added to different steps during brewing. Addition points of nsLtp1 were ‘mashing begin’ (b1), ‘kettle wort’ (b2), ‘begin boiling’ (b3) and ‘whirlpool’ (b4) (see Figure 25). For nsLtp1, 6 mg of the used lyophilisate were experimentally shown to be sufficient for gushing reduction induced by 2 mg of hydrophobin FcHyd5p in 0.5 L bottles of beer. The chosen amount of transgenic protein addition, which was extrapolated to result in 60 mg/0.5 L in finished beer, results in an excess of nsLtp1, even with a considered loss of 90 % during the brewing process. None of the finished brewed beers showed gushing. Brewing samples were taken and applied to ELISA. Relative amounts of nsLtp1 as determined by ELISA were calculated per volume of corresponding examined brewing step. Comparison of the four brews showed no significant differences in nsLtp1 content for samples as related to supplement of nsLtp1. Addition of heterologous protein was not measurable (Figure 27A). Of the samples that were not used further in brewing, namely ‘last running’, ‘spent grain’, and ‘trub’, only ‘spent grain’ showed significant levels of nsLtp1 in all brews. The relative amount of nsLtp1 detected in ‘kettle wort’ was higher when compared to ‘mashing end’. ‘Cast wort’ exhibited almost the same signal as ‘beer’ within one brew, indicating that no loss of nsLtp1 occurred during brewing in the processes of fermentation, filtering and filling (Figure 27A).
Accordingly, calculated amounts of nsLtp1 per brewing step, as displayed in Figure 27B, showed that lautering process had a positive influence on nsLtp1 content. But the detection decreased again after wort boiling, with lower total content of nsLtp1 in ‘cast wort’ and ‘trub’ as compared to the summarized lautering samples. Further brewing did not lead to changes in the measureable nsLtp1, since in beers the level was not significantly different to those of boiled wort samples. A decrease of nsLtp1 was, however, observed in ‘cooling wort’

as compared to ‘cast wort’ (Figure 27B). Across the whole brewing process an increase of nsLtp1 was detected by ELISA. This increase seemed to be caused by processes during lautering.

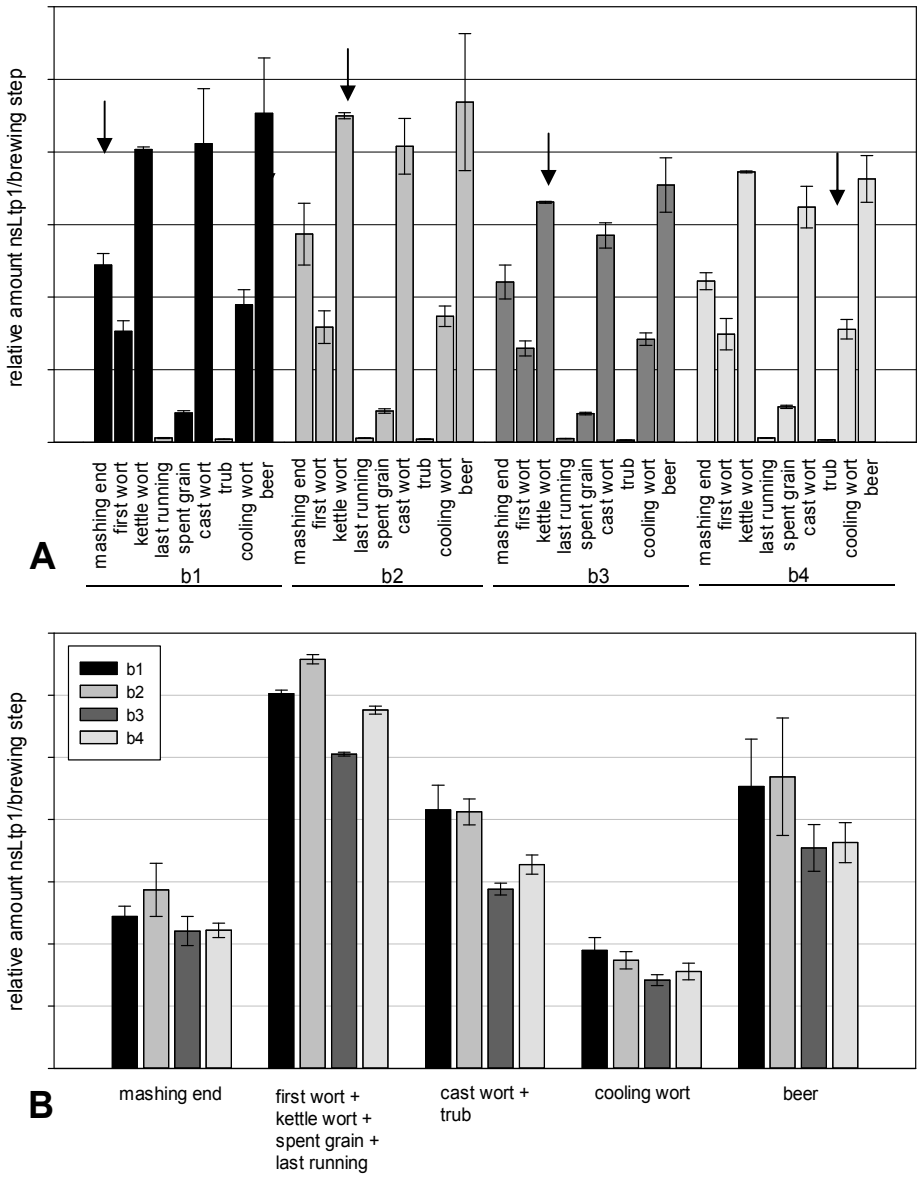

Figure 27: Content of nsLtp1 as relative amount as determined by ELISA per volume of brewing sample of brews after addition of transgenic nsLtp1 protein (120 mg/L) at different brewing steps (marked with arrows for brews b1-b4). A: amount of nsLtp1 per brewing sample; B: summarized amounts of nsLtp1 within corresponding brewing steps.

3.6 Investigation of contents of nsLtp1 and FcHyd5p in grain and malt samples

Artificial infection with *F. graminearum* or *F. culmorum* was expected to increase the content of hydrophobin in malt and cereals. It can further be expected that the expression of barley nsLtp1 will increase upon fungal infection of the plant. Infected samples of malt and grain were analyzed to confirm that the ELISA assays, established for detection of FcHydp5 and nsLtp1, were able to monitor the respective protein directly in samples. Results were compared to non-infected controls. The ELISA sample preparation was based on the weight of cereal and malt. An infection with fungi, however, leads to a decrease of protein content of grains (Sarlin et al., 2005a; Schwarz et al., 1996). Thus, less proteinogenic grain material would be used within the assay as compared to less or non-infected barley. To minimize this effect the ELISA results were analyzed with regard to the whole protein content of the sample.

3.6.1 Artificially infected grain

Barley was examined after artificial infection with *F. culmorum* in the field at the time of flowering. Samples of *Fusarium* inoculated and non-inoculated barley were provided by Andrea Linkmeyer (Lehrstuhl für Phytopathologie, Freising, Germany). Two varieties of barley, namely Marthe and Quench, with infected and control samples each of different infection years (2010, 2011) were used during the study. To estimate contamination rates, grains were plated on agar plates and fungal infestation was determined microscopically (Denschlag et al., 2013). Results of ELISA assays for the detection of nsLtp1 and FcHyd5p, and the infestation rates with fungi producing hydrophobin, which may be recognized by the antibody used against FcHyd5p (see chapter 3.2.1), are listed in Table 24.

Results of total protein determination by Bradford assay showed that infected barley contained 6 % - 16 % less protein than the corresponding negative controls.

For FcHyd5p the ELISA tests resulted in a positive signal in infected samples, and also in barley which had not been field infected with *F. culmorum*. The amount of hydrophobin was, however, increased in artificially infected barley when compared to the corresponding control without infection. Inverse ELISA signals increased significantly by 12 % - 52 % (Table 24).

The analysis of samples via nsLtp1-ELISA showed a significant difference between infected and non-infected samples for Marthe barley. For both test years the nsLtp1 content increased

significantly in the infected samples (P = 0.007 year 2010; P = 0.02 year 2011). Also, infected Quench samples of the year 2010 showed a significant increase compared to the corresponding control (P = 0.041). Samples of Quench of 2011 showed no difference in nsLtp1 amounts between infected and non-infected grains, which can be explained by the high standard deviation in the control sample. The ratio FcHyd5p:nsLtp1 increased in infected grain for both examined Quench samples and for Marthe sample of 2010 (Table 24).

Table 24: Fungal infestation rate with fungi producing FcHyd5p similar hydrophobin, as well as relative amount of FcHyd5p, and relative amount of nsLtp1 of samples of barley artificially infected with *F. culmorum* compared to respective control.

Infection	Yariety	Year of infection	% infestation	relative amount FcHyd5p per g protein	relative amount nsLtp1 per g protein	Ratio FcHyd5p: nsLtp1
-	Marthe	2010	8	5.37 ± 1.18	3.55 ± 0.19	1.51
F. culmorum	Marthe	2010	84	8.15 ± 0.49	4.50 ± 0.26	1.81
-	Marthe	2011	8	8.42 ± 0.14	4.36 ± 0.30	1.93
F. culmorum	Marthe	2011	82	10.06 ± 0.11	5.39 ± 0.37	1.87
-	Quench	2010	0	5.50 ± 0.33	3.81 ± 0.21	1.44
F. culmorum	Quench	2010	49	6.72 ± 0.45	4.29 ± 0.18	1.57
-	Quench	2011	n.d.	8.88 ± 0.14	5.72 ± 1.69	1.55
F. culmorum	Quench	2011	57	9.94 ± 0.02	5.39 ± 0.18	1.84

3.6.2 Artificially infected malt

Wheat malt, which was infected at start of malting by inoculation of fungal spores into the soft water, was analyzed by ELISA assays for FcHyd5p and nsLtp1. The malt was produced and provided by Ekaterina Minenko (Lehrstuhl für technische Mikrobiologie, Freising, Germany). For the infection, *F. graminearum* wild type and a mutant of *F. graminearum* with knockout of the gene coding hydrophobin *hyd5* were used. A control malt with no infection served as negative control.

With the ELISA assay, differences in the FcHyd5p content were already visible without correction for total protein content. Infected wheat with wild type *F. graminearum* showed a significant 1.3 fold increase of the signal as compared to the negative control (P = 0.043). After correction for the total protein content, a significantly higher amount of FcHyd5p was present in the wild type infected malt, which increased by 65.5 ± 10.4 % as compared to the negative control (Figure 28). The infection with a *hyd5* deficient *F. graminearum* strain resulted in a reduction of FcHyd5p, but the ELISA still detected more than in the non-

infected control with an increase of 16.5 ± 4.5 % (P = 0.038) of the reverse ELISA signal (Figure 28).

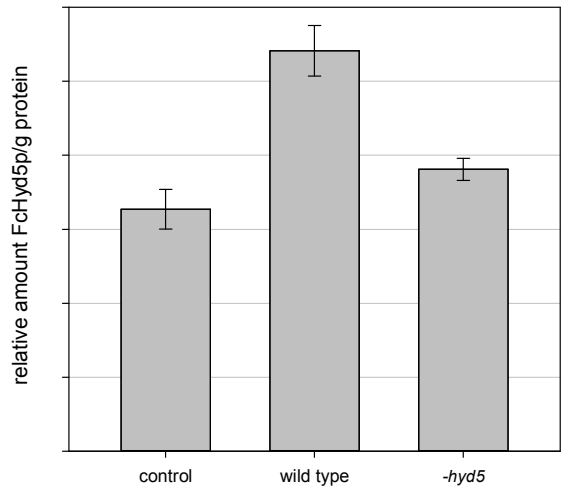

Figure 28: Relative amount of FcHyd5p in artificially infected wheat malt. Wheat malt was inoculated with spores of *F. graminearum* during malting. control: malt without inoculation; wild type: malt inoculated with wild type spores; *-hyd5*: malt inoculated with *hyd5* deficient strain.

The content of nsLtp1 in the wheat malt was also determined. As the antibody used also recognized Ltp of wheat (see chapter 3.3.1) the application of the ELISA was possible. No influence of malt infection on the nsLtp1 content was observed. Neither direct content nor nsLtp1 level corrected for total protein in the malt was related to infection with *F. graminearum* during malting. Also, no significant difference occurred when the FcHyd5p-knockout strain was used for infection. A similar signal in ELISA was measured for all three samples (data not shown).

3.6.3 Malt with determined gushing potential

Gushing and non-gushing malt were examined with regard to the occurrence of nsLtp1 or FcHyd5p. In addition, the correlation between concentrations of the proteins and gushing potentials in corresponding samples was investigated. Therefore, malts which had previously been tested for their gushing potential by either the Donhauser test or MCT were examined with the two ELISA assays developed during the current study.

3.6.3.1 Analysis of malt tested with the Donhauser test

Malt samples of wheat and barley, previously tested for their gushing potential with the Donhauser test, were supplied by BLQ (Forschungszentrum Weihenstephan für Brau- und

Lebensmittelqualität, Freising, Germany). The overfoaming volume of the samples ranged from 3 g to 599 g. Of the 11 barley samples, 7 had been tested to be gushing instable (gushing volume > 30 g), 3 were labile (gushing volume 10 g to 30 g) and one was declared as stable towards gushing (gushing volume < 1 g). All three wheat malts examined had been tested to be gushing instable. No correlation between total protein content in the malt extracts and the corresponding overflow volume in the Donhauser test was detected.

ELISA results showed that for barley malts a negative correlation between nsLtp1 content per g total protein and the overfoaming volumes of the corresponding malt samples was detectable with a coefficient of correlation of $R^2 = 0.52542$ (see Figure 29). No correlation was found, however, when wheat malts were analyzed in the same way.

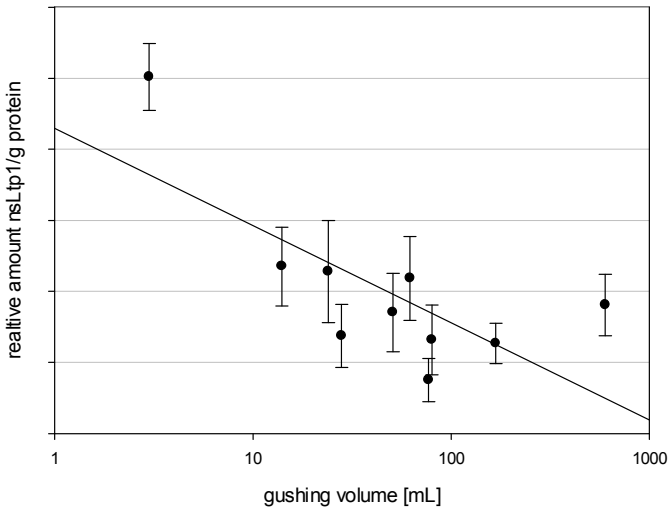

Figure 29: Relative amount of nsLtp1 in barley malt plotted against the overflow volume determined by Donhauser test.

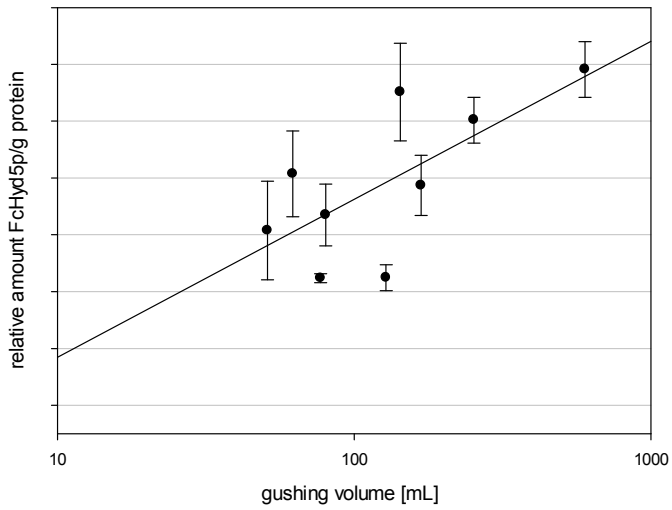

Figure 30: Relative amount of FcHyd5p in barley and wheat malt predicted to be gushing instable plotted against the overflow volume determined by Donhauser test.

For FcHyd5p no correlation between the amount of hydrophobin and gushing volume was observed when all malt samples were taken into account. However, when comparing only the malts which were predicted to be gushing instable, a positive correlation with a correlation factor of $R^2 = 0.4835$ was found between loss of volume in the Donhauser gushing test and FcHyd5p contents per g total protein (Figure 30).

By comparing the ratio between FcHyd5p and nsLtp1 with the gushing volumes of corresponding malt samples, a positive logarithmic correlation with a correlation factor of $R^2 = 0.5467$ was detected, when only barley malt samples were taken into account (data not shown).

3.6.3.2 Analysis of malt tested with the modified Carlsberg test (MCT)

Barley malt samples dating from 2010 to 2012 were supplied by a German brewery. Samples had been tested for their gushing potential at the brewery's own lab using the modified Carlsberg test (MCT). A total of 49 malt samples were examined with 17 being gushing negative and 32 being gushing positive with overflow volumes between 35 g and 211 g.

No correlation between total protein content and gushing potential of the malt was observed. Relative amounts of nsLtp1 determined by ELISA did not show any difference between malt being predicted gushing positive or malt with no gushing potential. A relative amount of nsLtp1 per g protein of $1.348*10^{-2} \pm 0.718 *10^{-2}$ and $1.424*10^{-2} \pm 0.745*10^{-2}$ was determined for gushing and non-gushing malt, respectively. For FcHyd5p, also no significant differences of relative amounts of FcHyd5p between gushing negative malt and gushing malt was detected. ELISA resulted in a decrease of absorbance per total protein content of 1.90 ± 1.22 % and 2.28 ± 1.30 % in gushing and non-gushing malt, respectively. Different to the Donhauser tested malt, no correlation between overflow amount in the MCT gushing test and the content of nsLtp1 or FcHyd5p appeared. Also after the classification of the malt according to the gushing potential, with less than 5 g loss no gushing, with 5 g - 50 g loss 50 % gushing probability and with > 50 g loss 90 % gushing probability, no correlation was found between gushing volume and either FcHyd5p or nsLtp1 content. The ratio of FcHyd5p to nsLtp1 was not significantly different between gushing and non-gushing malt. Also the difference in the ratio between malt with 50 % and malt with 90 % gushing probability was insignificant.

3.7 Investigation of contents of nsLtp1 and FcHyd5p in beer

3.7.1 Non-gushing beer of different types

The amount of nsLtp1 and FcHyd5p in beer of different types with no gushing occurrence was evaluated. The tested types of beer were lager beer, wheat beer and pilsner. For each type of beer, two bottles (0.5 L, purchased from retail) from the same batch were examined. The measured relative amounts of FcHyd5p and nsLtp1 in different beer types are illustrated in Figure 31.

In lager and wheat beer with 58.3 ± 8.6 % and 60.2 ± 10.9 % decrease in absorbance, respectively, a higher content of FcHyd5p was detected when compared to pilsner, with a decrease of absorbance of 47.1 ± 8.6 %. This difference, however, was only significant between pilsner and lager beer (P = 0.032). The amount of nsLtp1 was comparable between lager and pilsner beer with a reciprocal absorbance of about 0.7 ± 0.1. In comparison, wheat beer had a significantly higher amount of nsLtp1 with 2.6 ± 0.3 1/abs.

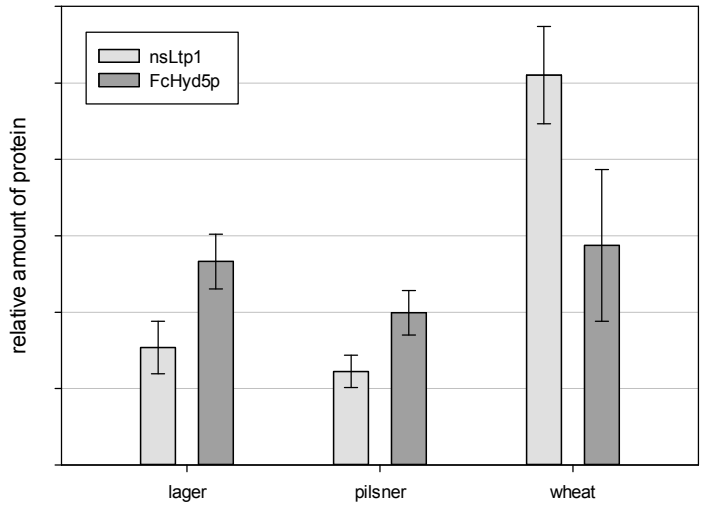

Figure 31: Relative amount of FcHyd5p and nsLtp1 in non-gushing beer of different types.

3.7.2 Comparison of gushing and non-gushing beer each of one brew

Gushing and non-gushing beers of one brewery were analyzed by ELISA for FcHyd5p and nsLtp1. All 12 gushing bottles were ‘Märzen’ type of the same brew. The 12 non-gushing bottles were of the same type, however, of a second brew. Before ELISA analysis, beer bottles (0.5 L) were submitted to gushing tests. After opening and measuring the weight loss, fractions ‘of’ and ‘btl’ were collected for ELISA tests. Unexpectedly, the beer which was

declared as non-gushing by the brewery, also showed gushing with even higher volume losses than gushing beer.

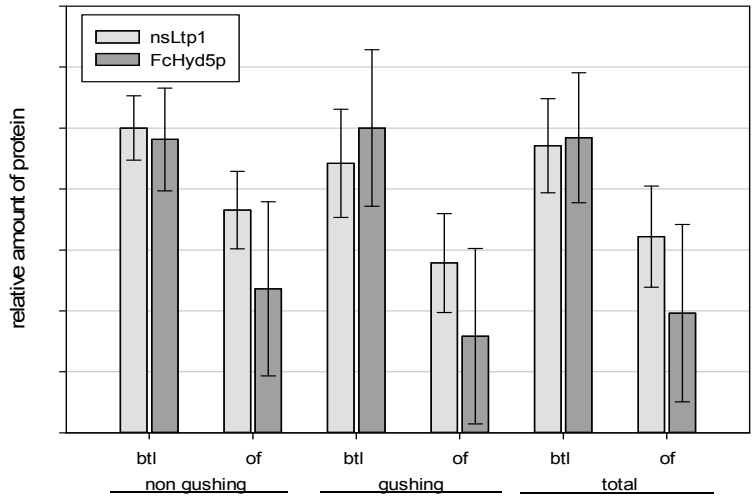

Figure 32: Relative amount of nsLtp1 and FcHyd5p in beer fractions overfoamed ('of') and rested in the bottle ('btl') after gushing. Values are given as average of declared non-gushing beers, gushing beers and the total of gushing and non-gushing beers, respectively.

ELISA tests for detection of nsLtp1 and FcHyd5p, respectively, in fractions 'of' and 'btl' were carried out. Results are shown in Figure 32. The nsLtp1 content in the 'btl' fraction was increased compared to the 'of' fraction ($P < 0.001$) for average of all beers. This was also true if the declared non-gushing beer ($P = 0.001$) and the declared gushing beer ($P < 0.001$) were viewed separately. A similar result was observed for FcHyd5p. A significant increase of FcHyd5p in 'btl' was detected in all calculations: separately for declared non-gushing or gushing beer and for the average of both (P values < 0.001) (Figure 32).

Regarding the relative protein amounts in the total beer as sum of both fractions, nsLtp1 was significantly decreased by 11.0 % in gushing beers in comparison to declared non-gushing beers ($P < 0.001$) (Figure 33). No correlation between gushing volume and nsLtp1 content was detected when all gushing or only as gushing declared beers were investigated. For declared non-gushing beers, however, a trend was observed with increased nsLtp1 content in beers that exhibited higher volume loss by gushing with a coefficient of correlation of $R^2 = 0.3062$ (Figure 34).

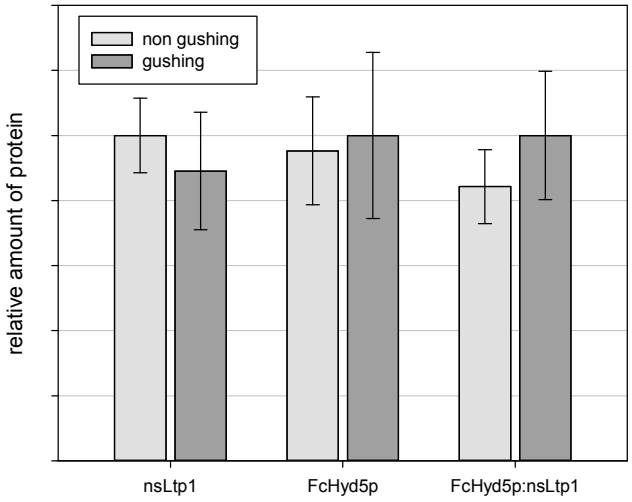

Figure 33: Relative amount of nsLtp1 and FcHyd5p, and the ratio of FcHyd5:nsLtp1 in gushing and non-gushing beer according to statements of the brewery.

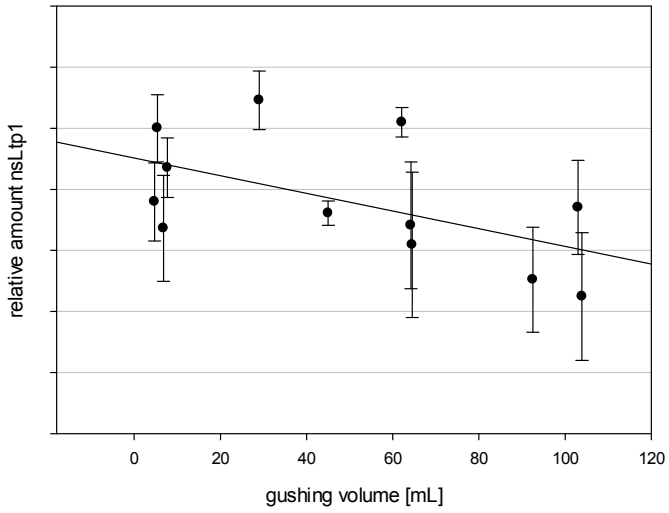

Figure 34: Relative amount of nsLtp1 plotted against the gushing volume of beer per bottle for beers declared as non-gushing.

No difference in the content of FcHyd5p between gushing and non-gushing beer was detectable (Figure 33). Also, no correlation between overflow volume and hydrophobin level existed. By comparing the ratio of relative amounts of FcHyd5p to relative amounts of nsLtp1 in beers a significant difference between gushing and non-gushing beer was detected. Gushing beer contained 18.7 % more FcHyd5p relative to nsLtp1 than non-gushing beer ($P = 0.025$) (Figure 33).

3.7.3 Comparison of gushing and non-gushing beer each of different brews

Gushing and non-gushing beer of different brews of same type and from the same brewery were examined. 4 types of wheat beer were obtained from a private brewery. Provided samples were bottles from 14 lots 'Urhefeweiße', 12 lots of dark wheat beer 'dunkle Weiße', 13 lots of 'Hefeweiße' and 8 lots of light wheat beer 'leichte Weiße'. Two lots of each beer type were negative gushing beers according to the brewery. Of each lot two bottles were analyzed as followed.

Before performing gushing tests 1 mL of pre-cooled beer (4 °C) was removed from each bottle and kept for ELISA assays. In this experiment gushing was defined as volume loss of at least 5 mL.

5 of the 12 analyzed dark beer lots showed gushing, the declared gushing negative lot did not show any overflow. In 'Hefeweiße' 8 out of 13 lots were gushing positive. One of the negative control bottles had a gushing volume of 22 mL. Also in light beer one of the 4 negative control bottles gushed with 5.2 mL overflow. In total 6 out of 8 light wheat beers were gushing positive. In 'Urhefeweiße' 5 lots out of 14 gushed, with one negative control bottle again showing gushing with 8.4 mL overflow volume.

Each beer type was separately analyzed by ELISA since previous results revealed different levels of protein amounts of nsLtp1 and FcHyd5p in different types of beer (chapter 3.7.1). Correspondingly, the absorbance of wheat beer type 'Urhefeweiße' (ur) had an increased reciprocal absorbance (0.370 ± 0.028), thus, a higher nsLtp1 content than the dark wheat beer (0.232 ± 0.021; $P < 0.001$). The level of nsLtp1 in 'Hefeweiße', with a reciprocal absorbance of 2.616 ± 0.664, was increased as compared to light wheat beer which had a reciprocal absorbance of 2.304 ± 0.420 ($P = 0.008$). Differences in the FcHyd5p content were detected between beers of type light, with 27.26 ± 10.92 % absorbance decrease, and both 'Hefeweiße' and dark beer. These had an increased amount of FcHyd5p with a decrease of absorbance of 45.84 ± 8.12 % and 49.56 ± 11.00 %, respectively.

The relative contents of nsLtp1 and FcHdy5p in gushing and non-gushing beers, as classified by the brewery or according to gushing tests, were investigated. Results are listed in Table 25. In all beer types, except light beer, a trend for higher nsLtp1 amount was observed in non-gushing beers classified by gushing tests. The increase, however, was only significant in dark beer with an increase of 4.5 % in reciprocal absorbance ($P = 0.032$). For the amount of FcHyd5p, no significant differences between gushing and non-gushing beer were detected in all tested types of wheat beer when gushing was determined by gushing tests (Table 25).

Table 25: Relative amount of nsLtp1 and FcHyd5p, and the ratio of FcHyd5p:nsLtp1 within gushing and non-gushing beer of different wheat beer types. Results are displayed for gushing classified after performed gushing test (gushing for > 5 mL overflow) and classified according to brewery statement. hefe: 'Hefeweiße'; light: light wheat beer; ur: 'Urhefeweiße'; dark: dark wheat beer.

Relative amount nsLtp1 [1/abs]				
Beer	Gushing determined by gushing test		Gushing according to brewery	
	gushing	non-gushing	gushing	non-gushing
hefe	2.554 ± 0.361	2.678 ± 0.751	2.538 ± 0.599	3.043 ± 0.123
light	2.322 ±0.363	2.252 ± 0.212	2.307 ± 0.352	2.296 ± 0.281
ur	0.366 ± 0.022	0.372 ± 0.025	0.367 ± 0.021 *	0.398 ± 0.014 *
dark	0.314 ± 0.016 *	0.328 ± 0.019 *	0.319 ± 0.016 *	0.342 ± 0.019 *
Relative amount FcHyd5p (decrease absorbance [%])				
Beer	Gushing determined by gushing test		Gushing according to brewery	
	gushing	non-gushing	gushing	non-gushing
hefe	45.61 ± 9.25	46.09 ± 7.18	46.44 ± 8.17	42.56 ± 8.00
light	26.64 ± 11.98	29.14 ± 8.01	25.80 ± 12.18	31.65 ± 4.20
ur	70.47 ± 3.70	69.03 ± 6.97	69.53 ± 5.02	70.34 ± 10.18
dark	53.75 ± 7.57	46.88 ± 12.13	50.76 ± 8.94	42.94 ± 18.81
Ratio FcHyd5p:nsLtp1 (relative amounts)				
Beer	Gushing determined by gushing test		Gushing according to brewery	
	gushing	non-gushing	gushing	non-gushing
hefe	18.467 ± 5.81	19.19 ± 8.36	19.69 ± 7.27	14.08 ± 3.20
light	11.66 ± 5.35	13.24 ± 4.660	11.39 ± 5.49	14.06 ± 3.33
ur	193.11 ± 17.27	184.91 ± 21.57	190.70 ± 19.34	176.20 ± 20.80
dark	170.96 ± 23,14	144.00 ± 39.37	159.80 ± 30.14	125.67 ± 54.55

*significant differences

When beers were classified according to negative control beers provided by the brewery, similar results were obtained. For light wheat beer an insignificant increase in nsLtp1 content in gushing beers was determined, whereas for 'Hefeweiße', 'Urhefeweiße' and dark beer the content of nsLtp1 in gushing beers was reduced compared to non-gushing beers. These differences of 7.2 % and 8.4 % were significant in dark beer ($P = 0.015$) and 'Urhefeweiße' ($P = 0.005$) (Table 25). The content of FcHyd5p in beers declared as gushing positive and in control beers was similar for all types of beer tested (Table 25).

No statistically significant relation between the gushing occurrence and ratio of FcHyd5p:nsLtp1 in analyzed beers was detected, irrespective of whether the declaration of gushing beers was according to performed gushing tests or to brewery statements (Table 25).

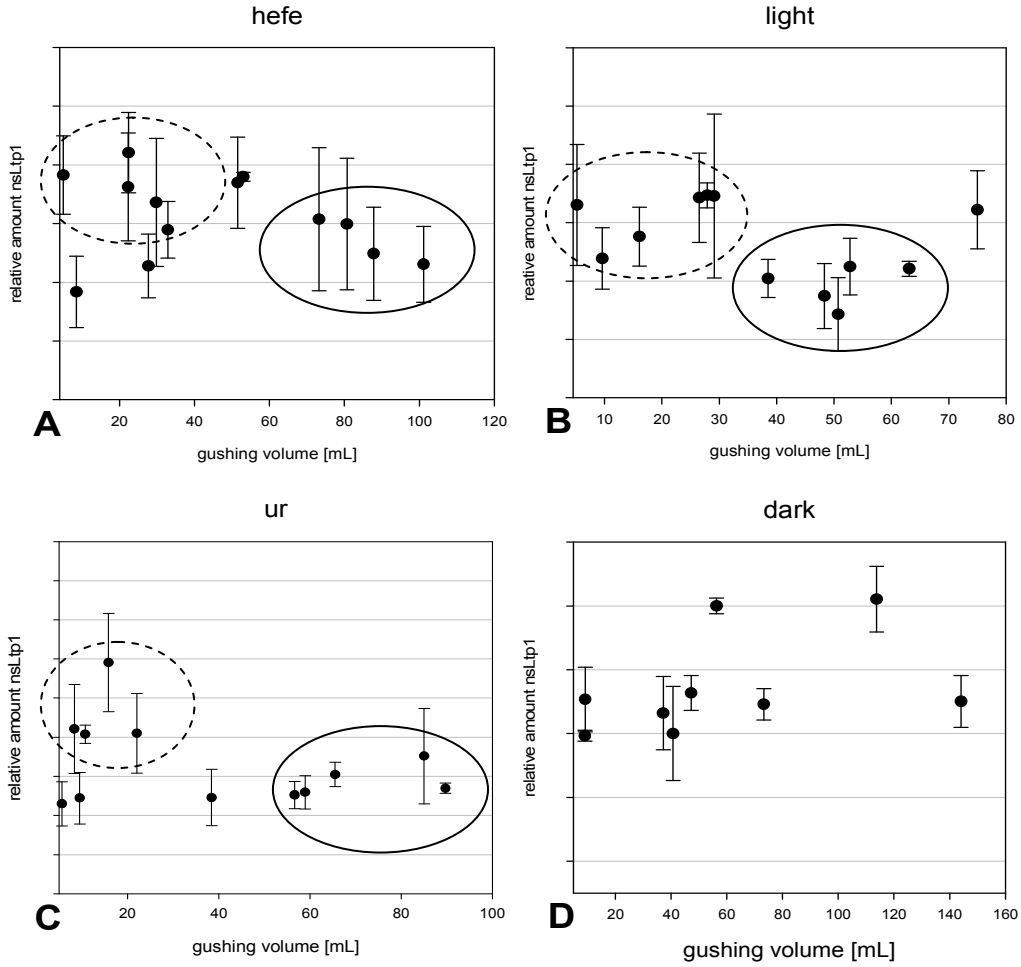

Figure 35: Relative amount of nsLtp1 plotted against the gushing volume per bottle for gushing beers. A: beer type 'Hefeweiße'; B: beer type light wheat beer; C: beer type 'Urhefeweiße'; D: beer type dark wheat beer. Clustering is shown in circles.

When comparing overfoam volumes of gushing beer with respective content of FcHyd5p no correlation was observed. Also, gushing volume did not correlate directly to nsLtp1 content. However, as shown in Figure 35, with nsLtp1 content plotted against overfoam volumes, two groups of gushing beer were distinguishable for types 'Hefeweiße', light wheat beer and 'Urhefeweiße'. For 'Hefeweiße' low gushing beers with overflow of 5 mL to 53 mL contained more nsLtp1 than a group of beers with high gushing (above 73 mL). The average nsLtp1-ELISA values for the low gushing cluster with 2.810 ± 0.225 1/abs were, however, not significantly higher than for high gushing beer with 2.409 ± 0.174 1/abs (Figure 35A). In light beer the difference between mean relative nsLtp1 content of 2.578 ± 0.236 1/abs in low gushing (up to 28 mL) and 1.968 ± 0.173 1/abs in high gushing (39 mL to 68 mL) beers proved to be significant ($P < 0.001$) (Figure 35B). In 'Urhefeweiße' beers two clusters also appeared. Beers with low overflow volumes of 10 to 22 mL contained a significantly higher nsLtp1 content of 0.391 ± 0.018 1/abs than high overfoaming beers with gushing volumes of

59mL to 90 mL and an average nsLtp1 content of 0.358 ± 0.008 1/abs (Figure 35C). No such clustering appeared when gushing volumes and nsLtp1 content of dark wheat beer were compared (Figure 35D). Regarding the ratio of FcHyd5p:nsLtp1 no relation between gushing volume and the ratio was observed, also no clustering occurred.

3.7.4 Correlation of FcHyd5p-induced gushing to nsLtp1 content

In addition to hydrophobin proteins the level of nsLtp1 was also assumed to be a detrimental gushing factor. To test this assumption, different beers of one type and from the same brewery were titrated with FcHyd5p. The volume loss induced by different concentrations of FcHyd5p was related to the level of nsLtp1 in the different beers.

Table 26: Gushing volumes induced by addition of 0.125 mg FcHyd5p to bottles (0.5L) of different beer lots and the corresponding level of nsLtp1 in these beers. exp 1 and exp 2 represent two individual experiments.

Samples		Gushing [mL]	nsLtp1 content [1/abs]
exp 1	beer 1	57.5	1.18 ± 0.14
	beer 2	15.5	1.95 ± 0.18
	beer 3	125.5	0.97 ± 0.20
exp 2	beer 1	2.2	0.72 ± 0.04
	beer 2	16.7	0.59 ± 0.04
	beer 3	13.7	0.60 ± 0.05

In the first experiment (exp 1 in Table 26) already before addition of hydrophobin a different gushing tendency in used beer lots was observed. For one brew (beer 3) bottles did lose some volume by overfoaming. At bottles of beer 1 a cap of foam arose after opening, whereas for the third brew (beer 2) no gushing tendency was visible. In correspondence with these findings, beer 3 with overflow upon opening gave highest overfoaming volumes induced by all concentration of FcHyd5p. Less gushing volume occurred in the ‘capping’ beer 1 and even lower overflow was observed for the completely non-gushing beer (beer 2), again for all used concentrations of FcHyd5p. Table 26 summarizes the results of gushing induced by addition of 0.125 mg FcHyd5p and the corresponding determined content of nsLtp1. Beer exhibiting the highest gushing volumes induced by FcHyd5p (beer 3; 125.5 mL) contained least amount of nsLtp1 with 1/abs of 0.97 ± 0.20. The ‘capping’ beer (beer 1), which showed intermediate induced gushing volumes of 57.5 mL, had a level of 1.18 ± 0.14 1/abs of nLtp1. In beer with the lowest overfoaming volumes (beer 2; 15.5 mL) the highest level of nsLtp1 with reciprocal abs of 1.95 ± 0.18 was measured. All differences in nsLtp1 amount were statistically significant.

In the second experiment (exp 2) only for hydrophobin concentrations below 0.3 mg/500 mL, the gushing volumes in beer bottles varied between different brews. With a hydrophobin concentration of 0.125 mg/500 mL two beers (beer 2 and 3) displayed a similar gushing volume of 16.7 mL and 13.7 mL, respectively, which was increased compared to that of beer 1 (2.2 mL). The gushing overflow was correlated to the level of nsLtp1. Beer 1 with 0.72 ± 0.04 1/abs contained significantly more nsLtp1 than beer 2 or 3, which comprised relative nsLtp1-ELISA values of 0.59 ± 0.04 and 0.60 ± 0.05, respectively (Table 26).

3.8 Cloning and production of protein Z4

By analyzing the amino acid sequence of Z4 with Signal.P3 software package no signal peptide sequence was detected. Thus, the Z4 encoding gene *Paz1* was cloned directly into the pPICZαA vector, resulting in vector pPICZαA_Z4. The *Paz1* gene construct was then cloned into the genome of the transformant strain *P. pastoris* X33 [pPICZαA_Z4]. Expression of *Paz1* was induced by cultivation of *P. pastoris* transformant strain X33 [pPICZαA_Z4] in medium containing methanol. Electrophoretic protein separation of the freeze dried culture supernatant by SDS-PAGE revealed the presence of a major band between 40 and 55 kDa after Coomassie Blue staining (Figure 37, lane 1). The size roughly matched the calculated mass of protein Z4 of 43 kDa. In control lyophilisate of cell free supernatant of wild type *P. pastoris* X33 culture, this band was not present (Figure 37, lane 6).

```
  1 MATTLATDVR LSIAHQTRFA LRLRSAISSN PERAAGNVAF SPLSLHVALS
 51 LITAGAAATR DQLVAILGDG GAGDAKELNA LAEQVVQFVL ANESSTGGPR
101 IAFANGIFVD ASLSLKPSFE ELAVCQYKAK TQSVDFQHKT LEAVGQVNSW
151 VEQVTTGLIK QILPPGSVDN TTKLILGNAL YFKGAWDQKF DESNTKCDSF
201 HLLDGSSIQT QFMSSTKKQY ISSSDNLKVL KLPYAKGHDK RQFSMYILLP
251 GAQDGLWSLA KRLSTEPEFI ENHIPKQTVE VGRFQLPKFK ISYQFEASSL
301 LRALGLQLPF SEEADLSEMV DSSQGLEISH VFHKSFVEVN EEGTEAGAAT
351 VAMGVAMSMP LKVDLVDFVA NHPFLFLIRE DIAGVVVFVG HVTNPLISA
```

Figure 36: Amino acid sequence of protein Z4 (in silico translation). Peptides detected by LC-MS/MS are underlined, they have sequence coverage of 42.2 % in relation to the whole protein. The RCL cleaving site is marked by triangles.

LC-MS/MS analysis of the corresponding band after trypsin digestion gave six peptide fragments, which showed 100 % identity with the published sequence of protein Z4 (accession no. CAA36015). These corresponded to a sequence coverage of 42.4 % of the published sequence. Peptides matching the aa sequence of Z4 are marked in the aa sequence

of protein Z4 in Figure 36. The marked position in Figure 36 between Met-357 and Ser-358 was described as the RCL site of protein Z4 (Dahl et al., 1996). At this binding site for proteases the terminal part of the protein is cleaved off upon protease binding. A partial sequence within the terminal part of the cleaving region was covered by one of the peptides analyzed by LC-MS/MS. This showed that the transgenic protein Z4 produced by the transformant of *P. pastoris* X33 [pPICZαA_Z4] is secreted in its native form.

3.9 Heat stability of protein Z4

Transgenic protein Z4 was incubated at different temperatures prior to separation by SDS-PAGE in order to examine its heat sensitivity. The Coomassie stained gel is shown in Figure 37.

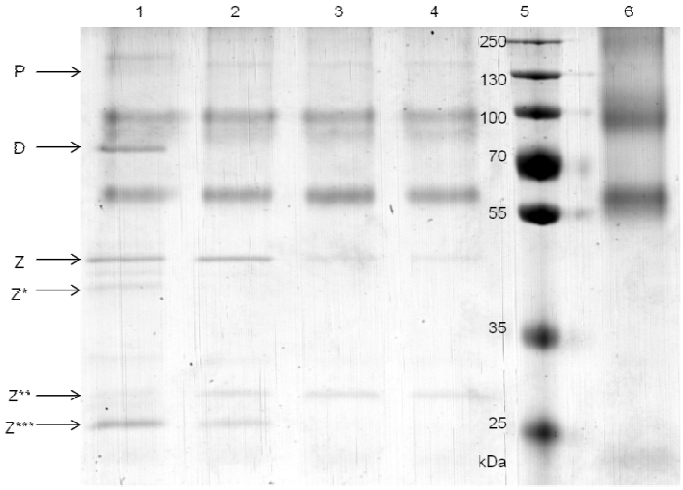

Figure 37: SDS-PAGE of protein Z4 incubated at different temperatures. Lane 1-4 protein Z4 0.3 µg, 25 °C (1), 70 °C (2), 90 °C (3) and 100 °C (4); lane 5 protein standards in kDa; lane 6 control X33.

With no heating two distinct bands occurred in the predicted size range of protein Z4. As validated by LC-MS/MS analysis (chapter 3.8), the upper band Z corresponded to the native form of the protein, which has a predicted size of 43.3 kDa. The lower band Z* was assumed to be the cleaved serpin, which was calculated to have a size of 38.8 kDa. A further band between 70 kDa and 100 kDa (D in Figure 37) occurred, which had the two fold size of protein Z4 and may represent a dimeric form of the native protein Z4. A band was present at all temperatures in a size between 130 and 250 kDa (P), which was suspected to be a polymer or a serpin-protease complex of Z4 and an inhibited protease. Two more bands at low kDa range at about 30 kDa (Z**) and 25 kDa (Z***) were present. They supposedly belonged to a size reduced version of the native protein Z4 and its cleaved form. Upon heating the lower band at 40 kDa (Z*) as well as the assumed dimer (D) diminished. These bands were only

visible in protein samples incubated at room temperature. Also the intensity of the upper 40 kDa band (Z) decreased with increasing temperature from 100 % at room temperature, over 99 % and 85 % to 39 % at 100 °C. Instead, a protein of 30 kDa (Z**) appeared. Compared to treatment at room temperature the intensity of the band Z** increased considerably with rising temperature (Figure 37).

3.10 Protease inhibition by protein Z4 and nsLtp1

As it belongs to the protein family serpin, protein Z4 was expected to inhibit serine proteases. Also nsLtp1 of barley is a probable inhibitor of green malt cysteine endoproteases. In order to examine the ability of the transgenic proteins to inhibit proteases, agar diffusion tests of proteases in combination with nsLtp1 and Z4 were performed. On a statistically significant level no inhibition of serine proteases trypsin and proteinase K was detected for nsLtp1 or Z4 (Table 27).

Table 27: Influence of the transgenic proteins Z4 and nsLtp1 on the proteolytic activity of proteinase K and trypsin on caseinate agar.

Type of protease	Protein added	Proteolytic zone diameter [mm]
proteinase K (60 µg/mL)	0	21.0 ± 1.0
	5 mg/mL Z4	20.0
	5 mg/mL nsLtp1	22.0
trypsin (60 µg/mL)	0	11.4 ± 1.5
	5 mg/mL Z4	12.5 ± 1.0
	5 mg/mL nsLtp1	11.8 ± 2.5

However, when an extract of barley malt was incubated with the transgenic proteins, the activity of undefined malt proteases was reduced. A decrease of the inhibition zone resulted from addition of Z4 or nsLtp1 to the malt. Application of untreated malt extract to caseinate agar diffusion test, resulted in an inhibition zone of 10.4 ± 1.2 mm diameter. As illustrated in Figure 38, supplemental protein Z4 decreased the zone to 80 ± 10 % ($P = 0.03$). nsLtp1 showed a similar protease inhibition by decreasing the inhibition zone to 82 ± 4 % ($P = 0.025$). Heat treatment of proteins prior to mixing with the malt extract significantly increased the diameter of the inhibition zone of malt proteases to a size similar to the protein Z4 and nsLtp1 free control (Figure 38).

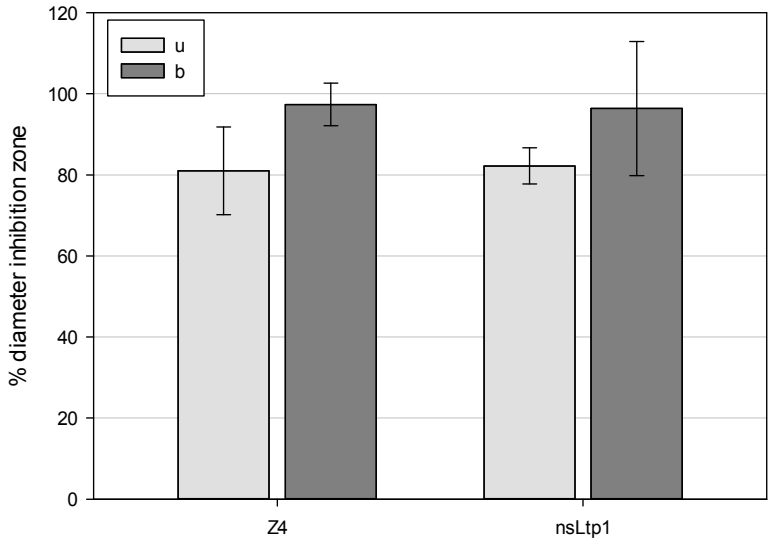

Figure 38: Inhibition of undefined malt proteases by protein Z4 and nsLtp1. Decrease of proteolytic zone diameters of malt extract in caseinate agar plates by co-incubation with protein Z4 and nsLtp1, in native (u) and heat treated (b) form.

3.11 Influence of protein Z4 on hydrophobin induced gushing

The influence of the transgenic protein Z4 on gushing in beer and carbonated water was analyzed. Protein Z4 did not induce any gushing when added to beer or carbonated water in high concentrations. Addition of Z4 to gushing beverages, which were pre-treated with hydrophobins of class 2, resulted in a decrease of the gushing volume. The addition of 2 mg of protein Z4 to beer previously treated with 2 mg FcHyd5p already decreased the volume loss by 11.6 %. In carbonated water higher concentrations of protein Z4 were necessary to reduce gushing. A significant decrease occurred only after addition of > 6 mg protein Z4. The gushing reducing effect was more pronounced at higher Z4 concentrations (Table 28). Also, gushing induced by 1 mg Hfb2 in carbonated water was decreased by addition of protein Z4. The reduction was even higher than for FcHyd5p induced gushing. The addition of 8 mg protein Z4 per bottle resulted in a decrease of volume loss of 65.1 %, whereas only 3.0 % of volume loss reduction was found for water pre-treated with FcHyd5p. Also, gushing which was induced by 4 mg of class 1 hydrophobin FcHyd3p in carbonated water was reduced by addition of Z4. 4 mg FcHyd3p resulted in a gushing volume of 38.7 ± 8.25 mL. By addition of 4 mg Z4 the overflow was decreased by 42.1 % (Table 28).

Table 28: Reduction of hydrophobin induced gushing by native protein Z4 in beer and carbonated water.

Protein added		Gushing volume [mL]	Difference to control [%]
Hydrophobin	Protein Z4	Gushing in beer	
FcHyd5p (2 mg)	none added	334.75 ± 7.14	-
FcHyd5p (2 mg)	2 mg	295.95 ± 11.24	-11.59
none added	2 mg	0.00 ± 0	-
		Gushing in carbonated water	
FcHyd5p (1 mg)	none added	180.53 ± 0.22	-
FcHyd5p (1 mg)	6 mg	173.55 ± 4.45	-3.86
FcHyd5p (1 mg)	8 mg	175.15 ± 1.25	-2.98
FcHyd5p (1 mg)	10 mg	143.75 ± 0.35	-20.37
FcHyd5p (1 mg)	12 mg	125.85 ± 8.25	-30.29
Hfb2 (1 mg)	none added	177.80 ± 0.90	-
Hfb2 (1 mg)	8 mg	62.10 ± 0.30	-65.07
FcHyd3p (4 mg)	none added	38.65 ± 8.25	-
FcHyd3p (4 mg)	4 mg	22.37 ±5.37	-42.12

Heat treatment of Z4 prior to addition to gushing water led to a lower gushing reduction. As illustrated in Figure 39, for FcHyd5p pre-treated water, native Z4 reduced gushing by 51.5 %. After heat treatment a reduction of only 24.1 % was observed. When heat treatment was performed in synthetic wort the effect of boiling was enhanced. The gushing reduction was then further decreased, reducing the gushing volume by only 13.5 %.

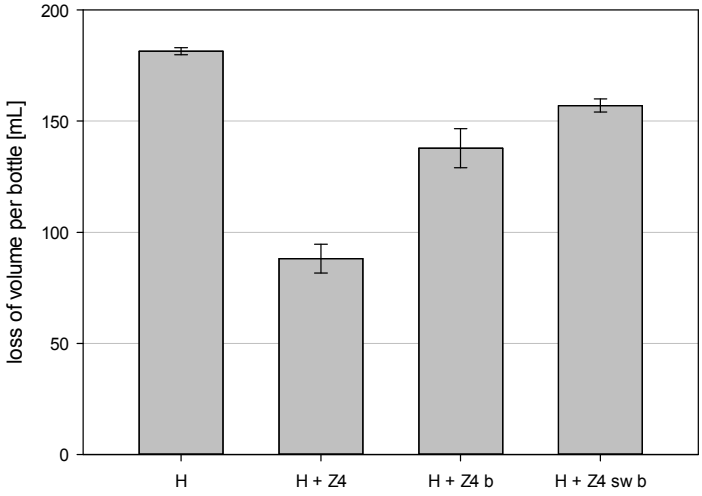

Figure 39: Influence of transgenic protein Z4 on hydrophobin induced gushing in carbonated water (0.33 L per bottle). Gushing induced by 1 mg FcHyd5p without inhibition (H) and gushing volumes by addition of FcHyd5p and 10 mg protein Z4 (H + Z4), FcHyd5p and 10 mg heat treated protein Z4 (H + Z4 b), and FcHyd5p and 10 mg protein Z4 heat treated in synthetic wort (H + Z4 sw b).

The influence of protease inhibition by protein Z4 on its gushing reducing properties was also investigated. As results from protease inhibition tests showed, activity of undefined

proteases in malt was reduced by Z4 (see chapter 3.10). Therefore, protein Z4 was incubated in malt extract before addition to carbonated water pre-treated with FcHyd5p. Results are shown in Figure 40. The addition of malt, without Z4, to gushing water already led to a reduction of the gushing volume of 13.2 ± 1.8 %. This reduction was weaker than that of Z4 alone, which showed a decrease of gushing of 19.8 ± 1.8 %. Protein Z4 incubated in malt extract prior to addition to gushing water resulted in a greater reduction of the volume loss (32.5 ± 0.6 %) when compared to protein Z4 or malt extract alone. Overall the relative reduction values of protein Z4 and malt extract alone (29.3 ± 3.4 %) corresponded well to the value found for the combined effect. The findings indicate that the gushing reducing properties of protein Z4 are presumably not influenced by its protease inhibition of barley malt proteases.

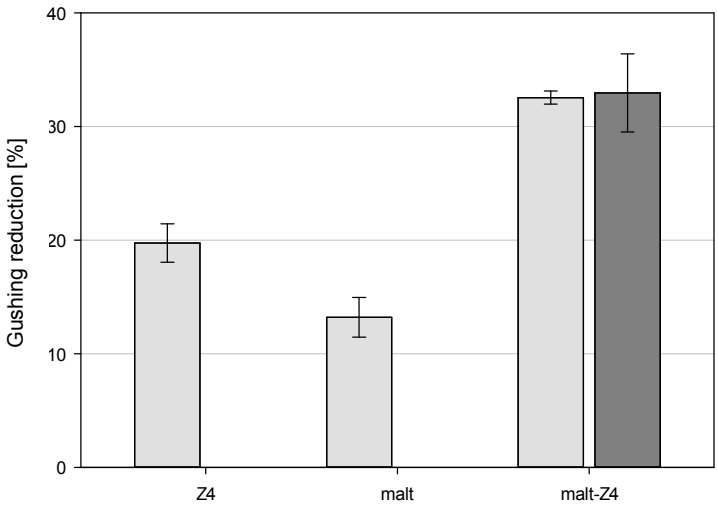

Figure 40: Influence of malt extract incubation on the gushing reduction property of transgenic protein Z4. The reduction of gushing volumes of hydrophobin induced gushing by protein Z4, malt extract, and protein Z4 incubated in malt extract (1.5 h) (malt-Z4) in carbonated water are shown.

3.12 Interaction of FcHyd5p with protein Z4 or nsLtp1

Both beer proteins, protein Z4 and nsLtp1, have the property to reduce hydrophobin induced gushing. It was assumed that these proteins interact with hydrophobin, altering its surface active properties, which in turn leads to a reduction of its gushing potential. Direct interaction was, therefore, investigated by performing SPR experiments with BIAcore, as well as DLS analysis of protein solutions.

3.12.1 BIAcore

Within the BIAcore system two approaches were tested by using two sensor chips coupled to either the anti-FcHyd5p-P3-IgG antibody or FcHyd5p as ligand. Via amino coupling each ligand was successfully immobilized onto a BIAcore sensor chip CM5. After activation, ligand coupling, and deactivation, a stable increase in RU of 18,580 was achieved for anti-FcHyd5-P3-IgG. Immobilization with FcHyd5p was less intense, resulting in an increase in RU of only 392. The coupling of FcHyd5p was proven by using anti-FcHyd5-P3-IgG as analyte. By injection of 10 µL of 0.1 mg/mL antibody an increase in RU by 370 occurred.

3.12.1.1 Protein interaction analysis on sensor chip with ligand anti-FcHyd5p-P3-IgG

FcHyd5p analyte was shown to interact with the coupled antibody on the chip. Injection of 3 mg/mL FcHyd5p in HBS-EP buffer pH 3.5 resulted in an increase in RU of 132.45 ± 14.22. Also at pH 7.4 binding was observed. The increase in RU was related to the amount of FcHyd5p applied. 0.035 mg/mL FcFyd5p increased the RU by 29.8, 0.35 mg/mL by 37.1, and 0.42 mg/mL by 39.4. Application of FcHyd5p in concentrations of 0.83 mg/mL, 1.75 mg/mL, and 3.5 mg/mL resulted in an increase in RU of 48.7, 75.6, and 65.5.

With interaction studies, performed by injection of already mixed proteins, no interaction between FcHyd5p and nsLtp1 was detected. The increase in RU for FcHyd5p alone and the mixture was similar. When FcHyd5p was first coupled to the antibody followed by injection of nsLtp1 in native or boiled form, no further increase in RU was detected, indicating no binding of nsLtp1 to FcHyd5p. No statement could be presented for Z4 interaction with FcHyd5p by this method because Z4 alone showed binding to the antibody leading to an increase of 211 RU after injection of 8.9 mg/mL. Indeed there was an increase in RU when protein Z4 was injected directly after FcHyd5p, or when FcHyd5p was injected after Z4. This increase, however, probably resulted from additional protein binding to the immobilized antibody.

3.12.1.2 Protein interaction analysis on sensor chip with ligand FcHyd5p

Binding sites, necessary for interaction between FcHyd5p and nsLtp1 or FcHyd5p and Z4, respectively, may be concealed by binding of FcHyd5p to the antibody. Therefore, FcHyd5p was used as ligand to alleviate possible concealment. Injection of nsLtp1 or heat treated nsLtp1, as well as injection of protein Z4, did not result in an increase of the RU level. No interaction between FcHyd5p and nsLtp1 or Z4, respectively, was detected.

3.12.2 DLS

In measurements with DLS by instrumentation with one angle setting, for a sample solution containing hydrophobin FcHyd5p, two particle classes were observed with mean diameter of 106.6 nm and 7.9 nm (Figure 41). For protein nsLtp1 a peak at particle size of 324.9 nm was detected (Figure 41C), which reduces to smaller particle sizes (299.4 nm) after heat treatment (Figure 41D). Z4 samples contained smaller particles than nsLtp1 with a size of 199.4 nm (Figure 41A). Also for Z4 the mean diameter of particles was reduced to 132.1 nm after heat treatment (Figure 41B).

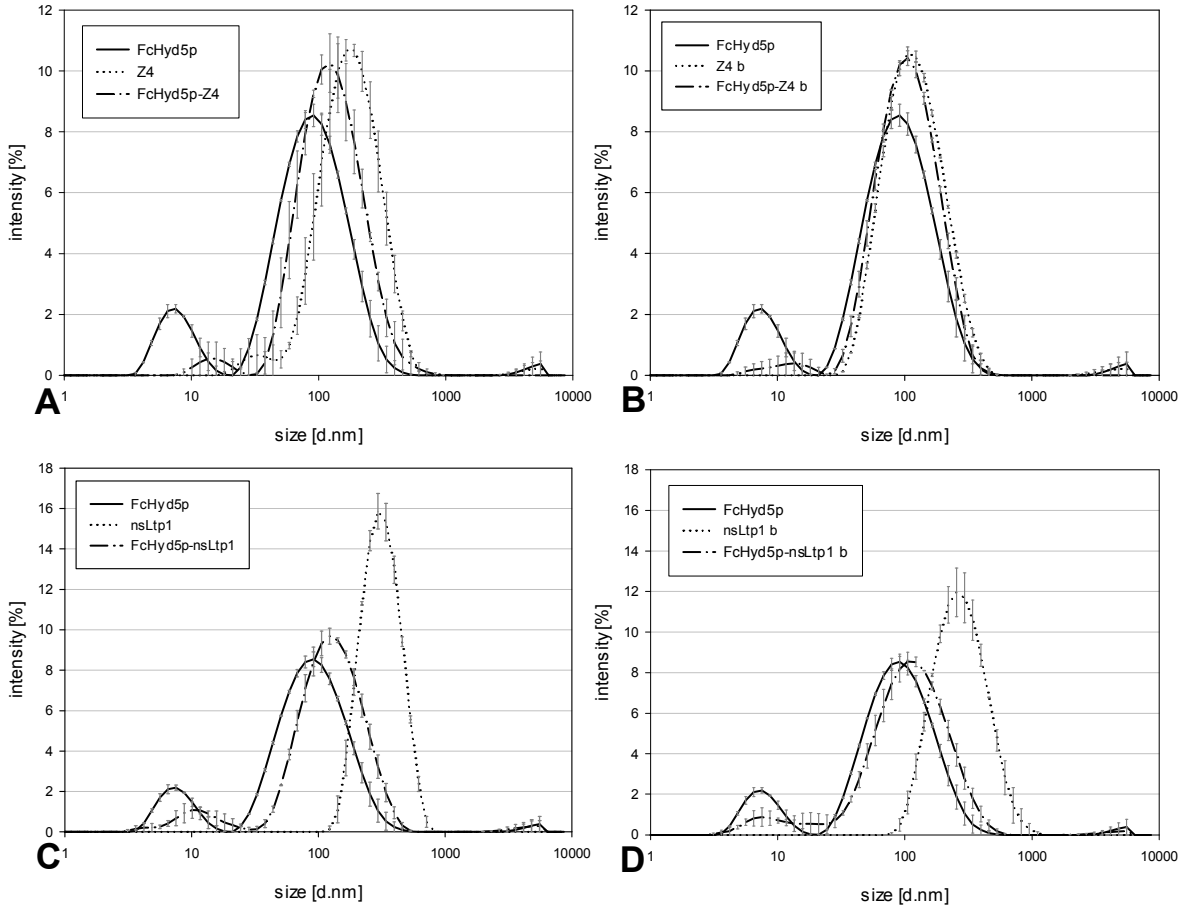

Figure 41: Particle size distribution of protein solutions of FcHyd5p, nsLtp1, protein Z4 and combinations of FcHyd5p with beer foam proteins in a 1:1 (v/v) ratio. A: particle size distributions of FcHyd5p, protein Z4, and combination of FcHyd5p with Z4 (FcHyd5p-Z4); B: particle size distributions of FcHyd5p, heat treated protein Z4 (Z4 b), and combination of FcHyd5p with heat treated Z4 (FcHyd5p-Z4 b); C: particle size distributions of FcHyd5p, nsLtp1, and combination of FcHyd5p with nsLtp1 (FcHyd5p-nsLtp1); D: particle size distributions of FcHyd5p, heat treated nsLtp1 (nsLtp1 b), and combination of FcHyd5p with heat treated nsLtp1 (FcHyd5p-nsLtp1 b).

When FcHyd5p was mixed with protein Z4 or Z4 b small particles of 8 nm vanished. Instead particles of size 15 nm and 12 nm occurred, representing an increase in size of 1.5 % to 1.9 %. The intensity of the larger particle sizes increased by 20 % and 22 %, respectively,

and shifted with particle diameters of 146 nm and 119 nm towards bigger particles as compared to pure FcHyd5p solutions with 107 nm (Figure 41A, B). Admixing nsLtp1 to FcHyd5p had a similar effect on the size distribution of FcHyd5p as Z4. The particle sizes increased from a peak of 8 nm to 12 nm, and from 107 nm to 145 nm or 134 nm by adding nsLtp1 or heat treated nsLtp1, respectively (Figure 41C, D).

A closer look at particle size distributions in protein solutions was gained by using DLS at multi angles. The mean particle peak sizes measured at angles 50°-150° are listed in Table 29. Solutions of FcHyd5p contained particles of a diameter of 2.4 ± 0.3 nm (p1), 7.0 ± 1.3 nm (p2), 37.6 ± 3.7 nm (p3), and 147.5 ± 28.7 nm (p4). These peaks of particle size could not be distinguished at all angle detections, but if not, a broader distribution was detected. In literature the diameter of class 2 hydrophobin Hfb1 is reported to lie between 2 and 3 nm (Hakanpää et al., 2004). Thus, one could suggest that monomers (p1, 2.4 nm) can form trimers resulting in p2 (7.0 nm), and higher aggregates with P3 being 15.3 ± 2.0 times p1 and p4 60.9 ± 12.0 times p1.

Table 29: Mean size of peaks 1-4 (p1-p4) in particle size distributions of protein solutions of a concentration of 30 mg/mL. Proteins nsLtp1, protein Z4, FcHyd5p in pure form and protein combinations of FcHyd5p with either nsLtp1 (FcHyd5-nsLtp1) or Z4 (FcHyd5p-Z4) in a ratio of 1:1 (v/v) were analyzed by DLS with detection at the angles 50°-150°.

Protein sample	Particle size d [nm]			
	Peak 1	Peak 2	Peak 3	Peak 4
nsLtp1	1.47 ± 0.87	14.00 ± 3.26		
Z4	3.00 ± 0.90	27.73 ± 4.00		
FcHyd5p	2.44 ± 0.28	6.95 ± 1.263	37.00 ± 3.74	147.50 ± 28.72
FcHyd5p-nsLtp1	3.30 ± 0.30	37.64 ± 3.85		
FcHyd5p-Z4	3.01 ± 0.79	31.00 ± 3.46		

Mixing FcHyd5p with Z4 or nsLtp1 resulted in a loss of particles in the size range of 7 nm, the assumed trimer. But particles of a size of about 3 nm were still present, representing p1 in pure FcHyd5p. Thus, one can assume that after addition of nsLtp1 or Z4 to FcHyd5p solutions monomers of FcHyd5p were still present, or, in the case of nsLtp1 addition also monomers or dimers of nsLtp1 (assumed size 1.7 nm, derived by Matejková et al., 2009). Large aggregates at 150 nm disappeared. Instead, the area of peaks with particles in the size range 30 nm to 37 nm got broader, indicating the presence of intermediates. This finding can be explained by an aggregation of an unordered type of hydrophobin and added protein molecules.

Because of the occurrence of rather big particles, an analysis of particles present in protein solutions was additionally performed by DDLS. Results showed that scattering of the examined samples, containing FcHyd5p or a mixture of FcHyd5p with nsLtp1 (1:1, v/v), was even lower than in control toluene. This implied that samples did not contain any particles that scatter depolymerised light, and is a strong indication that the formed aggregates were spherical (Voets I., personal communication).

3.12.3 Surface hydrophobicity

To test if there was any hydrophobic interaction between the hydrophobin and beer foam proteins, the relative surface hydrophobicity of protein solutions was determined. For determining the hydrophobicity, pH value was set to 5.0, representing the value of beer.

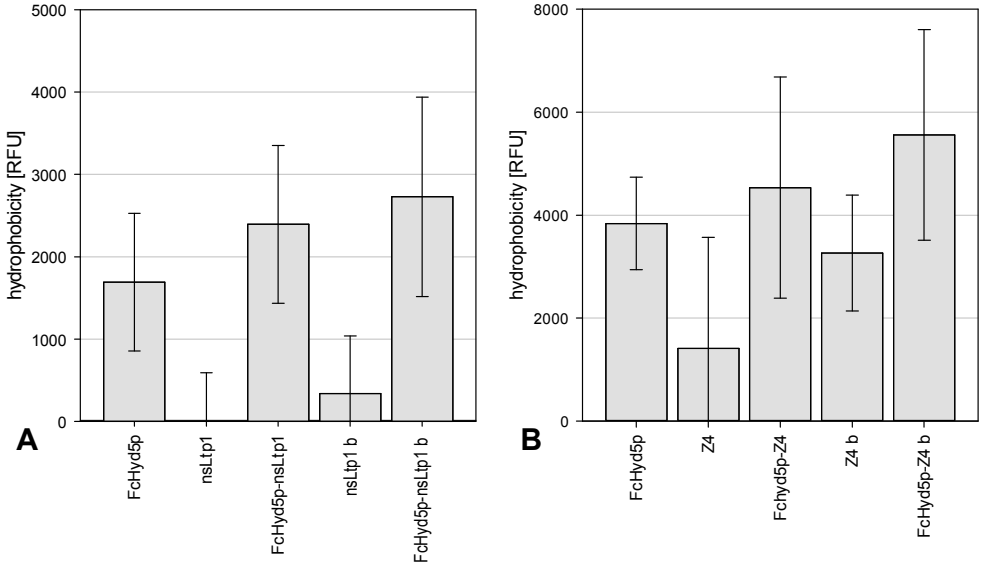

Figure 42: Surface hydrophobicity of protein solutions containing 0.1 % FcHyd5p, nsLtp1 or Z4 in citrate buffer pH 5.0. Hydrophobicity was measured by fluorescence caused by interaction with ANS and displayed as fluorescence values minus RFU of blank. A: surface hydrophobicity of FcHyd5p, nsLtp1, heat treated nsLtp1 (b), as well as combinations of FcHyd5p with either nsLtp1 or nsLtp1 b in the ratio 1:1 (v/v); B: surface hydrophobicity of FcHyd5p, Z4, heat treated Z4 (b), as well as combinations of FcHyd5p with either Z4 or Z4 b in the ratio 1:1 (v/v).

As illustrated in Figure 42A, measurement of pure nsLtp1 and nsLtp1 b at pH 5.0 resulted in a similar level of fluorescence as the protein free control. This indicated that, independent of the heat treatment, no accessible hydrophobic domains were present in the nsLtp1 molecule. Under the same conditions, FcHyd5p showed significantly higher fluorescence indicating that hydrophobic domains were accessible. No change in fluorescence was observed in mixtures of FcHyd5p with nsLtp1 or nsLtp1 b, respectively, when compared to pure

FcHyd5p samples. The hydrophobicity of the hydrophobin was not influenced by nsLtp1 (Figure 42A).

Contrary to nsLtp1, Z4 and heat treated Z4 possessed accessible hydrophobic domains at pH 5.0, as shown by detection of a higher fluorescent signal than for the control (Figure 42B). Thereby, heat treatment of Z4 had no significant influence on the fluorescent signal. The addition of Z4 or Z4 b to FcHyd5p led to an insignificant increase in hydrophobicity when compared to FcHyd5p alone (Figure 42B).

3.13 Influence of protein Z4 and nsLtp1 on properties of hydrophobin

3.13.1 Emulsion properties

3.13.1.1 Binding to oil droplets

Binding of proteins to oil in 20 % oil-in-water emulsions was evaluated by determining the relative amount of FcHyd5p and nsLtp1, respectively, in the corresponding water phase by ELISA. The bulk concentration of hydrophobin was reduced significantly by 20 % ($P \leq 0.001$) in emulsions containing only FcHyd5p as compared to the control (FcHyd5p containing solution without any oil addition). The decrease of FcHyd5p in the water phase is evidence for binding of the protein to oil droplets. Neither the addition of nsLtp1 nor of protein Z4, both in native or heat treated form, had an influence on the loss of hydrophobin in the water phase. Results indicated that these additional proteins did not influence the binding of FcHyd5p to oil.

Results of nsLtp1-ELISA experiments with emulsions containing nsLtp1 are illustrated in Figure 43. Compared to a control without oil addition, a significant decrease of 40 % ($P = 0.01$) of the relative amount of nsLtp1 was observed in the water phase of emulsions containing heat treated nsLtp1. In emulsions with combinations of heat treated nsLtp1 and FcHyd5p the content of nsLtp1 in the bulk increased by 35 % ($P = 0.009$) compared to emulsions prepared with nsLtp1 only. Thereby, no significant difference to the level of nsLtp1 in the control was measured (Figure 43). These findings suggested that FcHyd5p replaced nsLtp1 at the oil/water interface, consequently resulting in an increase in nsLtp1 concentration in the water phase.

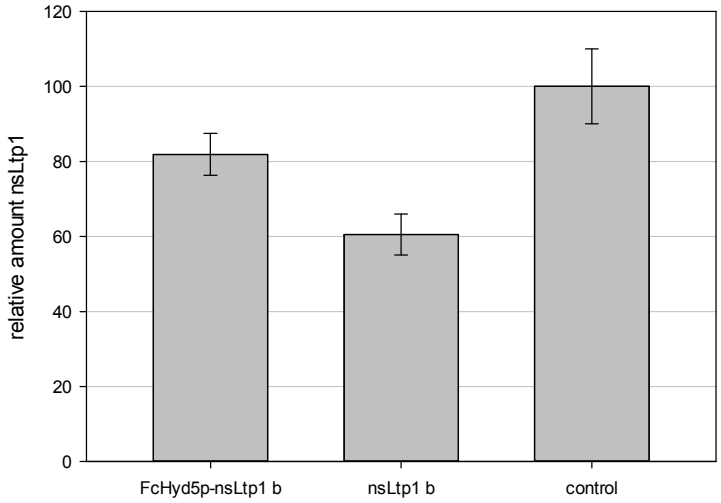

Figure 43: Relative amount of nsLtp1 in the water phase of 20 % oil-in-water emulsions, prepared with water containing heat treated nsLtp1 (b) or a combination of FcHyd5p with nsLtp1 b in the ratio 1:1 (v/v). As control served an aqueous solution of heat treated nsLtp1 without admixing oil.

3.13.1.2 Emulsion stability

The clearing behavior of emulsions containing 0.01 mM of protein is displayed in Figure 44. Emulsions formed with 0.01 mM of hydrophobin FcHyd5p displayed a high stability when compared to emulsions with nsLtp1 or protein Z4 in the same concentration. A reduction of turbidity of only 35 % was observed over 120 h for FcHyd5p, whereas nsLtp1 exhibited no emulsion stability. nsLtp1 containing emulsions showed a clearing over time resembling that of control emulsions without addition of any protein. Emulsions with 0.01 mM of protein Z4 also cleared fast but were always more stable than emulsions containing no protein. With a decrease of 22 % of absorbance values after 96.5 h incubation, emulsions prepared with mixtures of untreated nsLtp1 and FcHyd5p (1:1, v/v) showed less emulsion stability than emulsions containing only FcHyd5p. The absorbance recorded for emulsions with mixtures of FcHyd5p and Z4 (1:1, v/v) also decreased over the whole measurement period. However, values were increased when compared to pure Z4. Comparing emulsions of FcHyd5p mixed with either nsLtp1 or Z4, revealed an increased stability of emulsions containing nsLtp1 in addition to FcHyd5p (Figure 44).

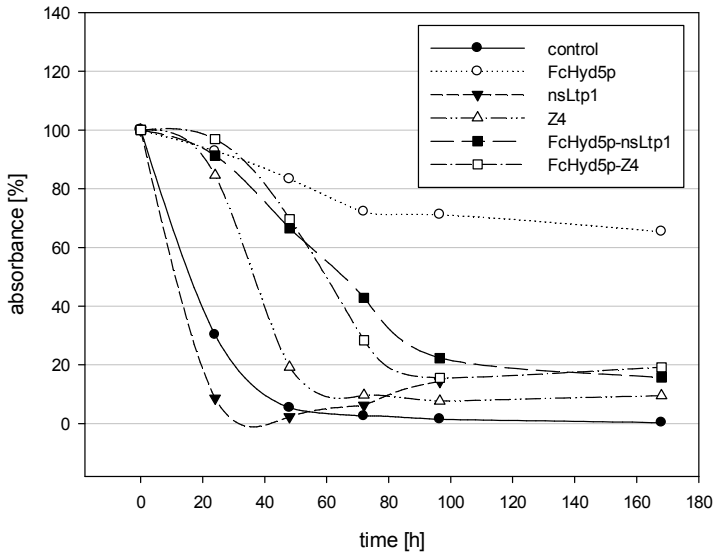

Figure 44: Emulsion stability of 20 % oil-in-water emulsions without proteins (control), as well as containing 0.01 mM protein FcHyd5p, nsLtp1, Z4 or combinations of FcHyd5p with nsLtp1 or Z4, respectively, in a 1:1 (v/v) ratio. Turbidity was measured by absorbance at 590 nm; percent turbidity was calculated from the starting value at time point 0 of each sample.

When prepared with a protein concentration of 0.75 mg/mL, oil-in-water emulsions showed a similar clearing pattern as samples adjusted to molarity (see Figure 45). Thereby, 0.75 mg/mL corresponded to 0.09 mM FcHyd5p, 0.08 mM nsLtp1, 0.09 mM protein in 1:1 (v/v) mixtures of FcHyd5p and nsLtp1, 0.03 mM protein Z4, and 0.06 mM in combinations of Z4 with FcHyd5p in a 1:1 (v/v) ratio. Again FcHyd5p stabilized emulsions over the whole measurement period. After 96 h and 120 h 16 % and 40 % clearing was measured in emulsions containing only FcHyd5p (Figure 45A, B). Emulsions with native nsLtp1 or heat treated nsLtp1 b showed fast clearing, with the one of nsLtp1 b clearing faster and reaching a lower level. Compared to emulsions containing 0.01 mM nsLtp1, emulsions with 0.08 mM were more stable and showed decreased clearing rates. Emulsions containing a combination of FcHyd5p with nsLtp1 were also very stable. With a decrease of absorbance of 26 % after 96 h, the stability was, however, decreased as compared to emulsions containing only FcHyd5p with 16 % clearing. Addition of nsLtp1 b to FcHyd5p emulsions had a more destabilizing effect than native nsLtp1. After 96 h resting 54 % clearing occurred (Figure 45A). The effect on emulsion stability of increasing the concentration to 0.75 mg/mL (0.03 mM) was more pronounced for protein Z4. Here a slower clearing rate was observed for Z4 resulting in 80 % decrease of absorbance after 120 h as compared to emulsions prepared with 0.01 mM with about 90 % clearing already after 72 h. For heat treated Z4 the ability to stabilize emulsions was similar. Addition of Z4 or Z4 b to FcHyd5p containing

emulsions did not alter the clearing when compared to emulsions with only FcHyd5p where proteins were used in the concentration 0.75 mg/mL (Figure 45B).

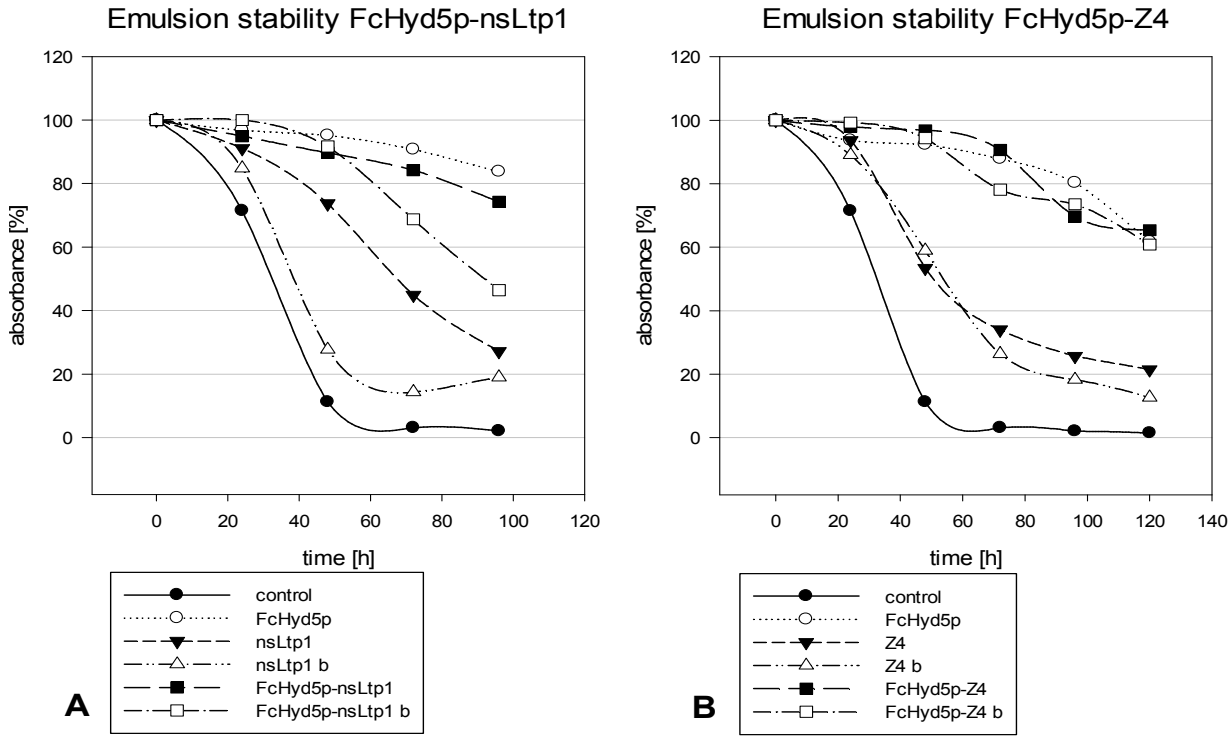

Figure 45: Emulsion stability of 20 % oil-in-water emulsions without proteins (control), as well as containing 0.75 mg/mL protein. A: emulsions prepared with proteins FcHyd5p, nsLtp1, heat treated nsLtp1 (nsLtp1 b), and combinations of FcHyd5p with nsLtp1 (FcHyd5p-nsLtp1) and FcHyd5p with heat treated nsLtp1 (FcHyd5p-nsLtp1 b) in a 1:1 (v/v) ratio, respectively; B: emulsions prepared with proteins FcHyd5p, Z4, heat treated Z4 (Z4 b), and combinations of FcHyd5p with Z4 (FcHyd5p-Z4) and FcHyd5p with heat treated Z4 (FcHyd5p-Z4 b) in a 1:1 (v/v) ratio, respectively. Turbidity was measured by absorbance at 590 nm; percent turbidity was calculated from the starting value at time point 0 of each sample.

3.13.1.3 Oil droplet size

The size of oil droplets in the different emulsions was analyzed by determination of the particle size distribution via light scattering. The volumetric size distribution of particles is shown in Figure 46. No significant difference between nsLtp1 and nsLtp1 b was detected. The particle sizes in emulsions prepared with FcHyd5p, nsLtp1 or nsLtp1 b were similar. However, with 7 % particles in the 1.5 µm fraction of the nsLtp1 emulsion had an increased volume, as compared to particles of the same fraction in the FcHyd5p emulsion with 6.5 % (Figure 46A). In the nsLtp1 and nsLtp1 b emulsions, particles of the 0.3 µm to 0.5 µm fraction had a volume of 1.5 %. Whereas in FcHyd5p, emulsion particles of this size corresponded to 2.0 % of volume (Figure 46A, B).

Oil droplets of emulsions formed with either native or heat treated protein Z4 had a different size distribution. With an even higher volume percentage of 7.7 %, a major peak again occurred in the 1.5 µm size fraction. However, emulsions prepared with Z4 contained no droplets in the size range below 0.7 µm. Instead, in both Z4 emulsions a peak at 30-40 µm was detected, representing 2.5 % and 1.0 % of the particles' volume for native and heat treated Z4, respectively (Figure 46C, D).

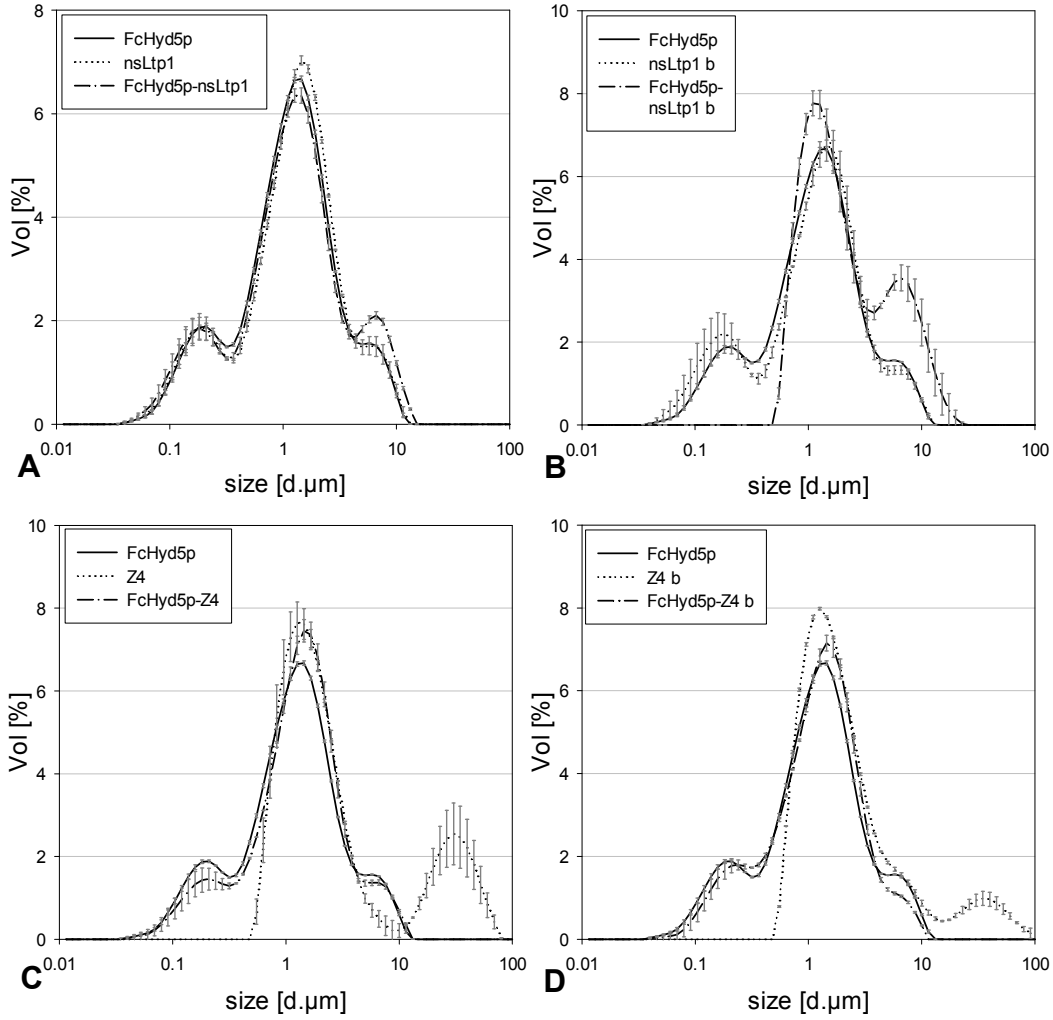

Figure 46: Volumetric particle size distribution in emulsions with 0.01 mM protein or mixed proteins in a ratio of 10:1 (v/v) measured by light scattering with particle size analyzer. A: FcHyd5p, nsLtp1, and combination of FcHyd5p with nsLtp1 (FcHyd5p-nsLtp1); B: FcHyd5p, heat treated nsLtp1 (nsLtp1 b), and combination of FcHyd5p with heat treated nsLtp1 (FcHyd5p-nsLtp1 b); C: FcHyd5p, Z4, and combination of FcHyd5p with Z4 (FcHyd5p-Z4); D: FcHyd5p, heat treated Z4 (Z4 b), and combination of FcHyd5p with heat treated Z4 (FcHyd5p-Z4 b).

When emulsions were prepared by combining FcHyd5p with nsLtp1 or FcHyd5p with nsLtp1 b, respectively, in a ratio of 10:1 (v/v), a change in particle size distribution was observed when compared to FcHyd5p emulsions. Mixing nsLtp1 with FcHyd5p appeared to

result in a significant increase in the number of medium and high sized oil droplets in favor of a decrease in the volume percentage of small sized particles. The percentage of big droplets in the 4-15 µm particle fraction was increased, whereas the volume percentage of the 1-2 µm particles decreased, when untreated nsLtp1 was mixed with FcHyd5p (Figure 46A). The effect was more pronounced when nsLtp1 b was added. When nsLtp1 b and FcHyd5p were mixed, the resulting emulsion no longer had particles in the size range of 0.1-0.4 µm. Instead, this emulsion showed a significant increase in volume of particles within the size ranges of 0.9-2 µm and 3-20 µm (Figure 46B).

For emulsions prepared with mixtures of Z4 and FcHyd5p, no particles were detected in sizes between 30 µm and 40 µm, which had been dominant in Z4 emulsions. Instead, the percentage in the 0.08-0.2 µm size range increased. Compared to the particle sizes of FcHyd5p emulsions, the volume of small particles with a peak at 0.2 µm decreased, whereas the volume of droplets with 1-2 µm in diameter increased. Native, as well as heat treated Z4 appeared to destabilize small droplets and raise the particle size when added to FcHyd5p emulsions. The effect was more pronounced for untreated protein Z4 (Figure 46C, D).

3.13.2 Foaming properties

Directly after foaming, the foam height of hydrophobin FcHyd5p containing solutions was significantly larger than foam heights of solutions with either Z4 or nsLtp1, both in untreated or boiled form. The foaming rate for FcHyd5p was 23.3 %, whereas nsLtp1 and nsLtp1 b resulted in a foaming rate of 10.1 % and 11.0 %, respectively. Thereby, boiling of nsLtp1 had no influence on foam formation capacity. In contrast, for Z4 the heat treatment increased the foam formation, raising the foaming rate from 6.2 % to 13.6 %. Mixed protein samples containing FcHyd5p and either Z4, Z4 b, nsLtp1, or nsLtp1 b in a 1:1 (v/v) ratio showed foam formation in the same percentage values as FcHyd5p alone.

Figure 47 illustrates the foaming rate calculated of the remaining foam after resting 1 h. Again, the foam height in solutions containing only FcHyd5p was increased as compared to nsLtp1 or Z4. After 1 h FcHyd5p had a foaming rate of 15 %. The foaming rate of heat treated Z4 (7.1 %) was still higher as compared to native protein Z4 (2.1 %). Native and heat treated nsLtp1 solutions had a similar foaming rate of 6 % after 1 h. By adding untreated nsLtp1 or Z4 to FcHyd5p the foaming rate after 1 h was not changed as compared to FcHyd5p. Foaming rates of 20 % and 17 % were calculated as the sum of individual foaming rate values of pure solutions of FcHyd5p and either native nsLtp1 or protein Z4. These values

were similar to the experimentally measured foam rates of corresponding protein mixtures. However, the addition of heat treated nsLtp1 or heat treated Z4 to FcHyd5p had a destabilizing effect on foam formed by FcHyd5p. Although initial foam formation in these combinations was not altered, foam height after 1 h decreased. These mixed protein solutions had a foaming rate of 9.2 % (FcHyd5p-nsLtp1 b) and 9.3 % (FcHyd5p-Z4 b), which was even below the foaming rate of FcHyd5p with 15 % (Figure 47).

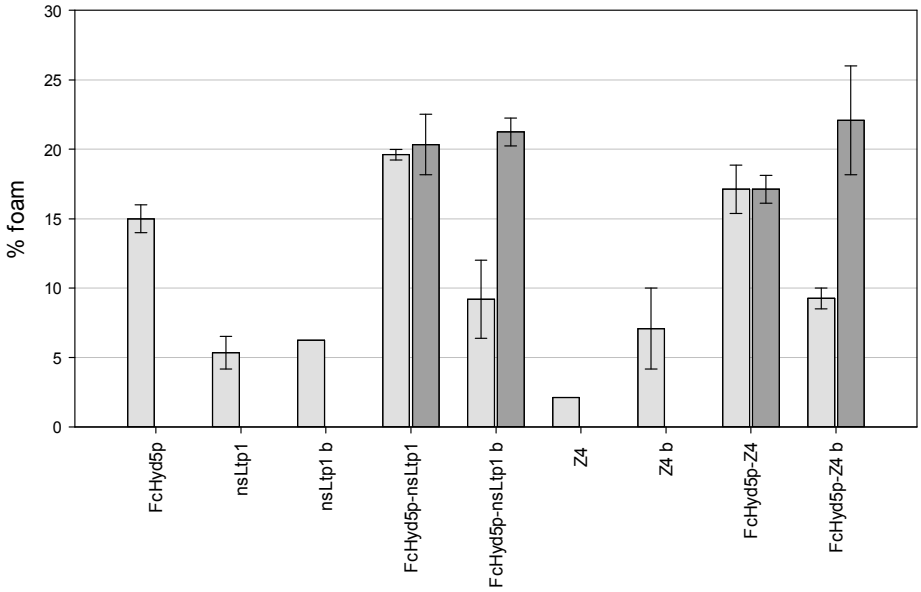

Figure 47: Foam stability of aqueous protein solutions. Pure samples containing protein FcHyd5p, nsLtp1, heat treated nsLtp1 (nsLtp1 b), protein Z4 or heat treated Z4 (Z4 b), as well as protein mixtures in a ratio of 1:1 (v/v) were allowed to rest for 1 h at ambient temperature after foaming. In dark gray the theoretical sum of foam percentage of pure proteins, which are present in the respective mixture, is shown.

In all samples foam decay occurred during 1 h. A high decrease of foam was observed for samples with pure Z4 and Z4 b with a loss of 73 % and 62 %, respectively. With a loss of 47 % and 43 % nsLtp1 and nsLtp1 b foams were more stable. For both proteins a higher decay was measured for untreated protein, thus, foam stabilization was increased by heat treatment. Foams formed with FcHyd5p solutions were the most stable with a foam decay of only 32 %. Addition of nsLtp1 or Z4 in untreated form to FcHyd5p did not alter the foam stabilization as compared to FcHyd5p alone. However, when comparing mixtures of FcHyd5p with either nsLtp1 b or Z4 b with pure FcHyd5p a considerable increase in foam loss was observed. A foam decay of 64 % and 51 % was measured for FcHyd5p-nsLtp1 b and FcHyd5p-Z4 b, respectively.

3.13.3 Surface tension

The influence of tested proteins on the surface tension of water against air is shown in Figure 48. Compared to surface tension of water (72 mN/m), for all samples a decrease in surface tension over time occurred. Already after drop formation time of 28 s, protein FcHyd5p reduced the surface tension to 68 mN/m. When compared to the other tested proteins, FcHyd5p displayed the lowest surface tension over the whole measured time (28 to 208 s).

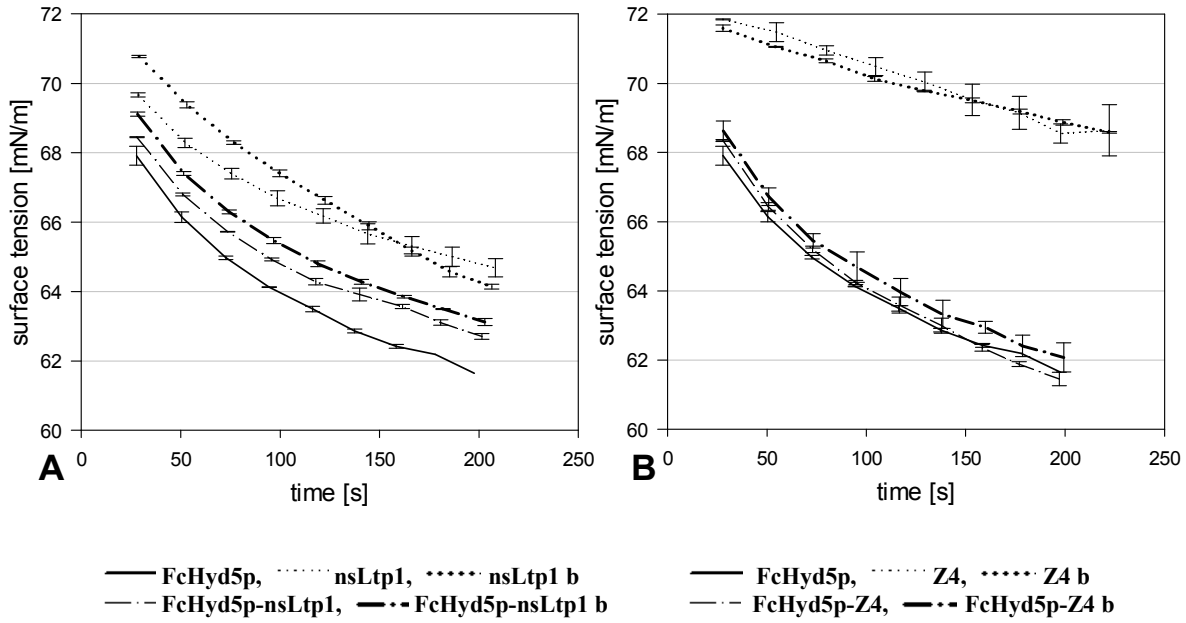

Figure 48: Impact of hydrophobin FcHyd5p and beer foam proteins on water surface tension at 20 °C. A: surface tension displayed by 1 mg/mL FcHyd5p, nsLtp1, heat treated nsLtp1 (nsLtp1 b), and mixtures of FcHyd5p with nsLtp1 (FcHyd5p-nsLtp1) or heat treated nsLtp1 (FcHyd5p-nsLtp1 b), respectively, in a 10:1 (v/v) ratio; B: surface tension displayed by 1 mg/mL FcHyd5p, Z4, heat treated Z4 (Z4 b), and mixtures of FcHyd5p with Z4 (FcHyd5p-Z4) or heat treated nsLtp1 (FcHyd5p-Z4 b), respectively, in a 10:1 (v/v) ratio.

Measurements with nsLtp1 and nsLtp1 b showed that both proteins exhibited a considerably higher surface tension than FcHyd5p (Figure 48A). For lower drop formation times heat treatment of nsLtp1 resulted in an reduced effect on surface tension. However, after 166 s the effect was reversed with native nsLtp1 now displaying a higher surface tension than the denatured one. Among the tested proteins, the lowest impact on surface tension was observed for protein Z4. For both heat treated and native Z4 proteins a similar effect was detected with a decrease of surface tension to 69 mN/m after 198 s (Figure 48B). At this formation time, FcHyd5p and native nsLtp1 decreased the surface tension to 62 mN/m and 65 mN/m, respectively (Figure 48A, B). The addition of 10 % Z4 to an FcHyd5p solution had no influence on the surface tension decreasing effect of FcHyd5p. Heat treated Z4 b added to

FcHyd5p resulted in a slight increase of the surface tension displayed by the hydrophobin (Figure 48B). nsLtp1, however, had a more pronounced impact on the surface tension of FcHyd5p. 10 % mixtures of nsLtp1 to FcHyd5p or nsLtp1 b to FcHyd5p, respectively, increased the surface tension of FcHyd5p solutions. Heat treated nsLtp1 had thereby a more pronounced effect leading to a higher increase. The surface tension of mixtures of FcHyd5p and nsLtp1 or nsLtp1 b lay between the one of the pure FcHyd5p and pure nsLtp1 proteins (Figure 48A).

3.13.4 Coating properties

The wettability of protein coatings on glass slides with oil was measured by determining the diameter of oil droplets, as well as by measuring the contact angle of the drops.

Diameters of oil droplets on protein films after 10 min are shown in Figure 49. The hydrophobin rendered the glass less oil wettable as compared to control, resulting in a decrease in droplet diameter from 0.26 cm to 0.2 cm. Oil droplets applied on Z4 coatings had a diameter of 0.28 cm. Heat treatment of Z4 significantly increased the wettability with oil ($P < 0.001$), with oil droplets on Z4 b films having a size of 0.32 cm. Both Z4 coatings were more wettable with oil as compared to the control. Oil droplet sizes on coatings with Z4 and Z4 b were increased by 15 % and 27 %, respectively, as compared to coatings with FcHyd5p (Figure 49). The droplet sizes on films of nsLtp1 and nsLtp1 b were in the same size range as those on coatings of Z4 b. They displayed a more hydrophobic surface on glass than FcHyd5p, resulting in an increase in oil droplet diameter of 26 % and 37 % when compared to FcHyd5p. In contrast to Z4, however, no significant difference in droplet diameter was observed between coatings of nsLtp1 and nsLtp1 b (Figure 49).

After 1 day of incubation at ambient temperature the diameter of the oil droplets increased only on coatings containing pure Z4 and Z4 b compared to day 0. The diameter of oil droplets showed an increase of 42 % and 54 %, respectively, when compared to oil droplets on coatings of FcHyd5p. For mixed protein coatings containing FcHyd5p and Z4 or Z4 b in a ratio of 1:1 (v/v) no significant difference in oil droplet size compared to pure coatings with FcHyd5p was detected neither after 10 min nor after 1 d. However, for 10:1 (v/v) mixtures of FcHyd5p-Z4 and FcHyd5p-Z4 b a small but significant increase in diameter of oil droplets by 14 % ($P = 0.005$) and 20 % ($P < 0.001$), respectively, as compared to pure FcHdy5p, was observed after 1 day incubation.

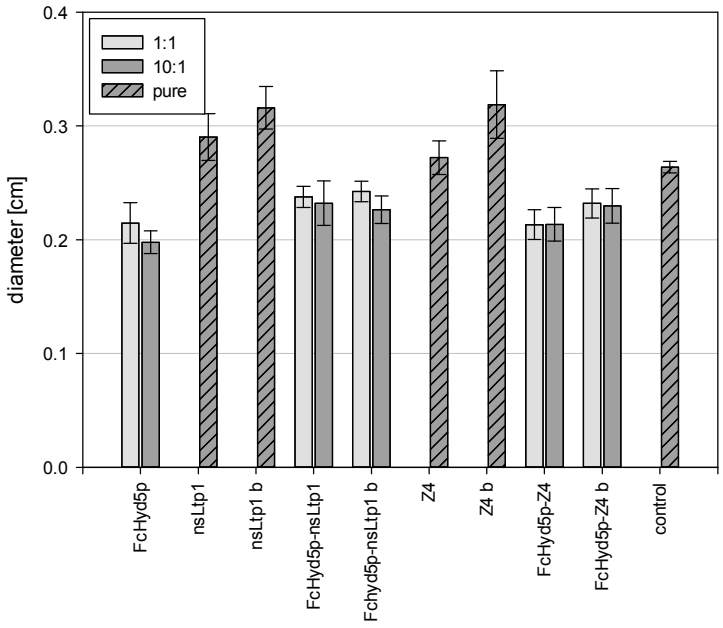

Figure 49: Wettability with oil of protein coatings on glass. Diameter of oil droplets after 10 min incubation on protein films of pure nsLtp1, heat treated nsLtp1 (nsLtp1 b), protein Z4 and heat treated protein Z4 (Z4 b) (shaded bars), as well as on mixtures of FcHyd5p with water (FcHyd5p), nsLtp1, nsLtp1 b, protein Z4 or protein Z4 b, respectively, in the ratios 1:1 (v/v, light gray) and 10:1 (v/v, dark gray). Glass surface without protein coating served as control.

Combining native nsLtp1 with FcHyd5p resulted in an increase in oil droplet diameters of 10 % ($P = 0.034$) and 17 % ($P = 0.008$) for mixing ratios 1:1 and 1:10 (v/v), respectively. nsLtp1 b added 1:1 or 1:10 (v/v) to FcHyd5p coatings led to an increase in oil droplet diameter of 13 % ($P = 0.015$) and 15 % ($P = 0.003$), respectively (Figure 49).

In accordance with diameter measurements, oil droplets on coatings of protein Z4 and heat treated Z4 displayed lower contact angles than FcHyd5p. Oil droplets on Z4 coatings had a contact angle of 27°. Z4 b was more oil wettable, resulting in a contact angle of 20°. Oil droplets on protein films of nsLtp1 and nsLtp1 b displayed a similar contact angle of 29°, whereas droplets on FcHyd5p coatings had increased contact angles of 43°. The slight increase in contact angles in 10:1 and 1:1 (v/v) mixtures of FcHyd5p with native and heat treated Z4, respectively, when compared to pure FcHyd5p, was insignificant. Also, by combining nsLtp1 or nsLtp1 b with FcHyd5p, either in a ratio 1:10 or 1:1 (v/v), no significant change in oil droplet contact angle was measured as compared to pure FcHyd5p coatings.

3.13.5 Correlation of proteins' surface properties

Hydrophobin FcHyd5p and beer foam proteins nsLtp1 and protein Z4, are believed to stabilize micro bubbles of CO_2 in carbonated beverages. Their surface properties differentially affect micro bubble formation and state and consequently gushing.

Emulsions were prepared in presence of the proteins and stability and oil droplet size were examined (see chapters 3.13.1.2 and 3.13.1.3). In order to check if the emulsion system was representative of the conditions of carbonated liquid, correlations of emulsion stability towards other surface properties tested for the proteins were evaluated. For correlation studies the following values were processed for better comparability reasons. The determined RFU values of surface hydrophobicity measurements were related to the values of FcHyd5p. Emulsion stability was calculated as a percentage decrease of absorbance after 268 h incubation time. To compare the impact on surface tension, the surface tension of aqueous protein solutions at a drop formation time of 197 s was used. Pearson product correlation factors, which were calculated by software SigmaPlot, are shown in Table 30.

Table 30: Correlation of emulsion stability, foaming properties, oil wettability of protein coats, surface hydrophobicity (surf. hydrop.) and surface activity. Correlation coefficient for parameters pairs of tested proteins FcHyd5p, nsLtp1, heat treated nsLtp1, protein Z4, heat treated protein Z4 and 1:1 (v/v) mixtures of hydrophobin and proteins Z4 and nsLtp1.

Pearson product monument correlation					
	foaming rate	foam decay	surface tension	oil wettability	surf. hydrop.
emulsion stability	0.767*	-0.694*	-0.743*	-0.886*	0.517
foaming rate		-0.558	-0.778*	-0.783*	0.87*
foam decay			0.735*	0.43	-0.164
surface tension				0.749*	-0.504
oil wettability					-0.683*

* pairs with P values lower than 0.050, corresponding to a significant relationship

In Figure 50 plots of emulsion stability versus the correlated surface properties surface tension, oil wettability, foam formation rate, and foam decay are shown. Emulsion stability was significantly correlated to all tested properties except surface hydrophobicity. A strong linear negative correlation between emulsion stability and surface tension (R^2 = -0.743), as well as between emulsion stability and oil wettability (R^2 = -0.886) was detected (Figure 50A, B; Table 30). Although Pearson calculation gave a significant negative correlation with

a correlation coefficient of R^2 = -0.694, the correlation between foam decay and emulsion stability displayed in Figure 50D proved to be insignificant due to high variations between repeated measurements. The correlation between foaming rate and emulsion stability proved to be nonlinear. Two clusters of data pairs can be distinguished in the plot of foaming rate vs. emulsion stability. Protein samples with a high foam formation rate over 20 % also had a high emulsion stability with over 50 %. The other cluster contained protein combinations with low foam formation rate (below 15 %) and low emulsion stability (below 50 %) (Figure 50C). Since the Pearson product moment, which calculated a significant relation with R^2 = 0.767, is based on the assumption of linearity, it cannot be taken as a reliable value.

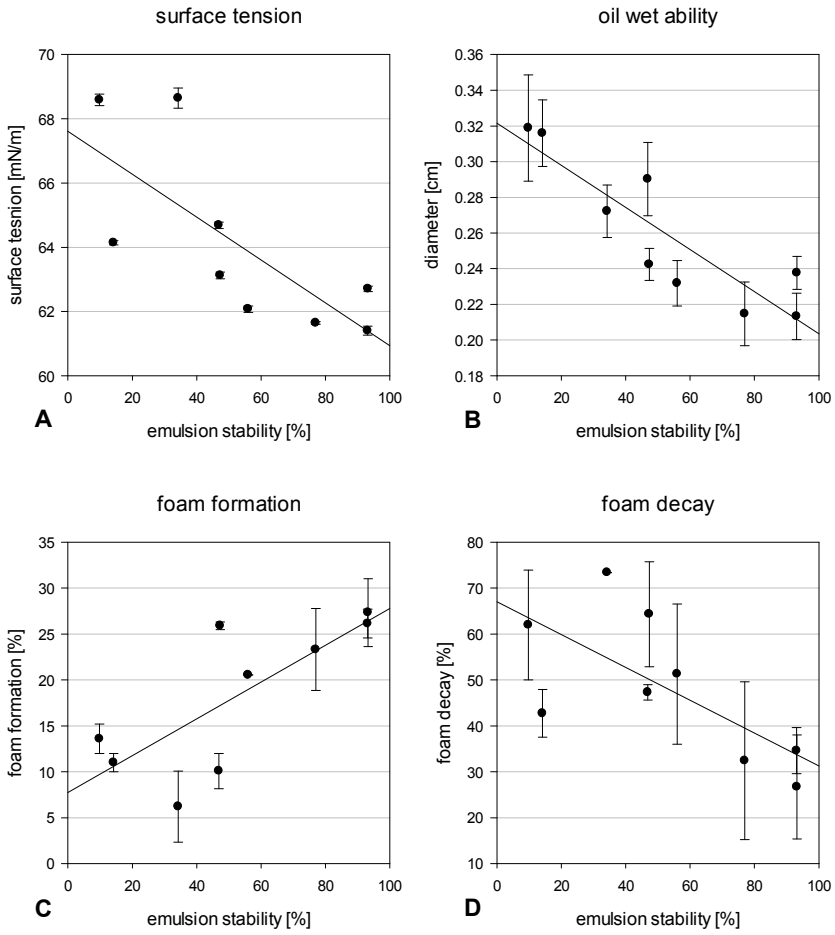

Figure 50: Correlation between the stability of 20 % oil-in-water emulsions containing proteins FcHyd5p, nsLtp1 and Z4 in native and heat treated form, as well as protein mixtures, and different surface property parameters. A: plot of emulsion stability vs. air/water surface tension after 196 s; B: plot of emulsion stability vs. oil droplet diameter on protein coated glass; C: plot of emulsion stability vs. foam formation rate; D: plot of emulsion stability vs. foam decay after 1 h.

Also for correlations between foaming rate and either oil wettability (R^2 = -0.783), surface hydrophobicity (R^2 = 0.87) or surface tension (R^2 = -0.778), which showed a significant correlation according to Pearson product moment, a nonlinear relation was observed. Again

two cluster pairs with high foam formation rate above 20 % and low surface tension, small oil droplet diameters on protein films, or high surface hydrophobicity occurred.

Linear correlations, which proved to be significant according to Pearson product moment calculations, existed between foam decay and surface tension (R^2 = 0.735). Oil wettability was not only correlated to emulsion stability, but also to surface hydrophobicity (R^2 = -0.6083), and in a highly positive way to foam formation rate (R^2 = 0.783) and surface tension (R^2 = 0.749).

3.13.6 Structure of protein films at air/water interface

Protein films formed at air/water interfaces were investigated by AFM. Thereby, the effect of contamination by nsLtp1 or protein Z4 on the hydrophobin film was examined.

The glass surfaces used had a homogenous and flat surface after cleaning where only a small height profile up to 0.3 nm was detected. Comparison of three different glass surfaces coated with FcHyd5p by drop transfer showed that all surfaces resulted in similar AFM picture profiles. In both scan sizes (10 µm and 0.5 µm) the height profiles were higher than those obtained from the empty glass surface, resulting in the conclusion that FcHyd5p was transferred onto the glass. The height with a mean average of 2.99 ± 0.76 nm in scan size 10 µm was increased as compared to empty surface with a height of 1.25 ± 0.18 nm. Small blobs of about 10-30 nm in diameter were observed, which were distributed uniformly over the surface. However, the lateral resolution of the used AFM was not high enough for precise determination of the size of occurring blobs.

Z4 and nsLtp1, respectively, were also transferred to the glass surface, as confirmed by the increased height in height profiles of the scanned images when compared to empty glass. Substrates contained relatively smooth areas with deviations in the range of 1 nm to 2 nm. In contrast to FcHyd5p, no blobs were visible. When surfaces of drops containing mixtures of proteins were transferred onto the glass, a great difference in height and roughness was detected by AFM. Addition of 50 % nsLtp1 or Z4 to FcHyd5p solutions, respectively, resulted in protein films with increased height profiles of the height retrace images. By comparing to FcHyd5p, at both scan sizes an increase up to 8 times (FcHyd5-nsLtp1) and 4 to 10 times (FcHyd5p-Z4) was detected. FcHyd5p substrates had an average height of 3.44 ± 0.20 nm at scan size 10 µm. Surfaces coated with protein mixtures showed an increased height of 11.66 ± 3.69 nm and 18.92 ± 4.83 nm with the addition of protein Z4 or nsLtp1, respectively. As shown in Figure 51, also for scan size of 0.5 µm an increased height

was observed with mixtures containing structures of 13.83 ± 2.61 nm (FcHyd5-Z4) and 11.173 ±5.17 nm (FcHyd5p-nsLtp1) in height, whereas substrates coated only with FcHyd5p showed an average height of 1.24 ± 0.24 nm.

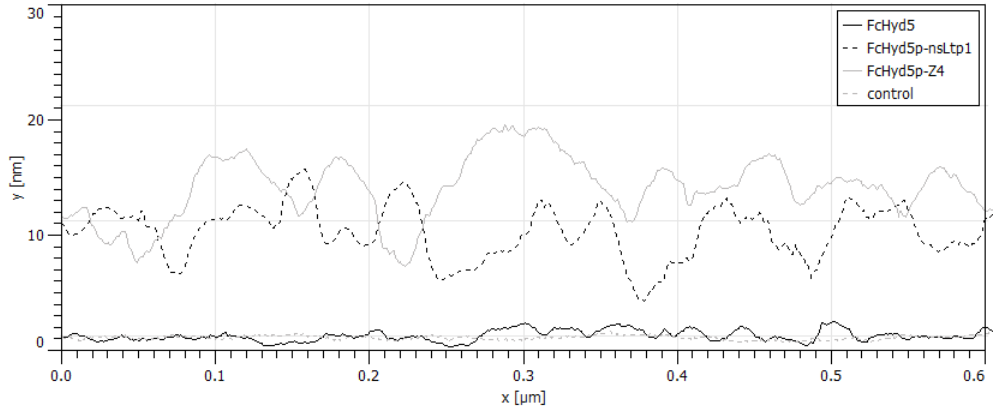

Figure 51: Height profile of height retrace images gained by AFM measurements of surfaces coated by drop transfer in scan size of 0.5 µm. Transferred proteins were FcHyd5p and protein combinations of FcHyd5p with nsLtp1, and FcHyd5p with *Z4* in a ratio of 1:1 (v/v). As control served glass surface without protein coating.

Looking at the structure of films, pure proteins displayed quite smooth surfaces. However, in the mixed protein films aggregates of a greater height interspersed by holes with low height were present. This structure resembled parts of the surface where less protein was present, represented by low height, whereas the high structures should contain large protein aggregates (Figure 52). This effect was more noticeable for mixtures containing nsLpt1 than for addition of Z4 in combination to FcHyd5p. Between the high sized structures and the holes a difference in height of 12.40 ± 3.32 nm for Z4 containing mixtures was measured. The mean diameter of the holes was 345.63 nm with a broad scattering of 140.34 nm. For FcHyd5p-nsLtp1 the height difference was similar with 11.72 ± 3.85 nm, but the determined average diameter of holes was increased to 409.31 ± 103.42 nm.

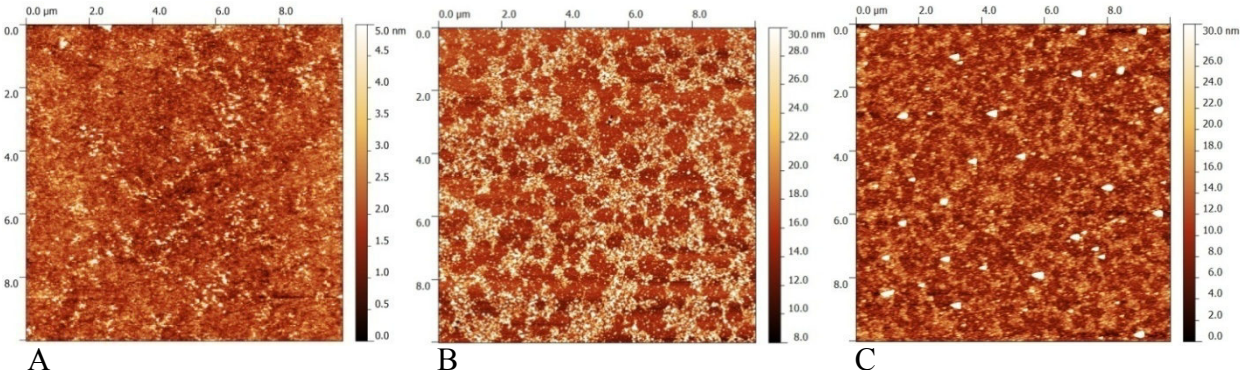

Figure 52: Height retrace images gained by AFM of glass surfaces coated by drop transfer in scan size of 10 µm. A: protein FcHyd5p; B: protein combination of FcHyd5p with nsLtp1 (1:1, v/v); C: protein combination of FcHyd5p with *Z4* (1:1, v/v).

4 Discussion

The basic thesis tested in the current study was that surface active beer proteins and their interaction with hydrophobin proteins play determinative roles in the gushing occurrence of beer. Results showed that indeed not only the presence of hydrophobin is relevant to gushing. ELISA experiments showed that in malt samples and beer samples which were classified into gushing and non-gushing the amount of hydrophobin played a minor role. While in non-gushing malt less hydrophobin was detected, in beer no relation could be found between gushing occurrence and the amount of FcHyd5p. However, for nsLtp1 not only was more nsLtp1 found in non-gushing malt, but also a decreasing level of nsLtp1 with raising gushing tendency existed. In contrast to FcHyd5p, for nsLtp1 a relation was found in beer. A higher amount of nsLtp1 was present in non-gushing beers.

An increasing ratio of FcHyd5p:nsLtp1 with increased gushing risk in malt was observed, and a higher ratio of FcHyd5:nsLtp1 was present in part of the gushing beers tested. Parallel occurrence and the amount of nsLtp1 compared to the amount of hydrophobin were suggested to be important for the ability of hydrophobin to cause gushing.

Further examination of the mutual effects of proteins which reduce or promote gushing, supported the importance of the presence of gushing negative acting proteins such as nsLtp1 or Z4 and their ratio to FcHyd5p. The gushing phenomenon is caused by micro bubble formation/stabilization and thereby linked to protein surface properties. The extraordinary properties of FcHyd5p, which enable the protein to stabilize micro bubbles and to induce gushing, were impaired by nsLtp1 and Z4. These proteins are included in the hydrophobin layer formed at surfaces. Thereby a negative impact on surface activity, and surface hydrophobicity occurred which led to a decrease of hydrophobin stabilized foams and emulsions.

4.1 Influence of protein Z4 on hydrophobin induced gushing

In addition to nsLtp1, protein Z is a major protein in beer. Similar properties concerning surface aggregation and effect on drainage and foam can be assumed, because both proteins are predominant in beer foam (Evans et al., 1999; Kaersgaard & Hejgaard, 1979; Sørensen et al., 1993). Hence, a similar behavior concerning gushing was also expected. The isoform Z4 was analyzed in regard to gushing because, of the two forms of protein Z occurring in beer, namely Z4 and Z7, protein Z4 is the dominant one, representing 80 % of the total protein Z content (Evans & Hejgaard, 1999).

Construction of a yeast transformant strain that produced and secreted protein Z4 upon methanol induction was successful. Sequence coverage of 42.2 % of peptides, found by LC-MS/MS analysis, confirmed the identity of Z4, which was cut off a band of about 40 kDa in SDS-gel. Z4 was at least partly produced in its native form with one peptide matching the protein part after the RCL cleavage site (Dahl, Rasmussen, & Hejgaard, 1996). However, SDS analysis revealed that also a cleaved form of the serpin was purified. In addition to the band at about 43 kDa, representing the native Z4 (Brandt, Svendsen, & Hejgaard, 1990), a shortened protein version running at about 38 kDa was present. This was assumed to be the cleaved serpin with a calculated mass of 38.3 kDa (Dahl et al., 1996). Presence of this protein spot indicated that protease inhibition by Z4 occurred already during the cultivation step, where Z4 inhibited proteases of *P. pastoris*.

This study indeed revealed that also beer protein Z4 was able to reduce gushing previously induced by hydrophobins. The effect was visible in beer and in carbonated water, with a higher reduction in beer. This was different to findings for nsLtp1 where more protein had to be added to the beer to achieve the same gushing reduction as in water. The suggested reason was the already high nsLtp1 content in beer (Lutterschmid et al., 2011). However, in contrast to nsLtp1, boiled Z4 caused a less effective gushing reduction than native Z4. As shown during the current study, this gushing reduction was even less effective after heating Z4 in synthetic wort instead of water. Therefore, during boiling in the brewing process the gushing reducing potential of Z4 in beer is reduced, and is negligible compared to that of nsLtp1, although, with 50-200 mg/L, even more protein Z was reported to be present in beer (Leisegang & Stahl, 2005). A higher gushing reducing effect of Z4 in beer may be due to cooperative gushing reduction of added protein Z4 with nsLtp1 already present in beer, which is missing in carbonated water. An interaction between nsLtp1 and protein Z was already suggested by Sørensen et al. (1993), who found that both proteins together positively affect the foam in beer.

SDS analysis revealed that transgenic protein Z4 was heat sensitive, which explained the reduced gushing activity after heating. Both bands of the suspected native and cleaved form of the serpin decreased in intensity with increasing incubation temperatures. Instead, a band of 30 kDa appeared, which was assumed to represent a degradation form of the native Z4 protein. In 2-D gels produced from barley malt and beer proteins an additional spot at 30 kDa was identified as a form of protein Z (Perrocheau et al., 2005). Additionally, a 30 kDa sized protein present in barley flour, malt, and beer was also previously identified as protein Z4

(Tanner et al., 2013). Both these findings indicate that this degradation form was present in beer. Upon heating, also the presumed dimer disappeared, which may explain the delayed decrease of native Z4. It was assumed that a complex between Z4 and an inhibited protease was visible as a further band at all temperatures at about 150 kDa. Such complexes are reported to not be destroyed by SDS treatment during electrophoresis, and therefore can be detected on SDS-gels (Dahl et al., 1996; Huntington et al., 2000). However, polymerization of serpin, which is generally known for serpin proteins, also has to be considered. Thereby intermolecular interaction between serpins can cause refolding of the molecules to result in lower energy folding (Devlin & Bottomley, 2005). For barley protein Z, formation of trimers and tetramers was suggested by Hejgaard (1982). In summary, results indicated that the native form of protein Z4 was degraded to a smaller peptide with a size of 30 kDa. Protein Z4 was shown to be sensitive to heat treatment. Although a heat stability due to stability of cleaved serpin forms was proposed (Brandt et al., 1990; Hejgaard, 1982; Stanislava, 2010), no proof was given in these reports. In fact, suggestions of at least a partial degradation of protein Z taking place during brewing were found in literature. In 2-D gel analysis of beer protein Z, spots were identified which clustered at 28-36 kDa next to the expected size around 40 kDa (Iimure et al., 2010, 2012; Perrocheau et al., 2005). For the Z4 type, sizes of about 43 kDa, and between 32 and 40 kDa, and 20 and 32 kDa were reported (Tanner et al., 2013). Even in beer a degradation fragment of Z4 was found to be present (Picariello et al., 2011).

The native form of Z4, studied here in regard to its gushing activity, was not assumed to be present in beer. During brewing either degradation or glycation is expected to happen due to boiling. These variations, experimentally simulated by heating in water or boiling in synthetic wort, possessed a less pronounced impact on hydrophobin induced gushing. Thus, protein Z4 naturally present in beer probably has a negligible impact on gushing, and compared to beer protein nsLtp1 only plays a minor role in the gushing of beer.

4.2 Protease inhibition by nsLtp1 and protein Z4

Heat sensitivity of at least native Z4 was further proven by the loss of its protease inhibition property after heating. Unspecified malt proteases showed less activity when native Z4 was added, whereas, after boiling of the serpin no change in protease activity occurred. The inhibition or reduction of malt protease activity due to Z4 is expected to lead to formation of the cleaved form of Z4. This process did not seem to affect the potential of Z4 to induce

gushing. Since Z4 belongs to the serpins, inhibition of serine proteases was suspected. Yet there was only experimental evidence for inhibition of cathepsin G (Dahl et al., 1996). Other proteases such as trypsin, subtilisin, pancreas elastase, and aspergillus protease were not affected in their activity by protein Z (Dahl et al., 1996; Hejgaard et al., 1985). Consequently, in this work no inhibition of the serine proteases, trypsin and proteinase K was observed.

Also nsLtp1 of barley is a probable inhibitor of green malt cysteine endoproteases. There was no suppression of papain or subtilisin, but activities of some serine proteinases were partially inhibited (Jones & Marinac, 1997; Jones, 2005). Results of this work confirmed that native nsLtp1 is capable of inhibiting proteases present in barley malt. But the tested serine proteases were not affected by nsLtp1. As with Z4, heat treatment of nsLtp1 resulted in the loss of inhibition property. This can be explained by defolding of the protein, which was also seen in ELISA assays and was supported by surface hydrophobicity measurements.

The tested proteases of malt were not further investigated. Proteases of all four classes are present in germinated barley. Most of the endoproteinases were reported to have pH optima below neutrality, but serine proteinases had a pH optimum at 8.0 or higher (Zhang & Jones, 1995). The protease inhibition tests were run at pH 7.4, indicating that indeed serine proteases were influenced by nsLtp1 and Z4.

4.3 Gushing reduction mechanism of nsLtp1 and protein Z4

In this study the interaction mode of the gushing factors fungal hydrophobin and beer foam proteins was investigated. According to Zapf (2006) beer foam proteins such as nsLtp1 form layers around CO_2 micro bubbles in beer and stabilize them. After pressure release a coordinated growth occurs, which results in beer foam on the beer surface. Zapf hypothesized that additional fungal proteins also aggregate at micro bubble surfaces. These were assumed to aggregate irreversibly, forming homogenous protein islands in between nsLtp1 areas on the bubble layer. A less elastic layer results, which does not withstand the increase in tension due to bubble growth upon bottle opening. An unimpeded uptake of CO_2 occurs resulting in bubble growth and bursting of the surface layer. The additional available bubble skin fragments thereby produced act as further condensation nuclei for CO_2. A fast CO_2 release is leading to gushing results (Zapf, 2006).

In accordance with this theory, results of the current work provide evidence that the gushing reduction properties of Z4 and nsLtp1 on hydrophobin induced gushing were not due to direct protein-protein interaction. In the BIAcore experiments no binding of nsLtp1 or protein

Z4 to FcHyd5p was observed, neither for hydrophilic nor for hydrophobic domain exposure of hydrophobin. Also no hydrophobic interaction could be detected by experiments on surface hydrophobicity of protein solutions. Because of hydrophobic protein interaction, it was suspected that hydrophobic parts were hidden and consequently not accessible, resulting in a decrease in surface hydrophobicity. Yet mixtures of FcHyd5p with beer foam proteins at pH value representing beer environment showed no differences in surface hydrophobicity as compared to pure protein solutions. Also, in the literature no evidence for a direct protein-protein interaction of proteins with hydrophobins was reported. No indication for a hydrophobic bonding between milk proteins and hydrophobin Hfb2 was found (Wang et al., 2013). In fact, even an interaction between different hydrophobins was reported to be unlikely (Szilvay et al., 2006).

However, some other attraction seemed to occur between nsLtp1 and FcHyd5p, as well as between protein Z4 and FcHyd5p. Particle size analysis of protein solutions by DLS during the current study showed that addition of nsLtp1 or Z4 to FcHyd5p resulted in the decrease of the presumed hydrophobin trimer at about 7 nm, whereas other peaks (12 nm at one-angle DLS) appeared or became broader or more intense (multi-angle DLS). These findings indicated that aggregation of molecules occurred. A clear statement, however, was difficult to make because resulting curves of the DLS measurements were overlapping, and covering of particle sizes because of wide distribution cannot be excluded. Big particle sizes in pure hydrophobin solutions were assumed not only to derive from protein aggregation, but also from bubble input during mixing and stabilization through the protein (Cox et al., 2007). The observed particle diameter of 148 ± 30 nm matched well with the observed micro bubble size of 100 nm in primary gushing water with added hydrophobin Hfb2 at atmospheric pressure (Deckers et al., 2011). Aggregate formation by hydrophobin proteins was reported and is believed to derive from hydrophobic protein interactions because of the hydrophobic patch (Basheva et al., 2011a; Kisko et al., 2008; Szilvay et al., 2007; Torkkeli et al., 2002; Wang et al., 2004; Zhang et al., 2011). Inhibition of hydrophobic interaction between hydrophobin molecules through protein molecules of nsLtp1 or Z4 can be imagined. This would prevent self assembly, formation of bigger aggregates and bubble stabilization. The assumption is supported by the fact that the big size particles with a mean diameter of 148 nm, which probably represent micro bubbles present in the solution, vanished in hydrophobin solution upon mixing with nsLtp1 or Z4. Another link between measured particle size distribution of FcHyd5p and gushing existed. A particle distribution analysis of gushing and non-gushing

beer showed that in gushing beer two particle classes with a mean size of about 3 nm and 100 nm were present. In non-gushing beer, only one particle class ranging from 100 nm to 300 nm was detected (Christian et al., 2011; Hagemeyer, 2012). One angle DLS measured particle size of FcHyd5p revealed the presence of the same two particle classes reported in gushing beer. Assumed monomers at 3 nm vanished when beer foam proteins were added, resulting in a particle size distribution similar to the one found in non-gushing beer.

Although no evidence for direct interaction between hydrophobin and beer foam proteins was found, an impact on aggregation behavior of proteins could be seen in the current work. The change in aggregation was also assumed to affect the protein aggregation on the bubble surface layer of CO_2-microbubbles. This corresponds to the incorporation of hydrophobin into nsLtp1 or Z4 formed films as assumed by Zapf (2006). The consequence of a simultaneous occurrence of hydrophobin and beer foam proteins would be a change of the extraordinary surface properties displayed by pure hydrophobins, eventually affecting the basic features needed for gushing induction. Considerations of Gardner (1972) also fit this assumption. The author stated that surface active anti-gushing substances must be assumed to compete for the surface layer resulting in less solid bubble layers and prevents stable micro bubble formation.

Results obtained during the current study showed that in combined samples of either nsLtp1 and FcHyd5p, or Z4 and FcHyd5p both proteins were indeed present in surface films. Experimental data showed that protein film coatings on glass which contained mixtures of the hydrophobin with either nsLtp1 or Z4 were less hydrophilic when compared to pure hydrophobin films but more hydrophilic than films formed by the pure beer foam proteins. The change in hydrophobicity indicates that both proteins were present in the protein film leading to an intermediate hydrophobicity. Furthermore, the surface activity of the hydrophobin was affected. All three tested proteins were able to lower the surface tension of water, indicating the property of protein assembly at the surface. After addition of nsLtp1, the surface tension decrease shown by FcHyd5p was less intense, indicating that both proteins were present at the air/water interface. For Z4, an effect was only observed when heat treated Z4 was added to FcHyd5p. The higher impact of heat treated beer foam proteins derived from structural changes, as indicated by surface hydrophobicity measurements. Thereby, defolding caused an increase in protein surface activity resulting in faster adsorption and better competition ability. In consequence, a facilitated integration of heat treated beer proteins into the hydrophobin film was achieved.

In addition to surface tension measurements and to results of coating hydrophobicity, AFM experiments showed the integration of nsLtp1 and protein Z4 into hydrophobin films formed at air/water interfaces. Substrate transferred from protein solution's air/water interface showed an increase in height for all tested proteins. The resolution of the AFM pictures was, however, not sufficient to elucidate whether differences in the film structures of the different proteins existed. Nonetheless, a structural change occurred for films of mixed protein samples. Mixing either nsLtp1 or Z4 with FcHyd5p, respectively, resulted in a film with increased height. Furthermore, areas of high and areas of low surface height emerged. Inhomogeneous protein distribution, as supposed by Zapf (2006) was concluded. Thereby, protein aggregation was assumed to lead to the high areas, whereas holes in the film explain the areas with low height representing the bare surface. In literature, a similar clustering of hydrophobin molecules at the surface was reported when they were mixed with whey proteins. Authors could prove that both proteins were present in the protein film. The hydrophobin was then found to separate into domains, which interconnected and vanished upon increasing hydrophobin concentrations. An irregular multilayer film formation was further suggested with the hydrophobin layer at the interface and an irregular layer of whey proteins at the bottom of the film (Blijdenstein et al., 2013). Bilayer formation was also suspected in a combined film of hydrophobin Hfb2 and β-Casein (Radulova et al., 2012). This would result in variations in protein layer height and may explain the picture in AFM images of mixed protein samples observed in this study. That no substitution of hydrophobin protein in mixed films happens was in accordance with results of emulsion experiments of this work. No increase in concentration of hydrophobin FcHyd5p was detected by ELISA in the aqueous phase of emulsions after addition of Z4 or nstp1.

The inclusion of beer foam proteins in hydrophobin formed protein layers was also supported by the negative impact of nsLtp1 and Z4 on foams and emulsions stabilized by FcHyd5p. It is well known that hydrophobins form protein layers at interfaces, causing high elasticity and giving rise to resistance against coalescence and disproportionation (Alexandrov et al., 2012; Basheva et al., 2011b; Blijdenstein et al., 2010; Cox et al., 2009, 2007; Milani et al., 2013). This results in formation of highly stable foams and stabilization of emulsions (Cox et al., 2009; Linder, 2009; Lumsdon et al., 2005; Niu et al., 2012). Accordingly, with FcHyd5p a good foaming and high stabilization was achieved. The addition of nsLtp1 or Z4 decreased FcHyd5p's foam stability. However, this was only true for boiled proteins nsLtp1 and Z4, matching the results of analysis of surface tension impact. A different result was observed for

the impact of nsLtp1 and Z4 on hydrophobin stabilized emulsions. Only nsLtp1 was able to reduce the emulsion stability of FcHyd5p, but now in native and heat treated form.

The different behavior of boiled and native beer foam proteins in foams and emulsions is due to the disordered structure gained by heat treatment improving surface activity. Higher surface activity enables boiled proteins to more easily overcome the energy barrier for adsorption (Damodaran, 2005). The energy barrier is higher at air/water interfaces in foams than at oil/water interfaces in emulsions (Damodaran, 2005). Therefore, only heat treated beer foam proteins influenced foam stability of FcHyd5p, whereas hydrophobin emulsions were also influenced by native nsLtp1. As already mentioned, the defolding of Z4 upon heating was indicated by increase in surface hydrophobicity. Defolding by heating of nsLtp1 was reported, and connected to increase in surface activity (Mills et al., 2009; van Nierop et al., 2004).

The increased protein size of protein Z4 (43 kDa) can explain that there is no effect of Z4 on stability and oil droplet size in emulsions formed by FcHyd5p. A more extensive, and less reversible adsorption of proteins at hydrophobic surfaces (Dickinson, 1999), like oil, leads to the assumption that smaller molecules of FcHyd5p, with fast adsorption, do not allow bigger protein molecules with slowed adsorption rates to compete for space at the interface. However, nsLtp1, with a lower molecular size, can compete with hydrophobin molecules. Yet results of surface hydrophobicity measurements of aqueous protein solutions showed that nsLtp1 gave a less hydrophobic protein surface than the hydrophobin, implying a reduced ability to oil adsorption. Consequently, emulsion adsorption for nsLtp1 was expected to be less intense as compared to FcHyd5p. ELISA measurements indeed showed that FcHyd5p was able to partly replace nsLtp1 from the oil surface, whereas FcHyd5p bound to the oil did not change upon addition of nsLtp1.

Destabilization in emulsions occurred via disproportionation and coalescence, which both result in an increase in oil droplet diameter. The occurrence of these effects was indicated by particle size analysis of emulsions with detection of bigger particles in less stable emulsions. Dynamic surface properties of bubble or oil droplet layers thereby determine stabilization. High elasticity and viscosity parameters prevent shrinkage as well as film rupture, and increase stability. Also, small oil droplets or bubbles are more stable (Bergeron & Walstra, 2005; Dickinson et al., 2002; Dutta et al., 2004; Kloek, van Vliet, & Meinders, 2001). The dense packing of hydrophobin proteins results in extraordinary viscosity and elasticity preventing coalescence and disproportionation (Alexandrov et al., 2012; Basheva et al.,

2011b; Blijdenstein et al., 2010; Cox et al., 2009, 2007; Milani et al., 2013). Accordingly, droplet diameters in emulsions containing FcHyd5p were small compared to emulsions prepared with mixtures of hydrophobin with beer foam protein. Incorporation of nsLtp1 and Z4 protein into the hydrophobin film can explain the negative effects on emulsion and foam stability of FcHyd5p. The protein surface film is then more susceptible to destabilization mechanisms, which is confirmed by the increase in oil droplets in emulsions. A lateral hydrophobic interaction of hydrophobin molecules (Hakanpää et al., 2004; Kallio, Linder, & Rouvinen, 2007; Paananen et al., 2003; Szilvay et al., 2007) within the film can be assumed to be distorted, resulting in a weaker protein layer, which was also proposed by Wang et al. (2013) for mixed protein films of hydrophobin and surface active milk proteins.

The detected change in hydrophobicity, displayed by protein films on a hydrophobic substrate for protein combinations, can also serve as explanation of further destabilization effects. Hydrophobin coatings turn the surface of hydrophobic substrate more hydrophilic. For hydrophobic carbon dioxide in beer this implies that CO_2 bubbles are surrounded by a protein layer exposing a hydrophilic surface to a hydrophilic medium, giving rise to good dissolution. However, bubbles with a hydrophobic protein layer, which is displayed by nsLtp1 and Z4, are expected to attract hydrophobic components, e.g. adjacent bubbles, leading to facilitation of merging and coalescence. Mixed protein layers were less hydrophilic than FcHyd5p alone. If coated by both proteins, bubbles therefore increased attraction to each other and consequently were more susceptible to destabilization. Significant negative correlations found between the oil wettability of protein films and the corresponding foam formation and emulsion stability, respectively, support this assumption.

4.3.1 Model of gushing mechanism

Both analyzed models of protein films at air/water interface and oil/water interface, represented by foaming and emulsion experiments, have to be taken into account to explain the gushing phenomenon. Gushing involves bubbles of CO_2 being in an aqueous phase. Thereby, the interface of CO_2/beer resembles air/water interfaces with CO_2 being a gaseous component. On the other hand, CO_2 bubbles are simultaneously a polar hydrophobic constituent comparable to oil droplets in oil-in-water emulsions.

Based on the obtained results, literature, and the theory presented by Zapf (2006) the following model for the gushing reduction mechanism of nsLtp1 and Z4 on hydrophobin induced gushing is suggested. A scheme of the model is given in Figure 53. In beer without

hydrophobin, surface active beer proteins, nsLtp1 and protein Z, assemble at CO_2 bubbles, which is supported by results of surface tension measurements and AFM. This only happens if CO_2 or gas was already incorporated into the liquid by the filling process and shaking of the bottle (Christian et al., 2009; Ilberg et al., 2008). Both proteins are capable of reducing the surface tension. Yet the decrease is not sufficient for the formation of stable bubbles. Further, no compact protein layer is assumed to be formed because of the capability of refolding at the interface, known at least for nsLtp1 (Euston et al., 2008; Euston, 2010). This leads to shrinkage and disappearance of the bubbles, which is supported by the low stability of foams and emulsions containing pure nsLtp1 or Z4, respectively. If bubbles are bigger than a critical diameter, they will grow and rise (Yount et al., 1984) resulting in the transfer of these proteins to the top and assembly at the interface between liquid and headspace. Upon bottle opening and pressure release, dissolved CO_2 can evaporate at natural particles and at glass walls (Gardner, 1973). Bubbles rise and when reaching the surface they collect nsLtp1 and protein Z, which previously accumulated there. Foam is then produced, stabilized by these proteins.

If hydrophobin proteins are present in the beer, they form a rigid layer at CO_2 gas brought into the liquid by shaking because of their extraordinary surface activity. Bubbles are formed, surrounded by this layer, which are stable as indicated by small oil droplet diameters in hydrophobin containing emulsions and great foam stability displayed by FcHyd5p. Stabilization is assumed to derive from lateral hydrophobic interactions (Hakanpää et al., 2004; Kallio et al., 2007; Paananen et al., 2003; Szilvay et al., 2007). The CO_2-concentration gradient between the inside of the bubble and the surrounding liquid, results in compression of the bubbles. Yet stable micro bubbles are formed because the hydrophobin molecules display a low surface tension. Moreover, hydrophobins do not desorb off the layer leading to a densely packed film which becomes almost solid. Due to the missing desorption, wrinkles are assumed to be formed in the layer when bubbles shrink (Alexandrov et al., 2012; Blijdenstein et al., 2010; Blijdenstein et al., 2013; Cheung, 2012; Cox et al., 2007; Stanimirova et al., 2013; Wang et al., 2013). Upon pressure release, CO_2 dissolved in the liquid diffuses into the micro bubble, increasing the diameter very fast. However, the rigid layer formed by hydrophobin is not elastic because of the previous compression and wrinkle formation. Expansion is not possible, leading to bursting of the bubble surface layer and release of gaseous CO_2. These assumptions are supported by findings and considerations of Alexandrov et al. (2012), Deckers et al. (2010; 2013), Draeger (1996), and Wang et

al.(2013). Additionally, the energy liberated by the explosion can break bonds between CO_2 and water molecules, as proposed by Deckers and co-workers (2013), resulting in fast evaporation and diffusion of CO_2. Furthermore, fragments of the bubble layer containing hydrophobin aggregates remain (Cox et al., 2007) as shown by the increased level of FcHyd5p in the 'btl' fraction, and can now act as condensation nuclei. As a consequence more bubbles are formed leading to further CO_2 evaporation and eventually to overfoaming. This phenomenon can explain the sudden release of CO_2 accompanied by the immediate occurrence of huge number of bubbles in the whole volume of gushing beer (Draeger, 1996; Pellaud, 2002).

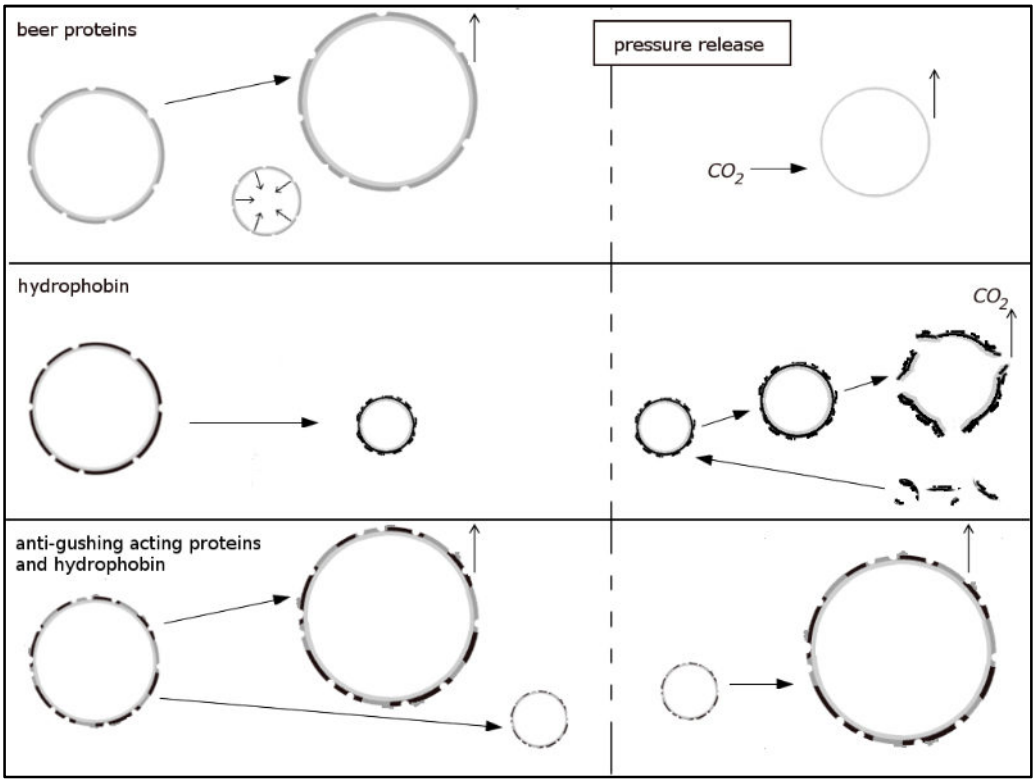

Figure 53: Model of the evolution of the gushing phenomenon by hydrophobin stabilized micro bubbles and the impact of beer proteins. Beer proteins (dark gray) alone cannot form stable micro bubbles, upon bottle opening natural bubble formation releases CO_2 (top). Stable micro bubbles are formed in the presence of hydrophobins (black), which grow and burst when pressure is released. Remaining fragments of hydrophobin containing bubble layers act as further nucleation sites (middle). If anti-gushing acting beer proteins nsLtp1 and protein Z4 are additionally present, they incorporate into the hydrophobin layer at the bubble surface. The layer gets more elastic, preventing burst and escalating of gas diffusion (bottom).

If in addition to hydrophobins, also a high number of beer proteins nsLtp1 and Z4 are present in beer, these will integrate into the hydrophobin film, changing its structure, leading to a more elastic surface after compression. Micro bubbles are formed, which can act as

condensation nuclei. However, because of the higher bubble surface film elasticity, the bursting of bubbles due to growth is diminished, reducing the extent of CO_2 liberation and consequently the severity of gushing. Furthermore, if a high extent of nsLtp1 or Z4 is present, micro bubbles will no longer be so stable. In addition to an increase of surface tension, destabilization by coalescence and disproportionation will occur, indicated by stabilization experiments of both foam and emulsions, as well as by increased diameters of oil droplets in mixed emulsions. As a result bubbles grow and ascend and, consequently, less micro bubbles are present which can act as evaporation site.

For hop constituents with inhibitory effect on gushing, like humulones, terpene, iso-α-acids, and linalool a similar mechanism was suggested. These surface active substances adsorb at the bubble surface, creating holes in the layer of gushing promoting substances and thereby prevent formation of micro bubbles and condensation nuclei (Shokribousjein et al., 2011). The formation of holes due to gushing reducing agents was supported in this work by results obtained in AFM experiments of protein films with combined proteins FcHyd5p and beer proteins.

4.4 Interaction of nsLtp1 and FcHyd5p in gushing samples

The presence of hydrophobins alone is not sufficient for gushing induction, but the ratio of hydrophobin and beer proteins appeared to be important for gushing performance. Gushing experiments by Lutterschmid et al. (2011) with nsLtp1, as well as findings of Zapf et al. (2005) and Hippeli & Hecht (2007) led to the conclusion that high levels of nsLtp1 in beer prevent gushing. This effect was supported by studies in this current work.

In ELISA experiments a correlation of the level of nsLtp1, but not of the level of hydrophobin FcHyd5p, to gushing and partly to overflow volumes was detected. High amounts of nsLtp1 were found in non-gushing beer. In gushing beers a lower content of nsLtp1 was present, with a trend to lower amounts of nsLtp1 in beers with higher overflow volumes. The variance in correlation between nsLtp1 content and gushing volumes was assumed to be due to other factors, such as hop compounds or the other major beer foam protein Z, which affect gushing (Christian et al., 2011; Gardner et al., 1973; Lutterschmid et al., 2011, 2010). For the level of hydrophobin no differences between beer with and without gushing was detected. Probably the contents were too low to be detected by the ELISA assay, with only small amounts needed for gushing induction (Linder, 2009; Sarlin et al., 2012, 2005a; Stübner et al., 2010). Titration experiments further showed that indeed the nsLtp1

content of beer is a determining factor for gushing. Beers with increased nsLtp1 content exhibited less overfoaming upon addition of the same amount of FcHyd5p than beers containing lower nsLtp1 contents.

Sarlin and co-workers detected a relation between hydrophobin level and gushing potential in malt determined with MCT, with increased gushing risk for concentrations above 250 µg/g. However, no clear correlation between overfoam volumes in the *in vitro* test and levels of hydrophobin was observed (Sarlin et al., 2005b; Sarlin, 2012). During the current work no correlation of hydrophobin content and gushing occurrence or gushing intensity as determined by MCT was observed. The different observations can be explained by the fact that gushing tests strongly depend on the instrumentation and execution, which may vary between laboratories (Haikara et al., 2005; Rath, 2008). Furthermore, fluctuations in determined overflow volumes lead to imprecise prediction of the gushing potential (Christian et al., 2011). However, in the current work, for malt tested for its gushing potential by the Donhauser test, a correlation between gushing and hydrophobin level existed for barley samples classified as instable towards gushing. The positive logarithmic correlation indicated that higher amounts of FcHyd5p yield higher overflow volumes in that particular gushing test. The different relations of the gushing tests to the amount of hydrophobin can be explained by the different boiling procedures applied in both tests. For the Donhauser test the malt is mashed completely, whereas in the MCT only an extract of malt is boiled. By using only malt extract in the MCT, gushing relevant particles, such as hydrophobin proteins, may be lost during extraction leading to lower gushing values (Christian et al., 2011). The removal of hydrophobin together with solid particles is supported by the fact that in brewing samples hydrophobin was found in spent grain. In line with this assumption, the Donhauser test is reported to be more sensitive (Rath, 2008). The differences in gushing test execution also explain differences in the relation of nsLtp1 and the corresponding gushing volumes within both tests. No correlation was observed when gushing malt classified by MCT was compared to the level of nsLtp1. This result was in accordance with findings of Hégová et al. (2009) who could not find a correlation between nsLtp1 amount and degree of gushing determined by Carlsberg test. However, gushing volumes of barley malt determined by Donhauser test increased with lower nsLtp1 contents. Thus, for prediction of the gushing potential of malt by Donhauser test it can be concluded that not only the hydrophobin content is determinative, but also the amount of nsLtp1. As in beer, the ratio of FcHyd5p to nsLtp1 in malt should be taken into account and is most likely crucial for gushing potential.

4.5 Influencing gushing by changing protein contents through brewing settings

4.5.1 Influence of environmental treatments on FcHyd5p

The antibody used for the detection of FcHyd5p in ELISA experiments recognized hydrophobin in samples of beer and mashing, without further cross reactions. It was therefore possible to detect and to follow FcHyd5p in brewing. Not only was FcHyd5p presumed to be quantified, but also other class 2 hydrophobins possibly present in samples. The peptide chosen as antigen could be aligned with class 2 hydrophobins of 26 *Ascomycetes*. By measuring extracts of barley grain which was field infected by *F. culmorum,* a possible application of the test in complex samples was confirmed. Since hydrophobin proteins are important for fungal infection (Ebbole, 1997; Tucker & Talbot, 2001), cereal *Fusarium* infection is believed to result in production of hydrophobins and was shown for *F. culmorum* (Sarlin et al., 2007). In malt artificially infected with *F. graminearum* during steeping, an increased level of FcHyd5p was detected by the ELISA assay. Again, this can be explained by fungal production of hydrophobin in order to infect the grain (Ebbole, 1997; Tucker & Talbot, 2001). During malting, fungal growth is expected because of favorable conditions (Gjertsen et al., 1963). Fungal growth and an increase of hydrophobin level during malting was reported (Oliveira et al., 2012; Sarlin et al., 2007; Schwarz et al., 1995) and is in accordance with findings of this study. By also testing a malt sample which was infected by a strain deficient for the FcHyd5p corresponding gene, the applicability and specificity of the ELISA test was validated again.

The hydrophobin FcHyd5p was shown to induce gushing in carbonated beverages (Lutterschmid et al., 2010; Stübner et al., 2010). Experiments were performed to detect critical steps during brewing, where hydrophobin concentrations can potentially be decreased in order to reduce the gushing potential of beer. FcHyd5p was added to different brewing steps but none of the produced beers showed gushing. In small scale brewing the surface/volume ratio of the vessels used is very high. Hydrophobins, which are known to be very surface active were reported to attach to hydrophobic surfaces in an unspecific manner (Linder et al., 2005; Wösten & de Vocht, 2000). It can be assumed that the proteins had been bound to the vessel's surfaces already during mashing and were therefore not passed on further through the brewing process into the final beer to induce gushing. Another reason why no gushing beer could be produced during the current study may have been the setting

of different brewing parameters, e.g. temperature, which may have favored the extraction and denaturation of beer proteins nsLtp1 or protein Z4, which negatively affect gushing (Lutterschmid et al., 2011; this study).

However, addition of the FcHyd5p at different steps of the brewing process could be detected in process samples. Monitoring FcHyd5p during the brewing process showed that mashing and wort boiling resulted in a decrease, whereas lautering increased its level. Although class 2 hydrophobins are believed to be heat stable up to 80-90 °C (Askolin et al., 2006; Torkkeli et al., 2002), the mashing step had a negative influence on the level of hydrophobin. Only temperatures up to 76 °C were reached in mashing, thus, other factors such as increased foaming (Ammer M., personal communication), or as described above, assembly of hydrophobin proteins to the vessel's surface may contribute to the loss of hydrophobin. Also a partial binding of the hydrophobin to malt particles and protein aggregation has to be taken into account. Sarlin et al. monitored hydrophobin throughout the brewing of gushing positive malt. They showed that hydrophobin proteins were partly extracted during mashing leading to a transfer of 20 % hydrophobin to wort (Sarlin et al., 2007). In contrast, in this study an increased level of hydrophobin was detected in wort samples as compared to the end of mashing. The reason being that both experiments were not comparable. Sarlin and colleagues already used infected malt for brewing where hydrophobin is expected to be present not only in soluble form at the beginning of mashing, but also bound to and inside malt kernels (Kang & Buchenauer, 2000; Oliveira et al., 2012). The increase of FcHyd5p in kettle wort detected in this study can be explained by the addition of water and sparging, partly dissolving and washing hydrophobin from the malt particles. A measured signal in spent grain supported this assumption. Loss of hydrophobin then occurs through spent grain and partly by last running, probably by binding of the surface active proteins to malt particles and grist. These results are in accordance with Sarlin and co-workers who also reported a loss of hydrophobin via spent grain (Sarlin et al., 2007). They, however, calculated a loss of 80 %, whereas here the detected loss was less severe with only 10 %. This can again be explained by the addition of solved hydrophobin directly into mash in contrast to usage of infected malt.

Preliminary experiments revealed that FcHyd5p boiled in synthetic wort was less sensitive towards the ELISA than samples incubated at 25-90 °C. The decrease of the FcHyd5p-level by wort boiling, thus, probably derived by a reduced detectablity. Thereby a loss over trub was not detected, indicating that no denaturation and agglomeration happened during boiling. This again is in contradiction to the studies of Sarlin et al. who reported a loss of

hydrophobin by cold break (Sarlin et al., 2007). A loss of hydrophobins and the corresponding gushing potential by wort boiling also is supported by the fact that more intensive wort boiling is reported to decrease the gushing risk (Kunert et al., 2001; Narziß, 1995). Another possibility why loss of hydrophobin occurs over boiling may be the same reason as loss after mashing. Hydrophobin may stick to the surface, preventing further transfer. This assumption is supported by the fact that in cold wort the hydrophobin content is further decreased. The increased level of FcHyd5p in beer in comparison to the previous brewing samples cast wort and trub was assumed to rise from masking of hydrophobin during wort boiling. Aggregate formation was suspected to happen, supported by the results of DLS measurements where next to monomeric particle size trimers and higher aggregates were also found. Alcohol, which is produced during fermentation process, is believed to partly dissolve aggregates, increasing the hydrophobin particles recognized by the antibody in beer. Breaking of hydrophobin aggregates into monomers by alcohol was shown to happen for the class 2 hydrophobin Hfb2 (Kisko et al., 2008).

The decrease in detection of hydrophobin by boiling in synthetic wort was assumed to be the result of protein modification during wort boiling. Lutterschmid et al. (2010) and Sarlin et al. (2012) suspected that the less effective gushing induction of hydrophobins after boiling in synthetic wort derived from structural changes by glycation. A decreased gushing induction for hydrophobin heated in synthetic wort was also confirmed in this work. The effect was thereby increased with increasing pH values. However, this study revealed by MALDI analysis that the native FcHyd5p was already glycated. This glycation of FcHyd5p probably occurred via enzymatic glycosylation during recombinant expression in *P. pastoris*. By N-linked glycosylation through the host *P. pastoris* an oligosaccharide chain composed of 8-11 mannoses and N-acetylglucosamine is added to the amino group of Asn: $Man_{8\text{-}11}$-$GlcNAc_2$ (Trimble et al., 1991). Since FcHyd5p has one glycosylation site for N-linked glycosylation (Gavel & von Heijne, 1990; Mellquist et al., 1998), this would at least result in a mass shift of 1502 Da, which is more than observed. Therefore, N-linked glycosylation was excluded. Moreover, the only aa motive for N-glycation found within the sequence of FcHyd5p lies in a α-helical structure and is thought to be inaccessible. *P. pastoris* is also capable of O-linked glycosylation, although not much is known about the mechanism and the specification (Cereghino & Cregg, 2000; Trimble et al., 2004). In a study by Duman et al. (1998) it was shown that α-1,2-mannans out of mainly dimers and trimers are linked to serine and threonine residues of the proteins. But tetrameric and pentameric oligosaccharides also occur.

The sequence of FcHyd5p contains 5 threonines and 5 serines and 5 major double peaks can be distinguished in the obtained MALDI spectrum. So it can be assumed that either one serine or threonine residue was glycosylated and the number of peaks correlated to length of the oligosaccharide chain, where 2 to 5 mannose residues can be linked. Whether hydrophobins are produced in glycosylated form in nature, is not clear. Filamentous fungi are able to carry out both glycosylation forms, i.e. O- and N-linked glycosylation (Deshpande et al., 2008). However, until now only for some class 1 hydrophobins an O-linked glycosylation was observed (Asgeirsdóttir et al., 1998; Kwan et al., 2006; Peñas et al., 2002).

Although an increase in glycation was measured by glycation assay after boiling FcHyd5p in synthetic wort, no change in the glycation pattern was detected by MALDI analysis. The used periodate glycation assay detects chain terminal C-OH adjacent to C-OH or C=O in the sugar chain (Ahmed & Furth, 1991; Furth, 1988). An increase in formaldehyde release and thus increase in assay signal occurs thereby if the sugar is present in reduced form. Then not only is the C1 but also the C6 able to form an aldehyde by reaction with periodate (Furth, 1988; Kennedy et al., 1993). Therefore, it was assumed that upon boiling in synthetic wort a reducing environment is supplied to FcHyd5p leading to reduction of already bound sugars, which in consequence results in an increase in assay detection. The assumption was supported by results of the MALDI analysis. After boiling in synthetic wort all occurring peaks observed in spectra of unboiled samples were ascertained, but in addition a peak with 16-17 Da less in mass arose in each main peak. Moreover, for each main peak the intensity of the second peak decreased in favor of the 16-17 Da smaller first peak. The mass difference of 16-17 Da corresponds to the mass of a hydroxyl molecule (OH).

The synthetic wort, representing the wort in brewing, is composed of four reducing sugars and a reducing environment of malt before fermentation was stated (Perrocheau et al., 2006). In combination with gushing experiments one can conclude that sugar reduction in glycated FcHyd5p due to heating in synthetic wort decreases the hydrophobin's gushing strength in beer. A slight correspondence with gushing volumes resulting by addition of FcHyd5p heated in synthetic wort was observed. Gushing induction was inhibited by incubation of FcHyd5p at pH 11, which was related to a high signal in the glycation assay, assumingly representing a high amount of reduced bond sugar molecules. Findings of Lutterschmid and colleagues (2010; 2011) for FcHyd5p and Hfb2 and of Sarlin et al. (2007) for Hfb2 demonstrated that boiling of hydrophobins in wort reduced overflow volumes in beer, and support this conclusion. Gushing experiments with FcHyd5p heat treated in synthetic wort prior to

addition to carbonated water revealed no influence by this kind of protein treatment on the hydrophobin's gushing intensity, in accordance with Lutterschmid et al. (2010). The effect of bound reduced sugars probably is greater in beer because of the decreased competition potential of the hydrophobin for micro bubble layer with other surfactant substances in beer, which are, however, missing in carbonated water (Liger-Belair, 2005). Results of foaming experiments showed that a more stable foam was formed by FcHyd5p after heating it in synthetic wort, yet the foam formation was not further increased with higher temperatures, supporting the explanation that initial bubble adherence is influenced only in a minor way.

4.5.2 Influence of brewing on the level of nsLtp1

The ELISA assay developed for detection of beer protein nsLtp1 followed the same principle as the one for FcHyd5p detection. The antibody used for nsLtp1-ELISA development was only able to recognize nsLtp1 after heat treatment. Unfolding of the protein seemed to occur allowing the antibody to bind. This was supported by experiments demonstrating that heating of nsLtp1 resulted in an increase in surface activity. Boiling in synthetic wort, led to an increased ELISA signal which was assumed to be a result of higher unfolding by glycation during heating (Jégou et al., 2001). The antibody was also sensitive towards nsLtp1 of wheat. Therefore, the ELISA was appropriate for quantification of nsLtp1 content as sum of nsLtp1 protein of wheat and barley nsLtp1, which had to be considered if wheat beer was analyzed.

Samples measured in different runs resulted in variable concentrations of nsLtp1. Moreover, the measured nsLtp1 contents of 122-400 mg/mL in beer did not match reports on the amount of nsLtp1 in beer present in literature. Depending on wort boiling temperature 2-3 µg/mL or 17-35 µg/mL were detected by van Nierop et al. (2004). The group of Jégou (2000) extracted ~40 µg/mL nsLtp out of beer. But the general presence and the relative amount of nsLtp1 in samples measured within one ELISA assay was comparable to results of Western blot analysis. Therefore, ELISA results were calculated in relative values, and only samples measured within one ELISA run were compared.

Fungal barley infection is reported to increase the expression of several Ltp genes, leading to the presumption of a role in the defense of plants. No studies on this topic were found concerning the examined barley protein nsLtp1. However, genes encoding LTP2, LTP3 and LTP4 in *H. vulgare* were up-regulated upon plant infection (Molina & García-Olemedo, 1993). In *Fusarium* infected wheat plants also an increase of nsLtp1 was reported (Hippeli & Hecht, 2008). An increase in nsLtp1 level in infected barley grain as determined in the

current study could therefore be explained and showed that the developed ELISA detected nsLtp1 in complex samples. The nsLtp1 content in examined infected wheat malt, however, did not vary. Expression of *ltp* genes of wheat is spatially and developmentally distributed. The gene corresponding to the Ltp which is recognized by the antibody in the ELISA, gave transcripts during maturation, germination and seedling (Boutrot et al., 2005), indicating that already gene expression is switched on and may not further be increased by infection during germination. Accordingly, the amount of nsLtp1 in malt of barley and wheat was reported to be unchanged in infected samples (Hégrová et al., 2009). Hippeli and Hecht (2008) observed an increase of nsLtp1 in green malt after infection, but the differences were less pronounced than for infected grain.

The addition of nsLtp1 at different steps within the brewing process could not be detected. In malt and beer samples a high level of the protein was already present, thus, the added amount was assumed to be too low to be distinguished. In literature a decrease during wort boiling was reported with a loss of about 75 % (Lusk et al., 2001a). Van Nierop and colleagues (2002) measured an even greater loss of Ltp1 of 97 % during boiling. Yet both these results were obtained by an ELISA which was directed against native Ltp proteins. However, it was shown that upon boiling nsLtp1 is defolded, undergoes reduction, and Maillard glycation throughout the brewing process, where structural unfolding happened during kettle boiling (Jégou et al., 2001; Perrocheau et al., 2006; van Nierop et al., 2004). The heat treated nsLtp1 was the foam active form and also had more impact on gushing reduction, and thus its remain and level in brewing was of great interest. The antibody used in the current work was only able to detect heat treated and therefore unstructured nsLtp1. With this antibody an increase during lautering was detected, which was decreased again during the wort boiling process. The increase can be explained by the liberation of nsLtp1 from grist particles. In first wort, which is mainly the liquid fraction of mashing end samples, a decreased content of nsltp1 was measured. A masking and partial removal of nsLtp1 by aggregates formed during heating in mashing was suspected. Only after sparging are nsLtp1 proteins presumed to be washed out, explaining the increase of the protein in kettle wort samples. A part of nsLtp1 still remained in the spent grain, which is to be expected since after heating partial precipitation was shown to occur (van Nierop et al., 2004). Moreover, nsLtp1 was already reported to be present in this brewing sample by Jégou et al. (2001).

The decrease in the level of nsLtp1 during wort boiling was also stated by Lusk et al. (2001) who in addition to the antibody against native Ltp protein, also used an ELISA with an

antibody directed against foam active nsLtp1. The foam active form was increased upon boiling, whereas the native form of nsLtp1 decreased, resulting in an overall decrease of nsLtp1 (Lusk, 2001a, 2001b). Also Robinson and David (2008) observed a decrease of nsLtp1 with ongoing wort boiling. Although nsLtp1 is heat stable, boiling in reducing environment in beer leads to defolding and denaturation (Lindorff-Larsen & Winther, 2001; Matejková et al., 2009; Perrocheau et al., 2006). High temperatures in wort boiling, thus, are assumed to denature already reduced Ltp proteins, leading to general decrease of nsLtp1 which was shown by the decreased level after wort boiling.

5 Summary

In this study the basics of primary gushing and the influence of beer foam proteins on this phenomenon were examined. The class 2 hydrophobin FcHyd5p was found to possess a reduced potential to induce gushing after heat treatment in synthetic wort, with an increased impact at higher pH values. Analysis of its glycation state by MALDI analysis showed that the native transgenic protein was already glycated and that the degree of glycation was not altered by boiling in the presence of sugars. By use of glycation assay, which detects not only glycation of proteins, but also the reducing state of bound sugars, an increased signal for heat treated FcHyd5p was detected. The decrease of gushing induction in beer was thus concluded to derive from the reduction of bound sugars at FcHyd5p due to the reducing environment of boiling wort, which was favored at higher pH values.

ELISA assays for detection of nsLtp1 and FcHyd5p in brewing samples were established, and a relative quantification was performed in gushing relevant samples.

Added FcHyd5p was monitored in brewing samples. A general increase from mashing to finished beer was observed. In the mashing and wort boiling stages a decrease of the signal was detected. A loss of hydrophobin due to its assembly at vessel surfaces and masking upon aggregate formation in wort boiling were assumed. Only a small loss occurred via spent grain and no loss over trub.

The addition of nsLtp1 to brewing was not visible by ELISA. An existing high amount of nsLtp1 in malt was assumed. In general the detection was increased during brewing. The increase in the level of nsLtp1 during lautering was suggested to be due to a wash out of proteins from particles by sparging. A part of nsLtp1 was removed by spent grain. Wort boiling decreased the nsLtp1 content, which was partly attributed to masking of nsLtp1 in the test by aggregate formation. In beer the amount of Ltp1 was increased again.

For malt classified as gushing positive by MCT no correlation between gushing occurrence and nsLtp1 or FcHyd5p content was observed. For malt tested by the Donhauser test the amount of FcHyd5p was positively correlated with overfoaming volumes of gushing instable malts, whereas for nsLtp1 the level decreased with increasing gushing volumes. By examination of gushing and non-gushing beers with ELISA, no relation between gushing and FcHyd5p was detected. For nsLtp1 increased amounts of protein were detected in non-gushing beers, with a trend to decreased overflow volumes for a rising level of nsLtp1. The ratio of FcHyd5p:nsLtp1 was increased in gushing beer and positively correlated to gushing volumes of malt determined by the Donhauser test.

For both proteins tested, nsLtp1 and FcHyd5p, the level was increased in the volume fractions which stayed in the bottle.

Results showed that next to hydrophobin, nsLtp1 is an even more influencing factor concerning gushing occurrence. This was further supported by the fact that beers that naturally contained a higher level of nsLtp1 showed less intense gushing by the addition of same amounts of FcHyd5p.

The other main foam protein in beer, protein Z4, was cloned in *P. pastoris* for heterologous production in order to analyze Z4 in regard of gushing. Z4 was also able to reduce hydrophobin induced gushing. The influence was decreased after heat treatment and still further after boiling in synthetic wort. This was shown to be due to heat instability. A degradation product with 10 kDa decreased size was observed by SDS analysis. The protein Z4 occurring in beer, was thus concluded to have only minor effect on gushing. Both examined beer proteins, namely Z4 and nsLtp1, were in addition shown to inhibit undefined malt proteases, probably of the serine type. The heat sensitivity of both proteins was further evidenced by the loss of protease inhibition after heating. Other tested serine proteases were not affected.

The effect of beer proteins on the gushing induction of hydrophobin was analyzed by examination and comparison of pure proteins and combinations of hydrophobin with beer proteins. A direct and also a hydrophobic interaction between FcHyd5p and nsLtp1 or Z4, respectively, was excluded due to negative results of BIAcore SRP experiments and analysis of surface hydrophobicity of protein solutions. Addition of nsLtp1 or Z4 to FcHyd5p resulted in aggregate formation in FcHyd5p solutions as detected by DLS. Particles of micro bubble size, however, vanished in solutions with combined proteins.

By surface tension experiments and analysis of oil wettability of protein films on glass, as well as by AFM of protein films transferred from drop surfaces, a joint appearance of both proteins in protein layers was shown, when FcHyd5p was combined with either of the two beer foam proteins. By AFM a structure change to thicker films with occurrence of areas with low and areas with high protein coverage was observed.

The parallel occurrence did negatively affect the stability of emulsions prepared with FcHyd5p. Observed destabilization was suggested to be due to increased coalescence and disproportionation, resulting in an increase of oil droplet diameters, as demonstrated by particle size distribution analyses. A negative influence of nsLtp1 and Z4 on foam stability displayed by FcHyd5p was also detected. Because of different surface properties and energy

barriers between air/water and oil/water interfaces, only heat treated nsLtp1 and Z4 decreased the stability of hydrophobin foams. The heat treatment resulted in a defolding giving rise to increased surface hydrophobicity and an increased surface activity as evidenced by surface tension measurements. Correlations were found between emulsion stability and foam stability, between both stabilities and surface tension impact, as well as between both stabilities and oil wettability of protein films. Results of experiments on these surface properties, thus, could be used for interpretations concerning the gushing phenomenon.

Based on these findings, a model for the influence of incorporation of nsLtp1 or Z4 into hydrophobin films, surrounding CO_2 bubbles in gushing beer, is proposed. By integration of beer foam proteins into the hydrophobin layer, bubbles are more susceptible to destabilization, and less micro bubbles are formed that can act as condensation site. Remaining micro bubbles further become more elastic giving rise to stabilization of micro bubbles, which would otherwise burst upon pressure release by bottle opening. A fast evaporation of CO_2 is hindered resulting in a reduction of gushing.

6 Zusammenfassung

In dieser Arbeit wurden die Grundlage von primärem Gushing und der Einfluss von Bierschaumproteinen darauf untersucht. Für das Klasse 2 Hydrophobin FcHyd5p war nach Hitzebehandlung in synthetischer Würze, insbesondre mit steigendem pH Wert, die Fähigkeit Gushing zu induzieren herabgesetzt. Mittels MALDI Analyse konnte eine Glykosylierung bereits bei transgenem nativem Protein nachgewiesen werden. Der Grad der Glykosylierung veränderte sich dabei während des Kochens in Anwesenheit von Zuckern nicht. Untersuchungen mittels eines Glykierungs-Testes, welcher nicht nur auf Glykierung, sondern auch auf Reduzierung der Protein-gebunden Zucker anspricht, ergaben ein erhöhtes Signal für in synthetischer Würze hitzebehandeltes FcHyd5p. Die beobachtete Gushingreduzierung in Bier wurde deshalb auf die Reduzierung von an das Hydrophobin gebundenen Zuckern zurückgeführt, wobei dies bei höheren pH Werten begünstigt war.

ELISA Tests für die Detektion von nsLtp1 und FcHyd5p in Brauproben wurden entwickelt, mit deren Hilfe eine relative Quantifizierung der Proteine in Gushing-relevanten Proben erfolgte.

Nach Zugabe von FcHyd5p zu verschiedenen Zeitpunkten im Brauprozess, wurde dieses während des Brauens verfolgt. Im Allgemeinen war eine Zunahme des Hydrophobingehaltes vom Maischen zu fertigem Bier erkennbar. Allerdings war nach den Braustufen Maischen und Würzekochen die Hydrophobinkonzentration verringert. Ein Rückgang von FcHyd5p aufgrund einer Anlagerung der Proteine an Kesseloberflächen, sowie Maskierung über Aggregatbildung während des Kochvorgangs wurde vermutet. Verlust von FcHyd5p über den Treber war gering und kein Ausfall fand mit dem Trub statt.

Mittels des ELISA Tests war die Zugabe von nsLtp1 in den Brauprozess nicht detektierbar. Dies wurde mit einem bereits hohen Anteil an nsLtp1 in Malz erklärt. Allgemein nahm die Detektion von nsLtp1 während des Brauvorgangs zu. Läutern erhöhte die Menge an nsLtp1, vermutlich aufgrund von Auswaschung der Proteine aus Partikeln. Dennoch wurde nsLtp1 teilweise über den Treber aus dem Brauprozess entfernt. Die ermittelte nsLtp1 Menge war nach dem Würzekochen verringert, was teilweise vermutlich auf Proteinmaskierung durch Aggregatbildung zurückführbar war, da im Bier der Gehalt an nsLtp1 wieder anstieg.

Gushingpotential von Malz welches mittels des MCT bestimmt worden war, zeigte keine Korrelation zu ermittelten Mengen an FcHyd5p oder nsLtp1 im Malz. In, mittels des Donhauser Tests, als Gushing-instabil eingestuften Malzproben, war der Level an FcHyd5p positiv mit den Überschäummengen korreliert. Für nsLtp1 dagegen sank für alle Gushing-

positiven Proben der Gehalt an nsLtp1 mit steigendem Überschäumvolumen. Bei der Untersuchung von gushendem und Gushing-negativem Bier mittels ELISA war keine Korrelation zwischen Gushingvorkommen bzw. –volumen mit FcHyd5p nachweisbar. Für nsLtp1, jedoch, wurden erhöhte Proteinmengen in nicht-gushenden Bieren ermittelt. Zudem war ein Trend zu verminderten Gushingvolumen mit steigendem nsLtp1-Gehalt erkennbar. Das Verhältnis von FcHyd5p:nsLtp1 war in gushendem Bier erhöht. Eine positive Korrelation bestand zwischen FcHyd5p:nsLtp1 und Überschäumvolumina in Malz, ermittelt über dem Donhauser Test. Der Level beider getesteter Proteine, nsLtp1 und FcHyd5p, war in der Bierfraktion erhöht, welche nach dem Überschäumen in der Flasche verblieben war.

Die Ergebnisse beweisen, dass nsLtp1, neben Hydrophobinen, ein sogar noch bestimmenderer Faktor für das Auftreten von Gushing ist. Dies wurde weiterhin gezeigt in Versuchen, bei denen in Bier mit natürlich erhöhtem nsLtp1 Gehalt, die gleiche Zugabe von FcHyd5p ein geringeres Gushing auslöste.

Das andere Hauptbierschaumprotein Protein Z4 wurde für heterologe Proteinproduktion in *P. pastoris* kloniert um Protein Z4 in Bezug auf Gushing zu analysieren. Z4 war in der Lage Hydrophobin–induziertes Gushing zu reduzieren. Die reduzierende Wirkung war nach Hitzebehandlung und v.a. nach Kochen in synthetischer Würze verringert. Untersuchungen mittels SDS-Gel-Analyse zeigten, dass dies auf Hitzeinstabilität des Proteins zurückzuführen war, da ein Abbauproduckt verkürzt um 10 kDa nachgewiesen wurde. Protein Z4 spielt somit, in der Form wie es im Bier vorliegt, in Gushing nur eine untergeordnete Rolle. Für beide untersuchten Bierproteine wurde weiterhin eine Protease-inhibitorische Funktion gezeigt. Die Aktivität von nicht weiter bestimmten Malzproteasen, vermutlich des Serinprotease Types, wurde inhibiert. Durch einen Verlust der Proteaseinhibition nach Hitzebehandlung, wurde überdies die Hitzesensitivität von nsLtp1 und Z4 bestätigt.

Die Funktionsweise der Bierproteine in Bezug auf Gushing, induziert durch Hydrophobine, wurde mittels Untersuchungen und Vergleich von Proteinlösungen der reinen Proteine, sowie von Proteinkombinationen von FcHyd5p mit nsLtp1 bzw. Z4 analysiert. Sowohl eine direkte als auch hydrophobe Proteininteraktion zwischen FcHyd5p und den jeweiligen Bierproteinen konnte aufgrund von SRP-Experimenten im BIAcore und Analysen der Protein-Oberflächenhydrophobizität ausgeschlossen werden.

Nach Zugabe von nsLtp1 oder Z4 zu Proteinlösungen von FcHyd5p konnte mittels DLS eine Aggregatbildung festgestellt werden. Partikel, die die Größe von Mikroblasen repräsentieren, verschwanden jedoch in den Proteinkombinationen.

Die gemeinsame Anwesenheit von beiden Proteinen, Hydrophobin und des jeweiligen Bierschaumproteins, in Proteinfilmen wurde gezeigt. Dazu wurden die Oberflächenspannung von Proteinlösungen, sowie die Öltropfen-Ausdehnung auf Protein-beschichtetem Glas untersucht. Zudem erfolgte eine Untersuchung von Proteinfilmen, transferiert von der Oberfläche von Protein-haltigen Tropfen, mittels AFM. Dabei war in Proteinkombinationen eine Zunahme der Dicke des Proteinfilms, sowie eine Bildung von Bereichen mit hoher bzw. geringer Proteinbedeckung erkennbar.

Die gleichzeitige Anwesenheit von Hydrophobin und nsLtp1 bzw. Z4 in Proteinfilmen hatte einen negativen Einfluss auf die Stabilität von FcHyd5p-Emulisonen. Die Destabilisierung konnte auf verstärkte Koaleszenz und Disproportionierung zurückgeführt werden, was in einem Anstieg der Öltropfengröße in diesen Emulsionen erkennbar war. nsLtp1 und Z4 beeinflussten zudem die Schaumstabilität von FcHyd5p negativ. Aufgrund von unterschiedlichen Oberflächeneigenschaften und Energiebarrieren von Luft-Wasser- und Öl-Wassergrenzen, war nur bei Hitze-denaturierten Bierproteinen ein negativer Einfluss auf die Schaumstabilität erkennbar. Hitzebehandlung führte dabei durch eine strukturelle Umfaltung zu einer erhöhten Oberflächenhydrophobizität und Oberflächenaktivität der Proteine.

Korrelationen zwischen Emulsionsstabilität und Schaumstabilität, sowie zwischen beiden Stabilitäten mit Oberflächenspannung bzw. Ölbenetzbarkeit von Proteinfilmen, wurden festgestellt. Ein Vergleich und Bezug der in dieser Studie ermittelten Protein-Oberflächeneigenschaften mit und zu Gushing war somit zulässig.

Ein Model wurde entwickelt, welches den Einfluss der Integration der Bierschaumproteine in Hydrophobinfilme um CO_2-Blasen in gushendem Bier erklärt. Durch die Integration von Z4 bzw. nsLtp1 in die Hydrophobinschicht sind die Blasen anfälliger für Destabilisierung. Dadurch sind weniger Mikroblasen vorhanden, die als Kondensationskeim dienen. Zudem werden die verbleibenden Mikroblasen elastischer, was zu einer Stabilisierung beim Anwachsen nach Druckentlastung führt. Mangels Zerplatzen von Mikroblasen wird somit eine schnelle CO_2-Entbindinung verhindert und Gushing reduziert.

7 References

Ahmed, N., & Furth, A. J. (1991). A microassay for protein glycation based on the periodate method. *Anal. Biochem.*, *192*(1), 109–111.

Aimanianda, V., Bayry, J., Bozza, S., Kniemeyer, O., Perruccio, K., Elluru, S. R., Clavaud, C., Paris, S., Brakhage, A. A., Kaveri, S. V., Romani, L., & Latgé, J.-P. (2009). Surface hydrophobin prevents immune recognition of airborne fungal spores. *Nature*, *460*(7259), 1117–1121.

Alexandrov, N. A., Marinova, K. G., Gurkov, T. D., Danov, K. D., Kralchevsky, P. A., Stoyanov, S. D., Blijdenstein, T. B. J., Arnaudov, L. N., Pelan, E. G., & Lips, A. (2012). Interfacial layers from the protein HFBII hydrophobin: dynamic surface tension, dilatational elasticity and relaxation times. *J. Colloid Interface Sci.*, *376*(1), 296–306.

Altschul, S.F., Gish, W., Miller, W., Myers, E.W. & Lipman, D.J. (1990). Basic local alignment search tool. *J. Mol. Biol., 215*, 403-410.

Asgeirsdóttir, S. A., de Vries, O. M., & Wessels, J. G. H. (1998). Identification of three differentially expressed hydrophobins in *Pleurotus ostreatus* (oyster mushroom). *Microbiology*, *144*, 2961–2969.

Askolin, S. (2006). Characterization of the *Trichoderma reesei* hydrophobins HFBI and HFBII. Doctoral thesis, Helsinki University of Technology, Finland.

Askolin, S., Linder, M., Scholtmeijer, K., Tenkanen, M., Penttilä, M., de Vocht, M. L., & Wösten, H. A. B. (2006). Interaction and comparison of a class I hydrophobin from *Schizophyllum commune* and class II hydrophobins from *Trichoderma reesei*. *Biomacromolecules*, *7*(4), 1295–301.

Askolin, S., Penttilä, M., Wösten, H. A. B., & Nakari-Setälä, T. (2005). The *Trichoderma reesei* hydrophobin genes hfb1 and hfb2 have diverse functions in fungal development. *FEMS Microbiol. Letts*, *253*(2), 281-288.

Bamforth, C. W. (1985). The foaming properties of beer. *J. Inst. Brew.*, *91*, 370–383.

Barr, K.A., Hopkins, S.A., & Sreekrishna, K. (1992). Protocol for efficient secretion of HAS developed from *Pichia pastoris*. *Pharm. Eng.*, *12*, 48–51.

Basheva, E. S., Kralchevsky, P. A., Christov, N. C., Danov, K. D., Stoyanov, S. D., Blijdenstein, T. B. J., Kim, H.-J., Pelan, E. D., & Lips, A. (2011a). Unique properties of bubbles and foam films stabilized by HFBII Hydrophobin. *Langmuir*, 2382–2392.

Basheva, E. S., Kralchevsky, P. A., Danov, K. D., Stoyanov, S. D., Blijdenstein, T. B. J., Pelan, E. G., & Lips, A. (2011b). Self-assembled bilayers from the protein HFBII hydrophobin: nature of the adhesion energy. *Langmuir*, *27*(8).

Beattie, G. B. (1951). British views on the fobbing and gushing beer problem. *Wallerstein* Laboratories Communications, 14, 81-99.

Bellmer, H.-G. (1995). Forschungsprojekt "Gushing." *Brauwelt*, *24/25*, 1167–1170.

Bergeron, V., & Walstra, P. (2005). Foams. In J. Lyklema (Ed.), *Fundamentals of Interface and Colloid Science*, *Vol. 5*, *Soft Colloids;*. Elsevier.

BIAacore - Sensor Surface Handbook. (2003), BIAcore Instrument Handbook.

Bidochka, M. J., St Leger, R. J., Joshi, L., & Roberts, D. W. (1995). The rodlet layer from aerial and submerged conidia of the entomopathogenic fungus *Beauveria bassiana* contains hydrophobin. *Mycol. Res.*, *99*(4), 403–406.

Blijdenstein, T. B. J., de Groot, P. W. N., & Stoyanov, S. D. (2010). On the link between foam coarsening and surface rheology: why hydrophobins are so different. *Soft Matter*, *6*(8), 1799–1808.

Blijdenstein, T.B.J., Ganzevles, R. A., de Groot, P. W. N., & Stoyanov, S. D. (2013). On the link between surface rheology and foam disproportionation in mixed hydrophobin HFBII and whey protein systems. *Colloids Surf. A, In Press*.

Bobálová, J., Petry-Podgórska, I., Laštovičková, M., & Chmelík, J. (2010). Monitoring of malting process by characterization of glycation of barley protein Z. *Eur. Food Res. Tech.*, *230*(4), 665–673.

Bordier, C. (1981). Phase separation of integral membrane proteins in Triton X-114 solution. *J. Biol. Chem.*, *256*(4), 1604–1607.

Boutrot, F., Guirao, A., Alary, R., Joudrier, P., & Gautier, M.-F. (2005). Wheat non-specific lipid transfer protein genes display a complex pattern of expression in developing seeds. *Biochim. Biophys. Acta*, *1730*(2), 114–125.

Bradford, M. M. (1976). A rapid and sensitive method for the quantitation of microgram quantities of protein utilizing the principle of protein-dye binding. *Anal. Biochem.*, *72*, 248–254.

Brandt, A., Svendsen, I., & Hejgaard, J. (1990). A plant serpin gene. *Eur. J. Biochem.*, *194*, 499–505.

Breu, V., Guerbette, F., Kader, J.-C., Kannangara, C. G., Svensson, B., & Wettstein-Knowles, P. (1989). A 10 kD barley basic protein transfers phosphatidylcholine from liposomes to mitochondria. *Carlsberg Res. Commun.*, *54*(2), 81–84.

Bruch, M., Weiss, V., & Engel, J. (1988). Plasma serine proteinase inhibitors (serpins) exhibit major conformational changes and a large increase in conformational stability upon cleavage at their reactive sites. *J. Biol. Chem.*, *263*(32), 16626–16630.

Carpenter, C. E., Mueller, R. J., Kazmierczak, P., Zhang, L., Villalon, D. K., Alfen, V., & N.K. (1992). Effect of a virus on accumulation of a tissue-specific cell surface protein of the fungus *Cryphonectria (Endothia) parasitica*. *Mol. Plant Microbe Interact.*, *4*(6), 55–61.

Casaretto, J. A., & Corcuera, L. J. (1998). Proteinase inhibitor accumulation in aphid-infested barley leaves. *Phytochemistry*, *49*(8), 2279–2286.

Casey, G. P. (1996). Primary versus secondary gushing and assay procedures used to assess malt / beer gushing potential. *MBAA TQ*, *33*(4), 229–235.

Cereghino, J. L., & Cregg, J. M. (2000). Heterologous protein expression in the methylotrophic yeast *Pichia pastoris*. *FEMS Microbiol. Rev.*, *24*(1), 45–66.

Cheung, D. L. (2012). Molecular simulation of hydrophobin adsorption at an oil-water interface. *Langmuir*, *28*(23), 8730–6.

Christian, M, Ilberg, V., Titze, J., Friess, A., Jacob, F., & Parlar, H. (2009). Gushing laboratory tests as successful methods for obtaining new cognitions on gushing. *Brewing Science*, *62*, 83–89.

Christian, Manuel, Jean, T., Illberg, V., & Jacob, F. (2011). Novel perspectives in gushing analysis : A review. *J. Inst. Brew.*, *117*(3), 295–313.

Cordero, M. J., Raventós, D., & San Segundo, B. (1994). Expression of a maize proteinase inhibitor gene is induced in response to wounding and fungal infection: systemic wound-response of a monocot gene. *Plant J.*, *6*(2), 141–150.

Cox, A. R., Cagnol, F., Russell, A. B., & Izzard, M. J. (2007). Surface properties of class II hydrophobins from *Trichoderma reesei* and influence on bubble stability. *Langmuir*, *23*(15), 7995–8002.

Cox, A. R., Aldred, D. L., & Russell, A. B. (2009). Exceptional stability of food foams using class II hydrophobin HFBII. *Food Hydrocoll.*, *23*(2), 366–376.

Curioni, A., Pressi, G., Furegon, L., & Peruffo, A. D. B. (1995). Major proteins of beer and their precursors in barley: Electrophoretic and immunological studies. *J. Agric. Food Chem.*, *43*, 2620–2626.

Curtis, N. S., Ogie, P. J., & Carpenter, P. (1961). Studies on gushing. II. Examination of some brewing factors. *J. Inst. Brew.*, *67*, 422–427.

Dahl, S. W., Rasmussen, S. K., & Hejgaard, J. (1996). Heterologous expression of three plant serpins with distinct inhibitory specificities. *J. Biol. Chem.*, *271*(41), 25083–25088.

Damodaran, S. (2005). Protein stabilization of emulsions and foams. *J. Food Sci.*, *70*(3), 54–66.

de Vocht, M. L., Reviakine, I., Wösten, H. A. B., Brisson, A., Wessels, J. G. H., & Robillard, G. T. (2000). Structural and functional role of the disulfide bridges in the hydrophobin SC3. *J. Biol. Chem.*, *275*(37), 28428–32.

de Vries, O. M. H., Fekkes, M. P., Wösten, H. A. B., & Wessels, J. G. H. (1993). Insoluble hydrophobin complexes in the walls of *Schizophyllum commune* and other filamentous fungi. *Arch. Microbiol*, *159*, 330–335.

Deckers, S M, Gebruers, K., Baggerman, G., Lorgouilloux, Y., Delcour, J. A., Michiels, C., Derdelinckx, G., Martens, J. & Neven, H. (2010). CO_2 -Hydrophobin structures acting as nano- bombs in beer, *63*, 54–61.

Deckers, Sylvie M, Lorgouilloux, Y., Gebruers, K., Baggerman, G., Verachtert, H., Neven, H., Michiels, C., Derdelinckx, G., Delcour, J. A., & Martens, J. (2011). Dynamic light scattering (DLS) as a tool to detect CO_2 -hydrophobin structures and study the primary gushing potential of beer. *J. Am. Soc. Brew. Chem*, *69*(3), 144–149.

Deckers, Sylvie M, Venken, T., Mohammadreza, K., Gebruers, K., Baggerman, G., Lorgouilloux, Y., Shokribousjein, Z., Ilber, V., Schönberger, C., Titze, J., Verachtert, H., Michiels, C., Neven, H., Delcour, J., Martens, J., Dederlinckx, G., & de Maeyer, M. (2012a). Combined modeling and biophysical characterisation of CO_2 interaction with class II hydrophobins: New insight into the mechanism underpinning primary gushing. *J. Am. Soc. Brew. Chem.*, *70*(4), 249–256.

Deckers, S M, Vissers, L., Gebruers, K., Shokribousjein, Z., Khalesi, M., Riveros-Galan, D., Schönberger, C., Verachtert, H., Neven, H., Delcour, J., Michiels, C., Ilberg, V., Derdelinckx, G., Titze, J. & Martens, J. (2012b). Doubly modified Carlsberg test combined with dynamic light scattering allows prediction of the primary gushing potential of harvested barley and malt. *Cerevisia*, *37*(3), 77–81.

Deckers, Sylvie M, Vissers, L., Khalesi, M., Shokribousjein, Z., Verachtert, H., Gebruers, K., Pirlot, X., Ilberg, V., Titze, J., Neven, H., & Derdelinckx, G. (2013). Thermodynamic view of primary gushing. *J. Am. Soc. Brew. Chem*, *71*(3), 149–152.

Denschlag, C., Vogel, R. F., & Niessen, L. (2013). Hyd5 gene based analysis of cereals and malt for gushing-inducing *Fusarium* spp. by real-time LAMP using fluorescence and turbidity measurements. *Int. J. Food Microbiol.*, *162*(3), 245–251.

Deshpande, N., Wilkins, M. R., Packer, N., & Nevalainen, H. (2008). Protein glycosylation pathways in filamentous fungi. *Glycobiology*, *18*(8), 626–637.

Devlin, G. L., & Bottomley, S. P. (2005). A protein family under “stress” - serpin stability, folding and misfolding. *Front. Biosci.*, *10*, 288–299.

Dickinson, E. (1999). Adsorbed protein layers at fluid interfaces: interactions, structure and surface rheology. *Colloids Surf. B*, *15*(2), 161–176.

Dickinson, E., Ette, Laie, R., Murray, B. S., & Du, Z. (2002). Kinetics of disproportionation of air bubbles beneath a planar air-water interface stabilized by food proteins. *J. Colloid Interface Sci.*, *252*(1), 202–13.

Donhauser, S., Weideneder, A., Winnewisser, W., & Geiger, E. (1990). Test zur Ermittlung der Gushinigneigung von Rohfrucht, Malz, Würze und Bier. *Brauwelt*, *32*, 1317–1320.

Douliez, J.-P., Michon, T., Elmorjani, K., & Marion, D. (2000). Mini review: Structure, biological and technological functions of lipid transfer proteins and indolines, the major lipid binding proteins from cereal kernels. *J. Cereal Sci.*, *32*(1), 1–20.

Douma, A. C., Mocking-Bode, H. C. M., Kooijman, M., Stolzenbach, E., Orsel, R., Bekkers, A. C. A. P. A., & Angelino, S. A. G. F. (1997). Identification of foam stabilizing proteins under conditions of normal beer dispense and their biochemical and physiochemical properties. In *Proceedings of the EBC Congress, Maastrict*, *26*, 671–679.

Draeger, M. (1996). Physikalische Überlegungen zum Thema Gushing. *Brauwelt*, *6*, 259–264.

Duman, J. G., Miele, R. G., Liang, H., Grella, D. K., Sim, K. L., Castellino, F. J., & Bretthauer, R. K. (1998). O-Mannosylation *of Pichia pastoris* cellular and recombinant proteins. *Biotech. Appl.Biochem.*, *28*, 39–45.

Dunn, M. A, Hughes, M. A, Zhang, L., Pearce, R. S., Quigley, A. S., & Jack, P. L. (1991). Nucleotide sequence and molecular analysis of the low temperature induced cereal gene, BLT4. *Mol. Gen. Genet.*, *229*(3), 389–94.

Dutta, A., Chengara, A., Nikolov, A. D., Wasan, D. T., Chen, K., & Campbell, B. (2004). Destabilization of aerated food products: effects of Ostwald ripening and gas diffusion. *J. Food Eng.*, *62*(2), 177–184.

Ebbole, D. J. (1997). Hydrophobins and fungal infection of plants and animals. *Trends Microbiol.*, *5*(10), 405–408.

Euston, S. R., Hughes, P., Naser, M. A., & Westacott, R. E. (2008). Comparison of the adsorbed conformation of barley lipid transfer protein at the decane-water and vacuum-water interface: a molecular dynamics simulation. *Biomacromolecules*, *9*(5), 1443–1453.

Euston, S. R. (2010). Molecular dynamics simulation of protein adsorption at fluid interfaces: a comparison of all-atom and coarse-grained models. *Biomacromolecules*, *11*(10), 2781–2787.

Evans, D. E., & Hejgaard, J. (1999). The impact of malt derived proteins on beer foam quality. Part I. The effect of germination and kilning on the level of protein Z4, protein Z7 and LTP1. *J. Inst. Brew.*, *105*(3), 159–169.

Evans, D. E., Sheehan, M. C., & Stewart, D. C. (1999). The impact of malt derived proteins on beer foam quality. Part II: The influence of malt foam-positive proteins and non-starch polysaccharides on beer foam quality. *J. Inst. Brew., 105*(2), 171–177.

Evans, D E., & Bamforth, C. W. (2008). Beer foam: Achieving a suitable head. In: C. W. Bamforth (Ed.), *Beer: A Quality Perspective* (pp. 1–48). Academic Press Inc.

Evans, D.E., Finn, J. E. C., Robinson, L. H., Eglinton, J. K., Sheehy, M., & Stewart, D. C. (2011). The effects of hop-α-acids and proline-specific endoprotease (PSEP) treatments on the foam quality of beer. *J. Inst. Brew.*, *117*(3), 335–342.

Fasoli, E., Aldini, G., Regazzoni, L., Kravchuk, A. V, Citterio, A., & Righetti, P. G. (2010). Les maîtres de l'orge: The proteome content of your beer mug. *J. Proteome Res.*, *9*, 5262–5269.

Finnie, C., Melchior, S., Roepstorff, P., & Svensson, B. (2002). Proteome analysis of grain filling and seed maturation in barley. *Plant Physiol.*, *129*, 1308–1319.

Fischer, S. (2001). Blasenbildung von in Flüssigkeiten gelösten Gasen. Doctoral thesis, Technische Universität München, Germany.

Furth, A. J. (1988). Methods for assaying nonenzymatic glycosylation. *Anal. Biochem.*, *175*, 347–360.

Garbe, L., Schwarz, P., & Ehmer, A. (2004). Beer gushing. In: C. W. Bamforth (Ed.), *Beer: A Quality Perspective* (pp. 185–212). Academic Press Inc.

Garcia-Olmedo, F., Molina, A., Segura, A., & Moreno, M. (1995). The defensive role of nonspecific lipid-transfer proteins in plants. *Trends Microbiol.*, *3*(2), 72–74.

Gardner, R.J. (1972). Surface viscosity and gushing. *J. Inst. Brew.*, *78*, 392–399.

Gardner, R J. (1973). The mechanism of gushing - a review. *J. Inst. Brew.*, *79*, 275–283.

Gardner, R.J., Laws, D. R. J., & McGuiness, J. D. (1973). The suppression of gushing by the use of hop oil. *J. Inst. brew*, *79*(3), 209–211.

Gasteiger, E., Hoogland, C., Gattiker, A., Duvaud, S., Wilkins, M. R., Appel, R. D., & Bairoch, A. (2005). Protein identification and analysis tools on the ExPASy Server. In: J. M. Walker (Ed.), *The Proteomics Protocols Handbook* (pp. 571–607). Humana Press.

Gastl, M., Zarnkow, M., & Back, W. (2008). Gushing - ein Multikausales Problem! *Brauwelt*, *32*, 896–899.

Gavel, Y., & von Heijne, G. (1990). Sequence differences between glycosylated and non-glycosylated Asn-X-Thr/Ser acceptor sites: implications for protein engineering. *Protein Eng.*, *3*(5), 433–442.

Gjertsen, P., Trolle, B. & Andersen, K. (1963). Weathered barley as a contributory cause of gushing in beer. In *Proceedings of the EBC Congress, Brussels,* 320–341.

Goswami, R., & Kistler, H. (2004). Pathogen profile heading for disaster: *Fusarium graminearum* on cereal crops. *Mol. Plant Pathol.*, *5*(6), 515–525.

Goujon, M., McWilliam, H., Li, W., Valentin, F., Squizzato, S., Paern, J., & Lopez, R. (2010). A new bioinformatics analysis tools framework at EMBL-EBI. *Nucleic Acids Res.*, *38*(Web Server issue), W695–699.

Grinna, L. S., & Tschopp, J. F. (1989). Size distribution and general structural features of N-linked oligosaccharides from the methylotrophic yeast, *Pichia pastoris*. *Yeast*, *5*(2), 107–115.

Guggenberger, J. (1962). Ein Beitrag zur Klärung von Fragen der Bindung und Entbindung von Kohlensäure in Bier und anderen kohlensäurehaltigen Getränken. *Brauwissenschaft 15*, 396-399.

Hagemeyer, D. (2012). Gushing unter Kontrolle? - Größenbestimmung an Kolloiden mit Eintauchsonde. *Brauindustrie*, *10*, 60–62.

Haikara, A., Kleemola, T., Nakari-Setälä, T., & Penttilä, M. (1999). Methods for determining a gushing factor for a beverage. US. *World Intellectual Property Organisation*, International Publication Number WO99/54725.

Haikara, A., Sarlin, T., & Home, S. (2005). Determination of gushing tendency of malt. *J. Inst. Brew.*, *111*(2), 247–247.

Hakanpää, J., Paananen, A., Askolin, S., Nakari-Setälä, T., Parkkinen, T., Penttilä, M., Linder, M., & Rouvinen, J. (2004). Atomic resolution structure of the HFBII hydrophobin, a self-assembling amphiphile. *J. Biol. Chem.*, *279*(1), 534–539.

Hakanpää, J., Szilvay, G. R., Kaljunen, H., Makismainen, M., Linder, M., & Rouvinen, J. (2006). Two crystal structures of *Trichoderma reesei* hydrophobin HFBI — The structure of a protein amphiphile with and without detergent interaction. *Protein Sci.*, *15*, 2129–2140.

Hall, T. (1999). BioEdit: a user-friendly biological sequence alignment editor and analysis program for Windwos 95/98/NT. *Nucleic Acids Symp.*, *41*, 96–98.

Hégrová, B., Farková, M., Macuchová, S., Havel, J., & Preisler, J. (2009). Investigation of relationships between barley stress peptides and beer gushing using SDS-PAGE and MS screening. *J. Sep. Sci.*, *32*(23-24), 4247–4253.

Heinemann, B. O., Andersen, K. V., Nielsen, R., Bech, L. M., & Poulsen, F. M. (1996). Structure in solution of a four-hleix lipid binding protein. *Protein Sci.*, *5*, 13–23.

Hejgaard, J., & Boisen, S. (1980). High-lysine proteins in Hiproly barley breeding: Identification, nutritional significance and new screening methods. *Hereditas*, *93*, 311–320.

Hejgaard, J. (1982). Purification and properties of protein Z - a major albumin of barley endosperm. *Physiol. Plant.*, *54*(2), 174–182.

Hejgaard, J., & Kaersgaard, P. (1983). Purification and properties of the major antigenic beer protein of barley origin. *J. Inst. Brew*, *89*, 402–410.

Hejgaard, J., Rasmussen, S. K., Brandt, A., & Svendsen, I. (1985). Sequence homology between barley endosperm protein Z and protease inhibitors of the alpha1-antitrypsin family. *FEBS letters*, *180*(1), 89–94.

Hippeli, S., & Hecht, D. (2007). Role of ns-LTP1 in the development of primary gushing. *Brewing Science*, *60*, 1–9.

Hippeli, S., & Hecht, D. (2008). Die Rolle von nsLTP1 und Proteasen bei der Entstehung des primären Gushing. *Brauwelt*, *32*, 900–904.

Hollemans, M., & Tonies, A. R. J. M. (1989). The role of specific proteins in beer foam. In *Proceedings of the EBC Congress,* Zurich, 561–568.

Horvath, A. J., Irving, J. A, Rossjohn, J., Law, R. H., Bottomley, S. P., Quinsey, N. S., Pike, R. N., Coughlin, P. B., & Whisstock, J. C. (2005). The murine orthologue of human antichymotrypsin: A structural paradigm for clade A3 serpins. *J. Biol. Chem.*, *280*(52), 43168–43178.

Hudson, B. (1962). Some observations on the treatment of gushing beers with nylon powder. *J. Inst. Brew*., 68, 460-466.

Hughes, M. A., Dunn, M. A., Pearce, R. S., White, A. J., & Zhang, L. (1992). An abscisic-acid-responsive, low temperature barley gene has homology with a maize phospholipid transfer protein. *Plant Cell Envir.*, *15*, 861–865.

Huntington, J. A., Read, R. J., & Carrell, R. W. (2000). Structure of a serpin-protease complex shows inhibition by deformation. *Nature*, *407*(6806), 923–926.

Huntington, J. A. (2011). Serpin structure, function and dysfunction. *J. Thromb.Haemos.*, *9*, 26–34.

Iimure, T., Takoi, K., Kaneko, T., Kihara, M., Hayashi, K., Ito, K., Sato, K., & Takeda, K. (2008). Novel prediction method of beer foam stability using protein Z, barley dimeric alpha-amylase inhibitor-1 (BDAI-1) and yeast thioredoxin. *J. Agric. Food Chem.*, *56*(18), 8664–8871.

Iimure, T., Nankaku, N., Hirota, N., Tiansu, Z., Hoki, T., Kihara, M., Hayashi, K., Ito, K., & Sato, K. (2010). Construction of a novel beer proteome map and its use in beer quality control. *Food Chem.*, *118*(3), 566–574.

Iimure, T., Kimura, T., Araki, S., Kihara, M., Sato, M., Yamada, S., Shigyou, T., & Sato, K. (2012). Mutation analysis of barley malt protein Z4 and protein Z7 on beer foam stability. *J. Agric. Food Chem.*, *60*(6), 1548–1554.

Ilberg, V., Titze, J., Christian, M., Jacob, F., & Parlar, H. (2008). Aktuelle Entwicklungen und Erkenntnisse in der Analytik des Gushingschnelltests. *Brauwelt*, *32*, 906–909.

Janssen, M. I., van Leeuwen, M. B. M., Scholtmeijer, K., van Kooten, T. G., Dijkhuizen, L., & Wösten, H. A. B. (2002). Coating with genetic engineered hydrophobin promotes growth of fibroblasts on a hydrophobic solid. *Biomaterials*, *23*(24), 4847–54.

Jégou, S., Douliez, J.-P., Mollé, D., Boivin, P., & Marion, D. (2000). Purification and structural characterization of LTP1 polypeptides from beer. *J. Agric. Food Chem.*, *48*(10), 5023–5029.

Jégou, S., Douliez, J.-P., Mollé, D., Boivin, P., & Didier, M. (2001). Evidence of the glycation and denaturation of LTP1 during the malting and brewing process. *J. Agic. Food Chem*, *49*, 4942–4949.

Jin, B., Li, L., Liu, G.-Q., Li, B., Zhu, Y.-K., & Liao, L.-N. (2009). Structural changes of malt proteins during boiling. *Molecules*, *14*(3), 1081–1097.

Jones, B. L., & Marinac, L. A. (1997). Purification, identification, and partial characterization of a barley protein that inhibits green malt endoproteinases. *J. Am. Soc. Brew. Chem.*, *55*, 58–64.

Jones, B. L., & Marinac, L. A. (2000). Purification and partial characterization of a second cysteine proteinase inhibitor from ungerminated barley (*Hordeum vulgare* L.). *J. Agric. Food Chem.*, *48*(2), 257–64.

Jones, B. L. (2005). Endoproteases of barley and malt. *J. Cereal Sci.*, *42*(2), 139–156.

Kader, J.-C. (1996). Lipid-transfer proteins in plants. *Annu. Rev.Plant Physiol.Plant Mol. Biol.*, *47*, 627–654.

Kaersgaard, P., & Hejgaard, J. (1979). Antigenic beer macromolecule an experimental survey of purification methods. *J. Inst. Brew.*, *85*, 103–111.

Kallio, J. M., Linder, M. B., & Rouvinen, J. (2007). Crystal structures of hydrophobin HFBII in the presence of detergent implicate the formation of fibrils and monolayer films. *J. Biol. Chem.*, *282*(39), 28733–28739.

Kang, Z., & Buchenauer, H. (2000). Cytology and ultrastructure of the infection of wheat spikes by Fusarium culmorum. *Mycol. Res.*, *104*(9), 1083–1093.

Kato, A., & Nakai, S. (1980). Hydrophobicity determined by a fluorescence probe method and its correlation with surface properties of proteins. *Biochim. Biophys. Acta*, *624*, 13–20.

Kennedy, D. M., Skillen, A. W., & Self, C. H. (1993). Colorimetric assay of glycoprotein glycation free of interference from glycosylation residues. *Clin. Chem.*, *39*(11), 2309–2311.

Kershaw, M. J., & Talbot, N. J. (1998). Hydrophobins and repellents: proteins with fundamental roles in fungal morphogenesis. *Fungal Genet.Biol.*, *23*(1), 18–33.

Kirkland, B. H., & Keyhani, N. O. (2011). Expression and purification of a functionally active class I fungal hydrophobin from the entomopathogenic fungus *Beauveria bassiana* in *E. coli*. *J. Ind. Microbiol. Biotechnol.*, *38*(2), 327–335.

Kisko, K., Torkkeli, M., Vuorimaa, E., Lemmetyinen, H., Seeck, O. H., Linder, M., & Serimaa, R. (2005). Langmuir–Blodgett films of hydrophobins HFBI and HFBII. *Surf. Sci.*, *584*(1), 35–40.

Kisko, K., Szilvay, G. R., Vuorimaa, E., Lemmetyinen, H., Linder, M. B., Torkkeli, M., & Serimaa, R. (2007). Self-assembled films of hydrophobin protein HFBIII from *Trichoderma reesei*. *J. Appl. Cryst.*, *40*, 355–360.

Kisko, K., Szilvay, G. R., Vainio, U., Linder, M. B., & Serimaa, R. (2008). Interactions of hydrophobin proteins in solution studied by small-angle X-ray scattering. *Biophys. J.*, *94*(1), 198–206.

Kleemola, T., Nakari-Setälä, T., Linder, M., Penttilä, M., Kotaviita, E., Olkku, J., & Haikara, A. (2001). Characterisation and detection of the gushing factors produced by fungi. In *Proceedings of the EBC Congress, Budapest*, 129–138.

Kloek, W., van Vliet, T., & Meinders, M. (2001). Effect of bulk and interfacial rheological properties on bubble dissolution. *J. Colloid Interface Sci.*, *237*(2), 158–166.

Kubicek, C. P., Baker, S., Gamauf, C., Kenerley, C. M., & Druzhinina, I. S. (2008). Purifying selection and birth-and-death evolution in the class II hydrophobin gene families of the ascomycete *Trichoderma/Hypocrea*. *BMC Evol. Biol.*, *8*, 4.

Kunert, M., Sacher, B., & Back, W. (2001). Ergebnisse einer Umfrage in deutschen Brauereien zum Thema "Gushing." *Brauwelt*, *141*, 350–362.

Kwan, A. H. Y., Winefield, R. D., Sunde, M., Matthews, J. M., Haverkamp, R. G., Templeton, M. D., & Mackay, J. P. (2006). Structural basis for rodlet assembly in fungal hydrophobins. *Proceedings of the National Academy of Sciences of the United States of America*, *103*(10), 3621–3626.

Kyte, J., & Doolittle, R. F. (1982). A simple method for displaying the hydropathic character of a protein. *J. Mol. Biol.*, *157*(1), 105–132.

Langevin, D. (2000). Influence of interfacial rheology on foam and emulsion properties. *Adva.Colloid Interface Sci.*, *88*(1-2), 209–222.

Leiper, K. A., Stewart, G. G., & McKeown, I. P. (2003). Beer polypeptides and silica gel Part II. Polypeptides involved in foam formation. *J. Inst. Brew.*, *109*(1), 73–79.

Leisegang, R., & Stahl, U. (2005). Degradation of a foam-promoting barley protein by a proteinase from brewing yeast. *J. Inst. Brew.*, *111*(2), 112–117.

Liger-Belair, G. (2005). The physics and chemistry behind the bubbling properties of champagne and sparkling wines: a state-of-the-art review. *J. Agric. Food Chem.*, *53*(8), 2788–2802.

Lin, K., Simossis, V. A., Taylor, W. R., & Heringa, J. (2005). A simple and fast secondary structure prediction algorithm using hidden neural networks. *Bioinformatics*, *21*(2), 152–159.

Linder, M., Selber, K., Nakari-Setälä, T., Qiao, M., Kula, M. R., & Penttilä, M. (2001). The hydrophobins HFBI and HFBII from *Trichoderma reesei* showing efficient interactions with nonionic surfactants in aqueous two-phase systems. *Biomacromolecules*, *2*(2), 511–517.

Linder, M. B., Qiao, M., Laumen, F., Selber, K., Hyytiä, T., Nakari-Setälä, T., & Penttilä, M. E. (2004). Efficient purification of recombinant proteins using hydrophobins as tags in surfactant-based two-phase systmes. *Biochem.*, *43*, 11873–11882.

Linder, M. B., Szilvay, G. R., Nakari-Setälä, T., & Penttilä, M. E. (2005). Hydrophobins: the protein-amphiphiles of filamentous fungi. *FEMS Microbiol. Rev.*, *29*(5), 877–896.

Linder, M. B. (2009). Hydrophobins: Proteins that self assemble at interfaces. *Curr. Opin. Colloid Interface Sci.*, *14*(5), 356–363.

Lindorff-Larsen, K., & Winther, J. R. (2001). Surprisingly high stability of barley lipid transfer protein, LTP1, towards denaturant, heat and proteases. *FEBS letters*, *488*(3), 145–148.

Lumsdon, S. O., Green, J., & Stieglitz, B. (2005). Adsorption of hydrophobin proteins at hydrophobic and hydrophilic interfaces. *Colloids Surf. B, 44*(4), 172–178.

Lusk, L. T., Duncombe, G. R., Kay, S. B., Navarro, A., & Ryder, D. (2001a). Barley β-glucan and beer foam stability. *J. Am. Soc. Brew. Chem.*, *59*, 183–186.

Lusk, L. T., Goldstein, H., Watts, K., Navarro, A., & Ryder, D. (2001b). Monitoring barley lipid transfer protein levels in barley, malting and brewing. *Proceedings of the EBC, Budapest, 28*, 663–672.

Lutterschmid, G., Stübner, M., Vogel, R. F., & Niessen, L. (2010). Induction of gushing with recombinant class II Hydrophobin FcHyd5p from *Fusarium culmorum* and the impact of hop compounds on its gushing potential. *J. Inst. Brew.*, *116*(4), 339–347.

Lutterschmid, G., Muranyi, M., Stübner, M., Vogel, R. F., & Niessen, L. (2011). Heterologous expression of surface-active proteins from barley and filamentous fungi in *Pichia pastoris* and characterization of their contribution to beer gushing. *Int. J. Food Microbiol.*, *147*(1), 17–25.

Mackay, J. P., Matthews, J. M., Winefield, R. D., Mackay, L. G., Haverkamp, R. G., & Templeton, M. D. (2001). The hydrophobin EAS is largely unstructured in solution and functions by forming amyloid-like structures. *Structure*, *9*(2), 83–91.

Maeda, K., Yokoi, S., Kamada, K., & Kamimura, M. (1991). Foam stability and physicochemical properties of beer. *J. Am. Soc. Brew. Chem.*, *49*(1), 14–18.

Matejková, M., Zídková, J., Zídek, L., Wimmerová, M., Chmelík, J., & Sklenár, V. (2009). Investigation of thermal denaturation of barley nonspecific lipid transfer protein 1 (ns-LTP1b) by nuclear magnetic resonance and differential scanning calorimetry. *J. Agric. Food Chem.*, *57*(18), 8444–8452.

Mitteleuropäischen Brautechnischen Analysenkommission (MEBAK) (1996). Band III. Pfenninger H. (Ed.). MEBAK, Freising, Germany.

Mellquist, J. L., Kasturi, L., Spitalnik, S. L., & Shakin-Eshleman, S. H. (1998). The amino acid following an asn-X-Ser/Thr sequon is an important determinant of N-linked core glycosylation efficiency. *Biochem.*, *37*(19), 6833–7683.

Milani, R., Monogioudi, E., Baldrighi, M., Cavallo, G., Arima, V., Marra, L., Zizzari, A., Rinaldi, R., Linder, M., Resnati, G., & Metrangolo, P. (2013). Hydrophobin: Fluorosurfactant-like properties without fluorine. *Soft Matter*, *9*(28), 6505-6514.

Mills, E. N. C., Kauffman, J. A., Morgan, M. R. A., Field, J. M., Hejgaard, J., Proudlove, M. O., & Onishi, A. (1998). Immunological study of hydrophobic polypeptides in beer. *J. Agric. Food Chem.*, *46*, 4475–4483.

Mills, E. N. C., Gao, C., Wilde, P. J., Rigby, N. M., Wijesinha-Bettoni, R., Johnson, V. E., Smith, L. J., & Mackie, A. R. (2009). Partially folded forms of barley lipid transfer protein are more surface active. *Biochem.*, *48*(51), 12081–12088.

Molina, A., & García-Olemedo, F. (1993). Developmental and pathogen-induced expression of three barley genes encoding lipid transfer proteins. *Plant J.*, *4*(6), 893–991.

Molina, A., Segura, A., & García-Olemedo, F. (1993). Lipid transfer proteins (nsLtps) from barley and maize leaves are potent inhibitors of bacterial and fungal plant pathogens. *FEBS letters*, *316*, 119-122.

Mosbach, A., Leroch, M., Mendgen, K. W., & Hahn, M. (2011). Lack of evidence for a role of hydrophobins in conferring surface hydrophobicity to conidia and hyphae of *Botrytis cinerea*. *BMC Microbiol:*, *11*(1), 10.

Müller, V., Besier, A., & Fröhlich, J. (2013). Überschäumen vermindern - Verfahren zur Behandlung des Phänomens Gushing. *Brauindustrie*, *1*, 18–21.

Murray, B. S. (2007). Stabilization of bubbles and foams. *Curr. Opin. Colloid Interface Sci.*, *12*(4-5), 232–241.

Nakai, S., Li-Chan, E. (1988). Hydrophobic interactions in food systems. *CRC Press, Boca Raton*.

Narziß, L., Reicheneder, E., Simon, A., & Grandl, R. (1990). Untersuchungen zum Gushing-Problem. *Monat. für Brauwiss.*, *9*, 296–305.

Narziß, L. (1995). *Abriss der Bierbrauerei*, 6th ed. Ferdindand Enke Verlag, Stuttgart.

Nečas, D., & Klapetek, P. (2012). Gwyddion: an open-source software for SPM data analysis. *Cent. Eur. J. Phys.*, *10*(1), 181–188.

Niessen, L., Donhauser, S., Weideneder, A., Geiger, E., & Vogel, H. (1992). Mykologische Untersuchungen an Cerealien und Malzen im Zusammenhang mit dem Wildwerden (Gushing) des Bieres. *Brauwelt*, *16/17*, 702–714.

Niessen, L. (1993). Entwicklung und Anwendung immunochemischer Verfahren zum Nachweis wichtiger *Fusarium*-Toxine bei der Bierbereitung sowie mykologische Untersuchungen im Zusammenhang mit dem Wildwerden (Gushing) von Bieren. Doctoral thesis, Technische Universität München, Germany.

Niessen, L., Hecht, D., Zapf, M. W., Theisen, S., Vogel, R. F., Elstner, E., & Hippeli, S. (2006). Zur Rolle oberflächenaktiver Proteine von Pflanzen und Pilzen bei der Enstehung des Gushing sowie zu den Möglichkeiten ihrer Beeinflussung. *Brauwelt*, *19-20*, 570–572.

Nishimura, S., Tatano, S., Gomi, K., Ohtani, K., Fukumoto, T., & Akimitsu, K. (2008). Chloroplast-localized nonspecific lipid transfer protein with anti-fungal activity from rough lemon. *Physiol. Mol. Plant Pathol.*, *72*(4–6), 134–140.

Niu, B., Wang, D., Yang, Y., Xu, H., & Qiao, M. (2012). Heterologous expression and characterization of the hydrophobin HFBI in *Pichia pastoris* and evaluation of its contribution to the food industry. *Amino Acids*, *43*(2), 763–771.

Oliveira, P. M., Mauch, A., Jacob, F., Waters, D. M., & Arendt, E. K. (2012). Fundamental study on the influence of *Fusarium* infection on quality and ultrastructure of barley malt. *Int. J. Food Microbiol.*, *156*(1), 32–43.

Østergaard, H., Rasmussen, S. K., Roberts, T. H., & Hejgaard, J. (2000). Inhibitory serpins from wheat grain with reactive centers resembling glutamine-rich repeats of prolamin storage proteins. Cloning and characterization of five major molecular forms. *J. Biol. Chem.*, *275*(43), 33272–33279.

Østergaard, O., Finnie, C., Laugesen, S., Roepstorff, P., & Svensson, B. (2004). Proteome analysis of barley seeds: Identification of major proteins from two-dimensional gels (pI 4–7). *Proteomics*, *4*, 2437–2447.

Paananen, A., Vuorimaa, E., Torkkeli, M., Penttilä, M., Kauranen, M., Ikkala, O., Lemmetyinen, H., Seimaa, R., & Linder, M. B. (2003). Structural hierarchy in molecular films of two class II hydrophobins. *Biochem.*, *42*(18), 5253–5258.

Pacios, L. F., Gómez-Casado, C., Tordesillas, L., Palacín, A., Sánchez-Monge, R., & Díaz-Perales, A. (2012). Computational study of ligand binding in lipid transfer proteins: Structures, interfaces, and free energies of protein-lipid complexes. *J. Comput. Chem.*, *33*(22), 1831–1844.

Pellaud, J. (2002). Gushing: State of the art. *Cervisia*, *27*(4), 189–205.

Peñas, M. M., Rust, B., Larraya, L. M., Ramírez, L., & Pisabarro, A. G. (2002). Differentially regulated, vegetative-mycelium-specific hydrophobins of the edible Basidiomycete *Pleurotus ostreatus*. *App. Environ. Microbiol.*, *68*(8), 3891–3898.

Perrocheau, L., Rogniaux, H., Boivin, P., & Marion, D. (2005). Probing heat-stable water-soluble proteins from barley to malt and beer. *Proteomics*, *5*(11), 2849–2858.

Perrocheau, L., Bakan, B., Boivin, P., & Marion, D. (2006). Stability of barley and malt lipid transfer protein 1 (LTP1) toward heating and reducing agents: relationships with the brewing process. *J. Agric. Food Chem.*, *54*(8), 3108–3113.

Petersen, T., Brunak, S., von Heijne, G., & Nielsen, H. (2011). SignalP 4.0: discriminating signal peptides from transmembrane regions. *Nat. Methods*, *8*(10), 785–786.

Picariello, G., Bonomi, F., Iametti, S., Rasmussen, P., Pepe, C., Lilla, S., & Ferranti, P. (2011). Proteomic and peptidomic characterisation of beer: Immunological and technological implications. *Food Chem.*, *124*(4), 1718–1726.

Pugh, R. (1996). Foaming, foam films, antifoaming and defoaming. *Adv. Colloid Interface Sci.*, *64*(95), 67–142. 4

Radulova, G. M., Golemanov, K., Danov, K. D., Kralchevsky, P. A., Stoyanov, S. D., Arnaudov, L. N., Blijdenstan, B. J., Pelan, E. G., & Lips, A. (2012). Surface shear rheology of adsorption layers from the protein HFBII hydrophobin: effect of added β-casein. *Langmuir*, *28*(9), 4168–4177.

Rasband, W.S. (1997-2012). ImageJ, U. S. National Institutes of Health, Bethesda, Maryland, USA.

Rath, F. (2008). Gushing im Jahre 2008 - Eine Bewährungsprobe für den "Modifizierten Carlsberg Test." *Brauwelt*, *32*, 910–913.

Roberts, T. H., Marttila, S., Rasmussen, S. K., & Hejgaard, J. (2003). Differential gene expression for suicide-substrate serine proteinase inhibitors (serpins) in vegetative and grain tissues of barley. *J. Exp. Bot.*, *54*(391), 2251–2263.

Robinson, L., & David, P. (2008). Improving foam quality through wort boiling optimisation. In *Proceedings of the 30th Convention, Auckland, New Zealand*, paper #12.

Rosenkrands, I., Hejgaard, J., Rasmussen, S. K., & Bjørn, S. E. (1994). Serpins from wheat grain. *FEBS letters*, *343*(1), 75–80.

Sarlin, T., Laitila, A., Pekkarinen, A., & Haikara, A. (2005a). Effects of three Fusarium species on the quality of barley and malt. *J. Am. Soc. Brew. Chem.*, *63*, 43–49.

Sarlin, T., Nakari-Setälä, T., Linder, M., Penttilä, M., & Haikara, A. (2005b). Fungal hydrophobins as predictors of the gushing activity of malt. *J. Inst. Brew.*, *111*(2), 105–111.

Sarlin, T., Vilpola, A., Kotaviita, E., Olkku, J., & Haikara, A. (2007). Fungal hydrophobins in the barley-to-beer chain. *J. Inst. Brew.*, *113*(2), 147–153.

Sarlin, T. (2012). Detection and characterisation of Fusarium hydrophobins inducing gushing in beer. Doctoral thesis, Aalto University School of Chemical Technology, Finland.

Sarlin, T., Kivioja, T., Kalkkinen, N., Linder, M. B., & Nakari-Setälä, T. (2012). Identification and characterization of gushing-active hydrophobins from *Fusarium graminearum* and related species. *J. Basic Microbiol.*, *52*(2), 184–194.

Schägger, H., & von Jagow, G. (1987). Tricine-sodium dodecyl sulfate-polyacrylamide gel electrophoresis for the separation of proteins in the range from 1 to 100 kDa. *Anal. Biochem.*, *166*, 368–379.

Scholtmeijer, K., Wessels, J. G. H., & Wösten, H. A. B. (2001). Fungal hydrophobins in medical and technical applications. *Appl. Microbiol. Biotechno.*, *56*(1-2), 1–8.

Schumacher, T. (2002). Gushing in Fruchtsaftschorlen. *Getränkeindustrie*, *7*, 8–10.

Schwarz, P. B., Casper, H. H., & Beattie, S. (1995). Fate and development of naturally occurring *Fusarium* mycotoxins during malting and brewing (1). *J. Am. Soc. Brew. Chem.*, *53*(3), 121–127.

Schwarz, P. B., Beattie, S., & Casper, H. H. (1996). Relationship between *Fusarium* infestation of barley and the gushing potentail of malt. *J. Inst. Brew.*, *102*, 93–96.

Shokribousjein, Z., Deckers, S. M., Gebruers, K., Lorgouilloux, Y., Baggerman, G., Verachtert, H., Delcour, J. A., Etienne, P., Rock, J.-M., Michiels, C., & Derdelinckx, G. (2011). Hydrophobins, beer foaming and gushing. *Cerevisia*, *35*(4), 85–101.

Simpson, W. J., & Hughes, P. S. (1994). Stabilization of foams by hop-derived bitter acids. Chemical interactions in beer foam. *Cerevis. Biotech.*, *19*(3), 39–44.

Skriver, K., Leah, R., Müller-Uri, F., Olsen, F. L., & Mundy, J. (1992). Structure and expression of the barley lipid transfer protein gene Ltp1. *Plant Mol. Biol.*, *18*(3), 585–589.

Sørensen, S. B., Bech, L. M., Muldbjerg, M., Beenfeldt, T., & Breddam, K. (1993). Barley lipid transfer protein 1 is involved in beer foam formation. *MBAA TQ*, *30*, 136–145.

Soufleri, I. A., Vergnolle, C., Miginiac, E., & Kader, J. C. (1996). Germination-specific lipid transfer protein cDNAs in *Brassica napus* L. *Planta*, *199*(2), 229–237.

Stanimirova, R. D., Gurkov, T. D., Kralchevsky, P. A., Balashev, K. T., Stoyanov, S. D., & Pelan, E. G. (2013). Surface pressure and elasticity of hydrophobin HFBII layers on the air-water interface: rheology versus structure detected by AFM imaging. *Langmuir*, *29*(20), 6053–6067.

Stanislava, G. (2010). A Review: The role of barley seed pathogenesis-related proteins (PRs) in beer production. *J. Inst. Brew.*, *116*(2), 111–124.

Stringer, M. A., & Timberlake, W. E. (1995). *dewA* encodes a fungal hydrophobin component of the *Aspergillus* spore wall. *Mol. Microbiol.*, *16*(1), 33–44.

Stringer, M.A., & Timberlake, W.E. (1993). Cerato-ulmin, a toxin involved in Dutch elm disease, is a fungal hydrophobin. *Plant Cell*, 5, 145–146.

Stübner, M., Lutterschmid, G., Vogel, R. F., & Niessen, L. (2010). Heterologous expression of the hydrophobin FcHyd5p from *Fusarium culmorum* in *Pichia pastoris* and evaluation of its surface activity and contribution to gushing of carbonated beverages. *Int. J. Food Microbiol.*, *141*(1-2), 110–115.

Subirade, M., Salesse, C., Marion, D., & Pézolet, M. (1995). Interaction of a nonspecific wheat lipid transfer protein with phospholipid monolayers imaged by fluorescence microscopy and studied by infrared spectroscopy. *Biophys. J.*, *69*(3), 974–988.

Sunde, M., Kwan, A. H. Y., Templeton, M. D., Beever, R. E., & Mackay, J. P. (2008). Structural analysis of hydrophobins. *Micron*, *39*(7), 773–784.

Szilvay, G. R., Nakari-Setälä, T., & Linder, M. B. (2006). Behavior of *Trichoderma reesei* hydrophobins in solution: Interactions, dynamics, and multimer formation. *Biochem.*, *45*, 8590–8598.

Szilvay, G. R., Paananen, A., Laurikainen, K., Vuorimaa, E., Lemmetyinen, H., Peltonen, J., & Linder, M. B. (2007). Self-assembled hydrophobin protein films at the air-water interface: Structural analysis and molecular engineering. *Biochem.*, *46*(9), 2345–2354.

Tagu, D., Nasse, B., & Martin, F. (1996). Cloning and characterization of hydrophobins-encoding ectomycorrhizal Basidiomycete *Pisolithus tinctorius*. *Gene*, *168*, 93–97.

Talbot, N. J., Ebbole, D. J., & Hamer, J. E. (1993). Identification and characterization of MPG1, a gene involved in pathogenicity from the rice blast fungus *Magnaporthe grisea*. *Plant Cell*, *5*(11), 1575–1590.

Tanner, G. J., Colgrave, M. L., Blundell, M. J., Goswami, H. P., & Howitt, C. A. (2013). Measuring hordein (Gluten) in beer – A comparison of ELISA and mass spectrometry. *PLoS ONE*, *8*(2), e56452.

Torkkeli, M., Serimaa, R., Ikkala, O., & Linder, M. (2002). Aggregation and self-assembly of hydrophobins from *Trichoderma reesei*: Low-resolution structural models. *Biophys. J.*, *83*, 2240–2247.

Torres-Schumann, S., Godoy, J. A., & Pintor-Toro, J. A. (1992). A probable lipid transfer protein gene is induced by NaCl in stems of tomato plants. *Plant Mol. Biol.*, *18*(4), 749–757.

Trimble, R. B., Atkinson, P. H., Tschopp, J. F., Townsend, R. R., & Maley, F. (1991). Structure of oligosaccharides on *Saccharomyces SUC2* invertase secreted by the methylotrophic yeast *Pichia pastoris*. *J. Biol. Chem*, *266*(34), 22807–22817.

Trimble, R. B., Lubowski, C., Hauer, C. R., Stack, R., McNaughton, L., Gemmill, T. R., & Kumar, S. A. (2004). Characterization of N- and O-linked glycosylation of recombinant human bile salt-stimulated lipase secreted by *Pichia pastoris*. *Glycobiology*, *14*(3), 265–274.

Tucker, S. L., & Talbot, N. J. (2001). Surface attachment and pre-penetration stage development by plant pathogenic fungi. *Annu. Rev. Phytopathol.*, *39*, 385–417.

Uruakpa, F. O. & Arntfield, S. D. (2006). Surface hydrophobicity of commercial canola grain proteins mixed with k-carrageenan or guar gum. *Food Chem.*, *95*, 255–263.

Vaag, P., Bech, L. M., Cameron-Mills, V., & Svendsen, I. (1999). Characterization of a beer foam protein originating from barley. In *Proceedings of the EBC Congress, Cannes,*157–166.

van Nierop, S. N. E., Evans, D. E., Axcell, B. C., & Cantrell, I. C. (2002). Does the presence of lipid transfer protein 1 (LTP1) in whole malt extracts influence yeast fermentation performance? In *Proceedings of 27th Convention, The Institute of Brewing, Asia Pacific Section, Adelaide*, paper #2.

van Nierop, S. N. E., Evans, D. E., Axcell, B. C., Cantrell, I. C., & Rautenbach, M. (2004). Impact of different wort boiling temperatures on the beer foam stabilizing properties of lipid transfer protein 1. *J. Agric. Food Chem.*, *52*(10), 3120–3129.

Viterbo, A. D. A., & Chet, I. (2006). *TasHyd1*, a new hydrophobin gene from the biocontrol agent *Trichoderma asperellum*, is involved in plant root colonization. *Mol. Pplant Pathol.*, *7*(4), 249–258.

Wagacha, J. M., & Muthomi, J. W. (2007). *Fusarium culmorum*: Infection process, mechanisms of mycotoxin production and their role in pathogenesis in wheat. *Crop Protection*, *26*(7), 877–885.

Wang, X., Graveland-Bikker, J. F., de Kruif, C. G., & Robillard, G. T. (2004). Oligomerization of hydrophobin SC3 in solution: From soluble state to self-assembly. *Protein Sci.*, *13*, 810–821.

Wang, Y., Bouillon, C., Cox, A., Dickinson, E., Durga, K., Murray, B. S., & Xu, R. (2013). Interfacial study of class II hydrophobin and its mixtures with milk proteins: relationship to bubble stability. *J. Agric. Food Chem.*, *61*(7), 1554–1562.

Wershofen, T. (2004). Gushing. Ein überschäumend spritziges Erlebnis. *Brauwelt*, *35*, 1061–1063.

Wessels, J. G. H., de Vries, O. M. H., Asgeirsdóttir, S. A., & Springer, J. (1991a). The *thn* mutation of *Schizophyllum commune*, which suppresses formation of aerial hyphae, affects expression of the Sc3 hydrophobin gene. *J. Gen. Microbiol.*, *137*(10), 2439–2445.

Wessels, J. G. H., de Vries, O. M. H., Asgeirsdottir, S. A., & Schuren, F. H. J. (1991b). Hydrophobin genes involved in formation of aerial hyphae and fruit bodies in *Schizophyllum*. *Plant Cell*, *3*(8), 793–799.

Wessels, J. G. H. (1994). Developmental regulation of fungal cell wall formation. *Annu. Rev. Phytopathol.*, *32*(1), 413–437.

White, A. J., Dunn, M. A., Brown, K., & Hughes, M. A. (1994). Comparative analysis of genomic sequence and expression of a lipid transfer protein gene family in winter barley. *J. Exp. Bot.*, *45*(281), 1885–1892.

Wösten, H. A. B., De Vries, O. M. H., & Wessels, J. G. H. (1993). lnterfacial self-assembly of a fungal hydrophobin into a hydrophobic roldet layer. *Plant Cell*, *5*, 1567–1574.

Wösten, H. A. B., & Wessels, J. G. H. (1997). Hydrophobins , from molecular structure to multiple functions in fungal development. *Mycoscience*, *38*, 363–374.

Wösten, H. A. B., van Wetter, M. A., Lugones, L. G., van der Mei, H. C., Busscher, H. J., & Wessels, J. G. H. (1999). How a fungus escapes the water to grow into the air. *Curr. Biol.*, *9*(2), 85–88.

Wösten, H. A. B., & de Vocht, M. L. (2000). Hydrophobins, the fungal coat unravelled. *Biochim. Biophys. Acta*, *1469*(2), 79–86.

Wösten, H. A. B. (2001). Hydrophobins: Multipurpose Proteins. *Annu.Rev. Microbiol.*, *55*, 625–646.

Yokoi, S., Maeda, K., Xiao, R., Kamada, K., & Kamimura, M. (1989). Characterization of beer proteins responsible for the foam of beer. In *Proceedings of the EBC Congress, Zurich.* 593– 600.

Yoo, B.-C., Aoki, K., Xiang, Y., Campbell, L. R., Hull, R. J., Xoconostle-Cázares, B., Monzer, J., Lee, J.-Y., Ullmann, D. E., & Lucas, W. J. (2000). Characterization of *Cucurbita maxima* phloem serpin-1 (CmPS-1): A developmentally regulated elastase inhibitor. *J. Biol. Chem.*, *275*(45), 35122–35128.

Yount, D. E. (1979). Skins of varying permeability: A stabilization mechanism for gas cavitation nuclei. *J. Acoust. Soc. Am.*, *65*(6), 1429–1439.

Yount, D. E. (1982). On the evolution, generation, and regeneration of gas nuclei. *J. Acoust. Soc. Am.*, *71*(6), 1473–1481.

Yount, D E, Gillary, E. W., & Hoffman, D. C. (1984). A microscopic investigation of bubble formation nuclei. *J. Acoust. Soc. Am.*, *76*(5), 1511–1521.

Zapf, M. W., Theisen, S., Vogel, R. F., Hecht, D., Elstner, E. F., & Niessen, L. (2005). Characterization of surface active proteins from *Fusarium* spezies and grain affecting foam stability. In F. H. Carl (Ed.), *Proceedings of the EBC Congress, Prague*.

Zapf, M. W. (2006). Charakterisierung oberflächenaktiver Proteine aus Fusarium spp. und deren Einfluss auf die Blasenstabilisierung in Bier. Doctoral thesis, Technische Universität München, Germany.

Zapf, M. W., Theisen, S., Vogel, R. F., & Niessen, L. (2006). Cloning of wheat LTP1500 and two *Fusarium culmorum* hydrophobins in *Saccharomyces cerevisiae* and assessment of their gushing inducing potential in experimental wort fermentation. *J. Inst. Brew.*, *112*(3), 237–245.

Zhang, N., & Jones, B. L. (1995). Characterization of germinated barley endoproteolytic enzymes by two-dimensional gel electrophoresls. *J. Cereal Sci.*, *21*, 145–153.

Zhang, X. L., Penfold, J., Thomas, R. K., Tucker, I. M., Petkov, J. T., Bent, J., Cox, A., & Grillo, I. (2011). Self-assembly of hydrophobin and hydrophobin/surfactant mixtures in aqueous solution. *Langmuir*, *27*(17), 10514–10522.